

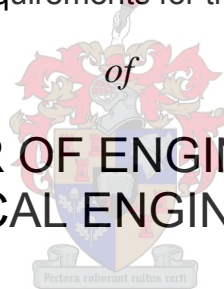
Surface water ultrafiltration pre-treatment through in- line coagulation and shallow bed media filtration

by

Patsy Maree

Thesis presented in partial fulfillment
of the requirements for the Degree

of
MASTER OF ENGINEERING
(CHEMICAL ENGINEERING)



in the Faculty of Engineering
at Stellenbosch University

Supervisor

Prof. A. J. Burger

March 2017

Declaration

By submitting this thesis electronically, I, Patsy Maree, declare that the entirety of the work contained therein is my own, original work, that I am the sole author thereof (save to the extent explicitly otherwise stated), that reproduction and publication thereof by Stellenbosch University will not infringe any third party rights and that I have not previously in its entirety or in part submitted it for obtaining any qualification.

Signed: Patsy Maree

Date: March 2017

Copyright © 2017 Stellenbosch University

All rights reserved

Abstract

High concentrations of organic and microbial matter in surface water cannot always be removed sufficiently through conventional water treatment methods. Ultrafiltration (UF) membranes are preferred for this purpose, as the low feed pressures required are cost effective, and a smaller footprint area is required compared to a conventional plant. UF membranes effectively clarify and disinfect surface water.

One notable hindrance to the use of UF for surface water treatment is the tendency of the membranes to foul. Particularly with the first annual rains, very high organic and solids loadings enter rivers. UF membranes can foul rapidly under these conditions. Therefore, this project investigated the use of in-line coagulation and integrated shallow-bed media filtration as low-cost pre-treatment prior to UF.

The media filter and UF were filtered and backwashed at the same intervals, using UF filtrate to simultaneously backwash both units. A shallow media bed with a depth of 250 mm promoted fractional particle retention and floc modification, by promoting contact between destabilised coagulated particles. The media filter, which acted as pre-filter (PF), was characterised for low turbidity river water of 12 NTU, represented by a prepared (synthetic) suspension of 20 mg/L humic acids (HA) and 30 mg/L bentonite. Design and operating parameters were chosen such that the PF could produce filtrate with turbidity below 1 NTU as feed to the UF, for 40-60 minutes. Backwashing the combined system at 4 PF displacement volumes (for 2 minutes) effectively restored the retention capacities of and initial pressure drops over both filters. The system was operated at an average downflow rate of 10 m/h through the PF and a flux of 46 LMH through the membrane. Keeping the parameters selected during characterisation fixed, the performance of the combined system was tested with higher turbidity synthetic suspensions. The improvement brought about to membrane performance by the PF was of interest.

For the low (12 NTU) and high (31 NTU) turbidity suspensions, reversible fouling occurred on the membrane, with a large percentage of the loading removed by the PF. No discernible irreversible membrane fouling took place. For low turbidity water, pre-treatment completely reduced TMP over the membrane, while at high turbidity water (25 mg/L HA, 100 mg/L bentonite), TMP was reduced by 70%. For the latter, breakthrough occurred after 15 minutes for 10 m/h PF filtration rather than after 50 minutes.

With a very high solids feed loading (400 mg/L bentonite) at 8 m/h PF downflow, the filtration duration had to be shortened to 50 min for effective PF backwashing. The PF could still reduce TMP by 60%, and allowed a more gradual turbidity filtrate profile to be filtered by the UF. High

organics loading of 70 mg/L HA did not present the same problem, and were effectively coagulated in such a manner that 99+% of TMP could be reduced through pre-filtration.

On-site testing confirmed lab findings that most of the turbidity load could be removed by the PF, indicating that overall system recovery can be increased by prolonging filtration duration. However, this work unfortunately took place at a time when the feed water was rather clean (6 NTU). On-site test work needs to be conducted with high turbidity feed to evaluate the performance of the unit under such adverse conditions.

Opsomming

Toenemend hoër konsentrasies van organiese en mikrobiese spesies in oppervlakwater kan nie altyd deur konvensionele watersuiweringstegnologieë tot 'n veilige mate verwyder word nie. Ultrafiltrasie (UF) membrane word verkies vir die behandeling van hierdie waterbron, as gevolg van die koste-effektiewe lae druk benodig om die stelsel te bedryf, asook die kleiner aanlegarea in vergelyking met konvensionele aanlegte. UF verwyder troebelheid asook patogene in water.

Die grootste hindernis tot die meer wydverspreide gebruik van UF in oppervlakwaterbehandeling, is die neiging van membrane om bevuil te word. Veral met die eerste jaarlikse reënval word hoë organiese en siltladings in riviere vervoer, wat membrane kan beskadig. Om hierdie rede was die moontlikheid ondersoek om koagulasie en 'n geïntegreerde vlak bed media filter te gebruik as UF voorbehandeling.

Die media filter en UF word terselfdertyd bedryf en teruggewas. UF permeaat word as waswater vir beide filters gebruik. 'n Vlak media bed met 'n diepte van 250 mm het turbiditeit gedeeltelik verwyder asook flokkulasie van destabiliseerde partikels aangehits. Die media filter, wat as pre-filter (PF) gedien het, was vir sintetiese water (bestaande uit 20 mg/L humiese sure (HA) en 30 mg/L bentoniet) met 'n turbiditeit van 12 NTU gekarakteriseer. Ontwerps- en bedryfsparameters was so gekies dat die PF vir 40-60 minute filtraat kon lewer met 'n troebelheid onder 1 NTU. Deur die stelsel na deurbraak terug te was vir 4 verplasingsvolumes (2 minute) was die PF se filterkapasiteit en aanvanklike drukval oor beide filters effektief herstel. Die stelsel was vir gemiddeld 10 m/h vloei deur die PF en 46 LMH flux deur die membraan bedryf. Karakterisasieparameters is konstant gehou vir behandeling van sintetiese waters met hoër turbiditeite. Die verbetering wat die PF aangebring het vir UF waterbehandeling was van belang.

Vir water met lae (12 NTU) en hoë (31 NTU) troebelheid was bevuiling omkeerbaar, en die PF het 'n groot lading van die membraan verwyder. Vir lae turbiditeit water het die PF TMP met 99+% verlaag. Selfs vir die hoë turbiditeit water (opgemaak uit 25 mg/L HA, 100 mg/L bentoniet) het die PF TMP met 71% verlaag. Vir laasgenoemde sintetiese oplossing het deurbraak na 15 minute plaasgevind eerder as die 50 minute waarvoor die laer turbiditeit water filtreer kon word.

Vir vloedtoestande met hoë bentonietlading (400 mg/L) moes die filtrasiesiklus verkort word na 50 minute vir 8 m/h PF filtrasie. TMP is met 60% verlaag, met 'n meer geleidelike PF filtraat turbiditeitskurwe wat deur die UF filtreer is. Vir 'n hoë organiese lading (70 mg/L HA) kon die PF die TMP met 100% verlaag.

Die opstelling is op 'n rivierwatersuiweringsaanleg getoets ten tye van relatiewe lae rivierwater troebelheid (6 NTU). Toetswerk het aangedui dat die meeste van die water troebelheid en feitlik 99+% van TMP deur die PF verwyder was vir kontinue filtrasie. Dit sal moontlik wees om onder sulke omstandighede die filtrasietydperk te verleng om terugwasverlies te verminder. Die opstelling moet op 'n aanleg getoets word op 'n tyd met hoër troebelheid water om die werking van die gekombineerde stelsel onder sulke omstandighede te toets.

Acknowledgements

Supervisor, Prof. André Burger, for the enriching research opportunity; invaluable wisdom and insight on water treatment; advice on and guidance throughout project work.

Process Engineering department, for financial support.

Wilhelm Frank Institute, for financing project costs.

Jos Weerdenburg and Anton Cordier, for assistance in construction, assembly and transport of my experimental set-up; also modifications made throughout and practical insights taught.

Francis Layman and Juliana Steyl, for assistance with procurement of equipment and reagents required, and logistical arrangements for site work.

Mark Miller from Grundfos, for provision of and effort in reprogramming feed pump.

Nardus Uys for electronic control of my set-up –PLC programming, wiring, calibration, advice.

Dr. LJ du Preez, for advice on thesis writing and data representation.

Ikusasa Water, and Overberg Water staff at water treatment plant, for facilitation of on-site test work.

Nearest and dearest family and friends for unwavering support, enthusiasm and understanding through all facets of project work.

CONTENTS

Abstract.....	i
Opsomming	iii
Acknowledgements.....	v
Nomenclature and definitions.....	xi
List of Figures.....	xiv
List of Tables.....	xviii
Chapter 1 : Introduction and project motivation	1
1.1 Background.....	1
1.2 Project motivation and rationale	2
1.2.1 Project scope.....	3
1.3 Key questions and objectives	4
1.3.1 Key questions	4
1.3.2 Objectives	4
Chapter 2 : Literature review	5
2.1 Surface water characteristics and treatment	5
2.1.1 Surface water characterisation	5
2.1.2 Surface water treatment technologies.....	9
2.2 Ultrafiltration.....	11
2.2.1 Background	11
2.2.2 Types and operation of membrane filters	12
2.2.3 Driving force and flux.....	17
2.2.4 Recovery for dead-end filtration	22
2.2.5 Membrane fouling	23
2.2.6 Backwash considerations.....	27
2.3 Media filtration principles	30
2.3.1 Pre-treatment to UF.....	30

2.3.2 Types and operation of media filters.....	30
2.3.3 Filtration directly following coagulation	34
2.3.4 Bed maturation	35
2.3.5 Pressure drop and head loss over media bed	36
2.3.6 Filtration efficiency	39
2.3.7 Backwash considerations for media filtration.....	40
2.4 Coagulation and flocculation	45
2.4.1 Distinction between coagulation and flocculation.....	45
2.4.2 Types of coagulant used in NOM removal	47
2.4.3 Coagulant dosing and dispersion	48
2.4.4 Effect of pH on water and subsequent effect on membranes.....	49
2.4.5 Jar tests and coagulant dosage determination.....	51
2.4.6 Combination of coagulation and filtration	52
2.5 Findings from literature	55
2.5.1 Configuration.....	55
2.5.2 Pre-filter filtration media	55
2.5.3 UF membrane	55
2.5.4 Downflow rate and filtration flux.....	56
2.5.5 Upflow rate and backwashing flux	56
2.5.6 Chemically enhanced backwash recipe	57
2.5.7 Coagulant and dosing.....	57
2.5.8 Suspension make-up	57
Chapter 3 : Research design and methodology	58
3.1 Operation of experimental set-up	58
3.2 Experimental set-up construction and assembly.....	61
3.2.1 Filtration units sizing and sourcing.....	61
3.2.2 Sand selection.....	62
3.2.3 Orifice mixing	63
3.2.4 Pump selection.....	64

3.2.5 Electronic requirements	64
3.3 Synthetic water make-up.....	65
3.3.1 Humic acid concentration	66
3.3.2 Bentonite concentration	67
3.3.3 Contribution of HA and bentonite to turbidity	67
3.3.4 Synthetic water composition	68
3.4 Flocculant dosage determination through jar tests	69
3.5 Chemically enhanced backwash procedure	71
3.6 Experimental plan.....	71
3.7 On-site test work.....	74
Chapter 4 : Filter characterisation.....	76
4.1 Pre-filter	76
4.1.1 Filtration media selection	76
4.1.2 Clean bed pressure drop and correlation with theory	78
4.1.3 PF bed depth.....	80
4.1.4 Effect of backwashing duration	87
4.1.5 PF particulate removal efficiency.....	92
4.1.6 Continuous filtration of synthetic water	94
4.2 UF membrane.....	97
4.2.1 Clean filter flux.....	97
4.2.2 Continuous filtration of synthetic water	97
4.3 Flood condition water composition selection	99
Chapter 5 : Effectiveness of combined shallow bed filtration and ultrafiltration	101
5.1 Low turbidity suspension filtration (12 NTU)	101
5.1.1 Low flux filtration (8 m/h; 37 LMH)	101
5.1.2 High flux filtration (10 m/h; 46 LMH).....	104
5.2 High turbidity suspension filtration (31 NTU).....	108
5.2.1 Filtration through membrane alone	109
5.2.2 Filtration through PF and UF	110

5.3 Flood condition suspensions	112
5.3.1 High solids loading (400 mg/L SS, 156 NTU).....	113
5.3.2 High organic matter loading (70 mg/L HA, 17 NTU)	117
5.4 Comparison of pressure drop data	120
5.5 On-site testing and performance evaluation	122
5.5.1 Selection of operation philosophy	122
5.5.2 Effect of pH on water quality	124
5.5.3 Surface water filtration through media and membrane filtration	125
5.5.4 Surface water filtration through flocculation on membrane.....	134
5.5.5 Temperature influence.....	141
5.5.6 Comparison with plant data	141
Chapter 6 : Conclusions and recommendations	142
6.1 Conclusions.....	142
6.2 Recommendations	143
Chapter 7 : References.....	145
Chapter 8 : Appendices	155
8.1 Appendix A: Characterisation of reagents and materials	155
8.1.1 MSDS sheets	155
8.1.2 Bentonite particle size distribution.....	156
8.1.3 Sand particle size distribution.....	157
8.1.4 Turbidity of humic acids and bentonite suspensions	158
8.1.5 Operation of conventional surface water treatment plant.....	161
8.2 Appendix B: Equipment construction and operation.....	162
8.2.1 Media filter Inventor drawing.....	162
8.2.2 Equipment list.....	163
8.2.3 Layout, construction and assembly of experimental unit.....	164
8.2.4 Commissioning of completed water treatment unit	165
8.2.5 Electronic requirements and instrumentation required.....	166
8.2.6 Final process flow diagram.....	166

8.2.7 Complete operating procedure for experimental set-up	168
8.2.8 Control philosophy.....	171
8.2.9 Southern Cape plant operation	174
8.3 Appendix C: Omitted graphs and data	175
8.3.1 Flocculated water turbidity.....	175
8.3.2 Pre-filter characterisation.....	175
8.3.3 Combined filter effectiveness	181
8.4 Appendix D: Sample calculations.....	187

Nomenclature and definitions

Symbol	Definition	Units
A_0	Orifice plate surface area	m^2
C	Concentration	mg/L
C_d	Discharge coefficient of orifice plate	--
d	Diameter of piping	m
F_g	Gravitational force	N
F_w	Force exerted by water	N
G	Velocity gradient measuring dispersion and mixing	s^{-1}
g	Gravitational acceleration	m/s^2
H	Height/depth of media bed	m
H_0	Initial bed height	mm
H_E	Bed height upon expansion	mm
h_L	Head loss	m
k	Kozeny's constant	--
K	Coefficient of permeability of media bed	m/s
M	Mass of dry media particles in bed	kg
m	Mass of specified material	kg
P	Pressure	kPa
P_{inlet}	Pressure at membrane vessel inlet	kPa
P_{outlet}	Pressure at membrane vessel outlet (in case of cross-flow)	kPa
$P_{permeate}$	Pressure of permeate stream	kPa
P_w	Power number	--
Q	Volumetric flow rate	m^3/s
Q_S	Volumetric flow rate at standard temperature, S	m^3/s
Q_T	Volumetric flow rate at temperature, T	m^3/s
R_F	Foulant layer resistance to flow through filter	m^{-1}
R_M	Filter medium (membrane/sand) resistance to flow through filter	m^{-1}
R_T	Total resistance to flow by filter media and foulant	m^{-1}
T	Temperature	$^{\circ}C$
t	Time	s
U	Superficial flow velocity	m/s
V	Volume of mixing vessel	m^3
V_B	Bed volume	m^3

v_{mf}	Minimum fluidisation velocity	m/s
W_F	Total volume of water filtered	L
W_B	Volume of water discarded during backwashing	L
x	Diameter of spherical particle	m
x_{sv}	Equivalent mean surface-volume diameter	m
β	Ratio of orifice plate diameter over approach diameter	--
ϵ	Voidage of packed bed	--
ϵ_0	Initial bed voidage	--
ϵ_E	Bed voidage upon expansion	--
Δ	Difference	--
μ	Dynamic viscosity of fluid	Pa.s
ρ_B	Bed density	kg/m ³
ρ_F	Fluid density	kg/m ³
ρ_s	Particle material density	kg/m ³
Π	Osmotic pressure	kPa

Abbreviations	Definition
CEB	Chemically enhanced backwash
CIP	Cleaning in place
CP	Concentration polarisation
DBP	Disinfection by-product
DV	Displacement volume
FA	Fulvic acid
Ga	Galileo's number
HA	Humic acids
HS	Humic substances
LMH	Units of membrane flux - (litres/hour)/m ²
MF	Microfiltration
MWCO	Molecular weight cut-off size
NF	Nanofiltration
NOM	Natural organic material
NTU	Nephelometric turbidity units
PES	Polyethersulphone
PF	Pre-filter

PVDF	Polyvinylidene fluoride
Re	Reynold's number
Re*	Reynold's number for flow through a packed bed
Re_{mf}	Reynold's number at minimum fluidisation point
RO	Reverse osmosis
SS	Suspended solids
TCF	Temperature correction factor
TDS	Total dissolved solids
TMP	Transmembrane pressure
UF	Ultrafiltration
UV-Vis	Ultraviolet visible light (spectroscopy)
VSD	Variable speed drive

Glossary

Downflow rate	Volumetric flow rate per media filter cross sectional area
Pre-filter	Shallow (<300 mm) media bed preceding UF with sand as filter media
Upflow rate	Backwashing volumetric flow rate per media filter cross sectional area

List of Figures

Figure 2-1: NOM composition	7
Figure 2-2: Active and support layers in anisotropic membrane.....	12
Figure 2-3: Cross-flow filtration operation.....	15
Figure 2-4: Dead-end membrane filtration operation	16
Figure 2-5: a) Adsorption in membrane pore, b) pore blocking and c) cake formation.....	23
Figure 2-6: Capture mechanisms in a) slow (surface) and b) rapid (depth) filtration.....	31
Figure 2-7: Media distribution within beds.....	33
Figure 2-8: Capture mechanisms within media bed	34
Figure 2-9: Residual turbidity profile over the course of a filtration cycle	35
Figure 2-10: Head loss as a function of time	38
Figure 2-11: Media particle fluidisation: a) The force of backwashing water, F_w , acts on the media particle. b) $F_w > F_g$, and the particle moves upwards and becomes fluidised.....	41
Figure 2-12: Effect of superficial velocity on bed height and pressure drop	42
Figure 2-13: Optimal residual turbidity removal for relatively low coagulant dosage.....	48
Figure 2-14: Particle size ranges for which treatment types are appropriate.....	52
Figure 3-1: Simplified PFD of experimentation set-up	60
Figure 3-2: Left: PF with transparent PVC body. Right: Inside view from top showing fine sieve supported by two coarse sieves.	62
Figure 3-3 : Bentonite and HA contribution to turbidity	68
Figure 3-4: Jar test set-up during coagulation dosage determination.....	70
Figure 3-5: Experimental plan	72
Figure 3-6: Selection of media grain type.....	72
Figure 3-7: Media bed characterisation sequence of experiments.....	73
Figure 3-8: Filtration experiments.....	74
Figure 4-1: Turbidity comparison for different filter media: 150 mm bed; 31 NTU suspension; 9 m/h downflow	77
Figure 4-2: Difference in residual turbidity between compacted and non-compacted bed: 250 mm bed; 12 NTU suspension; 10 m/h downflow	79
Figure 4-3: Residual turbidity at different downflow rates for 200 mm bed, 12 NTU suspension	82
Figure 4-4: Residual turbidity at different downflow rates for 250 mm bed, 12 NTU suspension	83
Figure 4-5: Residual turbidity at different downflow rates for 300 mm bed, 12 NTU suspension	84

Figure 4-6: Residual turbidity for different bed depths at 12 m/h downflow rate	86
Figure 4-7: Initial residual turbidity after different backwashing durations: 250 mm bed; 12 NTU suspension	89
Figure 4-8: Breakthrough at different backwashing durations: 250 mm bed; 12 NTU suspension	90
Figure 4-9: Effect of backwashing duration on water colour above fluidised expanded 250 mm bed.	91
Figure 4-10: Percentage turbidity removal for 250 mm bed at different downflow rates; 12 NTU suspension.....	93
Figure 4-11: Percentage 254 nm absorbance removed from 12 NTU water at 10 m/h downflow	94
Figure 4-12: PF pressure drop over 250 mm bed for continuous filtration of 31 NTU suspension	95
Figure 4-13: Residual turbidity curve past PF breakthrough: 250 mm bed; 31 NTU suspension	96
Figure 4-14: TMP increase for PF operation past breakthrough: 250 mm bed; 31 NTU suspension.....	96
Figure 4-15: TMP for direct flocculation onto membrane with 12 NTU suspension at 46 LMH..	98
Figure 4-16: TMP for direct flocculation onto membrane with 31 NTU suspension at 46 LMH..	99
Figure 5-1: TMP for direct filtration at 37 LMH of flocculated 12 NTU suspension	102
Figure 5-2: Pressure drop over PF for 8 m/h filtration of 12 NTU suspension	103
Figure 5-3: Average residual turbidity after PF for 8 m/h filtration of 12 NTU suspension.....	103
Figure 5-4: TMP for 37 LMH filtration of water filtered by the PF	104
Figure 5-5: TMP for direct filtration of flocculated 12 NTU suspension at 46 LMH	105
Figure 5-6: Pressure drop over PF for 10 m/h filtration of 12 NTU suspension	106
Figure 5-7: Average residual turbidity following PF for 10 m/h filtration of 12 NTU suspension	107
Figure 5-8: TMP for 46 LMH filtration of PF filtrate	107
Figure 5-9: TMP for direct filtration of 31 NTU suspension at 46 LMH.....	109
Figure 5-10: Pressure drop over PF for 10 m/h filtration of 31 NTU suspension	110
Figure 5-11: Average residual turbidity following PF for 10 m/h filtration of 31 NTU suspension	111
Figure 5-12: TMP for 46 LMH filtration of PF filtrate.....	112
Figure 5-13: TMP for direct filtration of flood SS suspension at 37 LMH	114
Figure 5-14: Pressure drop over media bed for flood SS suspension at 8 m/h.....	115
Figure 5-15: Residual turbidity following PF of flood SS suspension.....	115
Figure 5-16: TMP for cyclical operation at 37 LMH filtration of flood SS suspension	116

Figure 5-17: Cyclical operation of direct flocculation onto membrane of flood HA suspension	117
Figure 5-18: Pressure drop of cyclical operation of flood HA through PF	118
Figure 5-19: Residual turbidity following pre-filtration of flood HA suspension	119
Figure 5-20: TMP for cyclical operation at 37 LMH for flood HA suspension	119
Figure 5-21: Turbidity removal by PF at different downflow rates	123
Figure 5-22: Colour removal by PF at different downflow rates	123
Figure 5-23: Raw water properties over the course of experiment	126
Figure 5-24: Pressure drop over PF for site experiments	127
Figure 5-25: Percentage turbidity removal from site water by PF	128
Figure 5-26: Percentage colour removal from site water by PF	128
Figure 5-27: Day 1 TMP for filtration of PF permeate	130
Figure 5-28: Day 2 TMP for filtration of PF permeate	131
Figure 5-29: Day 3 TMP for filtration of PF permeate	131
Figure 5-30: Day 4 TMP for filtration of PF permeate	132
Figure 5-31: Day 5 TMP for filtration of PF permeate	133
Figure 5-32: Raw water turbidity and colour	134
Figure 5-33: Day 1 TMP profile for direct flocculation and filtration through UF	135
Figure 5-34: Initial TMP profile	136
Figure 5-35: Day 2 TMP profile for direct flocculation and filtration through UF	137
Figure 5-36: Day 3 TMP profile for direct flocculation and filtration through UF	138
Figure 5-37: Day 4 TMP profile for direct flocculation and filtration through UF	138
Figure 5-38: Day 5 TMP profile for direct flocculation and filtration through UF	139
Figure 5-39: Day 6 TMP profile for direct flocculation and filtration through UF	140
Figure 5-40: Non-normalised TMP plot	141
Figure 8-1: Bentonite particle size distribution	156
Figure 8-2: Silica sand grading and particle size distribution	157
Figure 8-3: Silica filtration media	157
Figure 8-4: Humic acid contribution to water turbidity	159
Figure 8-5: Bentonite contribution to water turbidity	159
Figure 8-6: Experimental set-up (left) side and (right) front view	165
Figure 8-7: Experimental sequence	172
Figure 8-8: Subprocesses for experimentation	173
Figure 8-9: Residual turbidity for flood HA coagulant dosage	175
Figure 8-10: Residual turbidity for 8 and 9 m/h downflow through coarse 150 mm bed	176
Figure 8-11: 11 m/h downflow rate through shallow bed of screened sand	176
Figure 8-12: Pressure drop over PF at 8 m/h downflow rate	177

Figure 8-13: Pressure drop over PF at 10 m/h downflow rate.....	177
Figure 8-14: Pressure drop over PF at 12 m/h downflow rate.....	178
Figure 8-15: Pressure drop over 200 mm PF	178
Figure 8-16: Pressure drop over 250 mm PF	179
Figure 8-17: Pressure drop over 300 mm PF	179
Figure 8-18: Residual turbidity for repeated 50 minute cycles of 10 m/h with 2 DV backwashing	180
Figure 8-19: Residual turbidity for repeated 50 minute cycles of 10 m/h with 3 DV backwashing	180
Figure 8-20: Residual turbidity for repeated 50 minute cycles of 10 m/h with 4 DV backwashing	181
Figure 8-21: Residual turbidity for repeated 50 minute cycles of 10 m/h with 6 DV backwashing	181
Figure 8-22: Pressure drop profile over media bed for 3x60 5x75 min 36 LMH cycles with 2 min backwashing.....	182
Figure 8-23: Residual turbidity profile following media filtration for 36 LMH operation with 2 min BW	182
Figure 8-24: Membrane pressure for 3x60 5x75 min 36 LMH cycles with 2 min backwashing	183
Figure 8-25: Pressure drop over media bed for 50 min 46 LMH.....	183
Figure 8-26: Residual turbidity profile following media filtration	184
Figure 8-27: Membrane pressure for 50 min 47 LMH cycles with 2 min backwashing	184
Figure 8-28: Pressure drop over pre-filter	185
Figure 8-29: Percentage turbidity removed by pre-filter	185
Figure 8-30: Percentage colour removed by pre-filter	186
Figure 8-31: Raw water properties over course of experiment	186
Figure 8-32: PF pressure drop calculation	189

List of Tables

Table 2-1: Comparison of groundwater and surface water	5
Table 2-2: Surface water turbidities for research studies	6
Table 2-3: Nominal pore sizes for UF membranes	13
Table 2-4: Comparison of PVDF and PES properties	14
Table 2-5 Typical UF operational fluxes for surface water filtration.....	19
Table 2-6: Typical UF surface water filtration durations between hydraulic backwashes	19
Table 2-7: Typical UF backwashing fluxes for surface water filtration	20
Table 2-8: Typical UF backwashing durations for surface water filtration.....	20
Table 2-9: Backwashing upflow rates from literature	41
Table 2-10: Recommended media bed expansion percentages.....	43
Table 2-11: Effect of alkaline pH on NOM-containing surface water coagulation.....	50
Table 2-12: Effect of acidic pH on NOM-containing surface water coagulation	51
Table 3-1: Filter fluxes and flow rates considered for operation	62
Table 3-2: Head loss and flow velocity for flow rates and orifice sizes considered	63
Table 3-3: HA concentrations from literature used to synthesize surface water	66
Table 3-4: Bentonite concentration representative of SS in surface water	67
Table 3-5: Resulting turbidity of synthetic surface water suspensions upon adding bentonite..	67
Table 3-6: Water compositions for different conditions considered.....	68
Table 3-7: Flocculant dosages for different water types.....	70
Table 4-1: Correlation between experimental and theoretical pressure drop: 250 mm bed; 12 NTU suspension	80
Table 4-2: Pressure drop for various flow rates with 12 NTU suspension	85
Table 4-3: Media bed depth and flow rate comparison with 12 NTU suspension	87
Table 4-4: Displacement volumes and backwashing durations for 250 mm bed.....	88
Table 4-5: Recovery at different backwashing durations: 250 mm bed.....	92
Table 4-6: Recovery for different flow rates and durations: 250 mm bed	92
Table 4-7: Clean membrane TMP.....	97
Table 5-1: Normalised pressure drop data for filtration experiments	120
Table 5-2: pH following UF and resulting residual Al	125
Table 8-1: Comparison of temperature normalisation effectiveness for Methods 1 and 2	194
Table 8-2: Determination of average turbidity and corresponding standard deviation	195

CHAPTER 1 : INTRODUCTION AND PROJECT MOTIVATION

1.1 Background

Developments in the field of membrane filtration technology have increased the use thereof in surface water treatment for the production of drinking water. Conventional treatment cannot remove pathogens and disinfection by-products to the same extent as membranes (Zhang, et al., 2014). The use of membranes reduces chemical requirement of the plant as the membranes serve a disinfection as well as clarification purpose (Drioli & Giorno, 2009). For the treatment of surface water, ultrafiltration (UF) is the preferred treatment type, as the pores are small enough to prevent the propagation of pathogens and suspended compounds, and the energy requirement is lower than that of nanofiltration and reverse osmosis. Water delivered is of a high and consistent quality. Membranes are periodically hydraulically and chemically backwashed to remove retained particles and recover the permeability of the membrane.

The largest hindrance to the more widespread use of membranes in water treatment is their sensitivity to fouling, which can be caused by suspended solids and organics particularly prevalent in surface water. Pre-treatment is thus typically used prior to membrane filtration, providing an additional barrier to incoming foulants. Each pre-treatment will introduce complications to the process, whether it is the addition of dead volume, high capital costs, regeneration costs of materials, regular replacement of disposable filters or additional chemical costs. In-line coagulation prior to sand filtration is included, as the formation of flocs is beneficial to the performance of both filters considered (Rebhun, et al., 1984), (Zhang, et al., 2008). Direct flocculation prior to sand filtration, with the omission of sedimentation, induces orthokinetic or contact flocculation. The growth of flocs takes place within the depth of the media bed, and large enough flocs are retained within the bed.

For the treatment of surface water, it is known that especially with the first annual rainfall, a high concentration of suspended material and dissolved compounds are washed down a river to a treatment plant, which could adversely affect the performance of the operating units. This is a particular problem for membrane filtration, as the sudden and drastic increase of transported material could damage membranes to such an extent that they have to be replaced.

1.2 Project motivation and rationale

UF membrane systems can sometimes rapidly lose capacity due to fouling when abnormally high levels of organic and suspended material are present in the feed water. This can, for example, happen at river water treatment UF plants when flash floods entrain high quantities of silt and other foreign material. Under such conditions, it is wise to have some mechanism of pre-clarification, along with standard pre-screening, as safeguard prior to UF. Various pre-treatment technologies could then be considered, e.g. clarifiers, or media filters.

To install a well-designed independent deep-bed media filtration system (including all peripheral equipment such as flocculation systems, backwash pumps and blowers) as pre-treatment almost defies the purpose of the UF and, furthermore, makes little financial sense if it is only needed for certain periods of the year. However, the system can be much more cost-effective when a relatively shallow sand bed pre-filter is installed as an integrated part of the UF system. In such a system, the same water is used to backwash the UF and the sand PF, with no separate backwash circuits and intermediate valves. Furthermore, if the bed is relatively shallow (i.e. less than 0.4 m) then:

- the pre-filter can be installed on top of the UF vessel, thereby minimising additional plant footprint requirements;
- additional pressure drop will be low; and
- less backwash water will be required to clean the bed (compared to deep-bed units).

Therefore, this project focused on the technical evaluation of a shallow sand bed – with in-line coagulation – as pre-treatment to UF.

Properties of the sand pre-filter were manipulated in such a manner that it could be operated for the same duration as the UF, with operational times of between 40 and 60 minutes, followed by hydraulic backwashing for between 0.5 and 3 minutes. The two filters were operated and backwashed in series using the same feed and backwash pumps. As the same water was used to backwash both units, the reduction in overall water recovery of the process was minimised.

Coagulation was used as pre-treatment to maximise the efficiency of both units. The sand bed could serve as floc modifier, promoting contact between coagulated particles and thus floc growth. The shear induced by the tortuous paths between filter media typically promotes agglomeration. Furthermore, it was also argued that residual micro-flocs passing through the sand bed would build up as a cake layer on the membrane surface rather than enter and restrict the pores.

1.2.1 Project scope

A scope for the project has to be defined in order to limit the range of variables changed. As the experimental unit had to be built from scratch, it is important to limit the type and range of variables changed which could affect the unit's overall performance.

- Selection of maximum bed depth

The bed depth of a typical full scale rapid media filter ranges from 0.4 m (GE Water) to 1.5 m (Cox, 1969), depending on the nature of water being treated and its application. No information could be found in literature on the use of a shallow media bed, with a depth not exceeding 0.4 m, as pre-treatment to UF. The purpose of the shallow pre-filter is not to act as full scale media filter, but as buffer which could retain a fraction of incoming particles and create a more gradual fouling profile to be filtered by the UF. The media particles will act as floc modifier, promoting the contact between destabilised particles and creating agglomerated microflocs, which will not irreversibly foul the membrane but rather be built up as a cake layer.

The depth of the bed shall not exceed 0.3 m, to support the logic that backwashing will happen regularly (e.g. every hour) and that additional head space and pressure drop requirements should be minimised. One media bed containing silica as single filtration media was selected. No additional equipment (pumps) is required for the pre-filter as it will operate in conjunction with the UF, and additional infrastructure is minimised by limiting the dimensions of the bed.

- Selection of maximum installation height of the pre-filtration set-up

For the maximum bed depth considered, a maximum bed expansion of 50% should be allowed to calculate the pre-filter column height. Therefore a height of 0.45 m was chosen. Accounting for the cap and base of the filter, ball valves above and below the installation to isolate it, and T-piece fittings for pressure sensors and gauges, a maximum installation height of 1 m was selected and fixed. The column height was kept unchanged for the use of different bed depths.

- Air scouring was not included in the backwashing regime

Although air scouring is known to improve the effectiveness of backwashing for both media and membrane filtration (Bessiere, et al., 2009), (Pradhan, et al., 2012), (Stevenson, 1997), it was not included for these experiments, because it was not necessary to prove the pre-filtration principle.

- Not all compounds are accounted for in the synthetic make-up of water

For the treatment of surface water with UF membranes, laboratory scale test work only considered the fouling of membranes through organic and colloid particles by using suspensions containing humic acids and bentonite. The effectiveness of the system was measured by its ability to remove organic matter and suspended solids through turbidity, and furthermore by measuring pressure drop as indicator of fouling.

- pH adjustment

The pH of the water was not adjusted for during test work, and water was coagulated at a neutral pH. Ferric chloride was selected as coagulant. The effect of pH on floc formation is not as pronounced for ferric chloride as it is for aluminium sulphate, which is another coagulant typically used in surface water treatment (Matilainen, et al., 2010).

1.3 Key questions and objectives

1.3.1 Key questions

1. Can media bed properties (grain size, bed depth) be modified within the scope of the project to effectively clarify a low turbidity suspension within typical ultrafiltration operational parameters (downflow and upflow rate, filtration and backwashing durations)?
2. What contribution does the pre-filter make to membrane performance for various test suspensions in terms of removing solids loading?
3. Would the media filter impede the operation of the UF membrane through operational limitations and how would this be mitigated?

1.3.2 Objectives

In order to answer the key questions for this project, a series of deliverables had to be met:

- Design and construct a pilot-scale set-up in which water can be coagulated in-line and subsequently filtered through a media bed and ultrafiltration membrane. Filters should be able to be operated individually and in series with automated operation.
- Select surface water composition representative of typical surface water, and treat water in experiments with coagulant dosage determined through jar tests.
- Find parameters for media filtration (grain size, depth of bed) suitable to clean water for the required operational duration and at required flow rates. Measure filtration performance throughout with turbidity testing.
- Determine suitable flow rates for required operational durations which deliver clean water throughout testing.

CHAPTER 2 : LITERATURE REVIEW

The literature study focused specifically on the type of water used and the technologies considered for the treatment thereof. A brief overview of surface water is discussed along with general treatment technologies, before an in-depth discussion on ultrafiltration, media filtration and flocculation.

2.1 Surface water characteristics and treatment

Water occurs naturally in fresh and saline sources both above and below the ground. As the focus of this project is specifically on surface water treatment, a comparison between fresh water sources is given in Table 2-1.

Table 2-1: Comparison of groundwater and surface water

Groundwater	Surface water
Extracted from underground aquifers	Extracted from rivers and dams
Low pH: dissolved CO ₂ from organic decomposition (Stevenson, 1997)	Wide possible pH range, seasonal variation dependent on run-off to rivers (Matilainen, et al., 2010)
Lower turbidity than surface water: filtered as it flows through ground (Tchobanoglous & Schroeder, 1985)	High turbidity (1-1000+ NTU): wide range suspended and dissolved components
Higher dissolved salt concentration: increased mineral contact (Tchobanoglous & Schroeder, 1985). High in iron, manganese (Stevenson, 1997)	High in natural organic material responsible for taste, odour, colour

Surface water typically has greater turbidity and organic species than groundwater, and its composition varies seasonally.

2.1.1 Surface water characterisation

a) Components in natural water and their analysis

Surface water contains variable levels of soluble and insoluble components which differ for each water source and season. It is thus impossible to characterize or give typical concentrations for suspended and organic matter in surface water (Tchobanoglous & Schroeder, 1985).

Turbidity causing compounds

Surface water can have a cloudy appearance due to suspended solids and colloids, present due to the attrition of stones and sand, or the transport of materials. The clarity of the water is measured as turbidity.

In a treatment plant, the turbidity of water is monitored on-line throughout operation. It is commonly used to trend the performance of filters. SANS standards govern that potable water should have a turbidity not exceeding 1 NTU (SANS 241-1:2011).

Turbidity measures the amount of visual light scattered by suspended solids in a suspension (Droste, 1997). The amount of light scattered or absorbed by the sample is expressed in nephelometric turbidity units (NTU). Prior to analysis the meter is calibrated, enabling the expression of absolute values. Dissolved organic materials such as humic acid (HA) will contribute to the turbidity reading, as it will also scatter light. The value in NTU is thus not merely representative of suspended solids, but will include dissolved materials.

Authors investigating treatment of surface water through membrane filtration have logged natural water turbidities that vary notably, shown in Table 2-2.

Table 2-2: Surface water turbidities for research studies

Surface water turbidity (NTU)	Research group
1.8-3.6	(Crozes, et al., 1997)
2-3	(Cho, et al., 2006)
2.8-7.6	(Fan, et al., 2001)
3.9	(Carroll, et al., 2000)
6	(Chae, et al., 2008)
6-20	(Guo, et al., 2009)
7.2-8.6	(Crozes, et al., 1997)
8.6	(Kimura, et al., 2004)
20	(Dong, et al., 2006)
21	(Guigui, et al., 2002)

Organic material

The umbrella term for organic compounds in water is natural organic matter (NOM). NOM can be responsible for the turbidity, pH, taste, colour and odour of the water (Matilainen, et al., 2010). Decaying plant and animal material, agricultural runoff wastewater and pollution are predominantly responsible for NOM in surface water (Tchobanoglous & Schroeder, 1985).

The make-up of NOM is illustrated in Figure 2-1, constructed using information from Carroll et al. (2000), with HS and non-HS characterisation information from work done by Rodrigues et al. (2008).

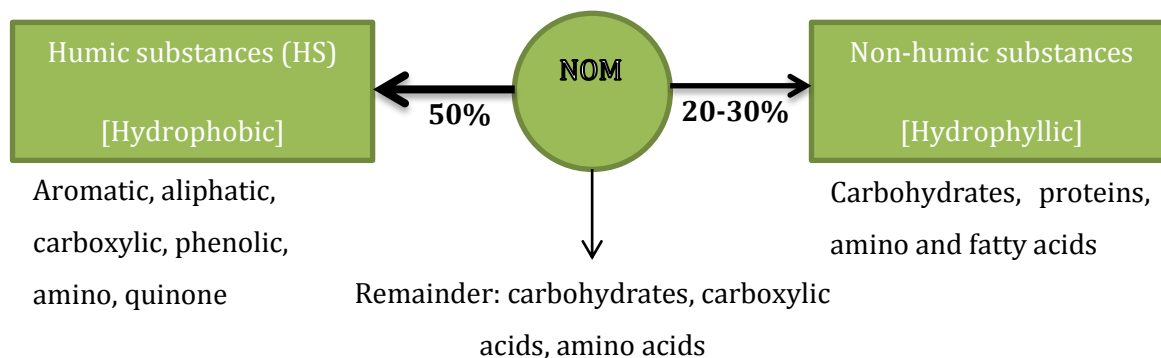


Figure 2-1: NOM composition

Humic substances (HS) consist of humic acids (HA) and fulvic acids (FA), and are characterised based on their solubility in acidic or basic substrates. HA can range in size from anything between 5-300 kDa (Zularisam, et al., 2006). It will have a negative charge when suspended in water due to dissociation of carboxylic and phenolic groups (Rodrigues, et al., 2008). HA is insoluble at low pH, while the opposite is true for FA. Upon reaction with chlorine during disinfection, HA can produce carcinogenic disinfection by-products (DBPs) (Peng, et al., 2005), (Park & Yoon, 2009), (Matilainen, et al., 2010), (Cho, et al., 2006), (Wang, et al., 2011).

Adsorption of HA within pores can occur during UF, causing highly undesirable and detrimental irreversible fouling (Zularisam, et al., 2006), (Crozes, et al., 1997), (Kimura, et al., 2008). Properties such as the hydrophobicity and charge will determine whether the compound adsorbs to the membrane surface or within its pores (Carroll, et al., 2000).

HA can effectively be removed through coagulation and subsequent solid-liquid separation. Ferric- and aluminium-based coagulants selectively aggregate suspended particles. Carroll et al. (2000) reports a preference for larger, hydrophobic and charged particles to coagulate. The remaining neutral hydrophilic fractions lend themselves out to irreversibly foul the membrane as reported by Fan et al. (2001). Coagulant type, dosage and a variable feed water composition may cause the components available for fouling in the water to fluctuate, causing variable foulant behaviour.

The organic compounds present in water can be measured through chemical oxygen demand, total organic carbon, total oxygen demand, biochemical oxygen demand or through colour measurement, expressed in platinum cobalt colour units.

In the case of HA present in surface water, the ultraviolet absorbance of HA at 254 nm is a widely used parameter to determine the concentration of HA and FA (Zularisam, et al., 2006), (Dong, et al., 2006), as HA concentration is proportional to the amount of UV light absorbed at the same wavelength (Rodrigues, et al., 2008). Turbidity is also used to determine the apparent colour of water, which is an easier and faster manner of analysis, while still being a reliable measure of filtration efficiency. Spectroscopic absorbance at 254 nm increases with the presence of more aromatic rings, total carbon and the molecular weight of larger HA compounds.

The presence of suspended solids (SS) in surface water will scatter light and affect the absorbance reading. Filtration of the sample prior to analysis will not only remove SS, but will also remove HS which aggregated with solids, influencing the accuracy of UV-Vis for HA measurement (Rodrigues, et al., 2008).

b) Interaction between HA and bentonite

The presence of certain colloidal foulants, such as silica, does not affect HA through adsorption (Li & Elimelech, 2006). Bentonite, with its given structure and large surface area, has been reported to adsorb HA, affecting the foulant behaviour (Kretzschmar, et al., 1998), (Pourrezaei, et al., 2010). If HA becomes adsorbed by the bentonite, there will be a less pronounced effect on fouling, as their bonding leads to a decrease in deposition of HA into the membrane pores (Zularisam, et al., 2006). The porosity of filtration cakes on membranes will be increased as it would be built up of larger particulates, which will greatly improve the filtration flux (Park & Yoon, 2009).

Research has been done on the adsorption of HA onto bentonite to assess to what extent bentonite can improve NOM removal. In some treatment plants, bentonite or kaolin clay is added to aid in NOM removal. The adsorption of HA onto bentonite is exerted because of Van der Waals forces between the differently charged particles in the water. Furthermore, cation exchange can take place between the organic compounds of HA (such as carboxyl groups), and alkaline cations in the clay mineral (such as the sodium, calcium or magnesium cations) (Park & Yoon, 2009).

2.1.2 Surface water treatment technologies

Suspended compounds in water have different sizes and properties, and are removed through various treatment processes. The treatment of water to produce potable water requires the elimination of potentially harmful and otherwise undesired species to within SANS 241 standard. According to SANS 241:2015, turbidity of the water should be less than 1 NTU, total coliforms less than 10 per 100 ml, and colour less than 10 mg/l Pt-Co.

a) Physical treatment methods

Membrane filtration

Filtration is a mechanical solid-liquid separation method involving the removal of suspended particulates from water by providing a physical barrier against their propagation (Degrémont, 2007). Suspended particles larger than a characteristic filter or pore size are retained, while smaller particles are able to pass through the barrier.

In recent years the use of membranes in water treatment through microfiltration (MF), UF and reverse osmosis (RO) has caused significant advances in the field of water treatment (Degrémont, 2007). UF is becoming increasingly common and preferred for the production of drinking water as opposed to conventional water treatment plants, due to its ability to produce water of a superior quality, and the inability of conventional treatment plants to maintain the stringent water quality standards regarding turbidity and the presence of pathogens (De Souza & Basu, 2013), (Guo, et al., 2009), (Zhang, et al., 2009). UF delivers water of a high and consistent quality (Shengji, et al., 2008). Membranes can effectively remove colour, taste, DOC and DBP from low quality water sources (Guigui, et al., 2002). The footprint of a membrane treatment facility is much smaller than the area required in building a conventional plant (Nakatsuka, et al., 1996). The operation of a conventional water treatment plant is discussed in Appendix A.

Apart from the effectiveness through which UF membranes disinfect water, the fact that clarification and disinfection can be carried out in a single step is unique to this unit operation (Konieczny, 1998). This lessens the dependence on other disinfection practices such as chlorination, ozonation and UV irradiation, of which some are inherently expensive and potentially unsafe (Zhang, et al., 2009), (De Souza & Basu, 2013).

Media filtration

Media filter beds are widely used and the media type, particle size, configuration and backwashing methods vary depending on the nature of the water treated (Drioli & Giorno,

2009). The quality of the treated water is proportional to the quality of the incoming water (Hillis, et al., 1998). Conventional plants can also not remove certain components, such as aluminium, to the same extent as membrane filtration can. Larger footprint areas and a greater dependency on chemicals are typical of conventional plants.

b) Chemical treatment methods

Coagulation and flocculation

Coagulation destabilises charged particles, and by promoting contact between the destabilised particles, they are agglomerated through flocculation. During this process, the sizes of the small particles are increased, making it easier to remove in subsequent treatment steps. Organic matter and colloidal colour is removed effectively through coagulation and flocculation, which is why coagulation and flocculation are generally used in conjunction with filtration and other treatments to clarify water (Stevenson, 1997).

Cox (1969) and Gomez et al. (2006) give detailed descriptions of the alternative chemical disinfection processes of chlorination, ozonation and UV irradiation. In particular they discuss disadvantages around each technology type, highlighting the relevance of UF as alternative disinfection method.

2.2 Ultrafiltration

Ultrafiltration is becoming the preferred technology for surface water treatment (Nakatsuka, et al., 1996). In many instances, UF plants are replacing conventional treatment plants, or are built supplementary to existing conventional plants in order to improve water quality.

The largest problem to its more widespread implementation is that membranes can be irreversibly fouled, especially by a sudden high influx of suspended materials or organics, which occurs following seasonal rainfall. For this reason, effective pre-treatment through the addition of a protective barrier is critical to protect membranes.

2.2.1 Background

According to Weber (1972), a membrane can be defined as a phase which prevents the propagation of either molecular or ionic species between the two phases that the membrane separates. Membranes allow for the selective transportation of certain compounds from one phase to another through a semipermeable barrier. Membranes enable separation through:

- Size exclusion through a permeable membrane
- Diffusion of molecules through the semi-permeable membrane under high pressure
- Adsorption to the membrane surface

MF, UF and nanofiltration (NF) use size exclusion, with the differences in their pore sizes distinguishing between the types of filtration. Particles larger than the nominal pore size are retained, and decrease membrane permeability.

The removal of salts in the treatment of saline or brackish water is done through reverse osmosis (RO), and in UF permeate will still contain salts and dissolved components. The UF pressure is used to overcome viscous forces of the fluid rather than osmotic forces as in the case of RO (Scott & Hughes, 1996).

UF is the preferred membrane treatment technology for surface water treatment for water potabilisation, as its relatively low required feed pressures renders it economically feasible. Pore sizes are small enough to retain pathogens, and it can be periodically backwashed to remove deposited particles. MF is characterised by larger particle sizes, which still allows for the passage of pathogens. NF will block easily when used as stand-alone process because of all the suspended material present in surface water, and cannot be as easily backwashed. The higher required feed pressure also incurs greater operational costs (Rautenbach & Albrecht, 1989).

2.2.2 Types and operation of membrane filters

Membranes can be distinguished based on characteristics discussed in this section:

- a) Configuration
- b) Materials
- c) Flow through membrane unit: cross-flow vs. dead-end
- d) Flow through capillaries: inside-out vs. outside-in
- e) Operation: constant flux vs. constant pressure

a) Configuration

Factors pertaining to the configuration of the membrane include pore distribution, membrane structure, morphology and selective barrier.

Pore distribution

Membranes can be made as isotropic or anisotropic. Isotropic membranes are symmetrical and have equivalently sized pores throughout. They are used for ion exchange, or macroporous MF (Drioli & Giorno, 2009). As illustrated in Figure 2-2, an anisotropic membrane consists of two distinct sections consisting of the active and support layers, making the membrane asymmetrical. This is the configuration of UF membranes. The active layer (0.1-1 micron) is responsible for filtration, with the support layer (50-250 micron) providing structural integrity (Chae, et al., 2008), (Gray, 2005).

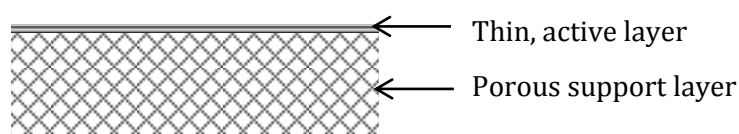


Figure 2-2: Active and support layers in anisotropic membrane

For the treatment of surface water, an anisotropic composited membrane is preferred as it is more resistant to fouling than an isotropic membrane (Chae, et al., 2008). The asymmetrical pore distribution promotes the formation of a cake layer on the membrane surface, which is advantageous to particle retention and membrane lifespan.

Membrane structure

Membranes can be made either as flat sheets, which are usually wound spirally for commercial units, or as hollow fibres. Spiral membranes can withstand large operational pressures and are preferred for RO. Hollow fibres with inner diameters less than 0.5 mm are classified as capillary

membrane fibres (Drioli & Giorno, 2009) while larger diameter fibres as referred to as tubular membranes. Capillary fibres are typically used for UF as they are strong enough to withstand UF operating pressures (Drioli & Giorno, 2009). Capillary membranes have lower pressure requirements, and are easier to backwash than spirally wound modules (Mierzwa, et al., 2008). Many small capillary tubes are packed in an UF module and a large surface area can be obtained per unit (Chae, et al., 2008). The surface area can be increased further by using multiple UF modules in arrangements, or racks.

Morphology

Fu et al. (2008) evaluated the effect of membrane morphology on fouling. According to them, it is the hydrophilicity, zeta potential and morphology of the membrane that most significantly affect fouling. By using the same material to eliminate the effects of hydrophilicity and zeta potential, the morphological contribution to fouling was investigated for surface water filtration. Differences in pore sizes and distributions significantly affected fouling behaviour. A membrane with lower porosity at the outer surface would experience more serious fouling than a membrane with greater outer layer porosity.

Selective barrier

The selective barrier of a membrane dictates the type of separation that takes place. Membranes are either made as porous or non-porous materials, and the membrane can also be modified to be charged or have a special chemical affinity (Drioli & Giorno, 2009).

If the pore size of the membrane closely overlaps the nominal size of suspended particles in water, pore blockage is more likely to occur. The membrane must either be chosen with this in mind, or properties of the incoming water must be adjusted through pre-treatment (Drioli & Giorno, 2009).

UF membranes for water treatment can have a range of pore sizes, depending on the final use of the treated water. Table 2-3 summarizes obtained information from manufacturers and literature.

Table 2-3: Nominal pore sizes for UF membranes

Pore size (µm)	Source
0.05	Memcor Vantage
0.04	Memcor CP II
0.03	DOW
0.02 (common size)	inge® dizzyer®, Zenon ZeeWeed
0.1	(Bessiere, et al., 2009)

Pore sizes are selected based on the size of unwanted compounds in the water. For instance, virus sizes range between 10 and 100 nm, and can only be confidently removed through UF and NF, and not MF (Scott & Hughes, 1996), (Fiksdal & Leiknes, 2006), (Zhang, et al., 2009), (Arnal, et al., 2004), (Chae, et al., 2008), (Crozes, et al., 1997). Pathogens are retained with absolute effectiveness if no damage is incurred to the membrane. Of the bacteria present in water sources, the prevalence particularly of *Escherichia coli*, *Camphylobater* and *Mycobacteria* species, which are responsible for gastroenteritis and other infections, are of concern (Gray, 2005).

b) Materials

Polymeric materials are predominantly used for manufacturing membranes, as they are highly versatile, widely available or relatively easy to manufacture, and the properties can be manipulated for specific applications (Drioli & Giorno, 2009). Ceramic membranes are used in certain systems (Konieczny, et al., 2006), and are highly effective but very expensive. Polymers are thus preferred, specifically with regards to UF.

Polyvinylidene fluoride (PVDF) (Gomez, et al., 2006), (Chae, et al., 2008), (Memcor CP II), as well as polyethersulfone (PES) (Katsoufidou, et al., 2005), (Katsoufidou, et al., 2008), (Konieczny, et al., 2009), (Fiksdal & Leiknes, 2006), (inge® dizzer®) are the most commonly used and most commercially available polymeric materials (Henley, et al., 2011). Disadvantages of polymeric membranes are that it is difficult to achieve regular pore sizing and spacing, and that the membranes are not as mechanically strong, thermally stable or chemically resistant (Drioli & Giorno, 2009). The differences in their properties are given in Table 2-4.

Table 2-4: Comparison of PVDF and PES properties

PVDF	PES
Hydrophobic material: fouls easier; greater extent of irreversible fouling due to organics adsorption (Katsoufidou, et al., 2005), (Drioli & Giorno, 2009)	Hydrophilic material: less amenable to fouling; higher flux recovery after hydraulic backwashing (Nakatsuka, et al., 1996), (Chae, et al., 2008)
More chemically robust (Gomez, et al., 2006)	Easily spun into fibres (Henley, et al., 2011)
	High strength due to characteristic SO ₂ (Henley, et al., 2011)
	Denser structure – better NOM separation (Kabsch-Korbutowicz, 2005)

Many new polymer modifications are constantly synthesized as research hones in on specific problems involved with materials. Properties such as the hydrophilicity, anti-fouling abilities, stability and the permeability can be improved through surface modification (Zhu, et al., 2014).

c) Flow through membrane unit: cross-flow vs. dead-end operation

With cross-flow operation, three streams enter or exit the membrane housing. The feed stream enters the vessel and is partially filtered through the membrane. Apart from the clean filtrate stream, which has passed through the membrane, the remainder of fed water is drawn off as a concentrate stream. The concentrate is often further processed to remove another filtrate fraction. This is a manner of concentrating liquid, and is also the manner in which RO plants operate. Figure 2-3 is redrawn from Kucera (2010):

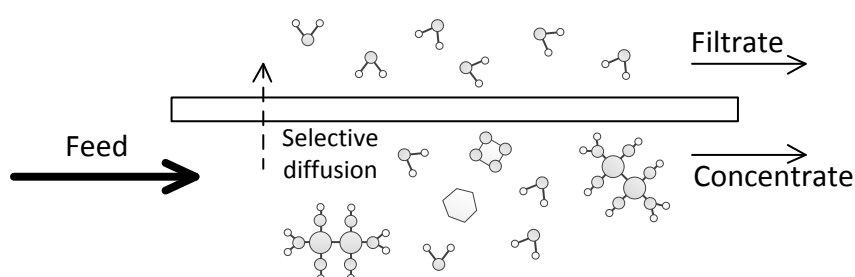


Figure 2-3: Cross-flow filtration operation

Cross-flow operation could induce concentration polarisation (CP) of ions in the suspension. CP is a polarising effect taking place on the membrane surface, which is detrimental to the passage of desired molecules through the membrane. If serious CP takes place, it could cause irreversible fouling and scaling (Drioli & Giorno, 2009). Tangential cross-flow, with incoming water flowing tangential to the membrane surface, decreases the large concentration gradient and increases the mass transfer coefficient.

Dead-end flow, which is typical for more dilute feeds, is considered in this project. A feed stream enters the membrane housing with the exit passage blocked. For water to pass through the housing, all water must pass through the membrane. All foulants larger than the nominal pore size are retained on the surface, as can be seen in Figure 2-4, and are periodically removed through backwashing. It is important to try ensuring homogeneous flow distribution to avoid localised fouling within membrane capillaries.

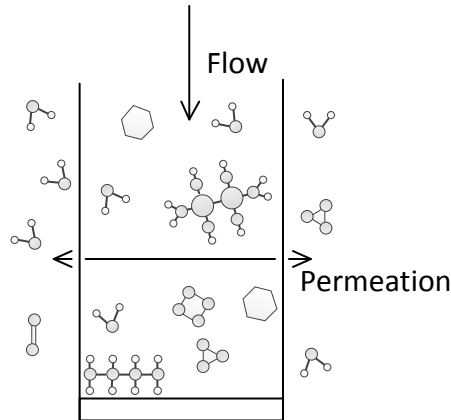


Figure 2-4: Dead-end membrane filtration operation

It has been found that dead-end cycles for relatively dilute feed water at a relatively low pressure, such as required for UF, is less energy intensive than a cross-flow system (Drioli & Giorno, 2009), especially because dead-end doesn't require an additional pump to transport concentrate as with cross-flow (Bessiere, et al., 2009). UF of surface water typically uses dead-end filtration, as water typically has relatively low suspended solids (SS) content.

d) Flow through capillaries: inside-out vs. outside-in

The direction of the flow through the capillaries plays an important role in membrane fouling. A membrane unit has resin cast around the top and bottom fibres to maintain capillaries in place. Water can thus enter either from the top or bottom of the housing, where the resin will force it to flow through the inside of the capillaries, or water will enter from the side of the vessel making contact with the outside of the capillaries. Pressure will force the water either outward or inward. This gives the two types of capillary flow, namely inside-out or outside-in, and is selected by the membrane manufacturer. The direction of flow is reversed during backwashing to remove foulants. The descriptions for the respective types of flow are only true for dead-end operation.

The flow configuration influences the type of fouling that will occur. In the case of the treatment of turbid water containing many suspended and dissolved compounds, the outside-in configuration is more desirable. The foulant layer will build up on the outside of the tubes, creating a cake layer. Outside-in flow gives a greater surface area for filtration (Serra, et al., 1999). On the other hand, inside-out filtration spreads the load of filtration through many pores. There is just the concern that pores can become blocked with a sudden influx of SS.

e) **Operation: constant flux vs. constant feed pressure**

Operation is done by maintaining either a constant feed flow rate or pressure. When operating at constant flux, an increase of the transmembrane pressure (TMP) will be required over time to maintain flow through the increasingly impermeable membrane. Alternatively, when operated at a constant feed pressure, a decline in membrane flux occurs with time as foulants deposit. Backwashing restores the permeability of the membrane once the performance has decreased significantly. For both operations, a lower flux will show a less rapid performance decline measured by aforementioned phenomena (Drioli & Giorno, 2009).

Constant pressure operation is typically used for small and lab scale work (Chen, et al., 2007), (Cho, et al., 2006), while constant flux is preferred for pilot and commercial filtration plants (Mosqueda-Jimenez, et al., 2008), (Guigui, et al., 2002), (Kimura, et al., 2004), (Guo, et al., 2009). Dead-end operated systems are usually operated at constant flux, either for a predetermined amount of time, or until a maximum TMP is reached and hydraulic backwashing is induced.

2.2.3 Driving force and flux

Different ways in which flow through the membrane are expressed, as well as typical operational and backwashing flow rates are discussed in this section.

- a) Transmembrane pressure
- b) Operational and backwashing flux
- c) Normalisation

a) **Transmembrane pressure**

TMP is a value expressing the driving force over a membrane enabling flow. It takes into account the feed pressure as well as pressure at the outlet of the system, which will be affected by losses occurring along the outlet line. In the case of crossflow filtration, the pressure of the permeate stream drawn off will also affect the driving force.

It is calculated as shown in Equation 2.1 (Crozes, et al., 1997), (Park et al., 2009):

$$TMP = \frac{P_{inlet} + P_{outlet}}{2} - P_{permeate} \quad [2.1]$$

In the case of dead-end filtration there is no side stream drawn off in the form of concentrate, and Equation 2.1 is simplified to the difference between the feed inlet and permeate pressures.

b) Operational and backwashing flux

Flow through membranes is expressed as flux, which has units of volumetric flow rate per surface area. Membrane flux is typically expressed as LMH ((litres/hour)/m²). Equation 2.2 shows flux is pressure driven and inversely proportional to viscosity and membrane resistance, R_T (Ma, et al., 2013):

$$J = \frac{\Delta P - \Delta \Pi}{\mu(R_T)} \quad [2.2]$$

The pressure term in Equation 2.2 refers to the difference between the TMP (ΔP) and the osmotic pressure of the water ($\Delta \Pi$). For UF calculations, the osmotic pressure is omitted. For RO, the osmotic pressure will increase as the brine stream becomes more concentrated, which will cause a decline in flux (Drioli & Giorno, 2009).

The intrinsic resistance of the membrane, R_M , and resistance caused by fouling, R_F , is summed and expressed as a total resistance, R_T in Equation 2.3 (Drioli & Giorno, 2009). The fouling resistance is made up both of reversible and irreversible fouling, R_{rev} and R_{irrev} , which are respectively removed through hydraulic and chemical backwashing (Kimura, et al., 2004).

$$R_T = R_M + R_F = R_M + R_{rev} + R_{irrev} \quad [2.3]$$

Typical operating fluxes and membrane loadings

The filtration flux of UF membranes varies greatly. Manufacturer guidelines would give a range of suggested fluxes for water of a certain nature and/or composition. Flux is selected based on the composition of the specific water source treated.

At lower fluxes fouling occurs more slowly; thus there is a trade-off between the operating flux of the system and the backwashing frequency (Katsoufidou, et al., 2005).

Table 2-5 summarises typical operating fluxes used by researchers in test work, while typical filtration durations are summarised in Table 2-6. Water turbidity for each flux included is given under Application. Unless otherwise stated, researchers and manufacturers specify parameters for surface water treatment.

Table 2-5 Typical UF operational fluxes for surface water filtration

Flux (LMH)	Pore size	Research group/manufacturer	Application
8-20	750 kDa	(Kimura, et al., 2004)	8.6 NTU
25-100	100, 30, 10 kDa	(Chang, et al., 2015)	5 mg/L HA
30	0.02 µm	Southern Cape water treatment plant	5-20 NTU
35-50	1, 3, 10, 30 kDa	(Mosqueda-Jimenez, et al., 2008)	3.2 mg/L HA
38	0.04 µm	(De Souza & Basu, 2013)	20 NTU
40-120	0.03 µm	(DOW, 2012)	<50 NTU
50-60	0.03 µm	(DOW, 2012)	5-60 NTU
55	200 kDa	(Ma, et al., 2013)	Low temperature surface water
60-90	0.02 µm	inge®	10-50 NTU
60-100	0.05 µm	(Guo, et al., 2009)	6-20 NTU
75	0.03 µm	(DOW, 2012)	2-5 NTU
75	0.04 µm	(Dialynas & Diamadapoulos, 2008)	2.8 NTU
75-110	50, 100 kDa	(Crozes, et al., 1997)	1.8-3.6 NTU
80	0.01 µm	(Bessiere, et al., 2009)	4-50 mg/L SS

Surface water membrane filtration isn't typically done at a rate greater than 100 LMH, with a flux of around 50 LMH appearing to be a fair average estimate. For the purpose of research, radical filtration conditions are sometimes used, such as a flux of 180 LMH (Chang, et al., 2015) in order to develop severe fouling with the aim of investigating backwashing conditions. For conditions simulating operation of an actual surface water treatment plant, these parameters are not realistic. Fluxes between 30-75 LMH are a more fair approximation.

Table 2-6: Typical UF surface water filtration durations between hydraulic backwashes

Duration (minutes)	Pore size	Research group/manufacturer	Application
15	0.04 µm	(De Souza & Basu, 2013)	20 NTU
20-25	0.03 µm	(DOW, 2012)	5-60 NTU
20-30	0.01 µm	(Zhang, et al., 2009)	Surface water (unspec.)
20-40	0.05 µm	(Guo, et al., 2009)	6-20 NTU
29-54	100, 30, 10 kDa	(Chang, et al., 2015)	5 mg/L HA
30-90	0.02 µm	inge®	<50 NTU
30	750 kDa	(Kimura, et al., 2004)	8.6 NTU
30	30, 150 kDa	(Nakatsuka, et al., 1996)	5-67 NTU
40	0.03 µm	(DOW, 2012)	2-5 NTU
60	10, 100 kDa	(Katsoufidou, et al., 2008)	10 ppm HA
60	200 kDa	(Ma, et al., 2013)	Low temperature surface water
60	1, 3, 10, 30 kDa	(Chen, et al., 2007)	5.4-37.6 NTU

Filtration duration typically does not exceed 60 minutes before backwashing is initiated.

Typical backwashing fluxes

Backwashing durations are short (see Table 2-8) and the durations of both sequences play a significant role in maximising recovery of a plant. Table 2-7 and Table 2-8 summarize typical flow rates and durations of hydraulic backwashing.

Table 2-7: Typical UF backwashing fluxes for surface water filtration

Flux (LMH)	Research group/manufacturer	Application
19	(De Souza & Basu, 2013)	20 NTU
100	DOW	2-5 NTU
230-250	inge®	<50 NTU
250	(Ma, et al., 2013)	Low temperature
250 (max)	Zenon ZeeWeed	General module information

It is recommended by Nagatsuka et al. (1996) to use a backwashing rate of at least twice the operational flux in order to ensure sufficient dislodgement of foulants. Manufacturers often have recommendations for specific applications.

Table 2-8: Typical UF backwashing durations for surface water filtration

Duration (seconds)	Research group/manufacturer	Application
10	(De Souza & Basu, 2013)	20 NTU
10-30	(Guo, et al., 2009)	6-20 NTU
20-70	(Nagatsuka, et al., 1996)	5-67 NTU
30	(Ma, et al., 2013)	Low temperature
30-60	(Zhang, et al., 2009)	Surface water (unspec.)
40-60	DOW	5-60 NTU
50-70	inge®	<50 NTU
60	(Chen, et al., 2007)	5.4-37.6 NTU
60-120	(Chang, et al., 2015)	5 mg/L HA

Backwashing duration is kept short in order to maximise recovery. Parameters from inge® and DOW for filtration and backwashing flux and duration aim at maintaining a recovery greater than 90%.

c) Normalisation

Temperature dependence of flux

Temperature of water critically affects its viscosity. For an increase in temperature, viscosity decreases and the activity of molecules increases. Water with a lower viscosity can easier pass through the pores of a membrane, and will thus have a slightly higher flux than at a lower

temperature. When measuring the flow rate of water, the effect of viscosity should be taken into account by including a correction factor to normalise flux to a standard temperature. This enables comparison for different experiments. The method to calculate temperature corrected flux is expressed in Equation 2.4 (Crozes, et al., 1997), (Shengji, et al., 2008):

$$Q_S = Q_T e^{-0.0239(T-S)} \quad [2.4]$$

For a particular flux at an elevated temperature, the normalised flux at the lower standard temperature will be lower in actuality, which in turn affects the amount of foulants deposited in a system.

Temperature dependence of pressure drop profile

No information was found in literature expressly normalising the pressure drop over UF membranes for constant flux operation. As the temperature during laboratory experiments and on-site test work differed significantly, the pressure drop data was not entirely comparable and had to be normalised to a common temperature.

Two different approximations were considered to try factor in the role of temperature in the fouling profile.

1. DOW (2012) proposes the following correlation in Equation 2.5 between flux, a temperature correction factor and the pressure over a reverse osmosis or nanofiltration unit.

$$Q_S = Q_T \cdot \frac{TCF_S}{TCF_T} \cdot \frac{\left(P_{feed} - \frac{\Delta P}{2} - P_{permeate}\right)_S}{\left(P_{feed} - \frac{\Delta P}{2} - P_{permeate}\right)_T} \quad [2.5]$$

The volumetric flow rate (Q), temperature correction factor (TCF) and pressure term measured at the experimental temperature (T), are substituted in Equation 2.5. The selected standard temperature (S) is used to calculate the standard volumetric flow rate and standard TCF.

The two temperature correction factors are given in Equations 2.6 and 2.7, and the flow rate at standard conditions is expressed in Equation 2.4.

$$TCF = e^{\left[3020\left(\frac{1}{298} - \frac{1}{273+T}\right)\right]}; T \leq 25^\circ\text{C} \quad [2.6]$$

$$TCF = e^{\left[2640\left(\frac{1}{298} - \frac{1}{273+T}\right)\right]}; T \geq 25^\circ\text{C} \quad [2.7]$$

The equation can then be rewritten to make the standard pressure term the variable.

This is a comprehensive and certain correction factor for RO and NF. NF, unlike RO, is at least semipermeable, similar to UF, and its effectiveness for UF temperature correction was tested.

2. The viscosity of the water was corrected to a standard temperature in order to enable comparison of data. If the assumption is made that for a constant flux, Equation 2.2 can be written in terms of both standard conditions and of operational temperature, the two equations can be combined as in Equation 2.8:

$$J = \frac{\Delta P_S}{\mu_S(R_T)_S} = \frac{\Delta P_T}{\mu_T(R_T)_T} \quad [2.8]$$

This is not entirely true, as the flux at standard conditions would be different to the operational flux, leading to differences in the volume of water passing through the membrane and thus the amount of foulants deposited (R_T). However, if this simplification is made, the equation can be simplified to Equation 2.9.

$$\Delta P_S = \frac{\Delta P_T \cdot \mu_S}{\mu_T} \quad [2.9]$$

2.2.4 Recovery for dead-end filtration

The recovery of a plant is expressed as the percentage water entering the plant that exits the plant as product. A fraction of filtered water is discarded as backwash.

In order to calculate percentage recovery, the volume of water filtered, W_F , is calculated, as well as the total volume of backwashing water for hydraulic backwashing and CEB rinsing, W_B . Calculations are based on the amount of filtration cycles completed between CEBs, which commence approximately once daily. Longer operational periods or shorter backwashing periods could cause an increase in membrane fouling, which is detrimental to operation in the long term terms of power requirement and chemical cleaning. The percentage recovery is calculated as shown in Equation 2.10.

$$Recovery = \frac{W_F - W_B}{W_F} \cdot 100 \quad [2.10]$$

Recoveries of up to 93% are attainable (Ma, et al., 2013) although not all plants are able to operate at such high recoveries. Zhang et al. (2009) reported recoveries between 79-91%, and Nakatsuka et al. (1996) reports higher recoveries of between 85-95%. Inge® recommends recoveries exceeding 90% for surface water treatment.

2.2.5 Membrane fouling

Fouling is a gradual decline in filter performance due to the deposition of foulants onto a membrane surface or within its pores. It manifests itself as a decline in permeability of the membrane, which leads to either a higher power requirement to maintain a constant flux, or a decline in flux when operated at constant pressure (Nakatsuka, et al., 1996), (Crozes, et al., 1997), (Zularisam, et al., 2006). It is the largest hindrance to the more widespread implementation of membrane systems on industrial scale (Wang, et al., 2008).

The manner in which fouling occurs as well as properties that influence it, are discussed in this section.

- a) Mechanisms
- b) Reversibility
- c) Factors influencing extent and type of fouling
- d) Normalisation: temperature dependence on pressure increase

The nature of water being treated, the kind of membrane and operating conditions plays a role in the type and extent of fouling.

a) Mechanisms

The mechanisms by which fouling typically occurs are illustrated in Figure 2-5:

- i. Pore constriction due to the adsorption of filtered species within the pores,
- ii. Pore blocking at the membrane surface, and
- iii. Cake formation (Katsoufidou, et al., 2005), (Katsoufidou, et al., 2008).
- iv. Combination of fouling mechanisms

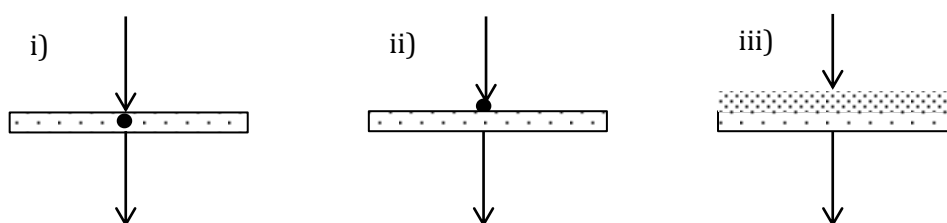


Figure 2-5: a) Adsorption in membrane pore, b) pore blocking and c) cake formation

i) Pore constriction

Pore constriction can either be a physical process, with the foulant being retained if it is caught in a tortuous channel within the membrane, or due to electrostatic forces, if the particle has an opposite charge to the membrane.

ii) Pore blocking

Pore blocking is a predecessor to cake formation, where particles are retained on the surface of the membrane. However, it does not create a permeable passage and can be removed by hydraulic backwashing.

iii) Cake formation

Although it is detrimental to the long-term functioning of the membrane, to a certain extent the reversible cake layer assists in filtration by aiding particle retention and acting as depth filter (Hillis, et al., 1998). It creates additional resistance to the passage of suspended particles in the water, creating a porous layer and causing a less rapid decline in flux (Zularisam, et al., 2006).

iv) Combination of mechanisms

Initially pore constriction or blockage due to adsorption is the predominant fouling mechanism (Zhang, et al., 2014), while cake layer build-up governs the fouling of the membrane over a long period (Katsoufidou, et al., 2005). It is common for more than one type of fouling to occur.

The pore restriction model and cake filtration model are typically used in modelling to determine the fouling behaviour of a type of water on a membrane, used in conjunction with previously obtained experimental data to determine which conditions promote the different types of fouling (Wang & Wang, 2006).

b) Reversibility

Fouling can either be reversible or irreversible by nature. The manner in which foulants are removed from the membrane surface determines the type of fouling (Kimura, et al., 2004). Hydraulic backwashing would remove reversible fouling while chemical cleaning is required to mitigate irreversible fouling. Permanent damage can be caused to the membrane when it gets chemically cleaned too often, which is why the frequency thereof should be minimised (Zularisam, et al., 2006).

c) Factors influencing extent and type of fouling

Both the properties of the membrane and properties of the water will influence the extent of fouling (Carroll, et al., 2000), (Katsoufidou, et al., 2008).

Components in water

– Hydrophobicity

The different fractions of HA have different fouling tendencies, depending on their size and structure. Properties like hydrophilicity and aromaticity affect their adhesion to the membrane, although the influences of these properties are not well elucidated (Katsoufidou, et al., 2005). Type and dosage of coagulant will determine which particles coagulate, and which remaining components are readily available for membrane fouling.

Matilainen et al. (2010) discussed the matter that hydrophobic NOM compounds can be removed to a greater extent than hydrophilic species, leaving the latter behind and thus readily available to foul membranes. Their findings are supported by the work done by Fan et al. (2001). Coagulation selectively agglomerates the hydrophobic NOM in the water, and the remaining hydrophilic fraction adsorbs to the membrane. The order of fouling potential is low aromatic hydrophilic neutral > high aromatic hydrophobic acids > transphilic acids > hydrophilic charged (Fan, et al., 2001). The decline in flux induced by the hydrophilic neutral fraction is due to both adsorption and colloidal deposition (Fan, et al., 2001).

Zularisam et al. (2006) again postulate that the hydrophobic fraction is responsible for rapid flux decline, as Chen et al. (2007) also state. The particles responsible for fouling are dependent on whether pre-treatment is carried out. Changing the solution chemistry of water by adding coagulant or altering the pH, will affect the charge of the HA functional groups and reduce the electrostatic repulsion that exists between them (Zularisam, et al., 2006).

– Particle size

Division exists around whether large or small particles play a more significant role in fouling. Carroll et al. (2000) report that small, neutral hydrophilic NOM components are largely responsible for irreversible fouling. Because of the high fouling potential of neutral hydrophilic particles, it is uncertain what role particle size plays. It could be that neutral hydrophilic particles only exist as small particles in water. Chen et al. (2007) argue that the smallest molecular weight NOM particles cannot be effectively removed through coagulation, and thus cause subsequent flux decline.

Fan et al. (2001) report that high molecular weight particles are responsible for major flux decline, and it is uncertain what role their charge played. Particle size and charge could be closely tied, although it appears that charge plays a bigger role than size.

– *Presence of calcium*

The presence of calcium enhances irreversible fouling on the membrane by promoting the formation of a foulant gel layer (Katsoufidou, et al., 2005). Furthermore, it reduces the solubility of HA and promotes their agglomeration by cancelling the electrostatic repulsion forces (Katsoufidou, et al., 2005), (Zularisam, et al., 2006).

Operating conditions and properties

– *Membrane material*

A hydrophilic membrane material is more averse to fouling as the cake detaches easier from the membrane surface (Crozes, et al., 1997), (Degrémont, 2007).

– *TMP*

TMP has a significant effect on the degree of membrane fouling. For prolonged filtration at TMP above 1 bar, Crozes et al. (1997) found that the degree of irreversibility of the fouling became more pronounced. Hydraulic backwashing did not recover the permeability of the membrane for high pressure operation. They postulate that the irreversibility is not due to the compaction of the fouling cake layer built up on the membrane, but rather due to NOM adsorption in the pores and on the membrane surface. Their comparisons with data from pilot plant studies showed increased prevalence of irreversible fouling of membranes at greater operational TMPs, with TMP above the threshold of 0.85-1 bar.

The operating flux will influence the rate of fouling, as a lower flux will show a less dramatic decline in membrane performance. Even if a low and high flux membrane are both operated for a required duration to attain the same R_F , the effect on performance of the membrane will be less pronounced for a lower flux membrane (Drioli & Giorno, 2009), (Mosqueda-Jimenez & Huck, 2006), (Katsoufidou, et al., 2005).

– *pH and temperature*

The pH of the feed water plays a vital role in the fouling behaviour of NOM on the membrane surface (Dong, et al., 2006). It affects the properties of HA as well as the extent of coagulation, and is discussed in further detail in 2.4.4.

Operation of the membrane system at low temperatures ranging between 6.5 and 11°C has been found to enhance irreversible fouling (Ma, et al., 2013).

– *Coagulation*

The conditions under which flocculation and coagulation takes place, as well as the coagulant dosage, have a significant effect on the degree of irreversibility of the fouling occurring on membrane systems (Kimura, et al., 2008). Kimura et al. (2008) also found that an increase in the coagulant dosage is responsible for promoting irreversible fouling on the membrane surface.

The use of in-line coagulation in a UF filtration process improves the reversibility of the foulant layer built up on the membrane surface, ensuring a greater removal of the cake layer during hydraulic backwashing and thus a greater flux recovery (Konieczny, et al., 2009).

Different types of coagulant can also significantly affect the fouling occurring on the membrane, with a significant difference to be found between a ferric and aluminium based coagulant (Konieczny, et al., 2009).

– *Backwashing frequency*

For a longer operational time, the reversible cake layer foulant that accumulates on the surface of the membrane could become compacted and its resistance to flow increased, which will be noted as an increase in TMP (Guigui, et al., 2002). The filtration cake will not necessarily completely develop into irreversible fouling when compacted (Crozes, et al., 1997), and while most of the resistance is reversible, Smith et al. (2006) found that cake layer compaction leads to irreversible fouling. Optimising the backwashing interval is crucial to maintaining the TMP increase per cycle to a minimum.

2.2.6 Backwash considerations

Optimal removal of foulants during hydraulic backwashing is critical in restoring the permeability of the membrane, and in reducing the dependency on chemicals for cleaning. The following factors pertaining to hydraulic backwashing are discussed in this section:

- a) Initiation and duration
- b) Improvement on backwashing effectiveness
- c) Chemically enhanced backwashing (CEB) and cleaning in place (CIP)

Backwashing of a UF membrane is conducted through hydraulic washing on a regular basis, and using chemical cleaning on a less regular basis. A hydraulic wash would commence after a filtration cycle by reversing the direction of flow to pump clean water in the opposite direction to filtration. This dislodges particles mechanically and enables them to be washed away. Certain components remain stuck to the membrane following a hydraulic clean, and chemical washing

is then used. The chemicals cause a reaction to take place which breaks the bond between the particle and the membrane (Chen, et al., 2003).

a) Initiation and duration

Backwashing of a membrane system usually occurs either when a significant head loss occurs over the system or when the permeate flux decreases significantly (Smith, et al., 2006). Backwashing is usually done regularly in order to improve the membrane filtration efficiency (Wang, et al., 2008). The interval selected is strongly dependent on the manufacturer, operating conditions and the nature of the water being treated. Backwashing durations and intensities are summarised in Tables 2.7 and 2.8.

After hydraulic backwashing, the initial TMP or permeate flux might not be the same as in previous cycles due to irreversible fouling. If initial TMP or permeate flux is deemed unfavourable, the system is subjected to chemically enhanced backwashing (CEB) and eventually cleaning-in-place (CIP), which is discussed later in this chapter.

Backwashing water is usually discarded due to high concentrations of pollutants, NOM, DBP and microorganisms (Zhang, et al., 2009).

b) Improvement on backwashing effectiveness

The addition of air scouring during backwashing can have a significant effect on the effectiveness of hydraulic backwashing. Pressurised air agitates capillaries and shakes foulants loose. It can also reduce the volume of water required to subsequently wash out foulants (Serra, et al., 1999).

Chen et al. (2003) statistically investigated backwashing factors. It appeared that the production interval between hydraulic backwashing cycles, the duration of backwashing as well as the pressure during forward flush are the most significant contributing factors to the effectiveness of the wash (Chen, et al., 2003).

The use of demineralised water for membrane backwashing has been suggested in a series of studies to improve the effectiveness of the filtration system by reducing the occurrence of irreversible fouling at low temperatures (Ma, et al., 2013). Treating UF filtrate further, for instance through dialysis or RO, produces more favourable backwashing water which improves the hydraulic cleaning efficiency (Chang, et al., 2015).

De Souza and Basu (2013) have found that the use of a relaxation period, when the permeate flow is halted briefly prior to backwashing, improves washing efficiency. This is more common

in membrane bioreactors, but can be beneficial to filtration operations in drinking water production.

c) Chemically enhanced backwashing (CEB) and cleaning in place (CIP)

Between hydraulic backwashing cycles, a gradual decline in membrane performance is typically observed, which can only be restored by chemical washing (Katsoufidou, et al., 2008). Strong acids, bases and disinfection agents are used. The chemicals selected for CEB target specific properties of adhered components in order to regain membrane permeability.

A high pH wash is usually conducted first in order to remove organic foulants, and is then followed by an acidic wash to remove inorganic foulants. Sodium hydroxide is usually used to remove organics, followed by an acidic wash typically done with hydrochloric or citric acid. The latter is effective in removing attached iron from the membrane surface, and is recommended for use when ferric chloride coagulant is used. DOW (2012) suggest 2% citric acid concentration. The membrane manufacturer would give the minimum and maximum pH values tolerable by the membrane material, and also note if the membrane is intolerant to high concentrations of chemicals. It is best practice to operate well within these parameters to prevent damage to the membrane.

DOW suggests performing on-line CEB every 1-7 day, and a more intensive off-line CIP every 1-12 months. Inge® proposes CEB from twice a day to once a week, depending on the nature of the surface water treated, and CIP conducted when necessary.

Chemical cleaning is of course crucial to effective membrane operations, but the use thereof has to be minimised if possible (Kimura, et al., 2004). The use of chemicals such as sodium hypochlorite can alter membrane properties and weaken the membrane, as reported by De Souza and Basu (2013). This further emphasises the need for the optimisation of hydraulic backwashing.

CIP is carried out on a much more seldom basis at about once per month. At times the same chemicals are used as for CEB, but with much longer recirculation and soaking times. More aggressive chemicals are also sometimes preferred to aid in flux restoration.

2.3 Media filtration principles

Media filtration is a physical clarification step that removes particles from water through retention by the tortuous paths between media particles. As time passes, more material is retained within the bed, providing increased resistance to flow until the breakthrough point is reached and residual turbidity starts increasing. After a certain amount of time the media needs to be backwashed to remove the retained particulates and restore its retention capacity (Henley, et al., 2011).

2.3.1 Pre-treatment to UF

Media filters are used in some studies as pre-treatment to UF (Mosqueda-Jimenez, et al., 2008), but in these cases the media filters are not operated in the same way as the UF. Filtrate from deep bed media filters are retained in a buffer tank, with UF feed drawn from the tank as required. In a study done by Mosqueda-Jimenez et al. (2008), and in another study referenced in their paper, water sent to the UF had already filtered through a graded media bed with backwashing done every 6-10 days and sent to a sump tank. No known references to shallow (referring to a bed depth less than 400 mm) media filtration before UF were found in literature.

2.3.2 Types and operation of media filters

As with membranes, media filters can be distinguished from one another based on properties like grain size and bed depth. The following factors determining filter type are discussed:

- a) Filtration rate
- b) Filter operation
- c) Media bed characteristics
- d) Capture mechanisms

Media filters used in conventional treatment plants are typically between 0.6 and 1.5 metres deep, and due to the large retention capacity of these deep beds can be operated for between 24 and 48 hours between backwashing cycles (Cox, 1969). It is not these types of filters that are of importance for this project, but their manners of operation and particle retention are of interest.

Filtration systems can either be described by the force driving filtration, by the depth of solids penetration, the type of media used, media size distribution, flow direction or the manner the water is pre-treated (Engineers, 1990). Sand, or silica, is the most commonly used media type (Cox, 1969) and the sizes of the particles mostly determine the type of filter and manner of filtration.

a) Filtration rate

The rate of filtration is influenced by media particle size. Slow filtration occurs when filtering water through beds with fine particles (diameter < 0.5 mm), resulting in down flow rates below 5 m/h (American Society of Civil Engineers, 2013). Because of how tortuous paths are, foulants are retained on the surface of the media bed. Compared to faster sand filters, they require a large surface area, are less flexible and are not as effective in the treatment of more turbid water, which is why rapid sand filters are preferred (Cox, 1969).

In rapid sand filters, particles are coarser than slow filters, resulting in higher down flow rates. The tortuous channels are of such a size that suspended particles are retained within the depth of the bed in a process called deep bed filtration (Gray, 2005). Pre-treatment is essential for the effective operation of coarser media beds. Figure 2-6 illustrates the difference in particle retention manner between slow filters on the left, and rapid (depth) filters on the right.

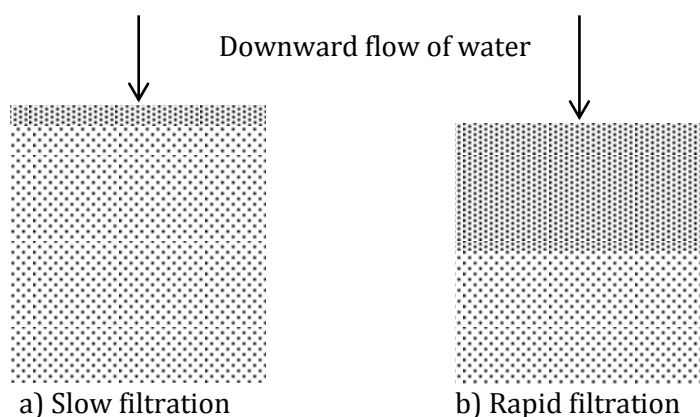


Figure 2-6: Capture mechanisms in a) slow (surface) and b) rapid (depth) filtration

While DOW (2012) would suggest downflow rates of between 10-20 m/h for rapid media bed filters, it seems to be a more widely accepted consensus that deep bed filters typically operate between 5 and 15 m/h (Crittenden, et al., 2012), (Gray, 2005), (Johir, et al., 2009). The quality of the filtrate could decrease above 10 m/h, and a flow rate of 7.5 m/h is typically recommended (Kawamura, 2000), (Jeong & Vigneswaran, 2013). Better particle retention occurs at lower down flow rates (Johir, et al., 2009).

With proper chemical pre-treatment, the aid of a flocculant and a deeper bed, a higher down flow rate would be obtainable (American Society of Civil Engineers, 2013).

b) Filter operation

As with membranes, media filters can be operated at constant pressure or downflow rate. During constant pressure filtration, flow rate will initially be high, with resistance of the bed

increasing as more foulants are retained. Downflow rate decreases with time and is recovered by backwashing. This method of filter operation is not preferred, as a large water storage volume is required to maintain constant head (Weber, 1972). When a constant downflow rate is maintained, increased deposit of foulant particles increases the resistance to flow and will require a greater pressure to filter water. Backwashing restores the initial pressure drop over the bed.

c) Media bed characteristics

- Grain size and equivalent diameter
- Voidage
- Support
- Graded beds

Grain size and equivalent diameter

Rapid sand filters have media particles between 0.5 and 1 mm in diameter (Gray, 2005), (Johir, et al., 2009), while some sources would cite even finer sizes of 0.35-0.5 mm (DOW, 2012). For a larger particle size, a deeper bed depth is required in order to clean the water to the same extent as finer particles (American Society of Civil Engineers, 2013). A finer particle size used will result in a greater pressure drop over the bed.

Equivalent diameters and sphericity of particles are crucial parameters required in media filter design, as particles are typically non-spherical. An equivalent diameter which reliably accounts for non-sphericity, is the equivalent diameter of a sphere that has the same surface to volume ratio as the non-spherical particles (Rhodes, 2008).

Voidage

The voidage or porosity of the bed, ε , is dependent on the nature of filter media used, as well as the processing treatment the media has been subjected to (i.e. backwashing and air scouring influence the voidage) (Stevenson, 1997), and can be determined as shown in Equation 2.11:

$$\varepsilon = 1 - \frac{M}{\rho_s V_B} \quad [2.11]$$

Where M is the mass of the media within the bed, V_B the total bed volume and ρ_s the density of the media used.

With the density and bulk density of sand of a particular size distribution known, the voidage can alternatively be determined with Equation 2.12 (Rhodes, 2008):

$$\rho_B = (1 - \varepsilon)\rho_S \quad [2.12]$$

A sand bed will typically have a voidage of 0.43-0.45 (American Society of Civil Engineers, 2013).

Support

Media particles are usually supported on a mesh, which serves as coarse screening and water distributor during backwashing, or most typically on a flat surface with outlets for downflow and nozzles to ensure homogeneous water distribution during backwashing (Degrémont, 2007).

Graded beds

Beds containing a range of particle sizes can either be left ungraded, or can be graded to have particles of different sizes in distinctive zones. Often a bed is graded fine to coarse, with finer particles at the inflow point of water. This assists filtration by creating faster flow rates at the bottom of the bed in order to pull water through. Beds graded in this manner, as well as uniform and ungraded beds, should settle back to their original configuration after the bed has been hydraulically backwashed. The following diagrams in Figure 2-7 are redrawn from Ives (1973).

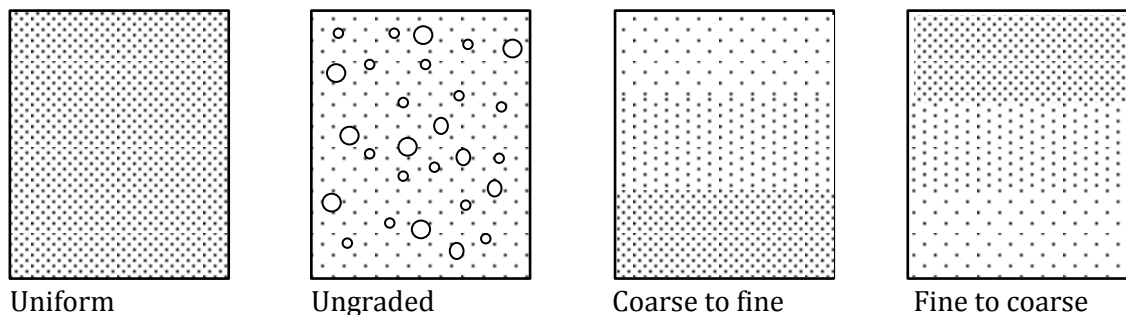


Figure 2-7: Media distribution within beds

Rapid sand filters with down flow rates of between 10-25 m/h usually use graded media beds, with a coarser media below a finer media, or alternatively a single grain size of between 1-1.4 mm effective size (American Society of Civil Engineers, 2013).

d) Capture mechanisms

As the water flows through the media bed, suspended particles can be retained in different manners. The description given below is illustrated in Figure 2-8 (redrawn) (Nazaroff & Alvarez-Cohen, 2001):

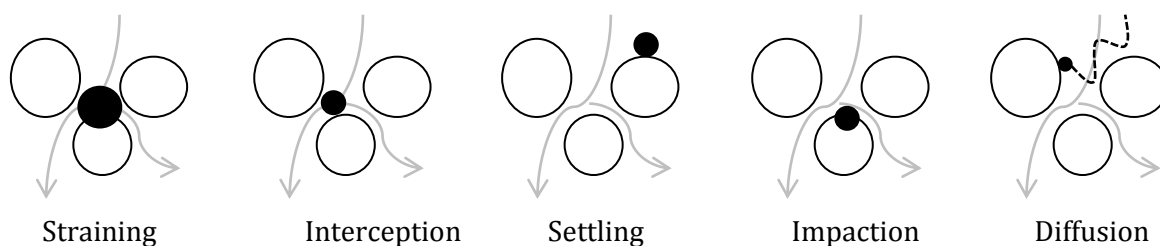


Figure 2-8: Capture mechanisms within media bed

Straining occurs when a suspended particle is larger than the opening between the media particles. Interception occurs due to adsorption surface forces when a particle follows the laminar stream line within a media bed and comes within close proximity to a media particle. Settling occurs under the influence of gravity. Impaction happens when particles in the water do not follow the path between media particles and directly collide with the media particles, where they remain deposited. Diffusion results from very small particles in the water attaching to media through Brownian motion.

2.3.3 Filtration directly following coagulation

Media filtration directly following coagulation, omitting flocculation and sedimentation, is known as orthokinetic flocculation. Orthokinetic flocculation involves the collision between coagulated particles due to shear through filtration through a media bed. Energy dissipates and promotes collisions between suspended particles (Stevenson, 1997).

The development of higher flow rate granular media filters has replaced the necessity of sedimentation prior to filtration, which decreases capital and operating costs (American Society of Civil Engineers, 2013). Instead of only filtering clear supernatant produced during sedimentation, as in conventional water treatment, the entire volume of water is filtered. Floc growth occurs as the water channels through the media filter (Degrémont, 2007). Micro flocculation instead of sweep flocculation is initiated and resulting flocs are voluminous enough to be retained through capture within the media bed.

Direct filtration is a preferred treatment method for water with slight colloidal turbidity and/or slight colour (Degrémont, 2007). The process will not necessary benefit from sedimentation, as the low turbidity will require a long settling time, and might not remove all suspended matter. The more colloids are present in the water, the more rapidly and effectively floc formation will occur (Stevenson, 1997). A reduced amount of coagulant can be used for orthokinetic flocculation (Degrémont, 2007), (Konieczny, et al., 2009), and the required flocculant dosage can be reduced by between 30 and 40% (Jeong & Vigneswaran, 2013). Relatively short filtration cycles are typical of in-line coagulation and media filtration. Breakthrough occurs relatively early while giving high quality water with a high removal efficiency of HA once maturation has

been attained (Rebhun, et al., 1984). Although shorter retention times are used with in-line coagulation, similar removal efficiencies have been reported to conventional flocculation (Leiknes, 2009).

2.3.4 Bed maturation

In order for a media filter to operate at its best possible performance, a period of bed maturation should be allowed for. It takes a while for particle attachment mechanisms to operate efficiently, and initially the water leaving a media filter has inferior quality. It is common to recycle this water back to the inlet and pass it through the bed again. A maturation period can range between 5-30 minutes before delivering high quality water.

Strategies used to minimise the maturation period include:

- Diverting the initial, more turbid permeate straight to drainage
- Adding a filter aid to the backwashing water to aid flocculation
- Resting the filter prior to filtration
- Filtering the water for a lower flow rate initially following backwashing (American Society of Civil Engineers, 2013).

Figure 2-9 illustrates effluent quality, and is redrawn from Amirtharajah and Wetstein (1980):

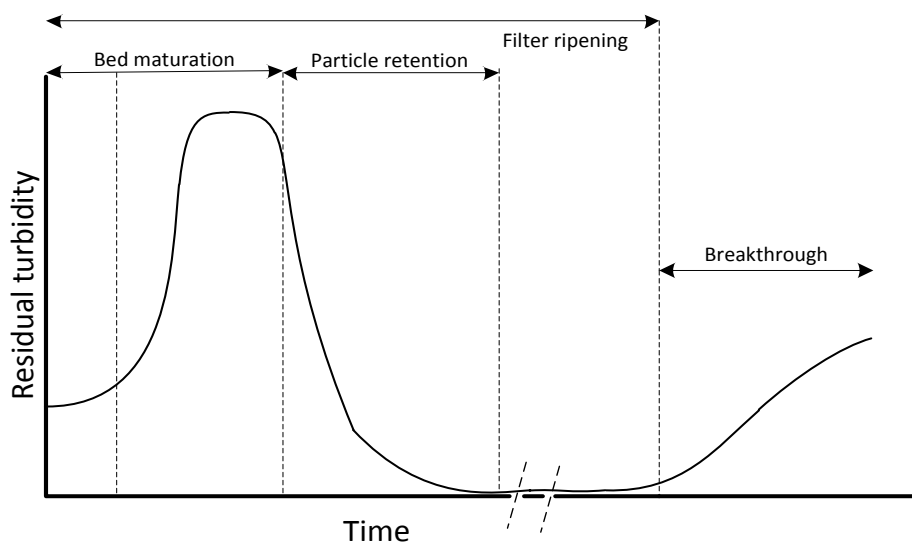


Figure 2-9: Residual turbidity profile over the course of a filtration cycle

Once the bed has matured, particle retention effectively occurs within the bed and water of a high quality is delivered. Residual turbidity remains low for a duration that depends on media

bed as well as raw water properties. After the maximum retention capacity of the bed is reached, breakthrough occurs. At the breakthrough point, turbidity increases to above a threshold turbidity limit specific to the process (Degrémont, 2007). Once a terminal residual turbidity has been reached, the bed is backwashed.

2.3.5 Pressure drop and head loss over media bed

Pressure drop occurs with time as more particles are retained in the bed and its retention capacity strives towards its maximum. Head losses under different conditions are investigated:

- a) Clean media bed
- b) During filtration
- c) During backwashing

a) Clean media bed

Darcy proposed an equation demonstrating the head loss of water as it flows through a granular filter bed. Energy is lost in the form of friction as the water passes through the grains, which translates into a head loss over the bed. Darcy describes head loss over a bed with height H in Equation 2.13:

$$\frac{\Delta P}{H} = R_{med} \mu U \quad [2.13]$$

Filtrater resistance, R_{med} , is a characteristic parameter for a clean media bed, and can be determined experimentally. It is indicative of the permeability of the filtration media.

The Kozeny formula in Equation 2.14 is a modification of Darcy's equation, including the effect of the porosity of the medium used:

$$\frac{\Delta P}{H} = \frac{k \mu (1-\varepsilon)^2}{\rho_F g \varepsilon^3} \left(\frac{a}{v} \right)^2 U \quad [2.14]$$

The value of k (Kozeny's constant) is approximately 5, and the $\frac{a}{v}$ grouping is the value of the specific surface area per unit of volume of filtering granules with a diameter of x . For spherical granules, this value is $6/x$.

Ergun has modified the Kozeny equation to account for kinetic loss of energy through the bed (Degrémont, 2007). Equation 2,15 models the pressure drop over a clean media bed (Rhodes, 2008):

$$\frac{\Delta P}{H} = 150 \frac{\mu U (1-\varepsilon)^2}{x^2 \varepsilon^3} + 1.75 \frac{\rho_F U^2 (1-\varepsilon)}{x \varepsilon^3} \quad [2.15]$$

The first term denotes the laminar component, and the second term denotes the turbulent component. U is the superficial velocity of water over the entire filtration area. The equation can be used for either flow regime. In the case of laminar flow, the laminar component will be dominant, and likewise for turbulent flow. If all the parameters of the bed and media grains are known, the head loss can be calculated. For laminar flow, the pressure drop is linearly proportional to the superficial velocity, whereas pressure is proportional to the square of linear velocity in turbulent flow (Rhodes, 2008).

Flow regime is determined by calculating the Reynolds number for a packed bed as shown in Equation 2.16 (Rhodes, 2008).

$$Re^* = \frac{xU\rho_F}{\mu(1-\varepsilon)} \quad [2.16]$$

The symbol x refers to the average diameter of particles within the bed (Rhodes, 2008). For a Reynolds number smaller than 10, flow through the bed is laminar, and for a Reynolds number larger than 2000, turbulent flow exists.

As silica particles are non-spherical, an equivalent mean surface-volume diameter is very important to determine. This is the correct parameter to use for a bed with particles that are not mono-sized (Rhodes, 2008). This x_{sv} parameter is determined using actual pressure drop data over a clean bed. For laminar flow, the pressure gradient will increase linearly with superficial fluid velocity if conditions such as temperature and properties such as voidage remain constant. This can be tested by plotting experimental pressure drop values against the superficial velocities. Equation 2.16 should also be used to determine that flow is laminar. The laminar component of Ergun's equation is expressed in Equation 2.17:

$$\frac{\Delta P}{H} = 150 \frac{\mu U (1-\varepsilon)^2}{x_{sv}^2 \varepsilon^3} \quad [2.17]$$

Using experimental data for the pressure drop at different flow rates, the value of x_{sv} can be determined through manipulation of Equation 2.17 to give Equation 2.18:

$$x_{sv} = \sqrt{\frac{150\mu U(1-\varepsilon)^2 H}{\Delta P \varepsilon^3}} \quad [2.18]$$

The value obtained for x_{sv} for varying flow rates should be similar. This value can then be substituted in Equations 2.14 and 2.15, and should closely approximate the actual pressure drop values.

The Ergun equation can be used with this equivalent diameter, negating the use of constants and factors which account for the non-sphericity. The Ergun equation is then written as:

$$\frac{\Delta P}{H} = 150 \frac{\mu U}{x_{sv}^2} \frac{(1-\varepsilon)^2}{\varepsilon^3} + 1.75 \frac{\rho_F U^2}{x_{sv}} \frac{(1-\varepsilon)}{\varepsilon^3} \quad [2.19]$$

b) During filtration

During filtration of surface water, suspended particles are retained within the bed, contributing to the efficiency of filtration and pressure drop over the bed. Different head loss patterns develop throughout the course of a cycle depending on the manner in which the filter is operated, and the nature of the filter media. Relevant to this project is deep bed filtration of suspended solids at different constant downflow rates. At higher flow rates greater head loss will occur, as more deposition of particles and more friction between the water and media particles result (Weber, 1972).

Many researchers have investigated the relationship between volume of filtrate that has passed through the bed, and head loss. When plotted against each other, a linear relation should be apparent. Formulas exist to determine theoretical filter capacity and determine the relationship between head loss and accumulated deposits (Rebhun, et al., 1984).

Breakthrough

Towards the end of a filtration cycle, the bed becomes saturated and foulants are no longer retained within the bed. It is indicative of the maximum operational time for a filter at the chosen conditions. Figure 2-10 illustrates head loss upon breakthrough, and is redrawn from Degremont (2007).

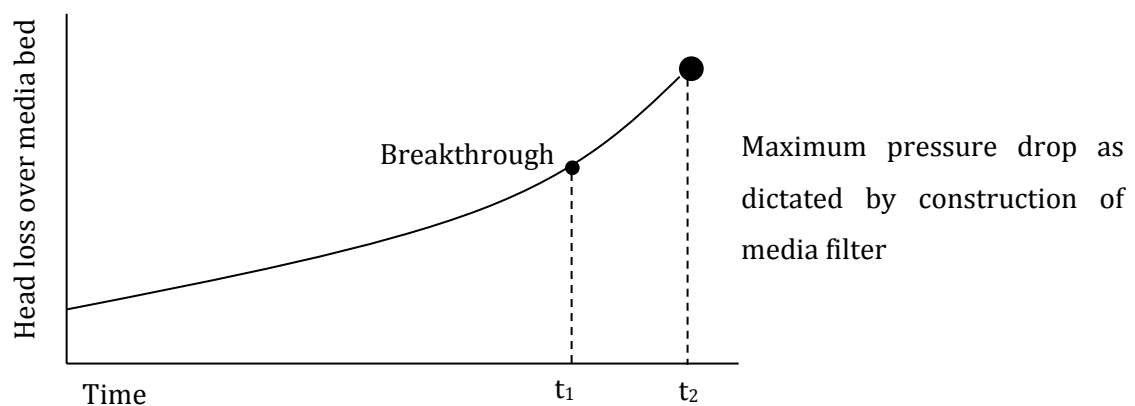


Figure 2-10: Head loss as a function of time

The breakthrough point occurs at t_1 , and is unique for a specific filter, water treated, flow rate and coagulant dosage. Head loss will increase until it reaches a maximum value at t_2 , specific to the filter and its operation.

During the maturation period as well as in the initial stages of filtration, the pressure drop will have a linear profile. Gradually more and more fouling will contribute to the pressure drop over the filter bed, making the profile increasingly more curvilinear. Eventually the entire profile will be curved and there will be no more sections of clean bed for the water to pass through. Once the entire depth of the bed has been penetrated by the filtration front, foulants will now pass through the bed and breakthrough occurs. For a deeper sand bed, it will take longer for breakthrough to occur (Degrémont, 2007).

Pressure drop is a function of the length of the filtration cycle, the depth and size of the media and the concentration of suspended particles. Triangular graphs are used to depict the correlation between these factors (Degrémont, 2007) and shows pressure drop with clean sand and during filtration of dirty water.

c) During backwashing

The assessment of backwash hydraulics is essential in order to determine the head loss during backwashing, at what backwash velocity the media starts to fluidise, and in order to determine how much the media bed will expand during backwashing (Van Duuren, 1997). The head loss through the bed during backwashing is determined by approximating the media filter bed as a fluidised sand bed and determining the head loss gradient as a function of the depth of the media bed with Equation 2.20 (Van Duuren, 1997):

$$\frac{h_L}{H} = \left(\frac{\rho_S - \rho_F}{\rho_F} \right) \cdot (1 - \varepsilon) \quad [2.20]$$

2.3.6 Filtration efficiency

The effectiveness of a filter is characterised by monitoring the head loss over the filter, and also the turbidity of the filtrate (Nazaroff & Alvarez-Cohen, 2001). It can be expressed in terms of the proportion of turbidity that has been removed, but typically the absolute product NTU is monitored. Filtration efficiency increases with time, up to breakthrough.

The filtrate turbidity is an important parameter in filtration performance monitoring, and the target range following treatment is 0.5-1 NTU (Nazaroff & Alvarez-Cohen, 2001). Filters used in the treatment of potable water, with a clarification step preceding it, are expected to remove between 80-90% of the incoming turbidity (Stevenson, 1997).

The recovery of the filter is calculated in the same way as for membrane filtration in Equation 2.10. It is defined as the fraction of raw water entering the filter that becomes product water (American Society of Civil Engineers, 2013). It is important to try maximise recovery without compromising filtrate quality.

2.3.7 Backwash considerations for media filtration

The manner in which backwashing is conducted and related topics are discussed in this section:

- a) Distribution of water during backwashing
- b) Rate and duration
- c) Bed fluidisation
- d) Improvement on backwashing effectiveness through air scouring
- e) Chemical cleaning of media particles

The backwash cycle is usually initiated either when a terminal head loss reaches a maximum, when breakthrough turbidity occurs or after a fixed operational duration (American Society of Civil Engineers, 2013). Clean water is forced upward through the media filter, typically at higher flow rates than filtration would occur. The backwash interval depends on various factors, including the size of the filter bed, characteristics of the media used and, most significantly, the nature of the water being treated.

a) Distribution of water during backwashing

During backwashing, water is pumped upward through the media bed. In order to prevent the channelling of a jet of water through the bed, which would prevent it from becoming uniformly cleaned, it is necessary to include distributors at the bottom of the media bed. Typically nozzles are installed to distribute the flow over a larger area of the media bed. A sieve support under the media bed assists with spreading out backwash water, but to a lesser degree than nozzles can.

b) Backwashing rate

The media bed is typically hydraulically backwashed at least twice the filtration rate. Table 2-9 summarises information gathered from literature on typical upflow rates.

Table 2-9: Backwashing upflow rates from literature

Upflow rate (m/h)	Grain size of media particles (mm)	Researcher
12-30		(Van Duuren, 1997)
15	0.6	(Jeong & Vigneswaran, 2013)
45	0.41	(Cox, 1969)
20-30		(Kawamura, 2000)
30-60	0.4-0.8	(Crittenden, et al., 2012)
40-50	0.35-0.5	(DOW, 2012)

The upflow velocity of the water needs to be of such a nature that it can adequately expand the bed, and wash out the particles loosened from agitation.

c) Bed fluidisation

- Minimum fluidisation velocity
- Fluidisation
- Bed expansion

Fluidisation

The rate at which backwashing takes place is typically at a higher volumetric flow rate than forward washing, at a rate sufficient to fluidise the bed. Fluidisation occurs when the force exerted on the particles by the upward flowing water is greater than the gravitational force exerted on the particle, causing it to become suspended and rise upward with a further increase in flow velocity, illustrated in Figure 2-11 (redrawn) (Ives, 1975).

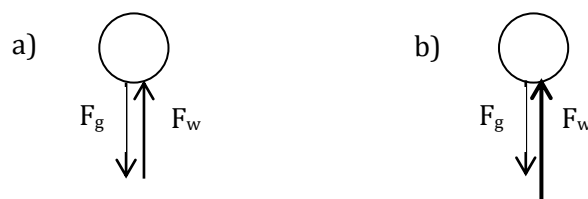


Figure 2-11: Media particle fluidisation: a) The force of backwashing water, F_w , acts on the media particle. b) $F_w > F_g$, and the particle moves upwards and becomes fluidised.

Before fluidisation occurs, there is a linear correlation between the pressure drop over the bed and the superficial fluid velocity over the bed, as illustrated in Figure 2-12 (redrawn) (Ives, 1973).

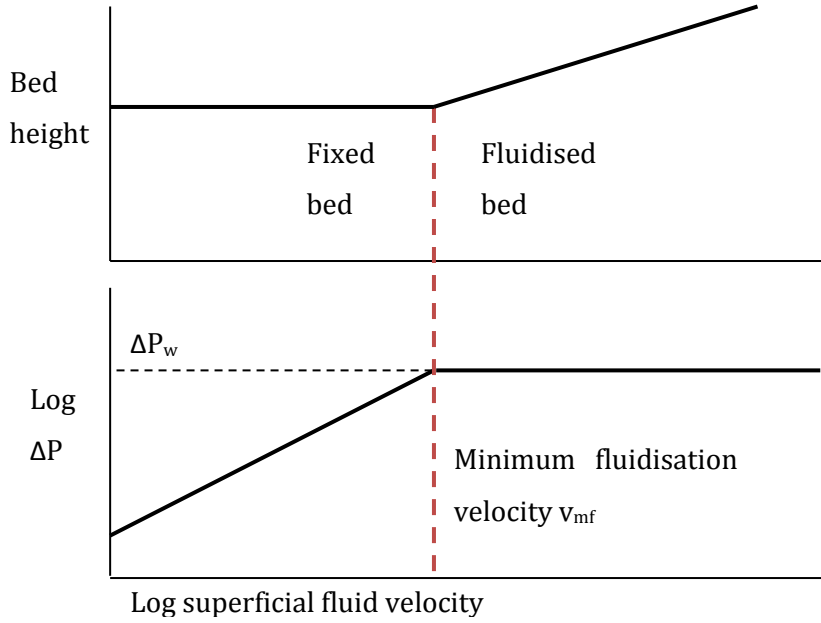


Figure 2-12: Effect of superficial velocity on bed height and pressure drop

Minimum fluidisation velocity

After fluidisation occurs the head loss gradient throughout the bed remains constant (Van Duuren, 1997). The head loss can be used to determine the minimum backwash velocity for fluidisation, which is expressed in terms of the Reynolds and Galileo numbers for a homogeneous and graded bed. For varying particle sizes, the minimum backwash velocity must be calculated for the largest particles to ensure that the entire bed is fluidised (Van Duuren, 1997), (Droste, 1997). Minimum backwash velocity is calculated using Equation 2.21:

$$v_{mf} = \frac{Re_{mf}\mu}{x_{sv}\rho_F} \quad [2.21]$$

With the minimum Reynolds number for fluidisation calculated in Equation 2.22:

$$Re_{mf} = \sqrt{33.7^2 + 0.0408 \cdot Ga} - 33.7 \quad [2.22]$$

And the Galileo number expressed as in Equation 2.23:

$$Ga = \frac{x_{sv}^3 \rho_F (\rho_s - \rho_F) g}{\mu^2} \quad [2.23]$$

As v_{mf} is a critical design parameter, Cleasby & Fan suggested incorporating an additional safety factor of 1.3 (1981).

Full fluidisation of the media bed is required to effectively backwash the filter. When backwashing above the point of fluidisation, the head loss over the bed remains constant (Stevenson, 1997), (Ives, 1975).

Bed expansion

The expansion of the bed can be controlled by controlling the upflow rate of water through the media bed. The rate at which water washes through the bed shouldn't be too high as to result in the washing out of media particles, and often low expansion percentages are sufficient to clean a media bed. Table 2-10 summarizes expansion percentages recommended by some researchers.

Table 2-10: Recommended media bed expansion percentages

Expansion (%)	Researchers
10	(Droste, 1997)
15-30	(American Society of Civil Engineers, 2013)
16-18	(Johnson & Cleasby, 1966)

At low expansions a large proportion of the maximum shear still exists in the bed (Slavik, et al., 2013), eliminating the need for excessive power usage to expand the bed to its maximum and making the process more economically viable.

Ives (1973) recommends using the porosity of the expanded bed as a guideline to find out at which point optimal hydrodynamic shear between media particles occurs. Using information of the bed, namely initial porosity (ϵ_0), initial bed height (H_0) and expanded bed height (H_E), the porosity at expansion (ϵ_E) can be calculated with Equation 2.24 (Ives, 1973):

$$H_0(1 - \epsilon_0) = H_E(1 - \epsilon_E) \quad [2.24]$$

Often bed expansion and optimal expansion for backwashing is given in terms of percentage bed expansion, but as the expansion of the bed and the values it can reach is constrained by particle size properties, the use of expanded bed porosity is a more universally sensible value.

The bed expansion will be greatly influenced by media size and bed porosity. Fractional expansion of the bed at the optimal backwashing flow rate can be determined by Equation 2.25 proposed by Kawamura (American Society of Civil Engineers, 2013):

$$Expansion = \frac{0.6 - \epsilon}{0.4} \quad [2.25]$$

d) Improvement on backwashing effectiveness through air scouring

In many conventional plants, air scouring is conducted prior to hydraulic backwashing. As air is bubbled through, media particles are agitated and the attached deposit is abraded (Van Duuren, 1997). Following air scouring, the bed is hydraulically washed to remove loosened particles. It also necessary to break up larger clumps of flocculant and foulant particles which have become too large to be washed out of the bed. The formation of these large foulant clumps is called mud balling and is detrimental to the functioning of the filter (Slavik, et al., 2013).

If it is not possible for air scouring to be used due to design or material constraints (air scouring could lead to abrasion and attrition of particles, particularly with anthracite coal), hydraulic washing can otherwise be optimised to improve cleaning. For instance, water can be pulsed, instead of maintaining a constant high flow rate. The intermittent relaxation periods preceding high flow rate water washed maximises shear in the bed and increases foulant removal (Slavik, et al., 2013).

e) Chemical cleaning of media particles

Periodically, and much less frequently than backwashing, the filter media has to be chemically cleaned to remove potential microbial material (Cox, 1969). Caustic soda can be used for this purpose to dissolve organic matter.

2.4 Coagulation and flocculation

Natural water sources contain myriad dissolved and colloidal particles (Weber, 1972). Particles with sizes up to 50 μm can settle under natural conditions depending on their density, but for smaller particles their removal through sedimentation is not feasible (Tebbutt, 1992). Chemical alterations promote the agglomeration of particles as flocs, which grow larger and can be separated from the fluid through solid-liquid separation (Weber, 1972). In this project, the treatment of NOM-rich surface water with low turbidity was investigated.

2.4.1 Distinction between coagulation and flocculation

Though often mentioned in the same sense, the processes of coagulation and flocculation are two separate processes working in conjunction with one another. There is a distinct difference between the mechanisms, although both can be brought about by the same reagent (Ives, 1975). Coagulation is responsible for the destabilisation of particles through the reduction of the zeta potential on the surface. Flocculation describes the agglomeration of the destabilised particles to form larger particles (Ives, 1975), (Van Duuren, 1997). Both the particle sizes and charges on the particles will influence the rate of settling and the settlability of the uncoagulated particles.

a) Coagulation mechanism

During coagulation, a chemical is dosed which either destabilises colloids which will not settle, float or filter naturally; or precipitates soluble NOM in the water (Stevenson, 1997). The destabilisation discussion is relevant to colloids, while NOM removal from water is discussed under Flocculation Mechanism.

Destabilisation

Colloids have sizes in the order of 10^{-4} m (Degrémont, 2007). Their small sizes and very large specific surface areas are conducive to the introduction of flaws to the crystalline network, giving them a negative charge and contributing to their stability in suspension (Van Duuren, 1997).

Colloids possess a zeta potential, pZ, which is a function of both the particle and the liquid medium (Degrémont, 2007). The zeta potential is the electric potential at the interface between the double electric layer around the particle and the bulk fluid (Ives, 1975). The addition of a coagulant compresses the electrochemical double layer, or can reduce the surface potential thereof (Gray, 2005). Surface charge is limited to a thin layer around particles, allowing them to come into closer contact with other colloids. The attractive body forces then become larger than

repulsive forces, which enables floc growth. The more colloids are present in the water, the more rapidly and effectively floc formation will occur (Stevenson, 1997).

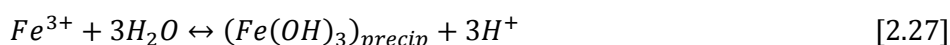
Dissolution and reaction

The counter ion used in the destabilisation of anionic suspended particles and HA should be cationic (Rodrigues, et al., 2008). In the case of this project, ferric chloride is selected as coagulant, which is discussed in 2.4.2. Upon addition of the ferric chloride coagulant, the following reactions take place (Degrémont, 2007):

- Dissolution of the coagulant takes place in the water.



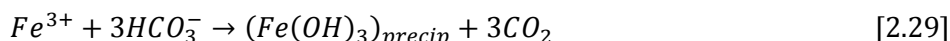
- The cations react with water molecules in a hydrolysis reaction, producing a hydroxide precipitate and a degree of acidity.



- The acidity-inducing hydrogen cation reacts with other species in suspension.



- The overall reaction can be formulated from Equations 2.26-2.28 into Equation 2.29:



The metal hydroxide formed during the dissolution reaction is responsible for the removal of the NOM (Cheng & Chi, 2002). The precipitates, or flocs, collide and grow into larger agglomerated particulates during flocculation (Stevenson, 1997).

The dosage of metal salts to water always exceeds the solubility of the metal in water (Weber, 1972), and thus the destabilisation of the colloids can be ascribed to the interaction with reaction intermediates as the metal becomes hydrolysed.

b) Flocculation mechanism

Following coagulation, the relatively slower flocculation stage commences and time is allowed for bonds to form between particles (Degrémont, 2007). Flocs are formed through various attachment methods. Micro or pin floc formation is the first stage of agglomeration, and agglomerate to form progressively larger flocs (Stevenson, 1997).

There are three mechanisms in which flocculation removes destabilised colloids and NOM from water (Tchobanoglous & Schroeder, 1985), (Matilainen, et al., 2010).

1. Adsorption

Charged soluble metal ions adsorb to the charged NOM functional groups

2. Complexation

Bonds are formed between NOM and metal hydroxides producing either an insoluble precipitate or resulting in adsorption

3. Precipitate enmeshment

NOM particles become enmeshed between metal hydroxide particles forming bonds

The type of reaction will be predominantly dependent on the pH and coagulant type, and more than one mechanism of NOM removal could occur (Jin, et al., 2003), (Cheng & Chi, 2002).

The resulting floc dimensions and properties are dependent on the type of coagulant as well as the water being treated (Wang, et al., 2011). Flocs can be characterized based on their morphological, physical and chemical properties. These properties could affect the effectiveness of subsequent treatments (Jin, et al., 2003), (Wang, et al., 2011), as well as affect the extent of membrane fouling (Wang, et al., 2008), (Cho, et al., 2006). Morphological properties involve the size distribution and fractal dimensions of flocs while physical properties evaluate the flocculating ability, viscosity, hydrophobicity and surface charge of the flocs. Floc structures are complex and difficult to predict or characterize (Jin, et al., 2003).

2.4.2 Types of coagulant used in NOM removal

In industry, inorganic ferric and aluminium coagulants are widely used, namely ferric chloride (FeCl_3), and aluminium sulphate, or alum, ($\text{Al}_2(\text{SO}_4)_3 \cdot 14\text{H}_2\text{O}$) (Konieczny, et al., 2006). Upon dosage of the coagulant, it produces the trivalent cations Fe^{3+} and Al^{3+} . A higher cation valency favours coagulation (Degrémont, 2007).

Although aluminium based coagulants have been shown in certain studies to remove turbidity more effectively than their ferric based counterparts (Konieczny, et al., 2009), there is controversy around its use. Residual aluminium in water had been linked to an increase in the prevalence of Alzheimer's disease (Konieczny, et al., 2006), (Matilainen, et al., 2010), (Droste, 1997). For this reason ferric based flocculants are preferred (Zhan, et al., 2010). Apart from the health advantage, ferric based coagulants have shown to better remove NOM than aluminium based coagulants, and are less sensitive to temperature changes (Matilainen, et al., 2010). Ferric flocs are also more resistant to stress forces (Guigui, et al., 2002).

The type of coagulant selected is dependent on water properties, suspended solids concentration and other water properties (Ives, 1975). The dosage thereof is determined through jar testing. The financial feasibility of a coagulant is also an important factor to consider.

2.4.3 Coagulant dosing and dispersion

a) Coagulant dosage

The optimal coagulant dosage for water with specific properties is determined through jar testing, discussed in 3.4. For flocculation of surface water, 3.5-10 mg/L of ferric chloride solution as FeCl_3 is recommended (Degrémont, 2007), which could increase to 10-30 mg/L (DOW, 2012) depending on the source.

It is often seen that coagulants remove a satisfactory degree of turbidity at relatively low dosages. Increased residual turbidity occurs when coagulant is dosed above this optimal range due to the restabilisation of colloids (Zhan, et al., 2010). Further increases in coagulant dosage lead to colloid removal through sweep flocculation. Figure 2-13 is redrawn from Weber (1972).

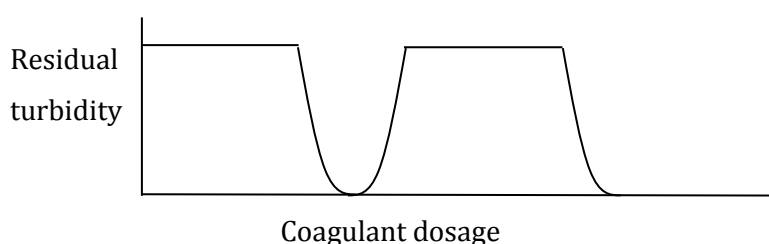


Figure 2-13: Optimal residual turbidity removal for relatively low coagulant dosage

Matilainen et al. (2010) postulates that a certain fraction of NOM cannot be removed through coagulation, possibly because of their small size. It could also be because of the electrostatic properties of the compounds, as hydrophilic neutral compounds are not removed through coagulation (Fan, et al., 2001).

The dosage has to be selected carefully, and with a fluctuation in feed water concentrations, has to be adjusted for at regular intervals to prevent over- and underdosing.

b) Dispersion of coagulant

In the case of this project, the coagulant was mixed through an orifice plate. A simple screw-in fitting could be made in-house in the Process Engineering Department workshop, and different types could easily be fabricated and tested. The aim of the mixer was simply to create a high

velocity and highly turbulent flow. An orifice plate was deemed as the simplest possible component to be used, while being highly effective in raising water velocity.

For a coagulant to work effectively, it has to be dispersed uniformly to avoid centralised compound removal (Degrémont, 2007). Coagulant is rapidly dispersed during flash mixing through the use of a turbulence inducing mixer. The velocity gradient of the mixing phase is indicative of the extent to which mixing has taken place. The velocity gradient is proportional to the probability of floc aggregation, although at very high values mechanical shear results in floc breakage. Power dissipated can be written in terms of the fluid properties and conditions (Weber, 1972), and is calculated as in Equation 2.30:

$$P = Q\rho_Fgh_L \quad [2.30]$$

With head loss through an orifice plate determined using Equation 2.31 (Dynamics, 2015) :

$$h_L = \frac{1}{2g}(1 - \beta^4)\left(\frac{Q}{C_dA_0}\right)^2 \quad [2.31]$$

The beta value is the quotient of the orifice diameter over the diameter of the pipe approaching the orifice. C_d is the discharge coefficient and is determined by the type of orifice plate used. In the case of the thin, sharp edged orifice plate used in the set-up, a C_d of 0.61 is appropriate. A_0 is the area of the orifice in the orifice plate.

Equation 2.32 specifies the velocity gradient for mixing within a vessel with a volume of V . For mixing through an orifice plate, the volume was calculated as the pipe area (in which the orifice plate is fitted) multiplied by ten times the pipe diameter. Once the head loss is calculated in Equation 2.31 and the power number determined through Equation 2.30, it is possible to calculate the velocity gradient through the following expression of the Camp-Stein equation in Equation 2.32 (Degrémont, 2007):

$$G = \sqrt{\frac{P}{V\mu}} \quad [2.32]$$

For coagulation, the acceptable range of values for G is between 400 and 1000 s^{-1} . A lower G value of around 70-100 s^{-1} is suitable for flocculation (Degrémont, 2007). Lower values will result in inadequate flocculation, and higher values can introduce shear (Tebbutt, 1992).

2.4.4 Effect of pH on water and subsequent effect on membranes

The pH has a very pronounced effect on the effectiveness of a coagulant. The suspension pH will not only affect the surface charge of NOM, but will also play a role in the hydrolysis product

produced (Zhan, et al., 2010). Furthermore, a different subsequent flocculation mechanism can ensue, causing a difference in floc structure and sizes (Wang, et al., 2011).

For water either more acidic or more alkaline than the proposed ideal operating range for a coagulant, floc size and structure could lead to ineffective NOM removal (Wang, et al., 2011).

Aluminium salts hydrolyse most effectively in water for a pH between 6 and 7.4, while ferric salts are optimal at between 5 and 6 pH (Degrémont, 2007).

a) Alkaline pH

At an alkaline pH, many phenomena take place as a result of complex interactions, which are summarised in Table 2-11. Some are contradictory, like Jung et al. (2005) and Sieliechi et al. (2008) stating opposite cases for the resulting humic macromolecule structure.

Table 2-11: Effect of alkaline pH on NOM-containing surface water coagulation

Phenomena	Mechanism	Researchers
Lower removal rate of NOM	Deprotonation carboxylic & phenolic acids - greater proportion negatively charged HA	(Cheng & Chi, 2002)
More expanded macromolecular complexes: easier to separate	Dissociation carboxylic & phenolic groups	(Kabsch-Korbutowicz, 2005)
Improved colloidal flocculation efficiency		(Wang, et al., 2011), (Zhan, et al., 2010)
Less effective removal of HA	Hydrolysis of polyferric sulphate favoured: decreases formation cations, less neutralisation HA	(Cheng & Chi, 2002)
Decreased NOM elimination	Adsorption of Al-hydroxides onto membrane; negatively charged pores	(Kabsch-Korbutowicz, 2005)
HA reorganise from stretched to coiled configuration		(Jung, et al., 2005)
Reaction takes place between ferric and HA: charged particles remain		(Cheng & Chi, 2002)
Stretched HA configuration	Electrostatic repulsion	(Sieliechi, et al., 2008)

Even with some contradictions in literature, which is to be expected due to the complex nature of NOM, the consensus on NOM removal appears to be that less effective removal of NOM occurs under alkaline conditions.

b) Acidic pH

For pH values below the optimal range for both coagulants, unique adverse factors can impede optimal NOM and turbidity removal. Table 2-12 summarises what is said in literature regarding acidic pH, and its subsequent effect on NOM removal and membrane fouling.

Table 2-12: Effect of acidic pH on NOM-containing surface water coagulation

Phenomena	Mechanism	Researchers
Greater removal of organics	Fixed Al-dosage: best removal in recommended optimal range	(Kabsch-Korbutowicz, 2005)
Better removal of HA by ferric salts than ferrous salts		(Park & Yoon, 2009)
Better agglomeration of HA	Promote charge neutralisation and complexation	(Sieliechi, et al., 2008)
Less removal of NOM		(Guigui, et al., 2002)
Increased hydraulic resistance of the HA		(Zularisam, et al., 2006)
Increase in water quality	NOM removal enhanced	(Dong, et al., 2006)
More severe membrane fouling behaviour	Enhanced adsorption of smaller NOM complexes onto membrane	(Dong, et al., 2006)
High concentration residual Al in filtrate	Smaller resulting floc size	(Matilainen, et al., 2010)
More NOM passing through membrane	Complex formation between Al and HA – form precipitates with small hydrodynamic radius	(Kabsch-Korbutowicz, 2005)
Greater irreversible fouling	Smaller flocs – pore blockage	(Kimura, et al., 2008)
More residual Al in water	Difference in hydrolysis mechanism and floc composition	(Kimura, et al., 2008)
Charge neutralisation of HA		(Cheng & Chi, 2002)
Decrease in UV ₂₅₄ absorbance	Carboxyl groups protonated, form large complexes which precipitated most HA; soluble FA remain	(Zularisam, et al., 2006)

If the pH decreases to below the optimal range, the effect on NOM removal, residual aluminium concentration and membrane fouling are very adverse. Acidic flocculation with aluminium below the optimal pH range increases aluminium concentration in the filtrate, due to the small size of flocs able to pass through membrane pores (Kimura, et al., 2008).

2.4.5 Jar tests and coagulant dosage determination

Jar tests are laboratory scale tests in which the optimal coagulant dosage to clarify water of a specific composition, is determined. Identical water suspensions are made up, and varying

dosages of coagulant are added. The water-coagulant mixtures are agitated by paddles and are subjected to a series of rapid and slow mixing sequences. Following mixing and allowing time for sedimentation, the turbidity of supernatant is measured to select an optimal coagulant dosage. The jar testing method is described in further detail in the Methodology section under 3.4.

2.4.6 Combination of coagulation and filtration

Flocculation and filtration are regarded as an effective combination of treatment methods, and are used in practice to specifically target particles of a particular size distribution, shown in Figure 2-14 (redrawn (Degrémont, 2007)). Filtration operations alone are unable to remove small particles, and coagulation and agglomeration is necessary for their removal.

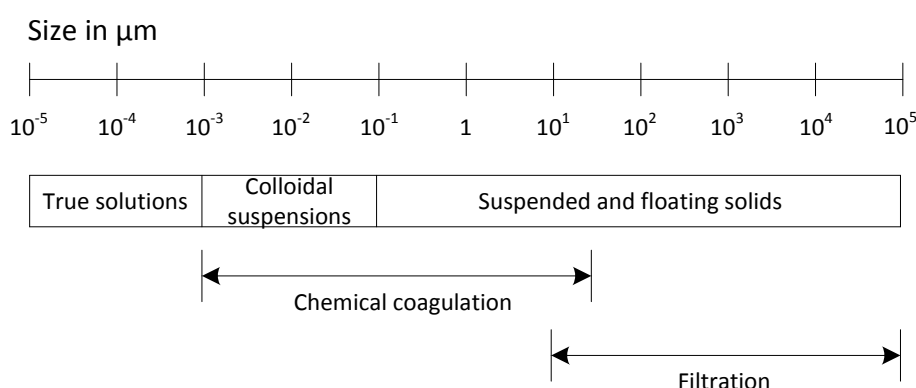


Figure 2-14: Particle size ranges for which treatment types are appropriate

There is no doubt that coagulation and flocculation improve the effectiveness of filtration, using both media and membrane filters. Many researchers have evaluated the effect the addition of coagulation has on the effectiveness of filtration, as discussed below.

a) Combination of coagulation and media filtration

Prior to the development of membranes, contact flocculation-filtration, or direct filtration, was used to improve the effectiveness of deep bed filtration (Rebhun, et al., 1984). The use of coagulation prior to media filtration increases the ability to remove colloids that would otherwise be too small to be retained (Weber, 1972). Furthermore, it aids in the permeability of the bed, by promoting particle agglomeration (Ives, 1975).

The extent to which media filtration is assisted by the retention of suspended particles is significant, as the quality of the permeate decreases when filtration commences immediately following backwash. Upon ripening, the additional resistance provided by the entrained

particles is beneficial to process operation up to the point when breakthrough occurs (Rebhun, et al., 1984).

b) Combination of coagulation and micro- and ultra-filtration

Many studies have been done on the combination of flocculation preceding either MF or UF, discussed below.

Filtrate quality

Systems combining coagulation and flocculation with filtration always performed better than systems where only one treatment method was used (Konieczny, et al., 2006), (Bergamasco, et al., 2011), (Wang, et al., 2012). Along with significant flux improvement, combining coagulation and flocculation with MF increases permeate quality (Guigui, et al., 2002). The pore sizes of UF membranes, and certainly also those of MF, are too large to reject the majority of dissolved organic materials in surface water, which is why coagulation is essential for high filtrate quality (Dong, et al., 2006).

Using both technologies in conjunction with one another improves the removal of NOM (Bergamasco, et al., 2011), (Judd & Hillis, 2001). This is especially important in MF where relatively large pores let more organic compounds through than UF (Carroll, et al., 2000).

Pathogen removal

In a study by Fiksdal and Leiknes (2006), MF systems could not without the assistance of coagulation and flocculation remove viruses to a satisfactory degree, and water is thus not disinfected properly. Without coagulation, no (MF) or only fractional (UF) virus removal was found. A high removal can still occur at relatively low dosages, with log 7 removal occurring at a coagulant dosage of 3 mg/L Al as opposed to the optimal 5 mg/L dosage (Fiksdal & Leiknes, 2006). The use of a coagulant prior to a membrane filter efficiently retains viruses suspended in drinking water (Kimura, et al., 2008).

Fouling

The addition of coagulation prior to filtration reduces the possibility for irreversible fouling occurring (Konieczny, et al., 2006). Agglomeration of suspended particles promotes the development of a cake layer on the membrane surface (Wang & Wang, 2006), (Chen, et al., 2007), (Dong, et al., 2006), (Zularisam, et al., 2006). Particles which would otherwise adsorb on the membrane surface are bound to nucleation sites on the coagulant (Wang & Wang, 2006), (Konieczny, et al., 2006). The cake layer is a more reversible form of fouling and can be removed through hydraulic backwashing. The development of reversible rather than irreversible fouling

ensures a higher permeate flux while also reducing the backwashing and chemical cleaning frequencies (Konieczny, et al., 2006). Furthermore the cake layer aids in filtration by capturing incoming particles (Konieczny, et al., 2009). This increases the lifespan of the membrane and reduces the backwashing frequency (Zhang, et al., 2009), (Cho, et al., 2006). The resulting floc cake resistance is lower than without pre-treatment (Guigui, et al., 2002) and results in a smaller increase in TMP during filtration as opposed to UF without pre-treatment (Wang & Wang, 2006).

High molecular weight hydrophobic compounds are reported to be responsible for rapid flux decline in UF without pre-treatment. Coagulation could remove these hydrophobic compounds, improving the permeability of the membrane. Low MW neutral hydrophilic compounds are not removed as effectively as larger hydrophobic compounds, and as they are left in the water, are responsible for flux decline in combined coagulation-UF systems. Once the coagulated flocs are retained on the membrane, they assist in the adsorption of neutral hydrophilic compounds and prevent them from adsorption onto the membrane (Chen, et al., 2007).

2.5 Findings from literature

From the literature study, operational parameters and fixed variables were established.

2.5.1 Configuration

A single media bed, which will be mounted next to the membrane on an experimental rig, is considered as pre-filter. The same pumps will be used to respectively feed and backwash both units simultaneously. As the UF membrane has more rigid guidelines with regards to filtration and backwashing duration, the operation of the entire unit will be governed by recommended UF operational parameters.

2.5.2 Pre-filter filtration media

Grain sizes used in rapid filtration range between 0.35-1 mm (Gray, 2005), (Johir, et al., 2009), (DOW, 2012). The use of 0.5 mm grain size silica sand was considered a fair average estimate. Silica sand was selected as filtration media. Different sand types are considered for pre-filter characterisation, both graded and uniform, and are discussed in 4.1.1.

The breakthrough point and termination of the filtrate cycle for pre-filtration is reached when filtrate turbidity exceeds 1 NTU, as per SANS 241-1:2011.

The filtration media was procured from Consol Minerals, with silica particle having a non-spherical shape, illustrated in Appendix A.

2.5.3 UF membrane

Inge® was selected as the manufacturer from which the pilot scale membrane was ordered. Their Dizzer® P4040 range was found to be the most appealing choice due to the material and available sizes. Their pilot scale membranes in the range considered have surface areas of 4 and 6 m². The membrane vessel has a length of 0.96 m and an outer diameter of 0.1 m.

The material used for their capillaries is PES, which is more fouling resistant than PVDF (Nakatsuka, et al., 1996), (Chae, et al., 2008). For their capillaries they use Multibore® fibres which consist of a single membrane fibre, with 7 hollow capillaries running through the length of the fibre. These fibres are stronger structurally than single fibres (www.inge.basf.com). The outer diameter of the capillary is 6 mm, and each of the 7 capillaries has a diameter of 1.5 mm.

Furthermore, this specific manufacturer was selected by recommendation based on its reliability in surface water treatment plants operational in the Southern Cape, which is the application for which this research could potentially be beneficial.

The membrane is operated in dead-end mode, with inside-out filtration through the capillaries.

2.5.4 Downflow rate and filtration flux

An operational downflow rate of 10 m/h flux through the pre-filter is considered as a fair average estimate for rapid gravity filters, as literature shows that down flow rates can range between 5 to 15 m/h (Crittenden, et al., 2012). Down flow rates between 5 and 10 m/h are most common (Gray, 2005), (Johir, et al., 2009), (Van Duuren, 1997) as the quality of permeate decreases above 10 m/h flux. It is decided to operate in a range of 8-12 m/h flux through the pre-filter.

As a relatively conservative estimate, but yet as an estimate comparable to typical fluxes used in practice, 50 LMH was selected as a design parameter for the average flux through the UF membrane. The range of filtration fluxes through the UF membrane depends on the surface area selected.

2.5.5 Upflow rate and backwashing flux

inge® recommends backwashing fluxes of 230-250 LMH for surface water treatment for water with a turbidity not exceeding 50 NTU. This recommended flux is suggested to backwash the membrane for 50-70 seconds. Another membrane manufacturer (DOW) cites a UF backwashing flux as low as 100 LMH.

A slightly more conservative backwashing flux of 200 LMH was selected, at 10% lower than the lower limit of the recommended range from inge® to account for the potential longer filtration duration. Backwashing between 0.5-3 minutes will be carried out during pre-filter screening.

Slightly decreasing the flux will benefit the recovery of the system without compromising the positive effect of vigorous hydraulic backwashing. This backwashing rate translates to 46 m/h upflow rate through the media bed, which is within the 40-50 m/h recommended range for surface water media filters (DOW, 2012). When using 230 LMH flux, an upflow rate of 53 m/h will be achieved, which exceeds the desired range.

2.5.6 Chemically enhanced backwash recipe

In the case of the pre-filter and UF being operated in series, the sand bed is chemically washed during the CEB regime carried out for the benefit of UF. Caustic is selected for the high pH wash, which has to be carried out first for organically fouled membranes (according to DOW). Sodium hypochlorite within the allowable free chloride range for the membrane selected, will be added to prevent biological growth. Following thorough rinsing, a low pH wash will be conducted with 1% citric acid. Soaking of both chemicals will take place for 20-30 minutes.

2.5.7 Coagulant and dosing

Ferric chloride is selected as the coagulant, as the use of aluminium sulphate is potentially linked to health risks (Konieczny, et al., 2006), (Matilainen, et al., 2010), (Zhan, et al., 2010). The dosage thereof was selected through jar testing with each of the specific synthesized suspensions considered.

The coagulant is mixed through an orifice plate directly following dosage. A velocity of 10 m/s flow through the orifice plate was selected as design basis for the orifice plate in order to ensure homogeneous dispersion of the coagulant.

2.5.8 Suspension make-up

The synthetic suspensions considered in lab experimentation was made up using humic acids and bentonite, due to its widespread use in membrane filtration research when making up a synthetic suspension (Wang, et al., 2011), (Katsoufidou, et al., 2005), (De Souza & Basu, 2013). The concentrations of each are discussed in further detail in 3.3.

CHAPTER 3 : RESEARCH DESIGN AND METHODOLOGY

In order to facilitate tests, a pilot scale treatment unit had to be constructed. The unit had to be able to operate within the desired parameters selected from the literature study. Once the unit had been commissioned, experiments were conducted to firstly determine optimal pre-filter (PF) parameters and to characterise both units. Following characterisation, the improvement brought about to membrane performance by sand filter pre-treatment was determined for a range of NOM-containing representative surface water compositions.

3.1 Operation of experimental set-up

The set-up was assembled as illustrated in the simplified PFD in Figure 3-1. The complete P&ID is included in Appendix B.

Equipment was constructed in such a manner that operation could either take place through the PF or ultrafilter alone, or through both units in series. The configuration was altered by opening and closing the appropriate ball valves around the units.

- Raw synthetic water was made up in T-101 with the required HA and/or bentonite.
 - The water was mixed with agitator M-101, to ensure homogeneous suspension.
- The forward flow rate set point, filtration duration and backwashing duration were entered on the touch screen.
- During experimentation, feed water was pumped with centrifugal pump P-101.
 - A fraction thereof was recycled to T-101, to assist in the suspension of particles.
 - During backwashing the feed pump maintained a low flow rate through the recycle line to avoid it being switched on and off at short intervals.
- Water was pumped firstly through the orifice plate.
 - Just before reaching the fitting, coagulant was dosed with P-102.
 - Passage through a short pipe flocculator followed to promote contact between coagulated particles.
- Water entered the PF.
 - When flowing through the sand, orthokinetic flocculation was induced.

- Following filtration through the PF, water was then filtered by the UF membrane.
 - Water enters through feed port at bottom, and exits feed exit side at top.
 - Filtration is in dead-end mode, with inside-out capillary filtration.
 - Clean filtrate was stored in a filtrate tank.
- Upon backwashing, the appropriate solenoids opened and closed to allow for the reverse flow of clean product water through the filters. P-101 is set to a low speed and P-103 switches on.
 - The rate of backwashing was controlled manually by adjusting ball valves.
 - The solenoid valve above the media bed opened during backwashing, allowing for the backwashing water to leave the system through drainage.

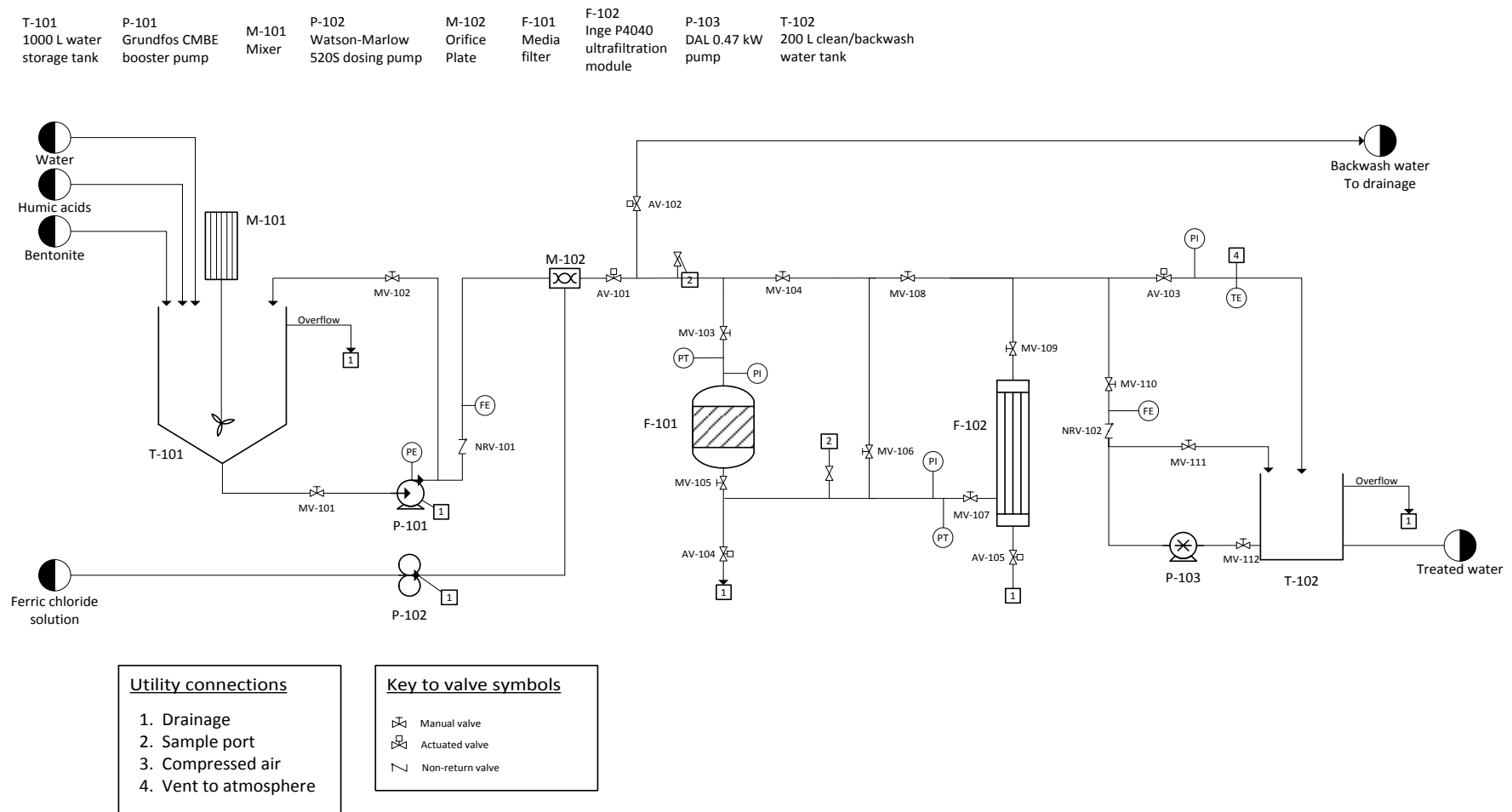


Figure 3-1: Simplified PFD of experimentation set-up

The PLC maintained a constant flow rate through the system by varying the speed of the centrifugal feed pump through its VSD. The PLC switched between operational and backwashing modes after the entered durations for each of the cycles had been reached, by switching the appropriate pumps (dosing and backwashing) on and off, and opening and closing the appropriate solenoid valves.

Dosing pump speed had to be set and calibrated manually. Backwashing flow rate was also set manually by throttling the pump and controlling the fraction of water recycled to the filtrate tank.

CEB took place through the normal backwashing pump and the same pathway. Caustic and citric acid solutions were made up in 50 L tanks which were then manually connected to the backwashing line.

The scope of the project poses limitations to the operation of the set-up:

- Air scouring during backwashing was not included
- Flow rate range capabilities are limited as surface areas of membrane and media bed are unalterable

3.2 Experimental set-up construction and assembly

From the operational conditions selected and discussed in 2.5, the appropriate process units had to be either procured or constructed. Construction and assembly occurred in-house with the author working alongside the Process Engineering Department's workshop. With the determination of the control philosophy based on the desired operational manner, the required electronic components were identified required to automate operation.

3.2.1 Filtration units sizing and sourcing

It was decided to use inge® membranes, as discussed in 2.5. An appropriately sized membrane had to be selected from their dizzer® P4040 range. The average membrane flux and PF downflow rate was used to determine suitable surface areas for each unit.

$$J_{UF}A_{UF} = J_{media}A_{media} \quad [3.1]$$

The 4 m² surface area membrane was deemed most suitable for the flow rates considered and commercial PVC tubing available. The required PF surface area was correlated to commercially available PVC pipe diameters, and a diameter of 0.154 m was selected. Transparent tubing was chosen for the body of the PF in order to observe and control expansion during backwashing.

Table 3-1: Filter fluxes and flow rates considered for operation

PF downflow rate (m/h)	Membrane flux (LMH)	Flow rate (L/min)
8	37.07	2.47
9	41.69	2.78
10	46.32	3.09
11	51.00	3.40
12	55.59	3.71

The base of the PF was capable of supporting a mesh sieve assembly, which would in turn support the filtration media. The media filter assembly and sand support mesh are shown in Figure 3-2.



Figure 3-2: Left: PF with transparent PVC body. Right: Inside view from top showing fine sieve supported by two coarse sieves.

The bottom of the base tapered conically downward to an exit port the same size as piping used in the system. To avoid channelling of water through the bed during backwashing, a screw-in distributor with equally spaced holes around the edge was inserted in the bottom of the bed under the mesh assembly.

3.2.2 Sand selection

Grain sizes in rapid media filtration are typically approximately 0.5 mm (Cox, 1969). Graded silica sand from Consol Industrial Minerals was bought from Cape Silica. The two procured graded sands respectively had particle size ranges of 0.18–0.50 mm, and 0.50–1 mm. It was also decided to screen the silica to grade it between 0.425–0.6 mm with mineral processing sieves, making the sand more representative of particle sizes in industry. Screening sand removes excessively large particles, improving filtration effectiveness; and fine particles, which can be washed out during backwashing and thus alter bed properties. These sands were used in initial

characterisation experiments with the most suitable sand selected for further consideration, as discussed in 4.1.1.

The column length needed to be appropriate for the required media bed depth, allowing for a potential maximum depth of 300 mm, as set out in the project scope, and a maximum expansion of 50%. A column length of 450 mm was selected to accommodate the maximum bed depth and its expansion. If a bed depth of less than 300 mm is used, or an expansion of less than 50% results, the excess volume within the filter assembly will contribute to the dead volume in the system. It was left as is and its variability accounted for during recovery calculations. Head space above the bed merely increased retention time of particles within the bed, but as orthokinetic flocculation only occurred within the depth of the sand bed, it was the bed depth that was of more importance for filtration effectiveness.

3.2.3 Orifice mixing

Rapid mixing of the coagulant with the water took place through an orifice plate. Ferric chloride was dosed through a port immediately preceding the orifice plate, and mixing was induced by the sudden expansion following the orifice. Three orifice plates of different sizes were made in the Process Engineering workshop, with variable diameters of 2, 2.5 and 3 mm in order to induce turbulence and homogeneous dispersion of the coagulant.

By testing the influence of the orifice plate sizes on flocculation efficiency, it was seen that a velocity above 10 m/s delivered cleaner water for a longer filtration period. Table 3-2 summarises velocities for water flow through the orifice plates at different flow rates, with the highlighted cells as the selected plates for the various flow rates. The velocity coefficient for each considered velocity plate is included.

Table 3-2: Head loss and flow velocity for flow rates and orifice sizes considered

	Water velocity through orifice (m/s)				
Downflow rate (m/h)	2 mm	2.5 mm	3 mm	h_L (m H ₂ O)	G (s ⁻¹)
8	13.1	8.4	5.8	23.5	35399
9	14.8	9.4	6.6	29.8	42268
10	16.4	10.5	7.3	15.1	31682
11	18.0	11.5	8.0	18.2	36568
12	19.6	12.6	8.7	21.6	41513

The high values of G are ascribed to the fact that an assumption had to be made in order to make the calculation. Equation 2.32 expresses G in terms of a mixing volume. For orifice plate mixing,

the mixing volume is expressed as 10 times the pipe diameter, which is potentially too small still for realistic G values to be obtained.

For coagulation, the acceptable range of values for G is between 400 and 1000 s^{-1} (Degrémont, 2007).

3.2.4 Pump selection

Three pumps were required for effective operation: a feed pump, backwashing pump and coagulant dosing pump.

The feed pump had a VSD to maintain a constant flow rate through both filters, as foulants would deposit in both filters and contribute to their resistances. A centrifugal Grundfos CMBE booster pump was reprogrammed to maintain constant flow. The forward flow rate signal and PID parameters from the PLC changed the pump speed to maintain the entered flow rate set point. It had a maximum flow of 2.2 m^3/h , which was more than adequate for the flow rates required; a rated head of 26.2 m; and maximum pressure of 5 bar.

A DAB centrifugal pump of 0.47 kW capable of delivering up to 2.16 m^3/h water with available head of 25 m was selected as backwashing pump. A recycle line was included to manually regulate the flow rate.

A Watson-Marlow 520S dosing pump was used to dose ferric chloride coagulant to the water. The appropriate bore size Marprene® tubing with an internal diameter of 0.5 mm was purchased and the pump was calibrated prior to each experimental run. The pump could deliver up to 9 ml/min, which at a coagulant concentration of 20% could deliver in excess of 10 mg/L (Degrémont, 2007) ferric chloride for the range of flow rates considered.

3.2.5 Electronic requirements

The temperature of water was measured with a J-type temperature probe from the Process Engineering Department. The sensor was calibrated with a thermocouple with a 1:1.05 agreement between the sets of data with an R^2 coefficient of 0.9999.

The flow rates of the both the filtration and backwashing water were measured by paddle wheel flow sensors, purchased from Netram Technologies. They had a measuring range of 0-30 L/min and were calibrated manually upon installation to ensure the accuracy of their readings.

Two A-10 pressure sensors from WIKA Instruments were used for the determination of pressure drop over the filters. The sensors were placed respectively above the PF and by the

membrane inlet. The sensors were capable of measuring pressures between 0-400 kPa in order to account for up to 100 kPa pressure drop over the UF, as TMP readings of around 100 kPa are typical in surface water treatment (Crozes, et al., 1997), along with a maximum pressure drop of 50 kPa over the PF, and additional minor losses in the system. The A-10 sensors had an uncertainty of 1% of their range which included the non-linearity of the sensors, meaning that their uncertainty stretched over 4 kPa.

Pressure gauges were added adjacent to both sensors, as well as at the exit of the membrane housing. The gauge before the media bed had a range of 0-160 kPa while the remaining two sensors could measure 0-100 kPa. This was for verification of sensor readings as well as TMP calculations.

Pressure drop over the media filter was calculated by adding and subtracting the hydrostatic pressure contributions of the water columns between the bed and the respective sensors. The minor loss contributions from the bends between the bottom of the bed and the pressure sensor at the outlet of the PF were considered, but the loss occurring over the sieve supporting the filter media could not be determined. As the actual pressure drop calculated from pressure readings and hydrostatic calculations corresponded very closely to theoretically predicted measurements, the sensor readings and calculations made were deemed accurate.

TMP was determined by calculating the average of the difference between the inlet and outlet pressure sensors. The outlet reading was measured by a pressure gauge, and only contained the loss constituted by a solenoid valve at the outlet.

Prior to the site visit it was decided to order more accurate sensors capable of minimizing the noise in measurements. Two S-20 sensors were ordered from WIKA Instruments, with an accuracy of 0.25 % of their measuring ranges. The media bed sensor was chosen to have a range of 0-160 kPa, corresponding with its gauge, and the membrane inlet sensor range was selected as 0-100 kPa. Much less noise in sensor readings was obtained along with the more accurate readings.

3.3 Synthetic water make-up

In the case of this project, surface water was represented with a synthetic water mixture during test work. The water was made synthetically to avoid reproducibility issues by ensuring consistent water composition over the course of many experiments, and to ensure the availability of the water when it was needed.

It had been shown that the presence of calcium ions has a significant effect on the fouling of the membrane, and CaCl_2 has been added in certain studies to incorporate the effect thereof on the system (Katsoufidou et al., 2008). Tap water was thus used to prepare the synthetic water suspensions, as it contains a small measure of calcium, and was more readily available than RO water in the laboratory.

Natural surface water turbidities are typically below 20 NTU for 60% of the year, as was seen from plant data obtained from a Western Cape treatment plant. Following the first rains of the season it is not uncommon to measure turbidities exceeding 500 NTU, although this is quantitatively a very seldom occurrence (less than 5% of operational time throughout a year). A range of conditions were selected representative of surface waters at different conditions, which is quantified later in this section.

3.3.1 Humic acid concentration

HA is typically used as a model substance representative of NOM (Katsoufidou, et al., 2008). HA concentrations used in studies by researchers interested in its effect on membrane fouling are summarised in Table 3-3. Typically other chemicals are also used to more closely mimic surface water, such as the inclusion of calcium, sodium alginate and fine clay, but for many researchers the effect of NOM fouling on membrane performance is of the most importance.

Table 3-3: HA concentrations from literature used to synthesize surface water

Concentration HA (mg/L)	Researchers
0.1-20	(Rodrigues, et al., 2008)
2-10	(Chang, et al., 2015)
7.5	(Wang, et al., 2008)
10	(Rebhun, et al., 1984)
10	(Rebhun, et al., 1984)
10	(Wang, et al., 2011)
10	(Katsoufidou, et al., 2005), (Katsoufidou, et al., 2008)
10	(De Souza & Basu, 2013)
20	(Li & Elimelech, 2006)
20-30	(Konieczny, et al., 2006)
50	(Fu, et al., 2008)

10 mg/L HA appears to be very representative for NOM content in surface water synthetic suspensions in membrane fouling tests. This corresponds to roughly 4 mg/L TOC (Konieczny, et al., 2006), which corresponds well to raw water TOC of 2.5 mg/L (Kimura, et al., 2008) and 7 mg/L (Konieczny, et al., 2006).

3.3.2 Bentonite concentration

Many researchers occupied with studies on the fouling effect of organic material on membranes will often include colloids to increase the turbidity of the water. Although concentrations aren't usually given, except for the few sources cited in Table 3-4, the resulting turbidity of the suspension is usually given. Turbidities to which organic suspensions have been adjusted are given in Table 3-5.

Table 3-4: Bentonite concentration representative of SS in surface water

Bentonite concentration (mg/L)	Research group
10	(Wang, et al., 2012)
4-50	(Bessiere, et al., 2009)
100	(Serra, et al., 1999)

Bentonite concentration added can be anything in a wide range. It is more standard practice to use residual turbidity as an indication of appropriate concentration.

Table 3-5: Resulting turbidity of synthetic surface water suspensions upon adding bentonite

Suspension turbidity (NTU)	Researcher group
15	(Wang, et al., 2011)
15-20	(Katsoufidou, et al., 2005)
20	(De Souza & Basu, 2013)
12.1	(Zhang, et al., 2014)

Suspensions with relatively low residual turbidities typically represent surface water in the cited studies.

3.3.3 Contribution of HA and bentonite to turbidity

Both HA and bentonite each contribute to the turbidity of the suspensions. Different concentrations of each were made up and the resulting turbidities were measured. Both HA and bentonite contributed linearly to the turbidity of the water, as can be seen in Figure 3-3.

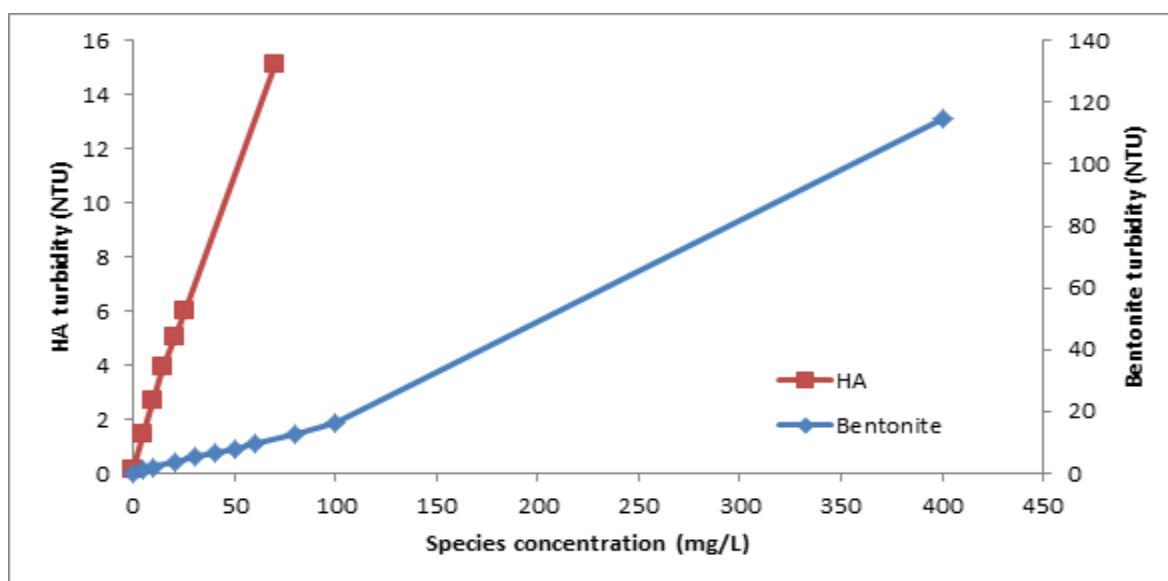


Figure 3-3 : Bentonite and HA contribution to turbidity

HA had a greater contribution to the turbidity of the water. At 20 mg/L, the HA had a turbidity of 5.0 NTU, compared to 3.5 NTU for 20 mg/L bentonite.

3.3.4 Synthetic water composition

Technical grade humic acid sodium salt (product code: H16752) and bentonite (product code: 285234) were ordered from Sigma Aldrich. A technical HA is selected because of the large amount of material required for experimentation, and because of the favourable use thereof in surface water studies (Wang, et al., 2008), (De Souza & Basu, 2013), (Katsoufidou, et al., 2008). The two components were dissolved in tap water (Mosqueda-Jimenez, et al., 2008). Bentonite particle size distribution is included in Appendix A.

A range of different surface water conditions were selected to replicate with the make-up of synthetic water compositions.

Table 3-6: Water compositions for different conditions considered

ID	Bentonite (mg/L)	HA (mg/L)	Turbidity (NTU)
Low turbidity surface water	30	20	12
High turbidity surface water	100	25	31
Flood: high SS	400	0	155
Flood: high organic	0	70	16.5

In order to replicate low turbidity surface water, 20 mg HA and 30 mg bentonite was decided on per litre of water, giving a turbidity of 12 NTU. This suspension was relatively more aggressive, with a slightly higher organic concentration than 10 mg/L typical of lab tests, in order to

accelerate fouling and gauge the improvement brought about by pre-filtration easier. The turbidity was close to those used in research papers for surface water.

A higher turbidity surface water suspension was synthesized using 100 mg/L bentonite and 25 mg/L HA, giving water with a turbidity of 31 NTU. The harsh water was used during media filtration characterisation to be able to screen the filterability of silica sand easier. Following characterisation tests with the cleaner surface water, the dirtier water was also used to gauge the load removed from the UF by the PF.

Following a series of tests conducted with both the low and high turbidity suspensions, flood conditions were simulated to see in extreme conditions what improvement the PF brought about to UF performance. Due to the interaction known to take place between bentonite and HA, it was decided to prepare separate worst case scenario water suspensions for each component to further aggravate the effect of fouling.

3.4 Flocculant dosage determination through jar tests

Jar testing was used to determine the optimal coagulant dosage for each water composition. Varying coagulant dosages were dosed to identical suspensions, and were then simultaneously subjected to a specific mixing regime. Different jar test sequences are proposed in literature. In each method, an initial rapid mixing phase to disperse the coagulant, slower mixing in which contact between destabilised particles is promoted, and settling is present. The optimal coagulant dose would be where residual supernatant turbidity is lowest.

The jar testing method described by Kawamura (2000) was selected, as the gradual stepwise decrease in the slow mixing speed for flocculation seemed most true to the conditions in flocculation chambers in industry where a gradual progression of slower speeds occur.

The jar test procedure was set up as shown in Figure 3-4 in the programmable Phipps and Bird jar tester available in the Process Engineering Department. Six 1 L beakers of water were prepared with the water composition selected. Upon addition of the coagulant, the paddles agitated the suspensions at 200 rpm for 2 minutes. A slow mixing phase then followed with the mixtures firstly stirred at 75 rpm for 7.5 minutes, then at 40 rpm for another 7.5 minutes, and lastly at 25 rpm for 5 minutes. A 20 minute settling period was allowed for the flocs formed to settle to the bottom of the jars as sludge.



Figure 3-4: Jar test set-up during coagulation dosage determination

A water sample was extracted from just under the surface of each beaker following settling, and the turbidity thereof was measured. Visual observation assisted in the selection of the coagulant, and the point at which pin floc formation occurred was noted.

At an insufficiently low dosage, water remained turbid. At a dosage approaching the optimal coagulant dosage, larger flocs were visible, but still too small to settle adequately. The optimal coagulant dosage had large flocs which settled to create a clear supernatant. The pH was not adjusted in this project as per the scope. Adequate colour removal was found. While an adjustment in pH would decrease the required amount of coagulant, another dosing pump would be required along with the appropriate chemicals.

Table 3-7 contains information on the optimal coagulant dosage for the different water suspensions considered for treatment in this project. Refer to Table 3-6 for the composition of the water suspensions.

Table 3-7: Flocculant dosages for different water types

Water suspension	Turbidity raw water (NTU)	Optimal dosage (mg/L FeCl₃)	Final water turbidity (NTU)
Clean river water	12	10	0.54
Dirty river water	30	14	1.51
Flood: high bentonite conc.	150	28	0.37
Flood: high HA conc.	26	16	1.8

An example of a residual turbidity graph for the selection of optimal coagulant dose is included in Appendix C.

3.5 Chemically enhanced backwash procedure

In order to restore the initial permeability of the membrane once irreversible fouling has taken place, it was necessary to wash the membrane with chemicals.

In the selection of base and acid concentrations, the minimum and maximum pH the membrane can handle was considered. In the case of the Inge® membrane, the pH should not go below 1 or exceed 13. The maximum tolerance for free chlorine is 200 ppm, which is considered in the addition of sodium hypochlorite. Deionised water was used to make up both the basic and acidic wash solutions.

In the high pH solution, sodium hydroxide was added to achieve a pH of between 11 and 12. The high pH is important for the removal of organic material. If biological fouling has taken place, the basic wash should occur first. Sodium hypochlorite was added as disinfectant to prevent biological growth on the membrane. Citric acid was used in the low pH wash as it can effectively remove iron or other metals that could adsorb onto the membrane. A 1% solution was made up and a pH of between 2 and 3 was used for washes.

Prior to CEB, the membrane was rinsed thoroughly with clean water. The membrane unit was then firstly flushed with a basic solution for 30 seconds at 100 LMH, before being washed at the normal backwashing rate of 200 LMH for 90 seconds. Ball valves right before and after the module were closed during the soak period, and the solution was left to soak for between 20-30 minutes. After soaking, the remainder of the basic solution was washed through the unit for a further 2 minutes after which the unit was again thoroughly rinsed with water. The washing sequence was then repeated with the acidic solution.

3.6 Experimental plan

Figure 3-5 summarises the sequence of experiments conducted. Double barred rectangles signify sub-processes, and are discussed in further detail in the figures following 3-5:

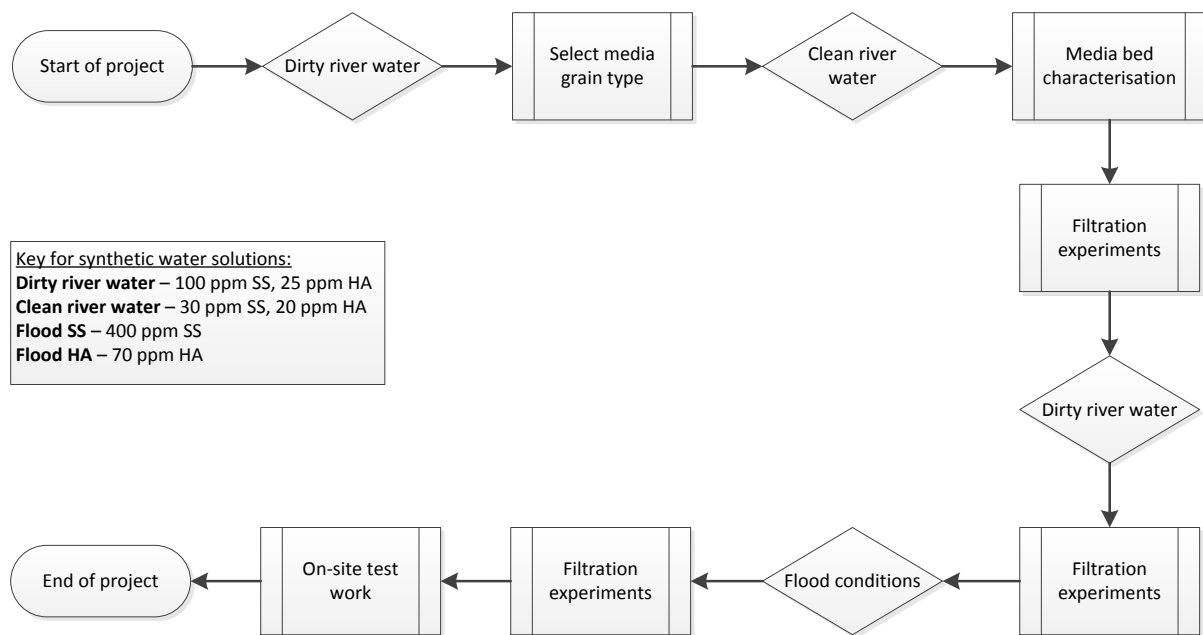


Figure 3-5: Experimental plan

Oval text shapes represent the beginning and end of a process. Diamond text shapes indicate a decision being made, regarding water composition selected, for example. Plain rectangles indicate actions that have to be taken.

Figure 3-6 illustrates the expected experimental sequence for the sub-process Select media grain type.

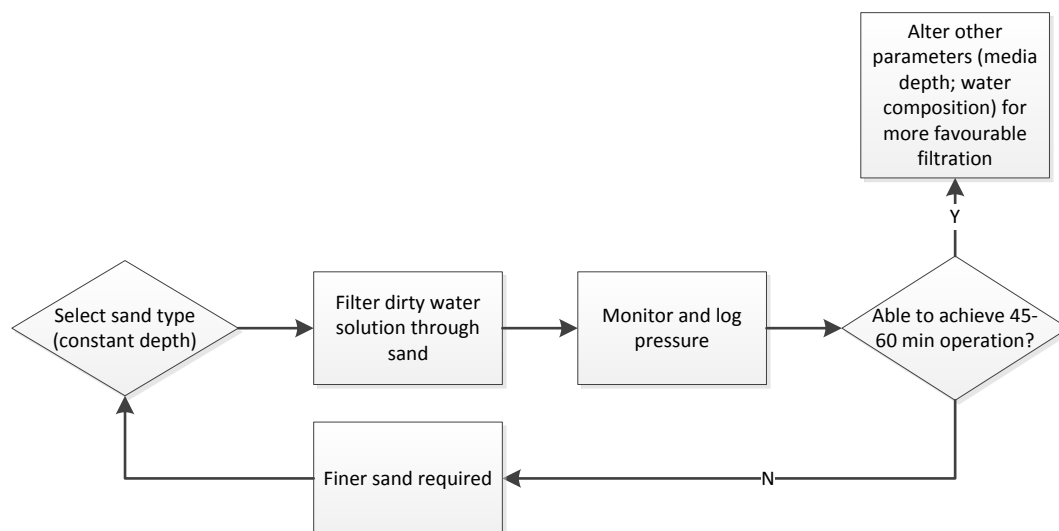


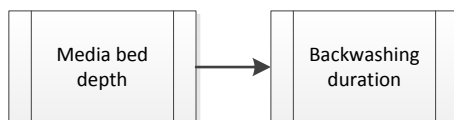
Figure 3-6: Selection of media grain type

Dirty river water was firstly used to compare the performance of different sand types, in order to enable a more certain selection of the most favourable sand type through coarse screening.

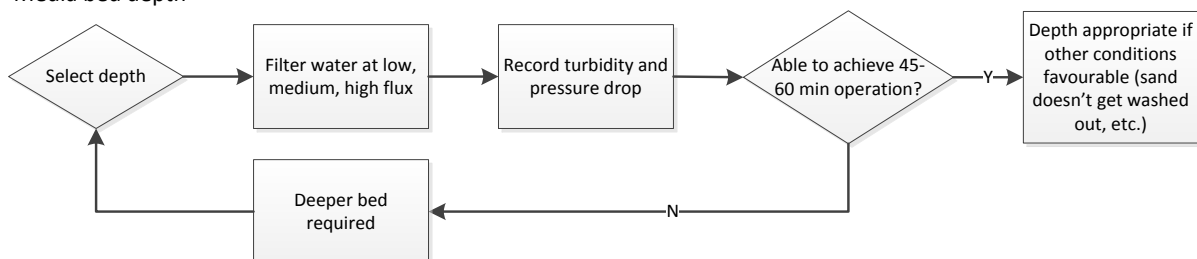
The characterisation of the media bed took place using the cleaner synthetic water. The cleaner water is more representative of the nature of the water which will be filtered for the most part of the year by a typical surface water treatment plant. Designing the media filter for these conditions rather than for flood conditions, which are experienced for a smaller fraction of the year, was a more economic choice. Designing a filter at the worst case conditions would result in a deep filter with a large head space, which is unnecessarily robust for the cleaner water filtered throughout the rest of the year. The extra depth would require a larger displacement volume to backwash, which will result in poorer recovery.

As Figure 3-7 shows, Media bed characterisation was two-fold, in which the Media bed depth first has to be determined before optimizing Backwashing duration.

Media bed characterisation



Media bed depth



Backwashing duration

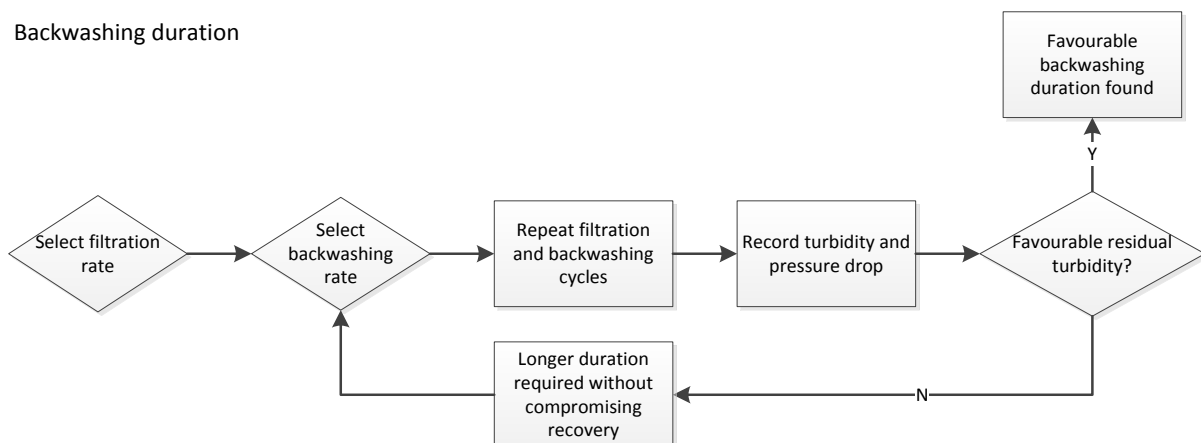


Figure 3-7: Media bed characterisation sequence of experiments

Once the media filter had been characterised for typical operation, the ultrafilter was introduced to the system. Filtration experiments are shown in Figure 3-8 and was repeated for the different water types considered.

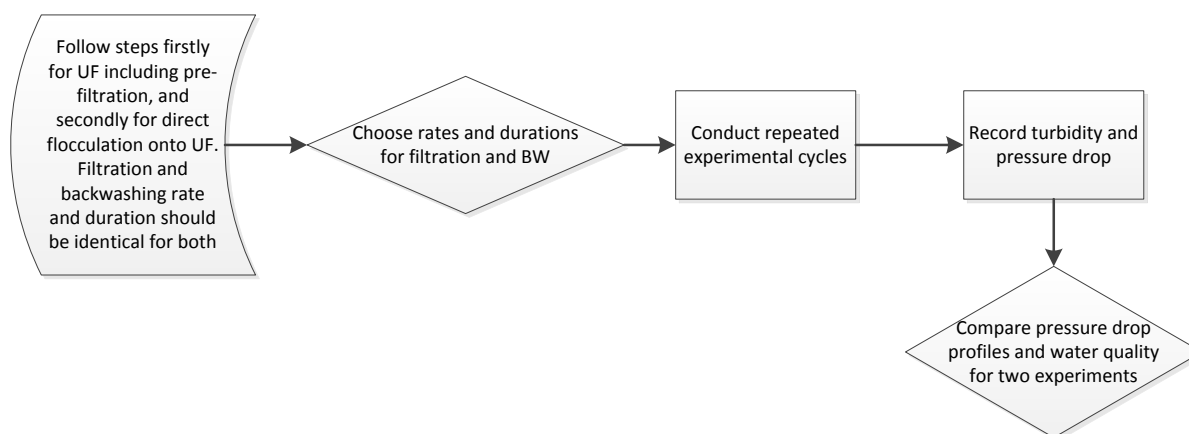


Figure 3-8: Filtration experiments

The performance of both the combined filters and ultrafilter alone were compared in order to determine the improvement brought about by the PF.

3.7 On-site test work

In order to gauge the long term performance of the set-up, on-site test work was conducted at a water treatment plant in the Southern Cape, in parallel with, and under approximately the same operating conditions as the actual UF plant. The manner in which the actual plant is operated, is included in Appendix B.

The pilot plant was transported to site and operated as closely as possible to the operating conditions used by the actual plant. Water was filtered at 37 LMH through the pilot plant, which was comparable to the 30 LMH flux at which the actual plant operated. The pilot plant was operated for 71 minutes with 2 minute backwashing intervals to achieve the same recovery of 82% achieved by the actual plant at the time of the site visit. As with the plant, a CEB was conducted every 24 hours.

Certain adjustments had to be made to more closely mirror conditions in the treatment plant. Prior to membrane filtration after coagulation and flocculation has commenced, the actual plant screened water through a 60 micron screen to remove larger flocs. As it was not possible to screen water in the pilot plant after coagulation, raw water was screened through a 150 then 75 micron screen prior to being pumped to the raw water storage tank. The feed rate to the tank was about the same as the rate of filtration in the pilot plant. This ensured good mixing in the tank, as confirmed by comparing the turbidity and colour of water pumped to the storage tank and water pumped to the experimental unit.

In order to further mirror site conditions, the same coagulant was used in the pilot plant as by the actual plant. Aluminium sulphate, or alum, was dosed at the same rate as the actual plant. The high dosage rate of aluminium sulphate rendered the water acidic, and another dosing pump had to be used on-site for pH adjustment. At very acidic conditions, inadequate removal of aluminium from the water occurs due to the different hydrolysis reactions taking place (Matilainen, et al., 2010). This was observed through on-site aluminium analyses. Sodium hydroxide was dosed to maintain the pH between 5.6 and 6.2 as done by the plant operators, in order to prevent aluminium from passing through the membrane.

The set-up was run continuously for 5 days for each of two sets of experiments, firstly operating the UF with its pre-filter, and secondly operating the UF by itself, with coagulation aiding filtration in both instances.

CHAPTER 4 : FILTER CHARACTERISATION

Prior to conducting experiments with synthetic surface water through the PF and the ultrafilter, the properties of these filters were firstly investigated through characterisation. Parameters such as grain size, bed depth and optimal backwashing duration first had to be established for the PF. Clean water and the synthetic suspensions were then filtered through the respective filters. Coagulation and flocculation was conducted throughout characterisation.

4.1 Pre-filter

4.1.1 Filtration media selection

In order to gauge the performance of a shallow media bed for different grain types, a synthetic water suspension with a high turbidity of 31 NTU was made up, consisting of 100 mg/L bentonite and 25 mg/L HA.

Sands of different grain sizes were considered. The viable sands' residual turbidity profiles were compared to determine the filtration effectiveness of the filter media. Particle size distributions and properties of the fine (AFS 45) and coarse (No. 1) sand are included in Appendix A.

Fine sand (0.18-0.5 mm)

The use of the fine graded Consol sand, AFS 45, was discredited as it caused operational problems. The fines were able to pass through the mesh support sieve, and were washed out of the bed upon backwashing. The fine sand entered solenoid valves above and below the PF and impeded their operation. It has an effective size of 0.32 mm, which is too fine compared to the average rapid media filtration grain size. A coarser filter media was considered instead.

Coarse sand (0.5-1 mm)

The No. 1 graded Consol sand had an effective size of 0.51 mm. The sand had a wide particle size distribution, but did not contain fines, which made operation more streamlined than the AFS 45 sand.

With the optimal coagulant addition, the coarse media bed was unable to effectively clarify the water, and breakthrough seemed instantaneous without any particle retention in the bed. The residual turbidity curve is plotted in Figure 4-1. The coarse No. 1 sand contained some particles with diameters exceeding 2 mm, which were not effective in promoting floc growth and

retention. Rebhun et al. (1984) also experienced inefficient clarification of water in their study on contact flocculation of humic substances when using sand with grain size of 1.2 mm, as opposed to a more effective 0.62 mm.

Screened sand (0.425-0.6 mm)

Following tests with coarse sand, sand was sieved to a narrower band of size distributions between 0.425-0.6 mm. The residual turbidity graph for the screened sand is plotted against the coarse bed residual turbidity graph in Figure 4-1, indicating a clear improvement on performance. For each of the sand types, a 45 minute cycle was conducted at 9 m/h downflow rate through the bed.

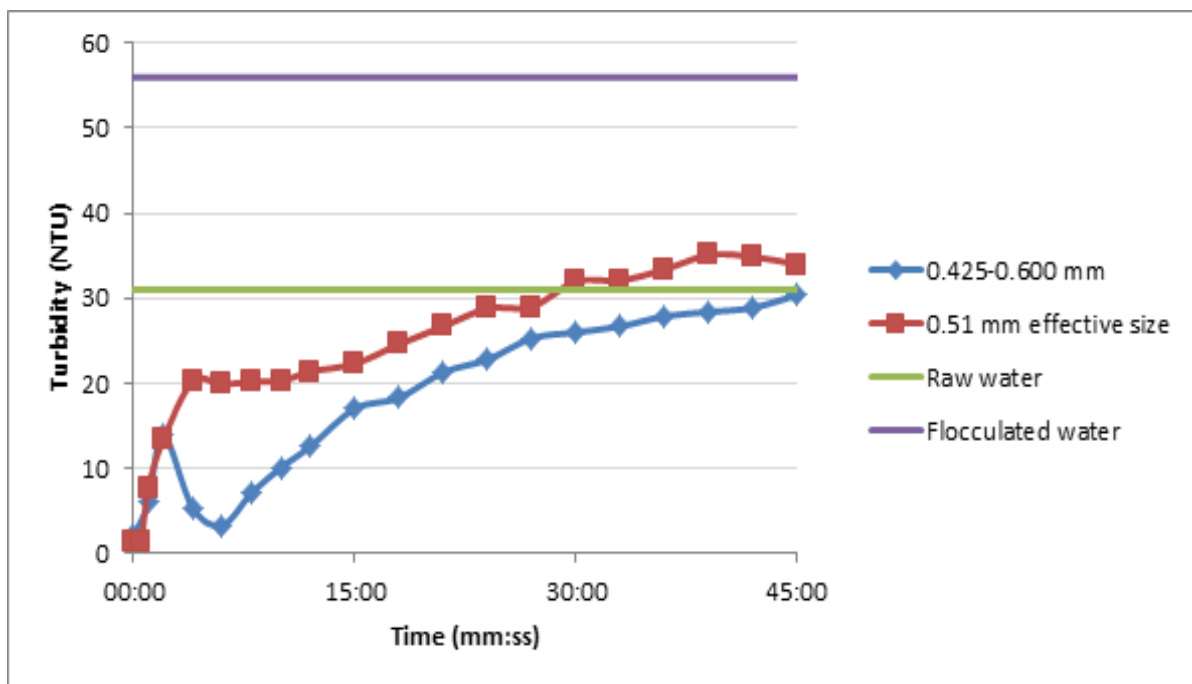


Figure 4-1: Turbidity comparison for different filter media: 150 mm bed; 31 NTU suspension; 9 m/h downflow

The initial spike in turbidity for the screened sand curve is characteristic of a media filter. Filtrate quality is initially poor, and improves once the bed has matured. This is indicative of effective particle capture.

Better floc retention and clarification was immediately apparent for the screened sand, with clarified water being delivered upon bed maturation, and the subsequent increase in turbidity rising more gradually than for the coarse sand. The coarse sand couldn't clarify water to the same extent as the screened sand, as the tortuous paths created between grains were not narrow enough to promote collisions of the destabilised particles and promote floc growth.

Pressure drop over both beds were comparatively similar at around 2.9 kPa, with the most significant difference being the water quality and ability of the bed to retain flocs. Screened sand was used in further testing.

4.1.2 Clean bed pressure drop and correlation with theory

The ability to predict clean bed pressure drop over the media bed was tested. The equivalent surface area to volume ratio sphere was determined from actual pressure drop data to account for the non-sphericity of the particles. This parameter was used to determine the theoretical pressure drop over the bed using the Ergun equation. The procedure and steps are described in more detail in 2.3.5 a).

Media bed voidage

For the 250 mm media bed selected through characterisation experiments, explained in 4.1.3, the voidage of the bed was determined using Equation 2.11. The mass of the dry sand (M) was determined gravimetrically, and by substituting the values for the density of silica, as well as the calculated volume occupied by sand in the filter, the voidage was determined as 0.45.

Following backwashing, the bed remained somewhat expanded at 275 mm rather than at its filled height of 250 mm. At this increased height, the voidage was increased to 0.5. It had to be accounted for in pressure drop calculations by using the correct bed voidage and bed depth.

Leaving the bed expanded was beneficial for operation, as a deeper bed had a greater retention capacity, and a bed with more voidage had more tortuous channels for water to flow through, without compromising filtration effectiveness. Qualitative improvements on filtrate quality were observed at expanded bed depth, with an example of residual turbidity improvement illustrated in Figure 4-2 at an operational flux of 10 m/h.

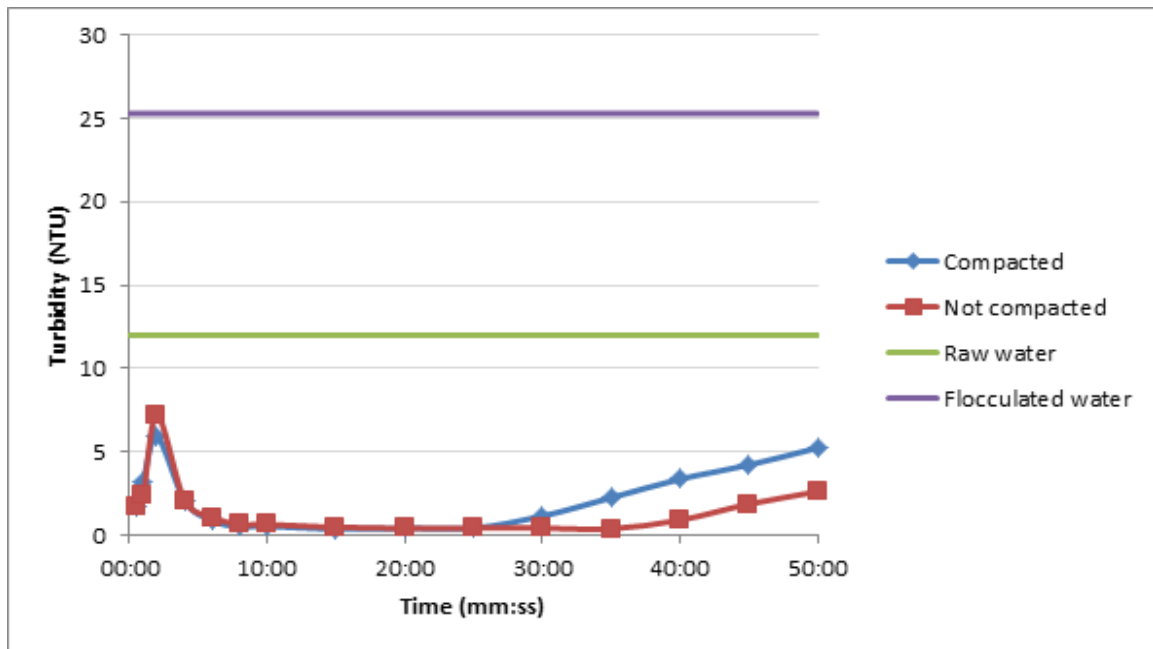


Figure 4-2: Difference in residual turbidity between compacted and non-compacted bed: 250 mm bed; 12 NTU suspension; 10 m/h downflow

Earlier breakthrough occurred when the bed was compacted, showing the benefit of a bed with slightly greater voidage. In this instance, filtrate turbidity exceeded 2 NTU at 35 minutes for the compacted bed, and at 45 minutes for the non-compacted bed.

The three distinct segments typical to these turbidity profiles were observed in Figure 4-2 and subsequent residual turbidity graphs:

1. after backwashing, bed maturation or ripening occurs where residual turbidity increases to a peak value before decreasing
2. low effluent turbidity of around 0.1 NTU is typical of the matured filter filtration cycle
3. breakthrough then occurs if residual turbidity exceeded the predetermined value (1 NTU)

The residual turbidity profiles shown above, as well as the linear pressure drop profiles included in Appendix C, are typical to rapid granular filtration (Crittenden, et al., 2012).

Pressure drop

Flow through the bed was laminar, determined by the Reynolds number for flow through a packed bed (Equation 2.16), and the corresponding term in the Ergun equation (Equation 2.19) was used to determine the theoretical pressure drop through the PF. Calculations and other bed parameters are included in Appendix D. Measured and predicted pressure drop values are given in Table 4-1.

Table 4-1: Correlation between experimental and theoretical pressure drop: 250 mm bed; 12 NTU suspension

Downflow rate (m/h)	Measured dP (kPa)	Theoretical pressure drop Ergun (kPa)
8	1.03	1.14
9	1.25	1.28
10	1.64	1.43
11	1.83	1.57
12	2.11	1.71

The Ergun equation over predicted at low flow rates, and under predicted at high flow rates. This could be because of the degree of non-sphericity of the particles, which could manifest itself as a greater drag effect through the bed in reality at higher velocities. Theoretical pressure drop increased linearly as per the linear relation between pressure drop and downflow rate for laminar flow. Measured pressure drop increased by a non-consistent larger magnitude.

The measured pressure drop over the PF remained consistent for experiments performed at different times. Although the pressure sensor reports an uncertainty of 1%, data remains consistent, and the pressure readings are assumed to be reliably accurate.

4.1.3 PF bed depth

Once the most suitable media type was selected, the depth of the PF had to be selected. It was decided to characterise the PF with a synthetic suspension representative of surface water conditions that occur throughout the largest part of the year. Surface water with turbidity below 20 NTU occurs for around 60% of the year, according to data from a surface water treatment site in the Western Cape. A suspension of 30 ppm bentonite and 20 ppm HA was used to synthesize water with a turbidity of 12 NTU for PF characterisation. The filter would be designed to operate until the breakthrough point was reached (PF filtrate turbidity of 1 NTU), allowing for turbidity removal in excess of 95% from water to be filtered by the membrane.

For feed water with a higher turbidity, the filtration duration selected during PF characterisation would be kept the same, with breakthrough occurring at an earlier point in the filtration cycle. While the PF would not be able to remove the same percentage turbidity as under characterisation conditions, a degree of turbidity removal will still occur. Most importantly, the PF will modify flocs by promoting contact between the coagulated destabilised particles as they flow through the tortuous interstitial filter media paths. Contact would lead to the formation of larger flocs, which should form a reversible cake layer on the membrane. The purpose of the PF is not to act as full-fledged media filter and remove all turbidity for all water

types considered. It should rather act as floc modifier, promoting contact between destabilised particles and remove as much turbidity as possible for the feed solids loading.

A PF designed for highly turbid water would include excessive dead volume for filtration with cleaner water, and would require longer backwashing to displace the head space volume, resulting in poorer recovery. Dirtier water and flood conditions would be used to test the performance of the PF at a later stage to determine the improvement brought about to membrane performance by the shallow PF.

UF operational parameters constrained PF parameters selected during characterisation, as UF properties cannot be altered. Typically an ultrafilter is operated for between 45-60 minutes, with backwashing durations of between 0.5-3 minutes (Ma, et al., 2013), (Zhang, et al., 2009), (Chang, et al., 2015).

Filtration efficiency of different bed depths

Three bed depths were considered and a range of flow rates were tested. Breakthrough turbidity of 1 NTU was used as indicator of ineffective filter performance, and the filtration duration for different downflow rates was noted.

Bed depths of 200, 250 and 300 mm were considered, as beds shallower than 200 mm were inefficient in delivering clean water, as tested for during screening and included in Appendix C. Downflow rates of 8, 10 and 12 m/h were tested to quantify the filtration efficiency of the bed at each depth. Residual turbidity was measured and the pressure logged. Each run was done until breakthrough was evident.

As expected, the shallow bed showed high residual turbidities and rapid breakthrough, especially at higher downflow rates, as the residual turbidity plot in Figure 4-3 indicates. Upon coagulation, feed water entering the PF had a turbidity of 25 NTU, roughly double that of the feed water suspension. Flocculated water turbidity was not included for clearer comparison of data.

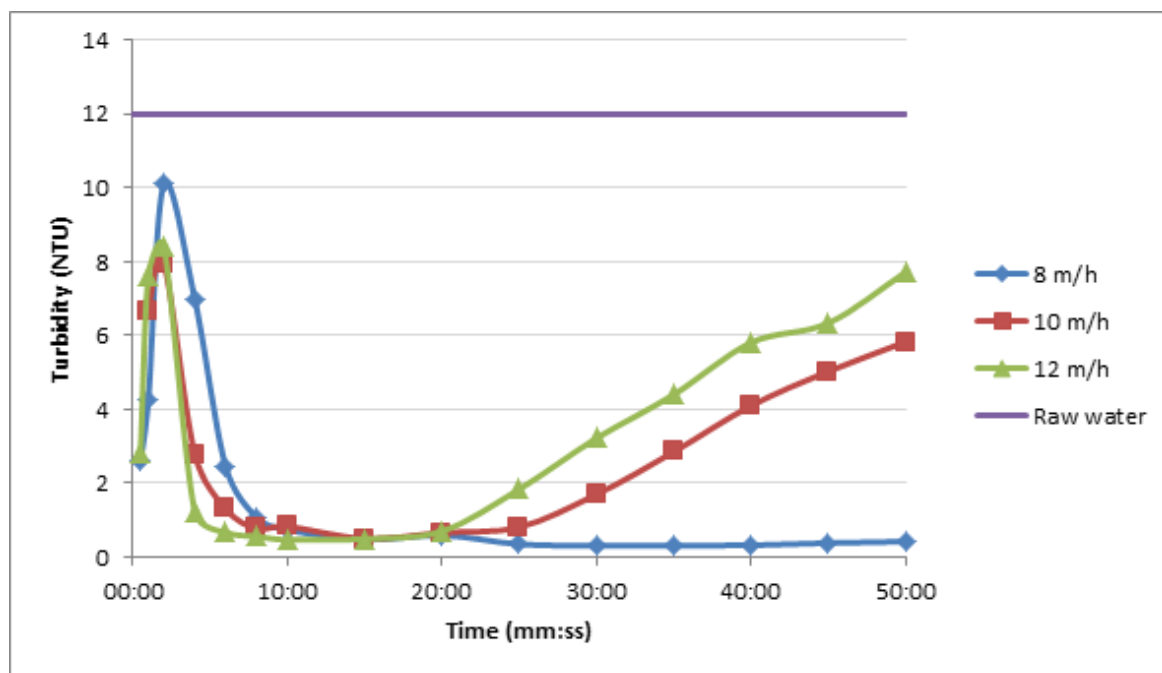


Figure 4-3: Residual turbidity at different downflow rates for 200 mm bed, 12 NTU suspension

The poor retention of particles at even the mid-range downflow rate rendered this bed depth an unviable option. Breakthrough occurred at 30 minutes for the 10 m/h downflow rate. Although the PF can be operated for a long duration at 8 m/h downflow rate before breakthrough occurs, the flow rates usable for operation were too limiting.

The poor particle retention was ascribed to the 200 mm bed not being able to adequately capture flocculated particles to initiate orthokinetic flocculation at a relatively high downflow rate. Water and flocs passing through the bed too rapidly were not retained within the PF bed long enough to aid in the agglomeration of destabilised particles. The effect of downflow rate on the ability of a shallow bed to promote orthokinetic flocculation was most pronounced at this shallow bed depth.

A trend apparent in all the bed depths considered was that at 8 m/h, the PF delivered clean water for much longer than projected from higher downflow rate breakthrough durations. At a low downflow rate, contact between destabilised particles within the media bed was enhanced as particles were not washed through the bed as quickly as at higher flow rates. Orthokinetic flocculation adequately manifests itself and the filter delivers cleaner water for a longer period.

Simultaneously, the residual turbidity curve for the 8 m/h downflow rate appeared to take longer to deliver clean water. Higher downflow rates promoted contact between destabilised particles more rapidly, shortening the required maturation period.

A deeper bed would thus be required to more adequately promote orthokinetic flocculation at the mid and high downflow rate and deliver clean water for longer. The bed depth was further increased to 250 mm, with residual turbidities for the flow rate range considered plotted in Figure 4-4.

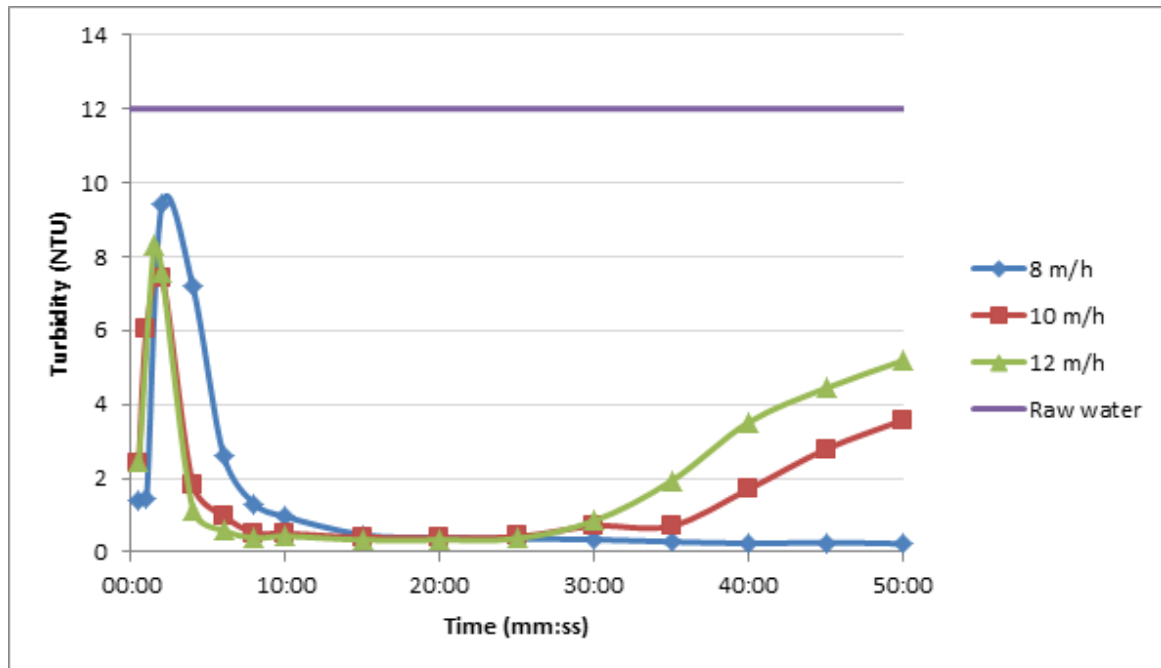


Figure 4-4: Residual turbidity at different downflow rates for 250 mm bed, 12 NTU suspension

Already a significant improvement in performance was seen for the slightly deeper bed. For a bed depth of 250 mm, the filter delivered water with turbidity below 1 NTU for 45 and 35 minutes at 10 and 12 m/h flux respectively. Clean water was delivered for up to 60 minutes for a low flux of 8 m/h.

Upon backwashing, the 250 mm media bed settled to a depth of 275 mm. The additional height of the media bed further contributed to the retention capacity of the bed.

Even longer effective filtration was found at a deeper bed depth of 300 mm, as shown in Figure 4-5.

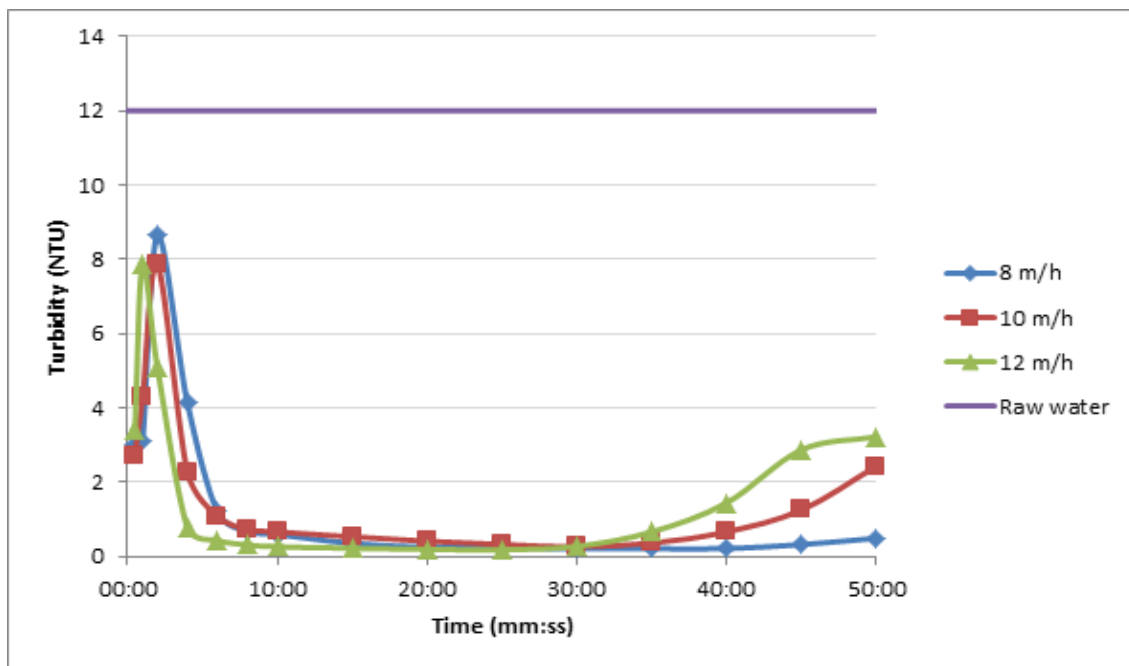


Figure 4-5: Residual turbidity at different downflow rates for 300 mm bed, 12 NTU suspension

Longer particle retention time occurred for the greater bed depth, with even the highest flow rate giving better performance. At 10 and 12 m/h, a 300 mm bed delivered water with a turbidity below 1 NTU for 45 and 40 minutes, as opposed to 40 and 35 minutes with a 250 mm bed. Filtration duration was only increased by 5 minutes for the aforementioned downflow rates. At a downflow rate of 8 m/h, duration was increased by 10 minutes from 70 to 80 minutes.

However, operating with a 300 mm media bed proved problematic for backwashing the bed in the fixed column height of 450 mm. The media bed settled to an expanded height of 330 mm. At the selected backwashing upflow rate, the bed expanded greater than the height of the transparent column. If the expansion height cannot be viewed, there is a risk that sand can be washed out, which will impede the operation of the backwashing solenoid valve and change media bed characteristics. For the same percentage of expansion as the 250 mm bed (52%), a column height of 530 mm would be required if the same head space above the expanded bed was included (safety ± 70 mm: expansion varies for different water compositions). The increased bed depth would increase the total system volume from 6.1 L to 7.3 L resulting in greater losses during backwashing, as the duration of backwashing is correlated to the amount of system displacement volumes. The average recovery for the two systems for the range of flow rates considered would be identical at 81.8%, not warranting the necessity of increasing the column height.

Because the media bed remained slightly more expanded following backwashing, the 250 mm bed was selected. Upon settling, the new height of the bed was 275 mm, which lay between the two best performance depths without the adverse effects found during backwashing of the 300 mm bed. It could be operated for the required duration of between 45-60 minutes at low and medium downflow rate. The 250 mm bed was thus selected for further characterisation.

A linear increase in pressure drop with an increase in flux was observed. The linear and steady increase in the pressure drop for each of the flow rates showed particle capture and growth occurred successfully within the bed. Graphs are included in Appendix C, with information summarised in Table 4-2.

Table 4-2: Pressure drop for various flow rates with 12 NTU suspension

PF depth (mm)	Downflow rate (m/h)	Pressure drop after 50 min (kPa)
200	8	2.3
	10	3.5
	12	4.8
250	8	3.4
	10	4.5
	12	6.3
300	8	4.8
	10	6.9
	12	8.1

Downflow rate

The downflow rate had a significant influence on the effectiveness of filtration. Downflow rates of between 8-12 m/h were initially considered as the operational range, with the duration of clean water production and pressure drop over the bed monitored.

Upon plotting residual turbidity plots for the different bed depths at different downflow rates, it was seen that 12 m/h downflow rate consistently performed worse than the lower downflow rates considered, with residual turbidity exceeding 1 NTU after a period shorter than the predetermined 45 minute minimum. Residual turbidity plots for different bed depths are plotted in Figure 4-6.

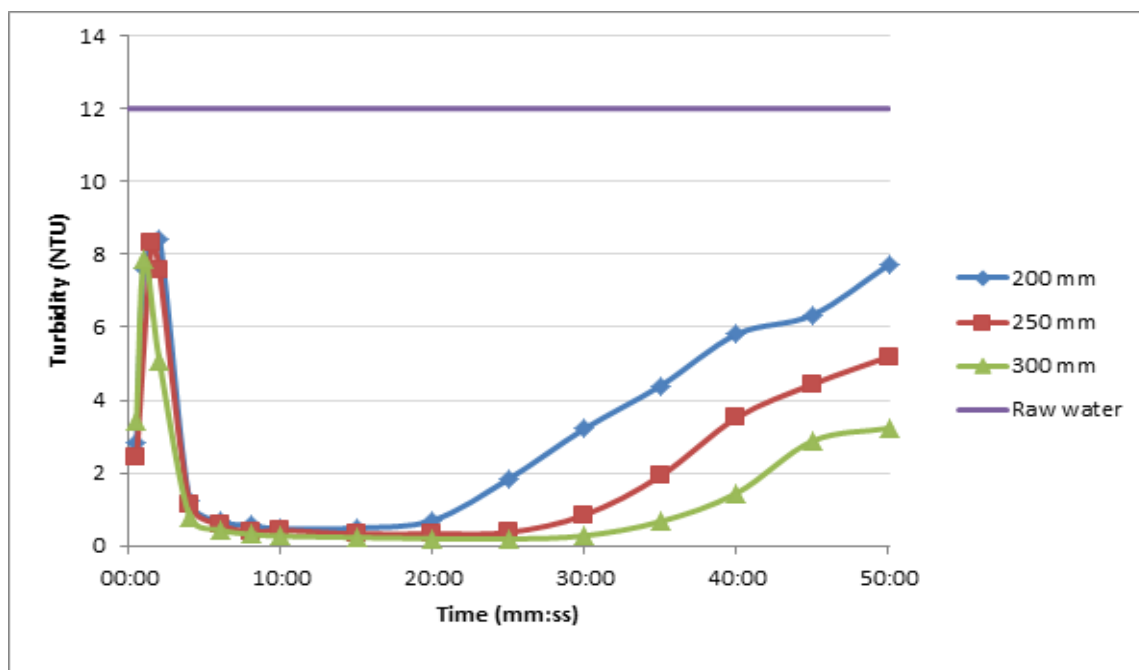


Figure 4-6: Residual turbidity for different bed depths at 12 m/h downflow rate

For water with a greater SS and HA loading, breakthrough would occur even earlier and from an early stage place greater strain on the UF membrane. The high downflow rate was of such a nature that bed maturation and satisfactory particle capture could not adequately manifest itself in the bed, resulting in poor filtrate quality. Very poor retention and short operational span was noted for the 200 mm bed, while the 250 and 300 mm bed performed somewhat better, with breakthrough occurring respectively at 40 and 45 minutes.

Information found in the literature study also suggested not operating at downflow rates exceeding 10 m/h, as a decrease in filtrate quality occurs (Kawamura, 2000). For this reason, the high flux of 12 m/h was not further considered in filtration tests and downflow rates of 8 and 10 m/h were used.

Operational duration

For each of the bed depths and downflow rates considered, the PF could be operated for the following durations before breakthrough turbidity of 1 NTU was reached.

Table 4-3: Media bed depth and flow rate comparison with 12 NTU suspension

Depth (mm)	Downflow rate (m/h)	Filtration duration until breakthrough (min)
200	8	65
	10	30
	12	25
250	8	70
	10	40
	12	35
300	8	80
	10	45
	12	40

The 200, 250 and 300 mm beds could comfortably be operated for 65, 70 and 80 minutes at a low downflow rate before breakthrough occurred. The slow movement of flocculated particles through the bed at a lower flow rate enabled more effective retention of particles within the bed and effective orthokinetic flocculation. At a lower downflow rate, less removal of maturing flocs occurred as the drag of the water through the bed was relatively low. High downflow operation of 12 m/h was discredited due to the short filtration durations obtainable.

4.1.4 Effect of backwashing duration

Following an operational cycle, the PF had to be hydraulically backwashed in order to recover the bed's retention capacity. As the ultrafilter was dependent on vigorous washing, a backwashing flux of 200 LMH was used, and sufficient head space had to be given to the PF to expand within the column at the selected upflow velocity. For the required UF flux of 200 LMH the system needs to be backwashed at 13.3 L/min, equivalent to an upflow velocity of 43 m/h, comparable to rates cited by researchers in Table 2-9.

Backwashing durations were selected based on what is typically recommended for UF membranes, which is a range of 0.5-3 minutes (Ma, et al., 2013), (Zhang, et al., 2009), (Chang, et al., 2015). The durations were correlated with the number of displacement volumes (DVs) of the media filtration system, and is summarised in Table 4-4. The system volume to be displaced is approximately 6.1 L.

Table 4-4: Displacement volumes and backwashing durations for 250 mm bed

DV	Duration to displace DV at 13.3 L/min (s)	Backwashing duration (min)
1 x	27.4	0.5
2 x	54.7	1
3 x	82.1	1.5
4 x	109.5	2
6 x	164.2	3

Several filtration cycles of 50 minutes each were repeated at 10 m/h downflow rate, with a different backwashing duration used in each set of experiments. After 50 minutes at 10 m/h downflow, the PF reached breakthrough, and at this point the filtration cycle was terminated and the bed backwashed. The high downflow rate was used as this would cause the deposition of more particles within the media bed. The backwashing duration selected for the set of filtration cycles had to be able to restore the retention capacity to ensure the delivery of clean filtrate in the following filtration cycle. Residual turbidity was measured in the selection of the most suitable backwashing duration.

For a backwashing time of 0.5 minutes, or one DV, the initial turbidity of the water was too high to be deemed suitable for consideration. Turbidities of between 20 and 80 NTU were observed within the first two minutes of operation, and water was never cleaned to below 1 NTU at any stage. It is for this reason that 2 DVs was considered as the minimum backwashing duration. The complete data sets for the experimental runs are included in Appendix C.

Figure 4-7 summarises the average initial turbidity for each set of experiments with different DVs. Flocculated and raw water turbidity of 25 and 12 NTU are not included in the figure as to enable easier visual comparisons between residual turbidity curves.

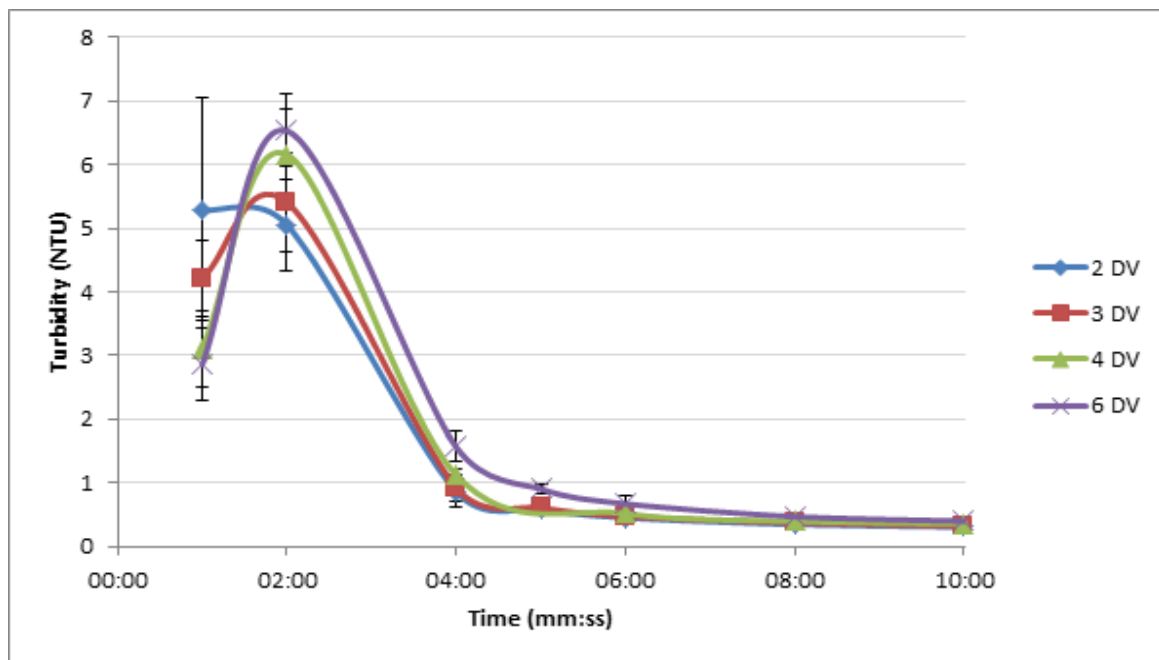


Figure 4-7: Initial residual turbidity after different backwashing durations: 250 mm bed; 12 NTU suspension

Again the residual turbidity peak appeared at 2 minutes, characteristic of the maturation period. Some difference in the magnitude of the initial turbidity was found for different DVs, but for each experimental set it fared well against raw water and incoming flocculated water. Variability of turbidity during bed maturation is largest, with more consistent and repeatable data once the bed has matured. Reliable performance occurs and turbidity remains consistently below 1 NTU. Water with turbidity below 1 NTU was delivered after 5 minutes of operation for all backwashing durations considered.

The longer backwashing durations of 4 and 6 DVs had a slightly higher initial peak. In the case of 2 and 3 DV, some of the remaining flocs that had not been washed out of the bed could have aided bed maturation, acting as seeding particles for orthokinetic flocculation and shortening the maturation period. For water with a greater concentration of incoming foulants, it could be problematic if a fraction thereof remained within the bed following backwashing.

It is the breakthrough period at the end which is of particular interest. Average residual turbidities upon breakthrough are summarised in Figure 4-8.

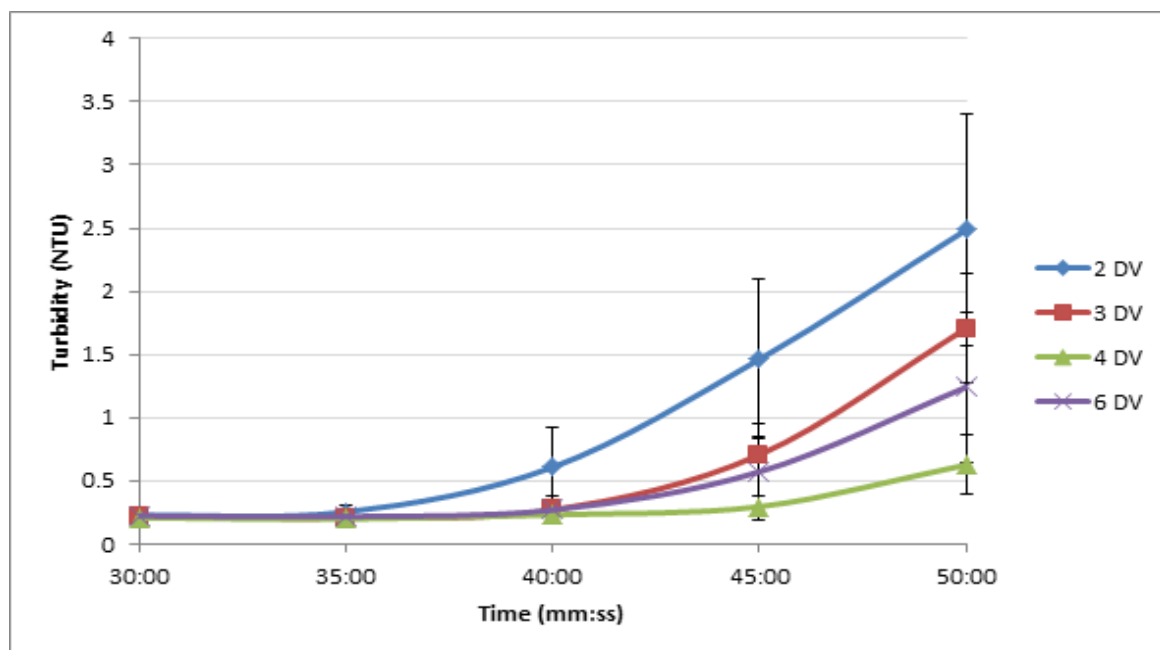


Figure 4-8: Breakthrough at different backwashing durations: 250 mm bed; 12 NTU suspension

For each of the durations considered, breakthrough occurred at around 45 minutes with a relatively small difference in performance. Two and three DV backwashing durations showed slightly earlier breakthrough, which could have been because of the residual flocs remaining in the PF after the shorter backwash. The presence of residual flocs could decrease the bed's retention capacity, resulting in the earlier breakthrough.

Lowest residual turbidity at the end of the filtration cycle occurred when 4 DVs were washed out during backwashing. Operating at 4 DVs gave good filtrate performance, while losing less water and operating at a greater recovery than would be the case for a 6 DV wash. The variability of terminal turbidity was smallest for 4 DV backwashing. Backwashing the PF for the duration of 4 DVs, or 2 minutes, was considered the optimal duration. The partial remainder of flocs after a 4 DV could aid in promoting floc growth and retention, while these aiding flocs are washed out after a 6 DV wash. Selecting a 4 DV wash gives more favourable recovery percentages than washing the bed for a duration of 6 DVs.

Figure 4-9 illustrates the difference in head space water colour at the end of a backwashing cycle.

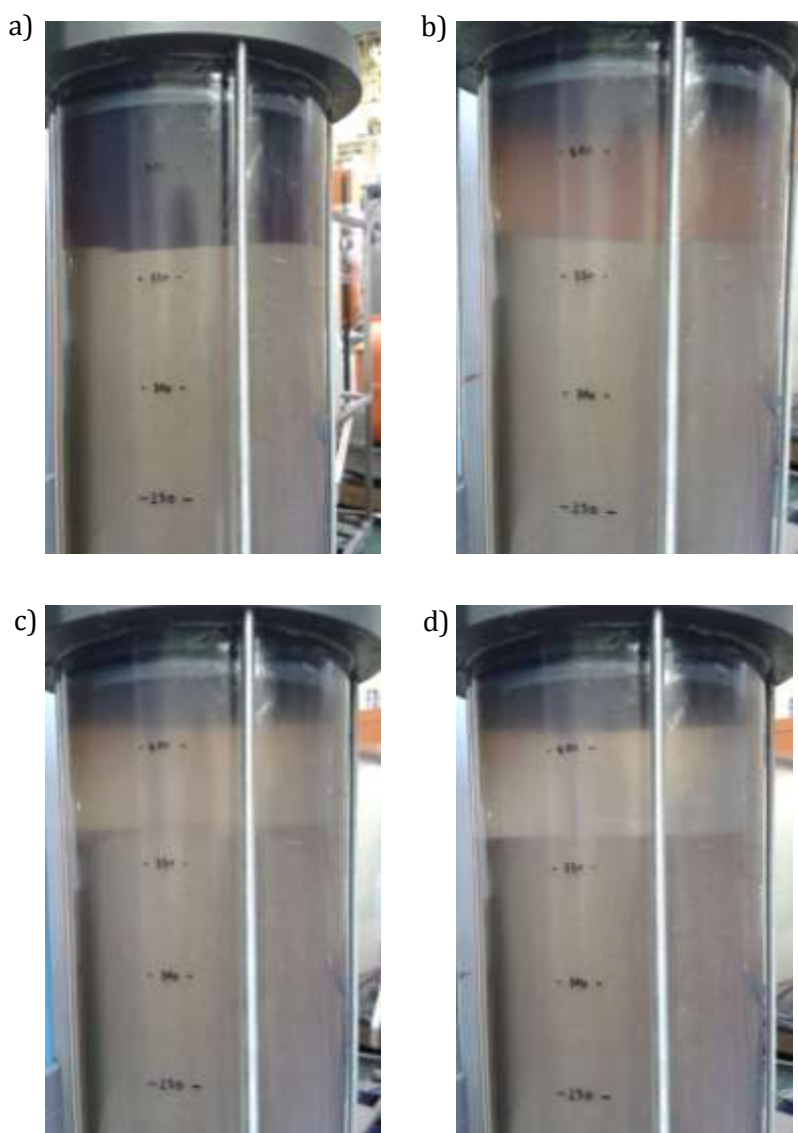


Figure 4-9: Effect of backwashing duration on water colour above fluidised expanded 250 mm bed.

a) 2 DV; b) 3 DV; c) 4 DV; d) 6 DV

The visual differences for water above the head space at the end of backwashing also indicated that 4 DVs is the minimum requirement to adequately clean PF filter media. Following 2 and 3 DV backwashing, the water remaining in the PF had a greater concentration of foulants present than for the 4 and 6 DV washes.

Recovery

The backwashing duration selected also affected the recovery of the system. Backwashing water was not recycled back to the filter, and as filtrate was used to backwash the bed, backwashing water is equal to lost product water. It is important to maximise the recovery of the system where possible. For filtration at 10 m/h downflow rate, a filtration cycle of 50 minutes is

attainable before breakthrough exceeding 1 NTU occurred. When the backwashing duration was varied, different recoveries were achieved, as summarised in Table 4-5.

Table 4-5: Recovery at different backwashing durations: 250 mm bed

Backwashing duration (min)	Displacement volumes	Recovery (%)
0.5	1	94.5
1	2	90.3
1.5	3	86.0
2	4	81.8
3	6	73.3

Recovery calculations included water lost during CEB, and was based on the amount of cycles completed in 24 hours. As stated in the previous section, 2 minutes backwashing was considered to be most favourable. Recovery was still greater than 80% for this duration, but can be increased if the two filters are operated past the PF breakthrough point.

Based on the operational durations until breakthrough for the flow rates considered, the following recoveries could be obtained following 2 minute backwashing:

Table 4-6: Recovery for different flow rates and durations: 250 mm bed

Downflow rate (m/h)	Duration (min)	Backwashing duration (min)	Recovery (%)
8	70	2	82.6
9	60	2	82.1
10	50	2	81.8

Recoveries were very comparable for the different filtration rates, due to the longer possible filtration durations at a lower downflow rates. Greater recoveries would be observed if the bed was operated past the breakthrough point, but for the aim of designing the PF for clean water filtration, the breakthrough point at 1 NTU was selected as the maximum operating point. For dirtier water, breakthrough would occur earlier.

4.1.5 PF particulate removal efficiency

Turbidity removal efficiency

The efficiency with which the PF removed turbidity was compared for different downflow rates filtered through the 250 mm bed. Water composition at 20 mg/L HA and 30 mg/L bentonite remained consistent. Removal efficiency could be expressed as the percentage turbidity causing components removed from the water over the course of a filtration cycle. Turbidity information are compiled in Figure 4-10 for comparison of filtration effectiveness.

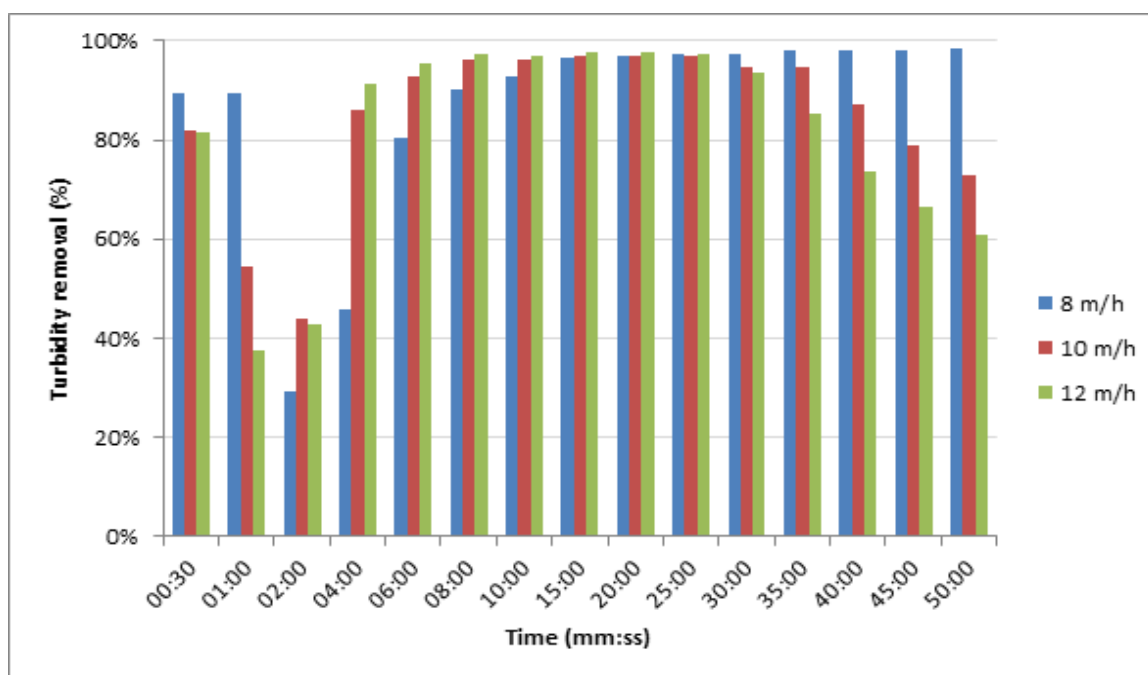


Figure 4-10: Percentage turbidity removal for 250 mm bed at different downflow rates; 12 NTU suspension

For each of the downflow rates, the poorest retention of turbidity causing components occurred at 2 minutes, with significant improvement thereafter until breakthrough occurred. Following maturation and before breakthrough occurred, turbidity removal exceeding 95% occurred for all downflow rates. Effectiveness was initially better but also deteriorated at a more rapid rate for higher downflow rates. Low downflow rate removed turbidity causing compounds for a longer duration following a more gradual maturation period.

UV-Vis removal of HA

In this project, UV Visible spectroscopy was not used as determining measurement in the selection of operating parameters. While HA present in the water would absorb the light at 254 nm, bentonite present in the filtrate would scatter light, affecting the reading and creating uncertainty around HA concentration. If samples were filtered prior to UV analysis, some of the HA could be removed if it adsorbed to bentonite. For this reason, residual turbidity is used during testing to select PF parameters during characterisation, as both bentonite and HA also contributed to this reading, and measurements could be made easier and more rapidly with the available equipment.

In order to determine what percentage of components that absorbed visible light at 254 nm was removed through the PF, and remained to foul the UF membrane, PF filtrate was analysed and compared to raw water absorbance. Water with 20 mg/L HA and 30 mg/L bentonite was used,

and filtered at 10 m/h downflow rate for 50 minutes, as done in previous characterisation experiments. Percentage removal is plotted in Figure 4-11.

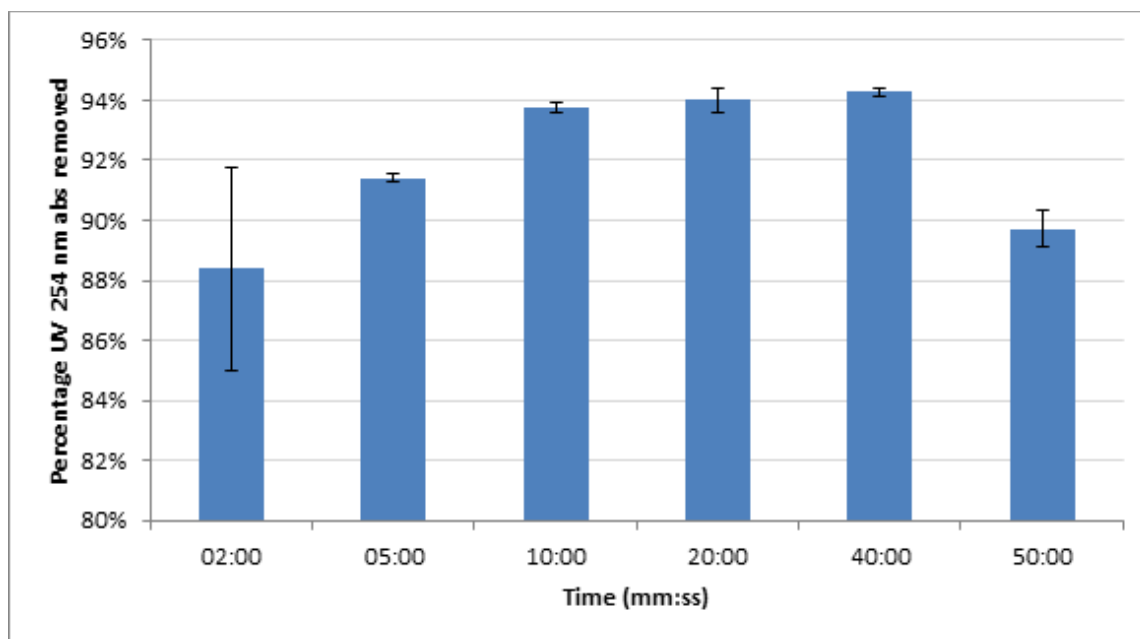


Figure 4-11: Percentage 254 nm absorbance removed from 12 NTU water at 10 m/h downflow

A much higher percentage removal of components absorbing UV visible light occurred, even before the PF bed had matured and even upon breakthrough. Removal percentages exceeding 88% consistently occurred. Initial removal at 2 minutes is variable as the bed had not yet matured and its potential to remove compounds in the water had not been fully reached. Greater removal of UV visible light components occurred compared to 30-40% turbidity removal prior to maturation, and 60-70% turbidity removal upon breakthrough.

It was postulated that coagulation had a more significant destabilising effect on HA in the water, and most of the HA were captured within flocs formed in the depth of the bed. The effectiveness with which orthokinetic flocculation of destabilised NOM occurred in the PF was very evident in especially the high initial removal rate of UV absorbance. The PF consistently effectively removed the majority of UV absorbance, which was assumed to be representative of HA. As HA is predominantly responsible for irreversible fouling of the membrane (Wang, et al., 2008), it could be seen that the PF would play a significant role in the reduction of irreversible fouling even at low percentage turbidity removal.

4.1.6 Continuous filtration of synthetic water

In order to gauge the PF capacity for HA removal, and the subsequent effect that particles that break through the PF had on membrane pressure drop, the combined set-up was filtered in series for an extended duration. The high turbidity synthetic suspension was used, with HA

concentration of 25 mg/L and bentonite concentration of 100 mg/L (turbidity of 31 NTU). Low turbidity water was not continuously filtered as it would take longer to develop a significant pressure drop profile over both filters. This test was not repeated with flood condition suspensions, as the concern existed that long term continuous filtration could irreversibly damage the UF membrane.

Figure 4-12 indicates the pressure drop experienced over the PF. The filtration cycle was terminated once a predetermined head loss of 5 kPa was found over the UF membrane. A downflow rate of 10 m/h, and 46 LMH flux through the membrane, was used as this would enhance the deposition of particles.

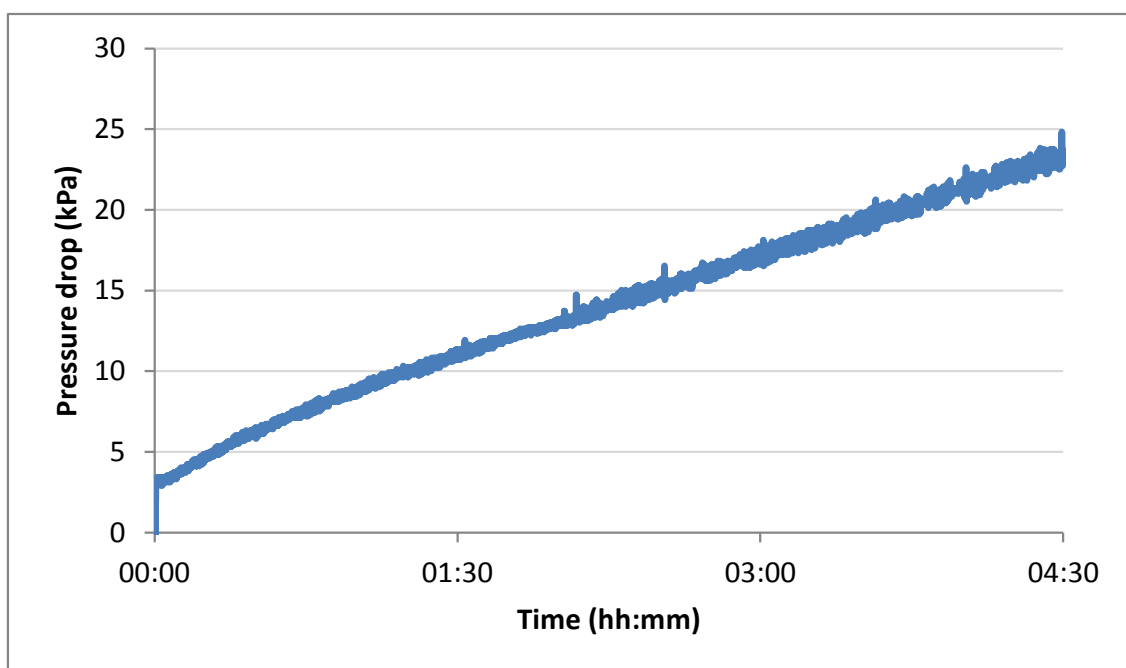


Figure 4-12: PF pressure drop over 250 mm bed for continuous filtration of 31 NTU suspension

A very high pressure drop occurred over the PF because of the high solids loading in the water. The pressure drop increased from the clean bed pressure drop of 2 kPa by approximately 20 kPa to the final pressure drop of 23 kPa. Pressure drop kept increasing linearly throughout experimentation, although it was expected that pressure drop would plateau once complete breakthrough had been reached. In order to determine the breakthrough profile, residual turbidity following the PF was plotted in Figure 4-13.

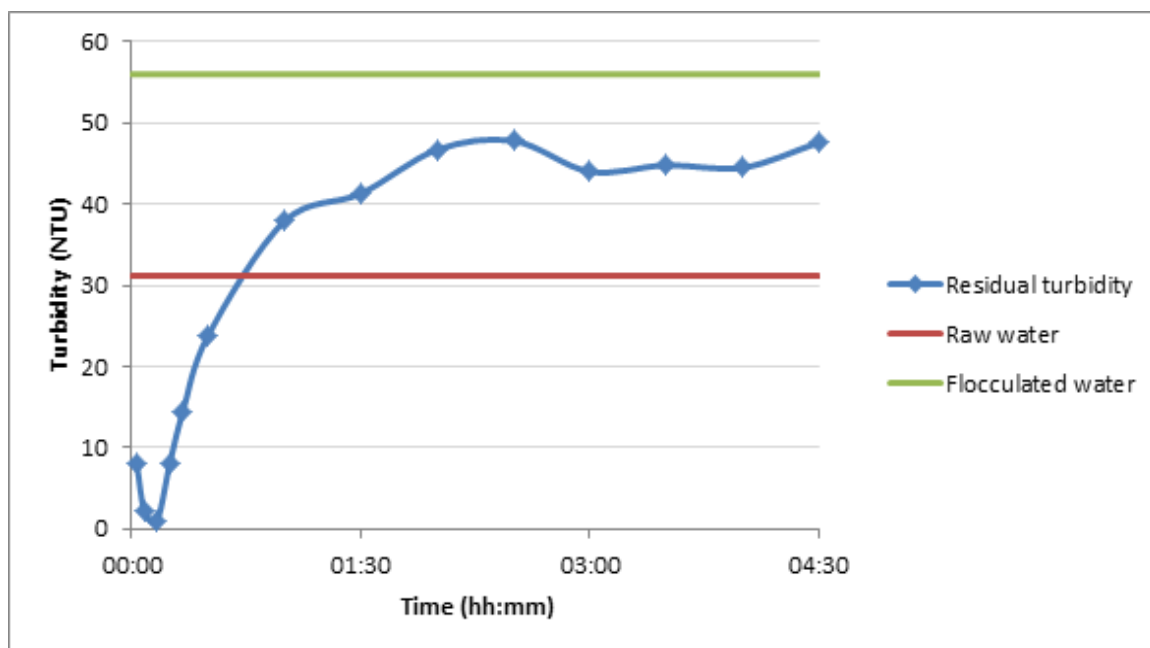


Figure 4-13: Residual turbidity curve past PF breakthrough: 250 mm bed; 31 NTU suspension

Breakthrough occurred after 15 minutes of filtration, with residual turbidity exceeding raw water turbidity after 45 minutes. The residual turbidity following PF never exceeded the turbidity of flocculated water entering the PF, meaning breakthrough was never complete. Orthokinetic flocculation continued to take place within the depth of the bed, which resulted in the growth and retention of flocs within the bed and continued increase in pressure drop.

Due to the high turbidity of the PF filtrate, a loading of solids was placed on the UF membrane with subsequent increase in TMP plotted in Figure 4-14.

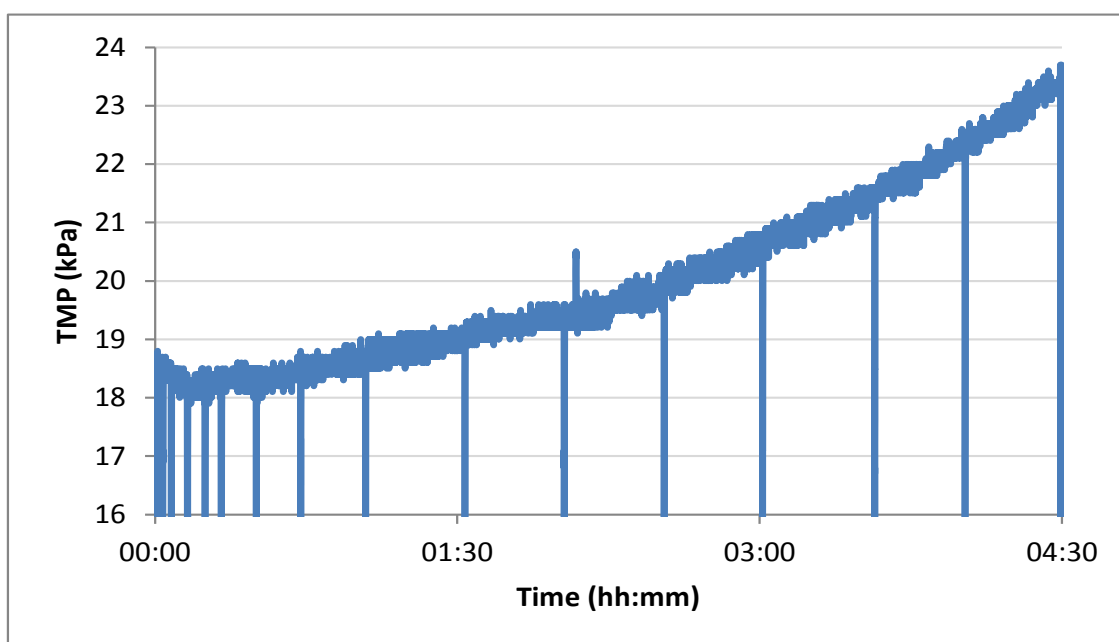


Figure 4-14: TMP increase for PF operation past breakthrough: 250 mm bed; 31 NTU suspension

Deposited particles contributed to the membrane resistance and increased the TMP by 5 kPa. The majority of the loading was carried by the PF. Fouling was reversible, with the permeability of the membrane restored upon backwashing. The continuous modification of flocs within the PF retained flocs that would otherwise have contributed to the TMP increase.

4.2 UF membrane

4.2.1 Clean filter flux

Throughout the operation of the filter, fouling will increase the TMP required to maintain a constant flux through the membrane. The TMP required at a later stage can be compared to initial clean filter TMP to determine to what extent the permeability of the membrane had been compromised by fouling.

The TMP for the fluxes considered, was calculated from logged pressure drops and pressure gauge readings at the five fluxes of interest. Sample calculations are included in Appendix D with TMP summarised in Table 4-7:

Table 4-7: Clean membrane TMP

PF downflow rate (m/h)	UF flux (LMH)	Feed P (kPa)	Feed exit P (kPa)	TMP (kPa)
8	37.1	27.5	10	17.5
9	41.7	28.4	10.5	18
10	46.3	29.8	11	18.8
11	51.0	30.8	11.5	19.3
12	55.6	31.9	12	20

TMP readings were relatively close to each other. Throughout an experimental cycle, TMP would increase and be restored following hydraulic backwashing. If fouling is irreversible, TMP could be used as an indicator for when CEB or CIP should be initiated. As more fouling takes place, an increase in TMP would occur, manifesting itself as a higher required driving force to overcome the fouling resistance and maintain a constant filtration flux.

4.2.2 Continuous filtration of synthetic water

In order to determine how the membrane performs under extended filtration periods, the low and high turbidity suspensions were filtered through the membrane. Incoming water was coagulated and directly filtered through the membrane until a predetermined pressure drop or filtration duration had been reached.

Low turbidity suspension (12 NTU)

The low turbidity water (30 mg/L bentonite and 20 mg/L HA) was flocculated directly onto the membrane at 46 LMH, with the pressure increase before the membrane being monitored with a manometer. Measurements were translated to TMP values and are plotted in Figure 4-15.

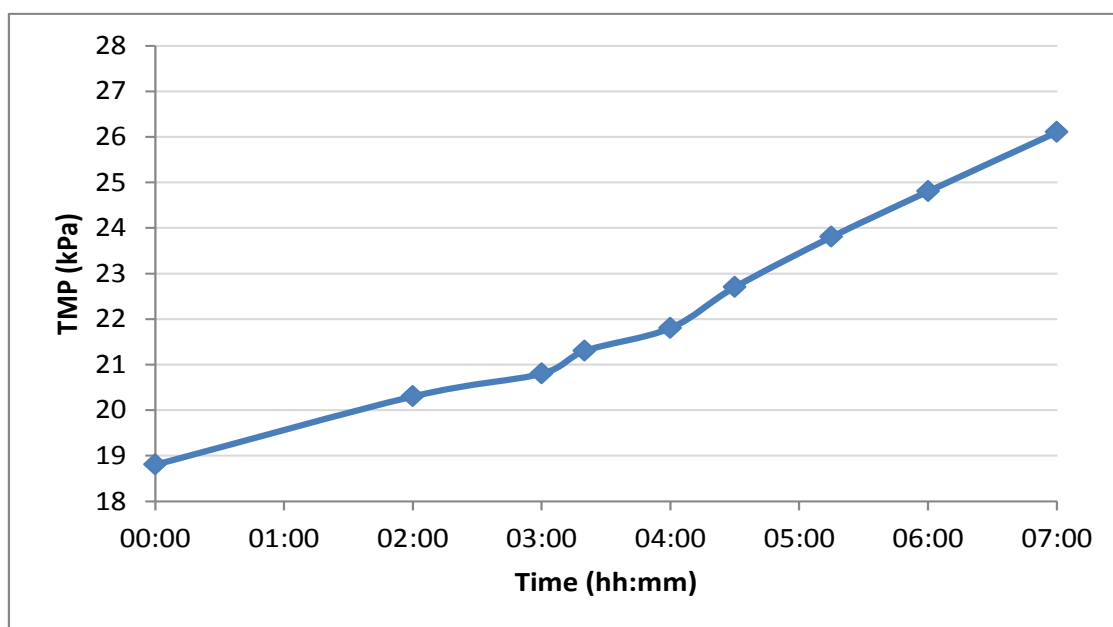


Figure 4-15: TMP for direct flocculation onto membrane with 12 NTU suspension at 46 LMH

Due to the low solids loading of the water and the large filtration area of the membrane (relative to the PF), the pressure recorded before the membrane increased at a rate of 1 kPa every hour. After 7 hours of flocculation onto the membrane, a TMP increase of 7.4 kPa was measured.

High turbidity suspension (31 NTU)

Continuous flocculation onto the membrane surface was repeated with the 31 NTU synthetic surface water suspension (100 mg/L bentonite and 25 mg/L HA). A high flux of 46 LMH was used and a TMP pressure drop curve was constructed with manometer and gauge measurements in Figure 4-16.

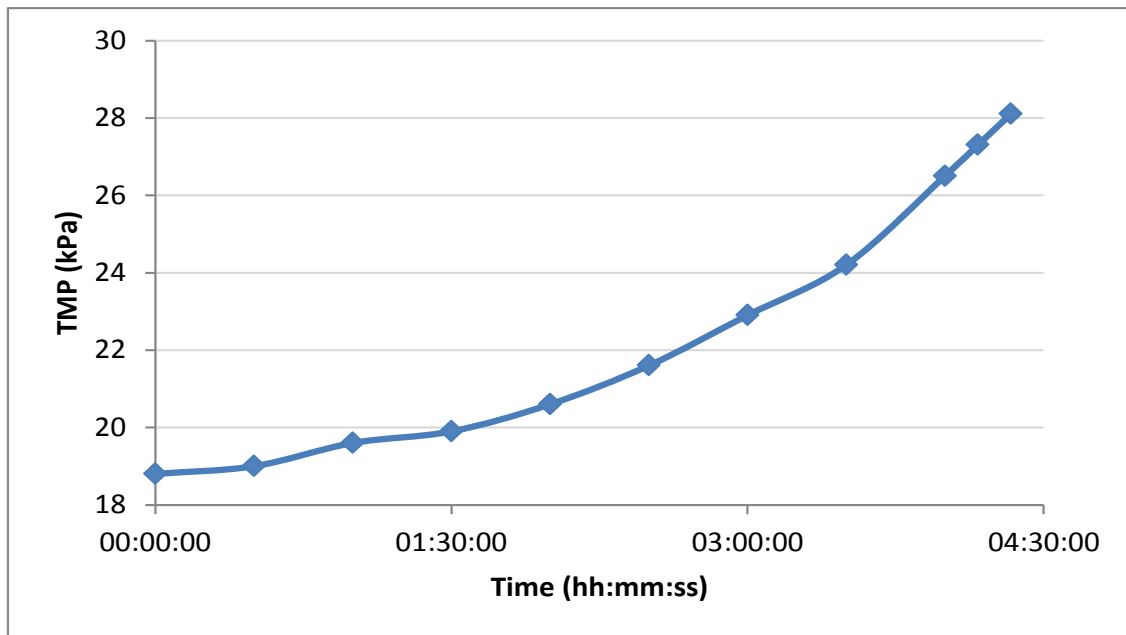


Figure 4-16: TMP for direct flocculation onto membrane with 31 NTU suspension at 46 LMH

A much more rapid increase in TMP of 9.3 kPa occurred after 4 hours 20 minutes of direct filtration. For the same filtration duration and flux, high turbidity suspension filtration including pre-treatment caused a TMP increase of 5 kPa. The PF removed 45% of the load that would have been deposited onto the membrane through retention. The addition of the PF does pose additional pressure drop in the system, but the removal of loading from the membrane is significant, and would protect it from sudden influx of high solids concentration to prevent damage and replacement.

4.3 Flood condition water composition selection

The concentrations of HA and bentonite in the flood condition suspensions were determined following initial testing with direct filtration of the two synthetic suspensions.

The highest concentration of HA for surface water treatment with UF found in literature was 50 mg/L (Fu, et al., 2008). The concentration of HA for high organics loading was selected at approximately 50% greater as 70 mg/L, in order to exaggerate the fouling effect. At this organics loading, it was expected that an increase in initial TMP will occur as a result of irreversible fouling.

The selection of bentonite concentrations for the flood condition suspension was primarily based on predicted pressure drop attainable. At a solids loading of 400 mg/L bentonite, a turbidity of 116 NTU is predicted. For similar filtration conditions to previous tests (46 LMH flux at 50 minutes filtration for direct flocculation onto the membrane), a TMP increase of 3 kPa

was predicted when correlated with the mass of suspended solids deposited directly onto the membrane. This was considered suitable for the investigation of the improvement brought about to UF performance by the PF under high SS conditions. The predicted turbidity is greater than the maximum surface water turbidity of 77 NTU observed at a Western Cape surface water treatment plant in the previous operational year.

CHAPTER 5 : EFFECTIVENESS OF COMBINED SHALLOW BED FILTRATION AND ULTRAFILTRATION

Following the characterisation of both filters, improvement in UF operation brought about by shallow media bed pre-treatment was evaluated. Tests were conducted using the various synthetic suspensions considered (HA concentrations of 20, 25 and 70 mg/L; bentonite concentrations of 30, 100 and 400 mg/L). The suspension was firstly filtered through the membrane alone, then through the PF and membrane under the same conditions. The TMP increase over the membrane was compared for the two sets of experiments to determine what contribution the PF makes to removing loading from the membrane for different water compositions. The increase in initial TMP was also monitored to determine whether irreversible fouling occurs.

5.1 Low turbidity suspension filtration (12 NTU)

Filtration with the low turbidity suspension (made up of 20 mg/L HA and 30 mg/L bentonite) was conducted both at a low and high flux. In-line coagulation was used at all times. The suspension was firstly filtered through the membrane alone, before adding the PF and determining the loading removed from the membrane and improvement brought about by pre-filtration.

During PF characterisation, it was seen that the PF removed in excess of 95% of turbidity from the low turbidity water, with the filtrate turbidity remaining below 1 NTU for the largest part of the cycle. Filtration durations selected during characterisation was used for filtration at the respective flow rates.

5.1.1 Low flux filtration (8 m/h; 37 LMH)

Filtration through membrane alone

To determine how much loading was deposited on the membrane during low flux filtration, water was coagulated and filtered firstly through the membrane alone. Water was filtered through the membrane alone for 70 minutes as well for comparison between UF performance with and without pre-treatment.

Due to the low solids loading, very gradual TMP increase was apparent as shown in Figure 5-1.

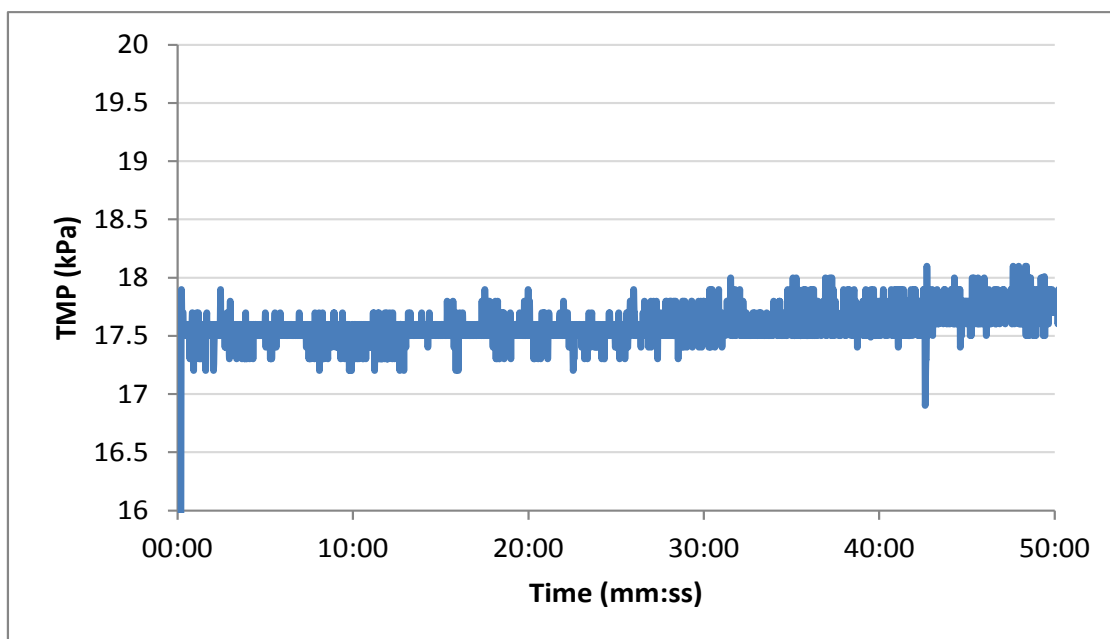


Figure 5-1: TMP for direct filtration at 37 LMH of flocculated 12 NTU suspension

The increase in TMP was approximately 0.4 kPa, which was low due to the low solids and organics loading. Another reason for the low increase in TMP was that the flocculated particles deposited on the UF filtration area were significantly larger than those deposited in the PF. For periods between rainfall when turbidity is low (around the 12 NTU used in testing), it appears that the membrane alone can handle the influx of incoming particles. However, operating without pre-treatment could be detrimental if the process isn't monitored carefully, and water quality suddenly changes.

The UF membrane was capable of removing 99%+ of turbidity, as UF filtrate turbidity was consistently below 0.2 NTU. Coagulated flocs retained by the membrane contributed directly to TMP increase.

Filtration through PF and UF

The low turbidity water was filtered at 8 m/h downflow rate through the PF, with corresponding flow through the membrane of 37 LMH. Operation is done for 70 minutes until breakthrough starts occurring through the PF, with backwashing conducted for 2 minutes. The resulting pressure drop is plotted in Figure 5-2, indicating loading retained by the PF.

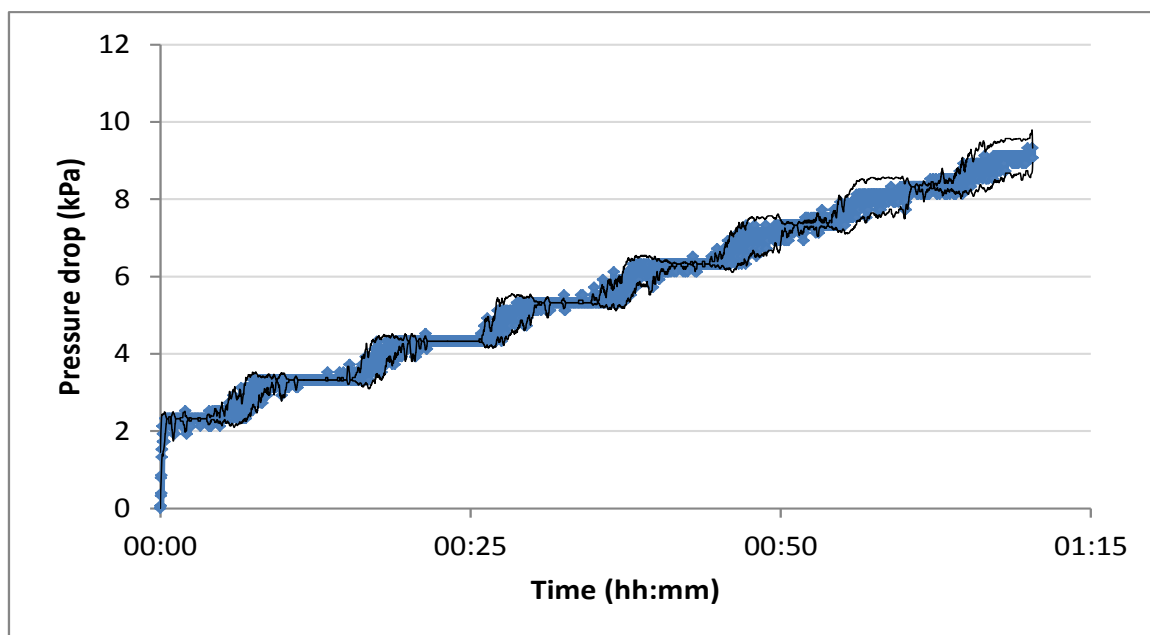


Figure 5-2: Pressure drop over PF for 8 m/h filtration of 12 NTU suspension

Pressure drop over the PF was approximately 7 kPa over the course of a 70 minute filtration cycle. The black lines above and below the blue plotted data points indicate the error of the readings, determined from the standard deviation of the data. Six filtration cycles were conducted with the average pressure drop and standard deviation plotted in Figure 5-2.

Floc growth within the bed manifests itself as increased resistance and thus as pressure drop over the bed. Pressure drop increases linearly and the filter was operated until filtrate turbidity reached 1 NTU, as plotted in Figure 5-3. Upon breakthrough, backwashing was initiated.

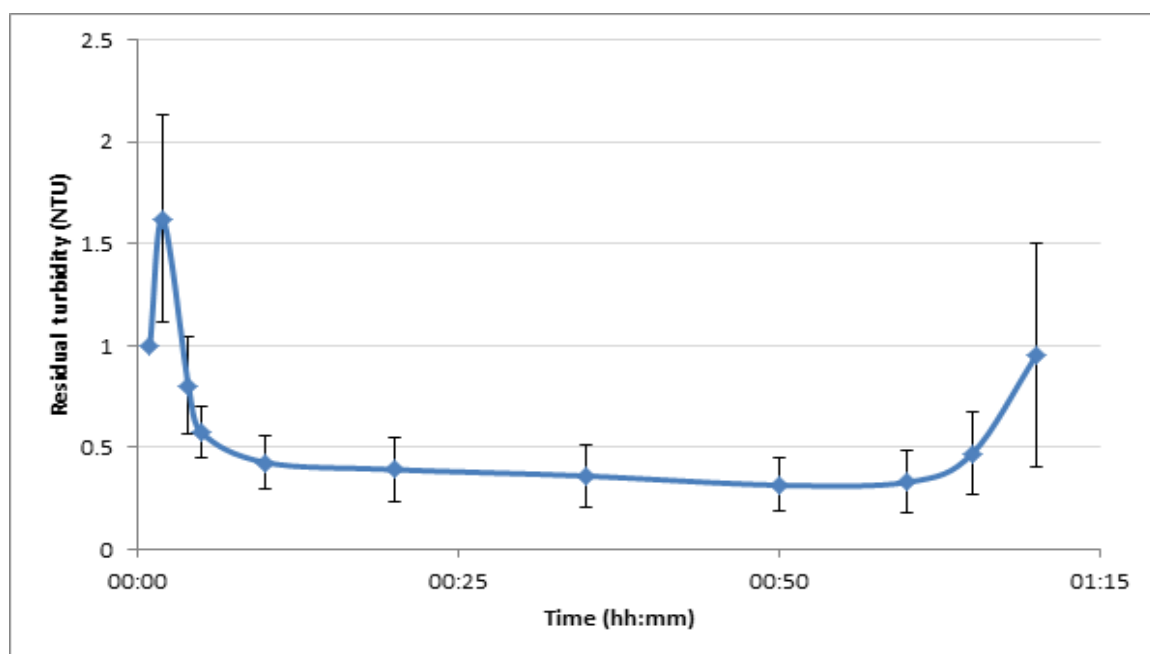


Figure 5-3: Average residual turbidity after PF for 8 m/h filtration of 12 NTU suspension

Even for initial turbidity spikes, residual turbidity was very low, indicative of the low loading that remained to be filtered by the membrane. The PF was very effective in reducing turbidity of the filtered water. Flocculated water entering the PF had a turbidity of 25 NTU, with 98%+ of incoming turbidity removed once the PF had matured.

For the six repeated filtration cycles, readings were most variable during maturation and breakthrough. Initially turbidity varies due to poor particle retention in the bed, which does not deliver a very consistent initial turbidity. While breakthrough occurs at consistent intervals, the magnitude of turbidity upon breakthrough varies. The matured filtration cycle is netter defined with small deviations in turbidity readings.

A very low load of suspended components remained after pre-filtration for deposition onto the membrane, which is evident from the TMP curve plotted in Figure 5-4.

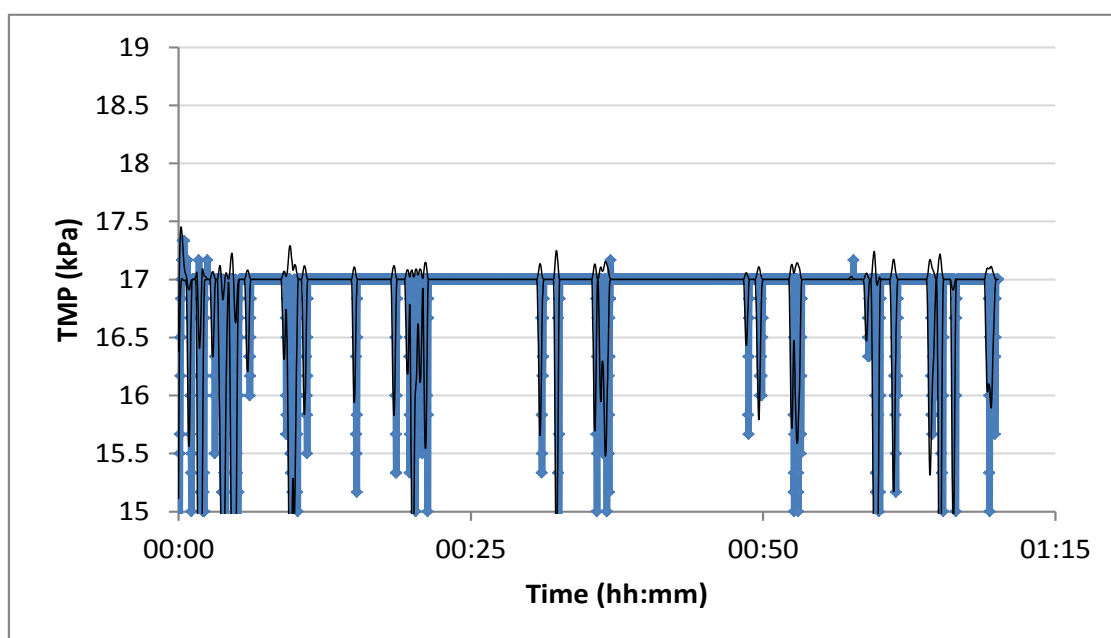


Figure 5-4: TMP for 37 LMH filtration of water filtered by the PF

No discernible increase in TMP occurred due to the insignificant amount of particles remaining in the PF filtrate for deposition. The PF effectively retained a large proportion of flocs, leaving the UF membrane to mainly perform a disinfection function only rather than clarification as well.

5.1.2 High flux filtration (10 m/h; 46 LMH)

The tests conducted previously were repeated at a higher flux, in order to deposit more particles and gain a larger difference between performance with and without pre-filtration.

The loading of solids in the water remained low, but were transported through both filters at a more rapid rate. During characterisation with low turbidity water it was found that the PF could be operated for 50 minutes at 10 m/h downflow rate before breakthrough occurred, which should be followed by 2 minutes of backwashing. These conditions were used for filtration tests and repeated filtration cycles are carried out.

Filtration through membrane alone

Operation for 50 minutes of flocculating onto the membrane at a flux of 46 LMH brought about a TMP increase of 0.4 kPa, shown in Figure 5-5.

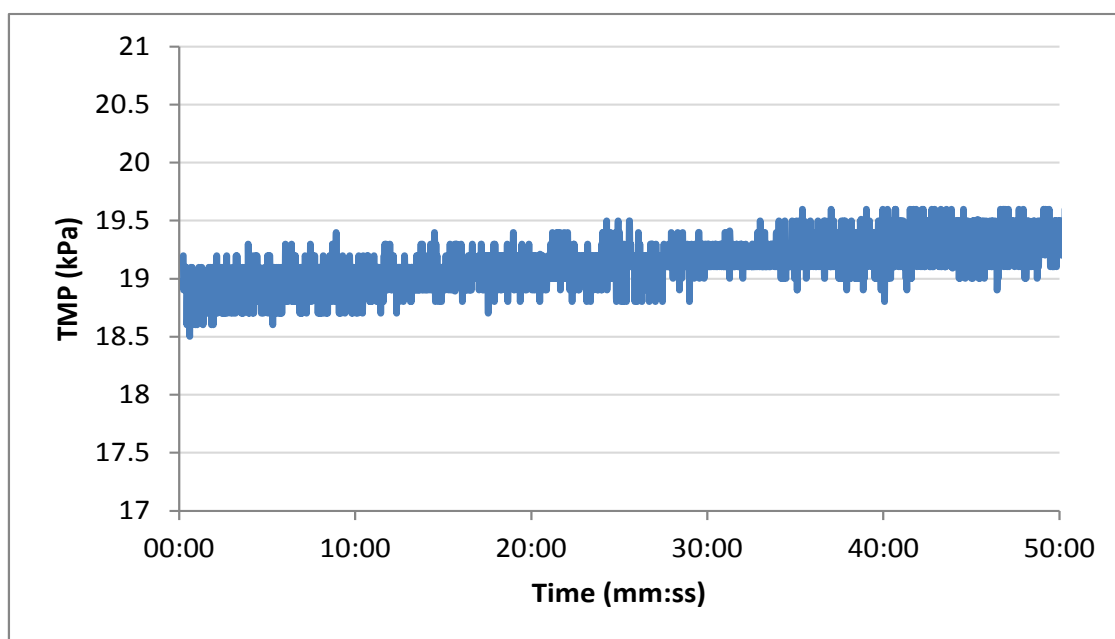


Figure 5-5: TMP for direct filtration of flocculated 12 NTU suspension at 46 LMH

The 0.4 kPa increase in TMP was the same increase as for direct flocculation and filtration through the membrane alone at 37 LMH. This was expected, as the mass of particles deposited are very similar for the two experiments: at a low flux and longer duration of 70 minutes, 8.5 g of suspended and dissolved particles are deposited on the membrane. At a higher flux with shorter filtration duration, 7.9 g material is deposited. It is assumed that all components in the synthetic water deposited onto the membrane, as filtrate turbidity was consistently less than 0.2 NTU.

The rate of deposition is the varying factor. It has been reported that it is more beneficial for long term use to operate at a lower flux (Drioli & Giorno, 2009), than to operate at a higher flux with the same fouling resistance contributed by deposited particles.

Filtration through PF and UF

Nine filtration cycles of 10 m/h downflow rate through the PF, and 46 LMH flux through the membrane, were carried out. Water was filtered for 50 minutes before being backwashed for 2 minutes. Again for the higher flux, water was filtered until PF breakthrough occurred, alleviating loading from the membrane by allowing only for relatively clean filtrate to be filtered by the membrane. The resulting pressure drop profile for the PF is plotted in Figure 5-6.

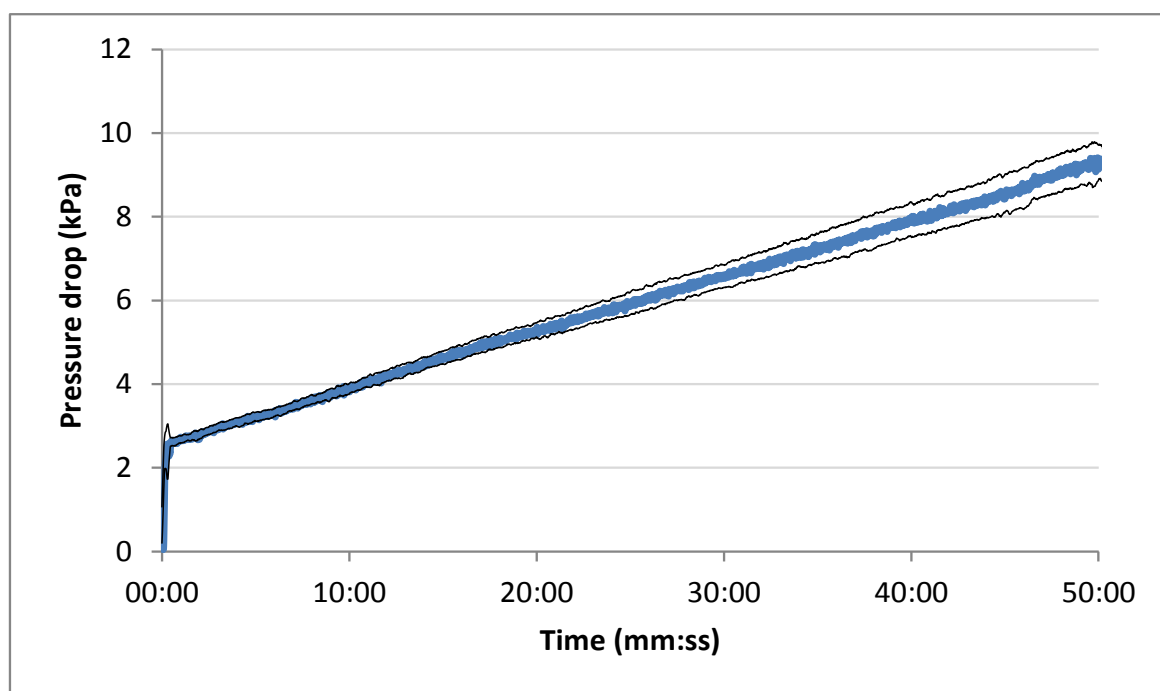


Figure 5-6: Pressure drop over PF for 10 m/h filtration of 12 NTU suspension

The media bed retained a large fraction of flocs, with linear pressure drop curves occurring consistently for the nine repeated cycles up to 7 kPa over the PF. The 2 minute backwashing period between cycles was sufficient to remove retained particles in order to restore the PF's retention capacity, which was also evident in initial filtrate quality. Filtrate had a very low particulate loading and low residual turbidity, with water with turbidity below 1.6 NTU delivered throughout the entire filtration cycle as shown in Figure 5-7.

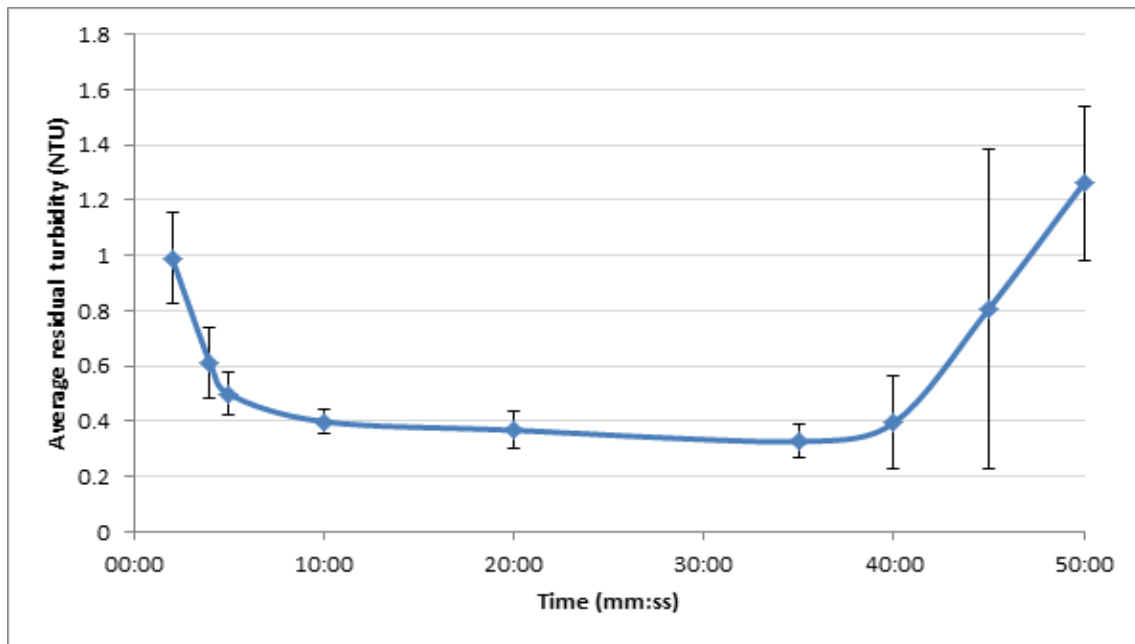


Figure 5-7: Average residual turbidity following PF for 10 m/h filtration of 12 NTU suspension

The PF filtration run was terminated once the turbidity exceeded 1 NTU. The PF removed a minimum of 83% turbidity with a negligible amount of solids passing through to the UF membrane. The initial turbidity spike during bed maturation is lower than for lower filtration flux. The maturation of the PF is thus enhanced at a greater filtration flux, as contact between destabilised particles occurs at a greater rate and accelerates floc growth and retention.

Due to the low solids loading of water exiting the PF, once more membrane operation remains at constant TMP for the nine repeated cycles, as shown in Figure 5-8.

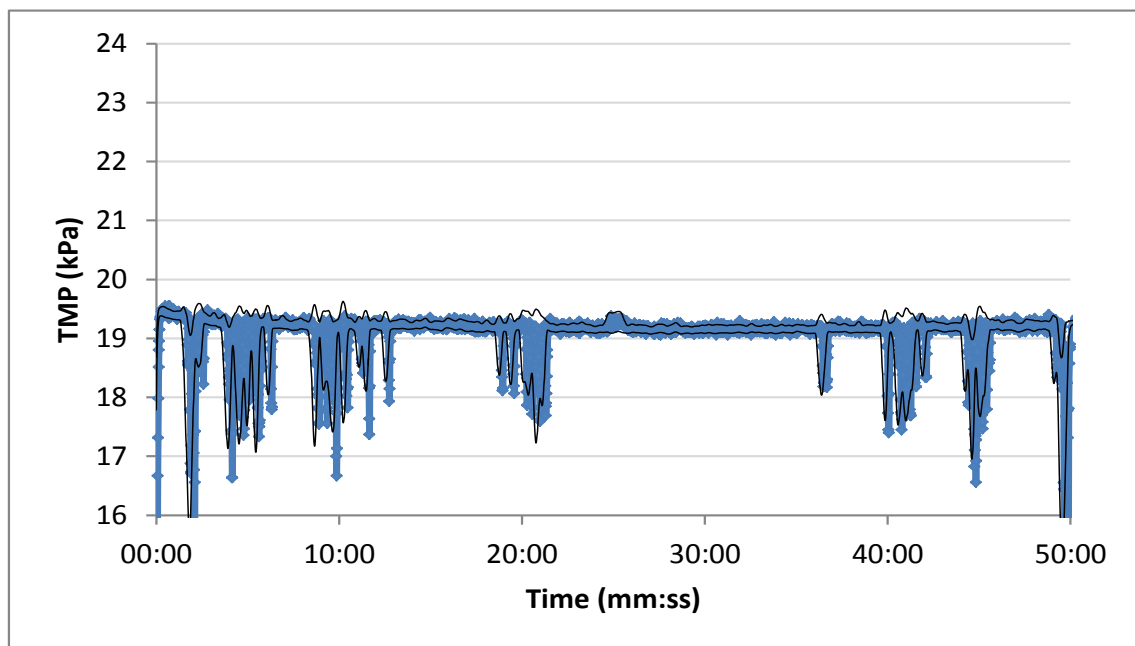


Figure 5-8: TMP for 46 LMH filtration of PF filtrate

Similar to lower flux operation through both filters, there is still a very small load of materials deposited on the membrane with no discernible increase in pressure. This is indicative of the effectiveness of particle retention by the PF.

At both a low and high flux, with termination of filtration at the PF breakthrough point, the PF retains the majority of flocs that would have otherwise deposited onto the membrane surface and caused an increase in TMP. Without pre-filtration, a TMP of 0.4 kPa would occur over the membrane at both fluxes considered. With pre-filtration, no discernible increase in TMP was noted over the membrane.

While for low turbidity the filter was operated only until breakthrough point, operation of the filter past breakthrough point and the subsequent effect on TMP is investigated next.

5.2 High turbidity suspension filtration (31 NTU)

The high turbidity suspension was used next to induce a more drastic pressure drop and TMP profile for both filters, and to gauge the performance of the PF and membrane at greater solids loading. At these conditions, breakthrough would occur much earlier than the low turbidity water for which PF operational parameters were selected. Rather than act as complete buffer to the membrane, the PF would rather act as floc modifier, allowing for agglomerated flocs to pass through the bed and deposit onto the membrane. The same filtration and backwashing flow rates were used as determined during characterisation.

High flux filtration of 46 LMH and 10 m/h was used, and filtration duration was extended to 60 minutes in order to get more radical results and further increase loading on the membrane. Through a longer duration, the improvement brought about by the addition of the PF would be more apparent. It is postulated that operation past the characterisation duration would be possible to increase overall system recovery from 82% at a high flow rate, to 84.5%. If no detriment is noted to the performance of the UF membrane at these conditions, it could be possible to increase recovery by extending filtration duration slightly.

The high turbidity water is made up of 25 mg/L HA and 100 mg/L bentonite, resulting in a raw water turbidity of 31 NTU. Once flocculated, the water had a turbidity of 56 NTU, which is the turbidity of water entering the first filter in the selected configuration.

5.2.1 Filtration through membrane alone

For higher flux operation, it was decided to operate the system at a duration longer than used in the clean water tests – at 60 minutes for 46 LMH rather than 50 minutes. The backwashing duration remained 2 minutes as determined in PF characterisation.

Operating the membrane under direct flocculation for five repeated cycles resulted in an average TMP profile plotted in Figure 5-9.

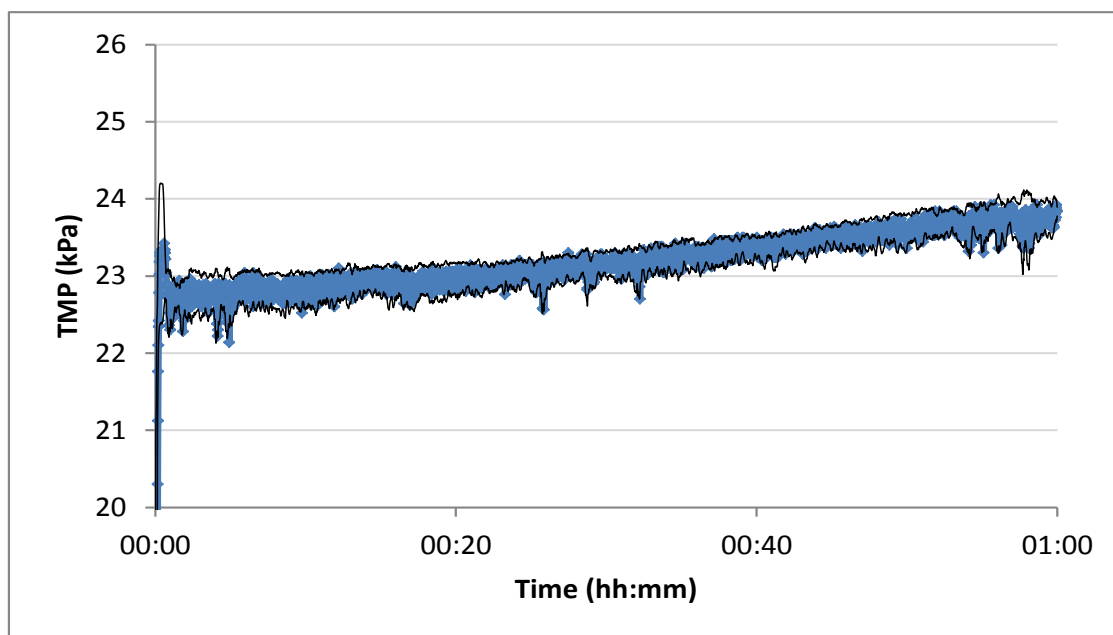


Figure 5-9: TMP for direct filtration of 31 NTU suspension at 46 LMH

The slightly higher initial TMP value is due to irreversible fouling from previous tests. The membrane had been CEB'ed prior to testing, and the increase in TMP was of importance. Black lines again indicate standard deviation from the average calculated TMP for five filtration cycles conducted successively. Initial TMP for each cycle was established and no increase had occurred.

Over the course of a 60 minute filtration cycle, an increase in TMP of approximately 1.2 kPa was noted. Following hydraulic backwashing, it appeared the membrane permeability was restored to the same initial TMP, indicating the reversibility of the fouling. Following five consecutive filtration cycles, the initial TMP remained the same, and no irreversible fouling occurred.

The TMP increase was proportional to the weight of deposited particulates. For low turbidity suspension direct filtration through the membrane, where HA and bentonite were present in 50 mg/L total, a TMP increase of 0.4 kPa was noted. After 50 minutes of direct filtration, the high turbidity water with HA and bentonite concentration of 125 mg/L total resulted in a TMP

increase of 1.2 kPa. The TMP seems linearly correlated with the mass of particles deposited onto the membrane. Again the membrane removed 99%+ turbidity with a consistently low filtrate turbidity not exceeding 0.2 NTU.

As HA is known to irreversibly foul membranes (Zularisam, et al., 2006), (Crozes, et al., 1997), it was thought that an increase in initial TMP would occur following sequential filtration cycles. It appeared that HA did not irreversibly adhere to the membrane, which could indicate that coagulation effectively destabilised HA. It could also be due to the known interaction taking place between the HA and bentonite. The HA could adsorb to the bentonite, creating a larger and easier filterable floc which does not block membrane pores and does not have the electrostatic potential to adsorb to the membrane. The number of cycles the experiment was repeated for is not sufficient to confidently make aforementioned assumptions, but for the specific set of filtration data at this duration it appeared true.

5.2.2 Filtration through PF and UF

The high solids loading water was filtered at 10 m/h downflow rate through the PF, and 46 LMH flux through the UF for 5 successive 60 minute cycles, with intermittent 2 minute backwashing. The pressure drop over the PF is plotted in Figure 5-10.

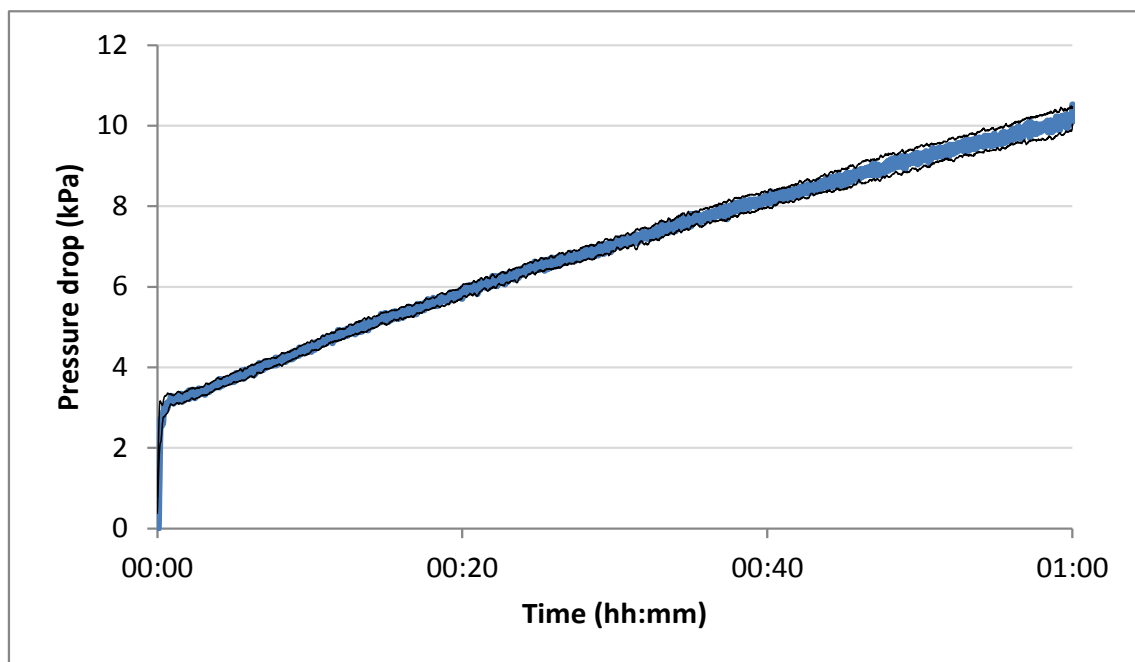


Figure 5-10: Pressure drop over PF for 10 m/h filtration of 31 NTU suspension

Consistent pressure drops of 7 kPa per cycle were observed for 5 repeated 60 minute cycles. Even for the longer filtration duration, the 2 minute backwashing period was effective in recovering the PF's retention capacity, as consistent pressure drop occurred with high quality

filtrate delivered for a short period upon bed maturation. Operation of the PF is continued well past the breakthrough point, as can be seen in the residual turbidity graph in Figure 5-11.

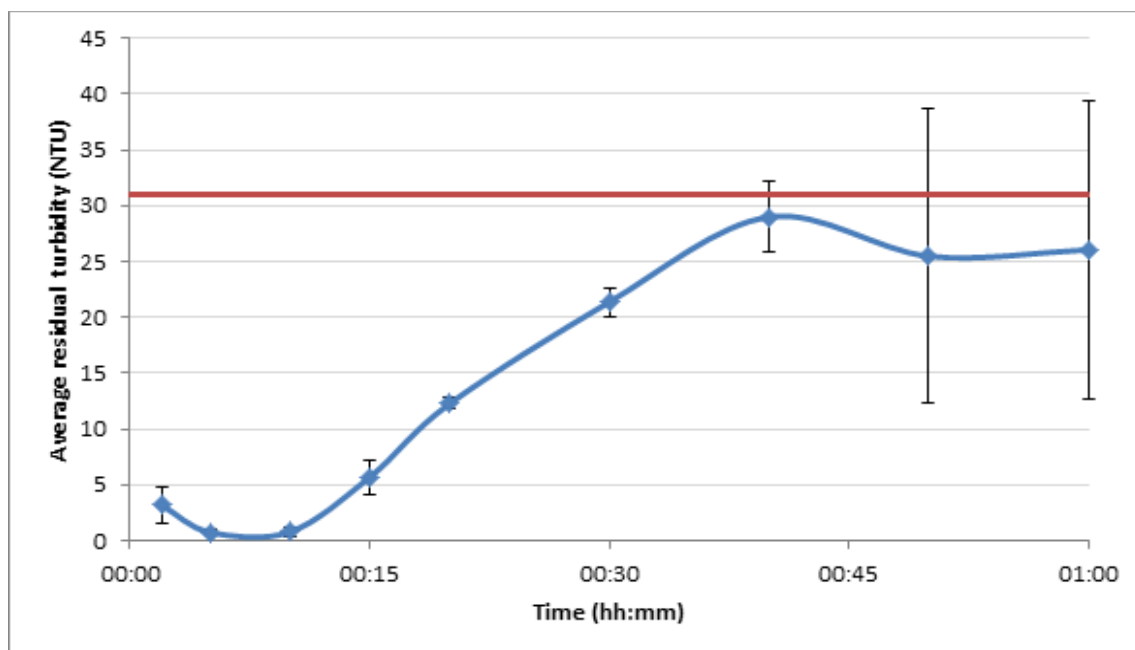


Figure 5-11: Average residual turbidity following PF for 10 m/h filtration of 31 NTU suspension

Effective particle retention initially occurred following bed maturation, with residual filtrate turbidity below 1 NTU delivered for the first 10 minutes of operation. Breakthrough occurred before 15 minutes, after which point residual turbidity increased until the turbidity was equal to the raw water turbidity at 40 minutes. Turbidity did not increase further, and remained lower than the incoming flocculated water turbidity of 56 NTU. This was indicative of orthokinetic flocculation continuously taking place within the depth of the bed, growing and retaining flocs and removing a fraction of incoming material. The continuous flocculation was also evident from the PF pressure drop plot, which did not plateau and kept increasing once breakthrough had occurred.

Operating the PF past breakthrough meant more solids could be deposited onto the membrane surface, which should indicate a larger rise in TMP. The membrane received a solids loading with a turbidity ranging from 2 to 30 NTU for the 45 min remainder of the filtration cycle following breakthrough, and the TMP profile is plotted in Figure 5-12.

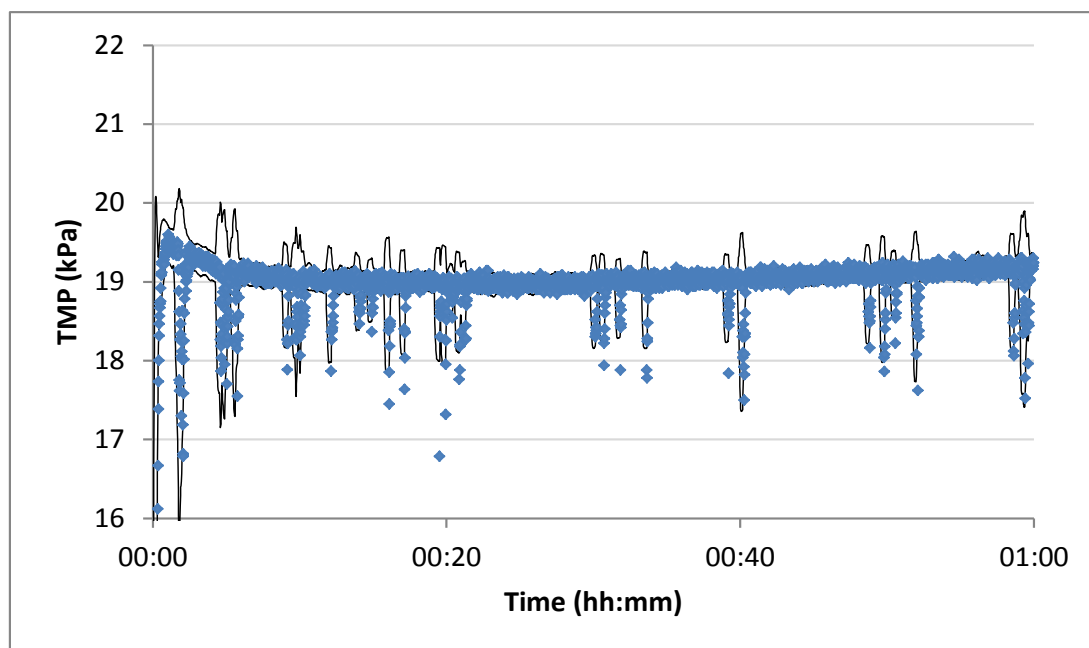


Figure 5-12: TMP for 46 LMH filtration of PF filtrate

A slight increase in the TMP was observed following an initial decrease. TMP was initially high but settled to a lower value which gets restored following hydraulic backwashing in subsequent cycles. Over the course of a 60 minute cycle, an average TMP increase of 0.3 kPa was noted consistently for the 5 successive filtration cycles conducted.

When compared to the TMP increase without pre-filtration, which is 1.2 kPa, it was found that the addition of pre-treatment removes 75% of the loading which would otherwise deposit onto the membrane. A slight difference in temperature between the two experiments occurred. The improvement brought about by the PF is discussed with normalised data in 5.4.

5.3 Flood condition suspensions

Following flood conditions, after heavy rainfall, two suspensions, respectively with a high solids loading and high organics loading, were selected for testing. The bentonite and HA suspensions were made up separately, due to the interaction that exists between the particles. With separate suspensions, the effect of each component on fouling could be seen separately to determine what performance improvement the use of a PF brings about.

TMP was slightly higher at this stage, as the membrane had been irreversibly fouled throughout the course of test work. This is however not a problem as it was the increase in TMP per experimental cycle that was of interest.

5.3.1 High solids loading (400 mg/L SS, 156 NTU)

A suspension of 400 mg/L bentonite (with no HA added), was selected for the high solids loading experiment, as discussed in 4.2.2. The predicted membrane TMP was more severe than in previous tests, but the loading is not made too radical as to cause permanent damage to the membrane.

This suspension was initially tested at a high flow rate, but due to the fine nature of the particles, it was not considered viable for operation within the selected parameters of 50 minutes filtration and 2 minutes backwashing. Similar problems occurred when attempting to filter the water at 8 m/h for 70 minutes. The loading of bentonite deposited in the bed gets too high after the aforementioned volumes of water have been filtered by the PF. Upon backwashing, the fines retained by the bed aided in expanding the bed volume beyond the visible column height due to the increased resistance imposed. The 2 minute duration selected during characterisation was also insufficient to clean the bed and restore its retention capacity following backwashing.

It was thus decided to operate the filter at a low flux of 8 m/h through the PF, and 37 LMH flux through the membrane. The operational duration had to be lowered to 50 minutes from 70 minutes. For 70 and 60 minute filtration through the PF, the mass of solids deposited in the bed was too high, and adequate backwashing after 2 minutes was not achieved. For 50 minutes of filtration, PF expansion during backwashing remained within the visible range, and the selected backwashing duration was sufficient to clean the PF and regain its retention capacity.

Filtration through membrane alone

The flocculated high SS water had a turbidity of 273 NTU, which was firstly directly filtered through the membrane for 8 successive filtration and backwashing cycles. A low filtration flux of 37 LMH was used, and the filtration duration was shortened from 70 minutes to 50 minutes, due to limitations in PF operation. The TMP profile is plotted in Figure 5-13.

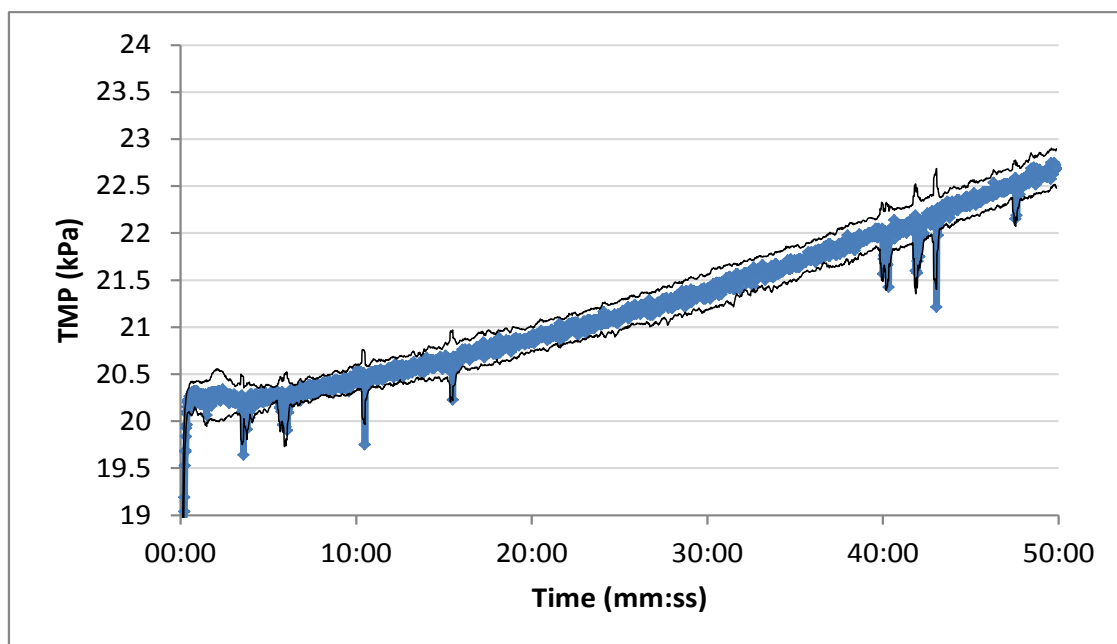


Figure 5-13: TMP for direct filtration of flood SS suspension at 37 LMH

TMP increases by 2.8 kPa for direct flocculation onto the membrane. Eight repeated cycles with 2 minutes of backwashing gave consistent TMP increases with no increase in initial TMP. The nature of fouling could have been reversible, or the backwashing duration was sufficient for foulant removal.

The turbidity removal by the UF membrane remained 99%+, with permeate turbidities below 0.2 NTU delivered throughout. The lack of increase in initial TMP was indicative that membrane pores did not suffer damage through clogging, which could cause irreparable damage to the membrane.

Filtration through PF and UF

Pre-treatment was then included by firstly filtering water through the PF, with filtrate filtered through the UF membrane. The experiment was run at 37 LMH flux for 50 minutes filtration, interspersed with 2 min backwashing between the eight filtration cycles. The PF pressure drop profile is plotted in Figure 5-14.

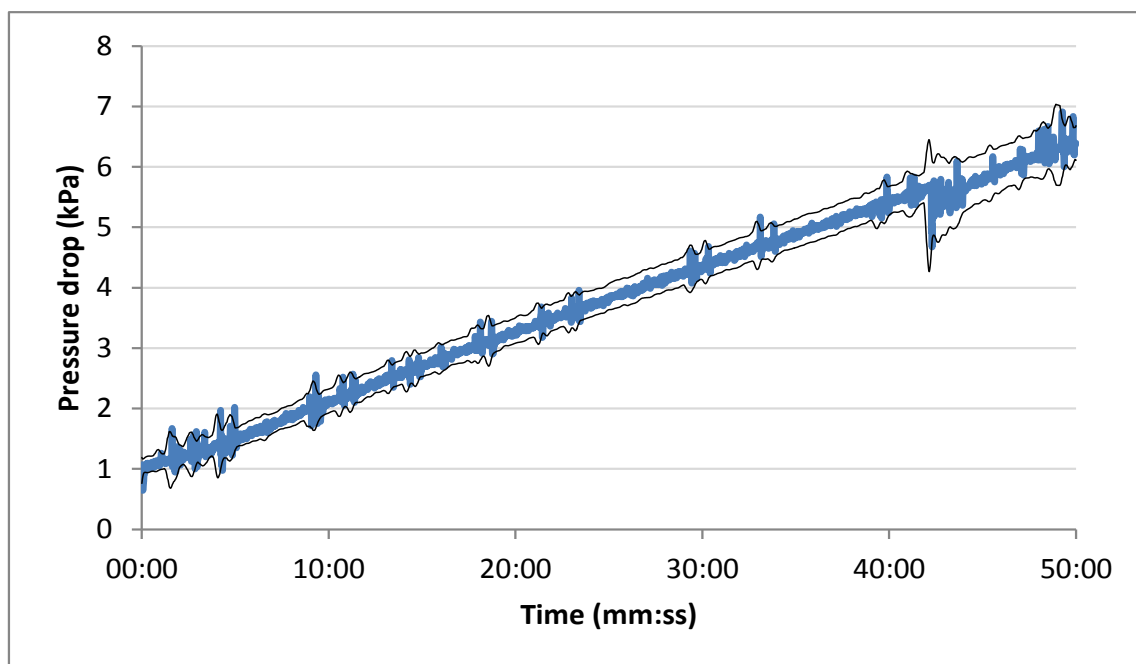


Figure 5-14: Pressure drop over media bed for flood SS suspension at 8 m/h

Initial pressure drop was equivalent to clean bed pressure drop of 1 kPa, with pressure drop rising constantly for the remainder of the cycle. Pressure drop over PF reached a maximum of 6.5 kPa over the course of the eight repeated filtration cycles. The relatively low pressure drop for synthetic water with such high solids loading could be due to inadequate particle retention within the bed, as seen from the residual turbidity graph in Figure 5-15.

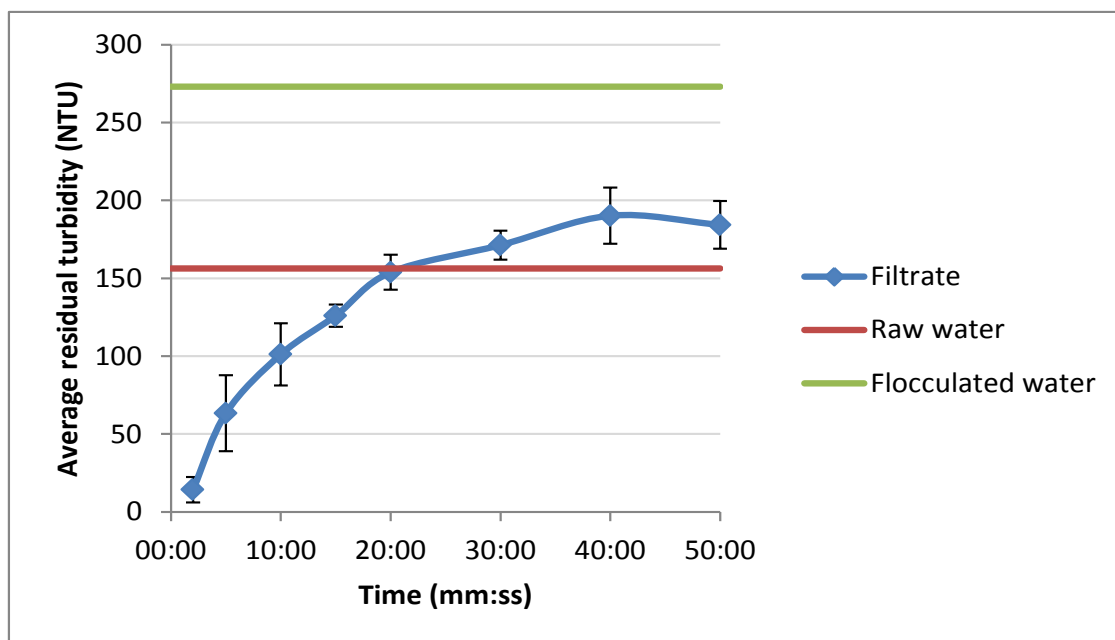


Figure 5-15: Residual turbidity following PF of flood SS suspension

Breakthrough occurred instantaneously, but the PF managed to remove the majority of the incoming 273 NTU flocculated water turbidity and allowed a gradual turbidity profile to pass through the PF bed and approach the membrane. Residual turbidities exceeded raw water turbidity at 20 minutes, but never reached the turbidity of the flocculated water. The plateauing of turbidity after 20 minutes indicated the continued effectiveness of orthokinetic flocculation in the PF. The filtration media kept modifying incoming flocs and retaining a fraction in the PF bed, which caused the continued increase in PF pressure drop. A high solids loading remained following pre-filtration to be deposited onto the membrane. The resulting increase in TMP is plotted in Figure 5-16.

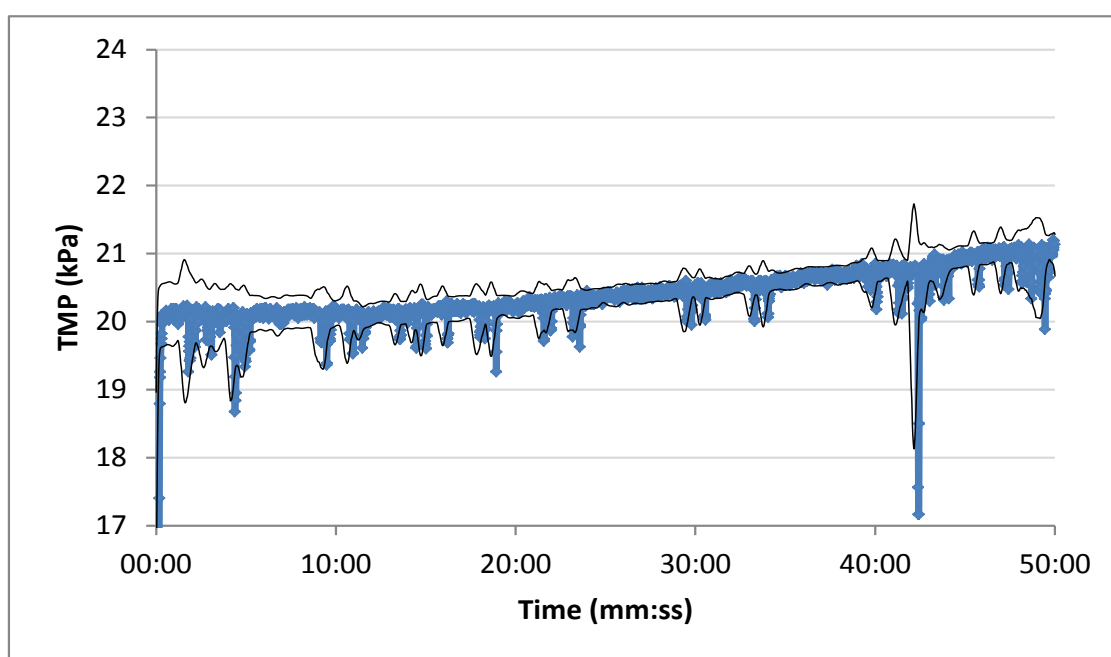


Figure 5-16: TMP for cyclical operation at 37 LMH filtration of flood SS suspension

The TMP profile showed a slow rise for the first 20 minutes of filtration, during which time the PF effectively retained the majority of flocculated bentonite. After 20 minutes, residual turbidity of the PF filtrate remained above 150 NTU, which caused a steeper slope in the TMP curve. Over the course of a 50 minute filtration cycle, a 1 kPa increase in TMP occurred.

When compared to membrane performance without pre-filtration, the effect brought about by pre-filtration was a removal of 67% of incoming TMP increasing flocs. The PF was highly effective in retaining incoming solids and creating a gradually increasing residual turbidity profile to be filtered by the membrane.

5.3.2 High organic matter loading (70 mg/L HA, 17 NTU)

A suspension containing 70 mg/L HA (with no bentonite added), was selected as the high organic matter flood suspension. Copying the procedure followed in the high solids loading test, the system was operated at 8 m/h flux through the media bed and 37 LMH flux through the membrane for 50 minutes. Comparison of membrane performance for operation through both filters, and flocculation directly onto the membrane, was done.

The organic material water has a raw water turbidity of 17 NTU, and flocculated water turbidity of 32 NTU. Whereas the turbidities are relatively low, it was predicted that the organic materials will irreversibly adsorb to the membrane surface.

Filtration through membrane alone

Flocculated water was filtered directly through the membrane at 37 LMH for eight successive cycles, with backwashing initiated every 50 minutes. The TMP profile is plotted in Figure 5-17.

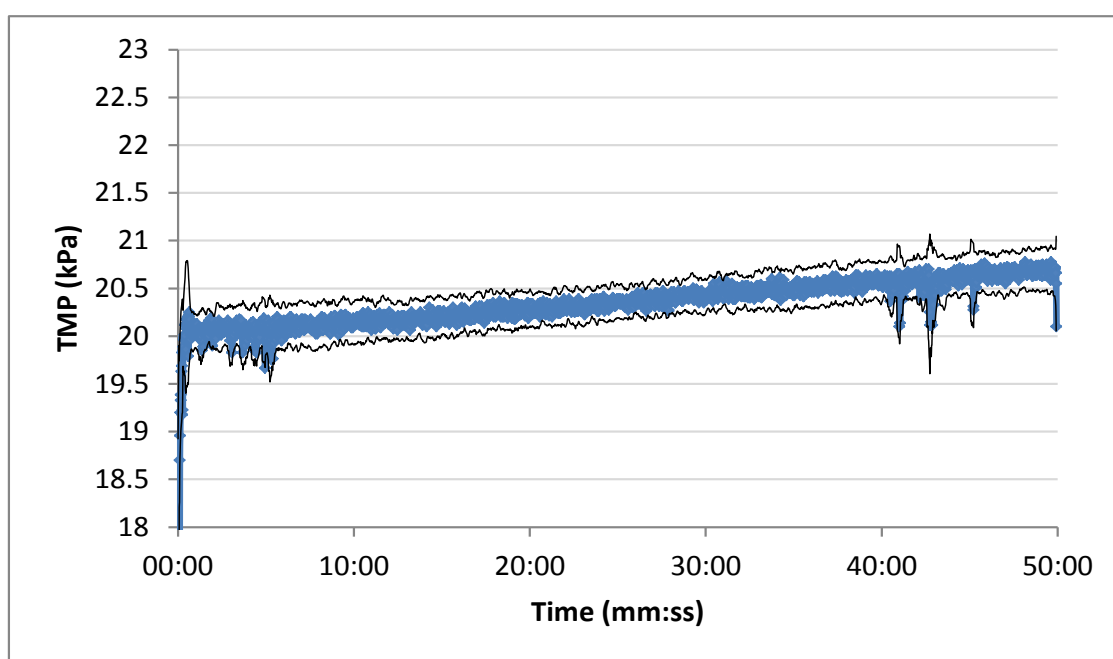


Figure 5-17: Cyclical operation of direct flocculation onto membrane of flood HA suspension

A repeatable, gradual increase in TMP was observed during direct flocculation onto the membrane. TMP increased with 0.7 kPa over the course of a 50 minute filtration cycle. The original TMP was restored upon hydraulic backwashing with no increase in initial TMP for 8 repeated cycles under these conditions.

The experimental duration was probably too short for irreversible fouling and manifest itself as an increase in the initial TMP. It was postulated that an experimental duration exceeding 24 hours, which is possible in site work, would show an increase in initial TMP.

It could also be that the floc formed during coagulation was effective in preventing irreversible fouling. Many studies emphasize the importance of coagulation prior to membrane filtration (Chae, et al., 2008), (Fiksdal & Leiknes, 2006), (Konieczny, et al., 2006), (Cho, et al., 2006). The coagulation of the organic material could form a reversible cake layer, which built up on the membrane surface rather than blocking pores. Coagulation and flocculation could take place successfully enough to prevent the occurrence of irreversible fouling for the short duration lab test work was conducted.

Filtration through PF and UF

The high organic concentration water was then filtered through both the PF and UF for eight successive cycles. The resulting PF pressure drop profile is plotted in Figure 5-18.

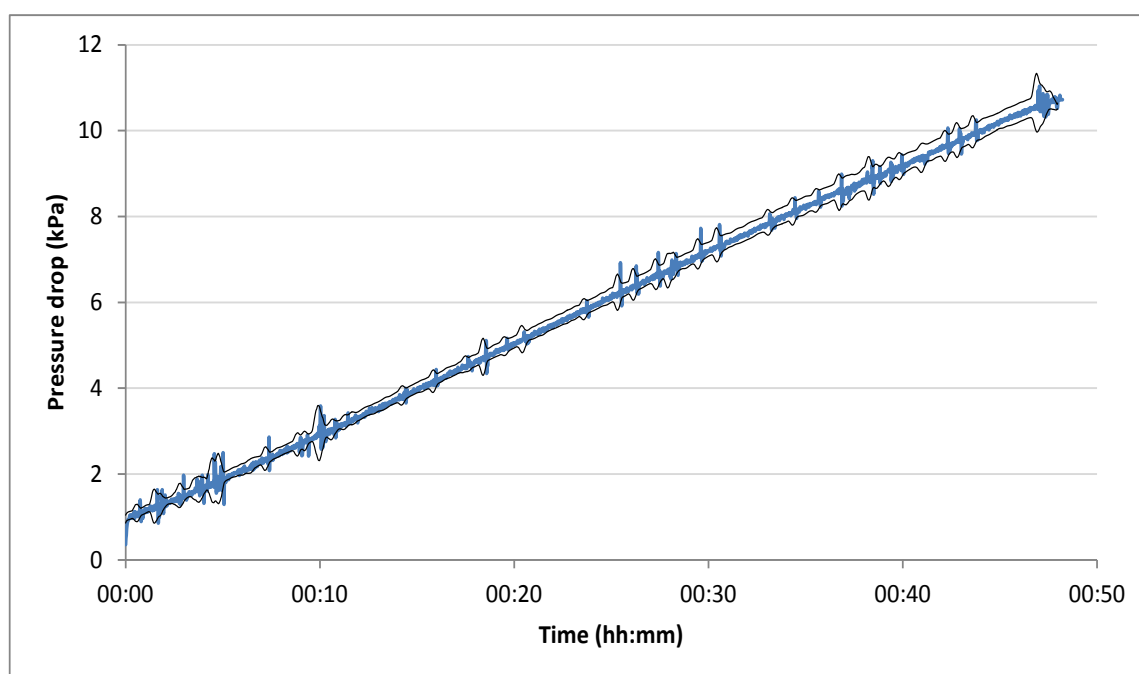


Figure 5-18: Pressure drop of cyclical operation of flood HA through PF

A constant pressure drop of 9 kPa is observed over the media bed for each of the eight cycles. Effective retention of particles occurred, as residual turbidity following the PF was low for the first 30 minutes of filtration before breakthrough occurs. The residual turbidities are plotted in Figure 5-19.

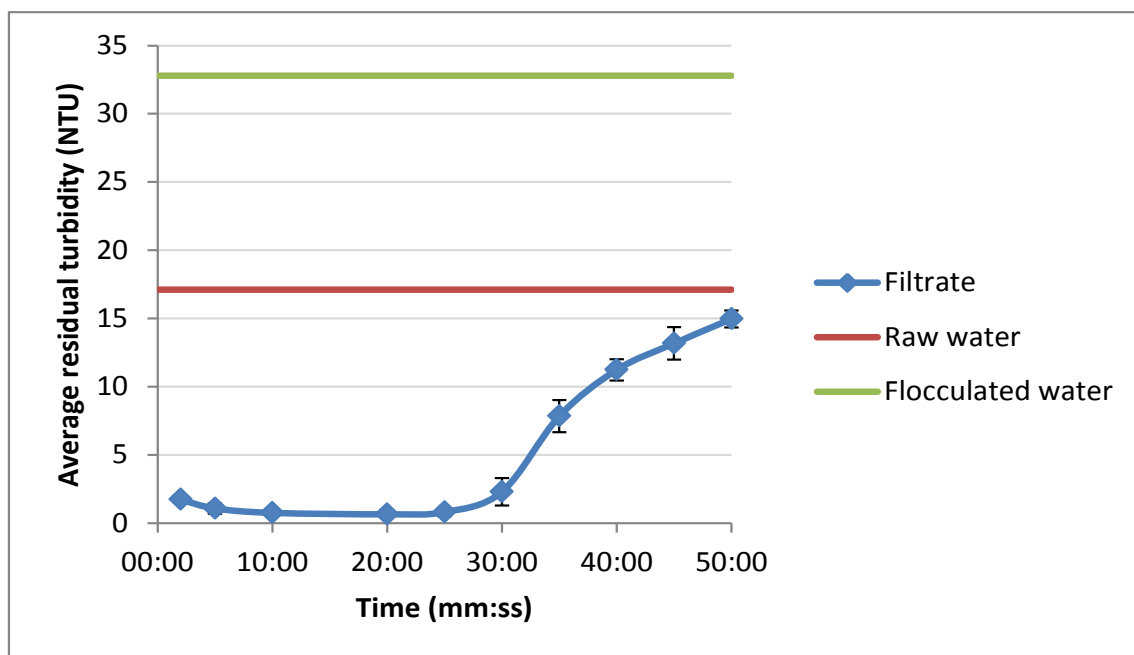


Figure 5-19: Residual turbidity following pre-filtration of flood HA suspension

The PF was successful in removing more than 50% of turbidity causing organic material after breakthrough occurred, resulting in a low organic fraction remaining to be deposited onto the membrane. The TMP over the membrane did not increase as it did for high suspended solids filtration, as seen in Figure 5-20.

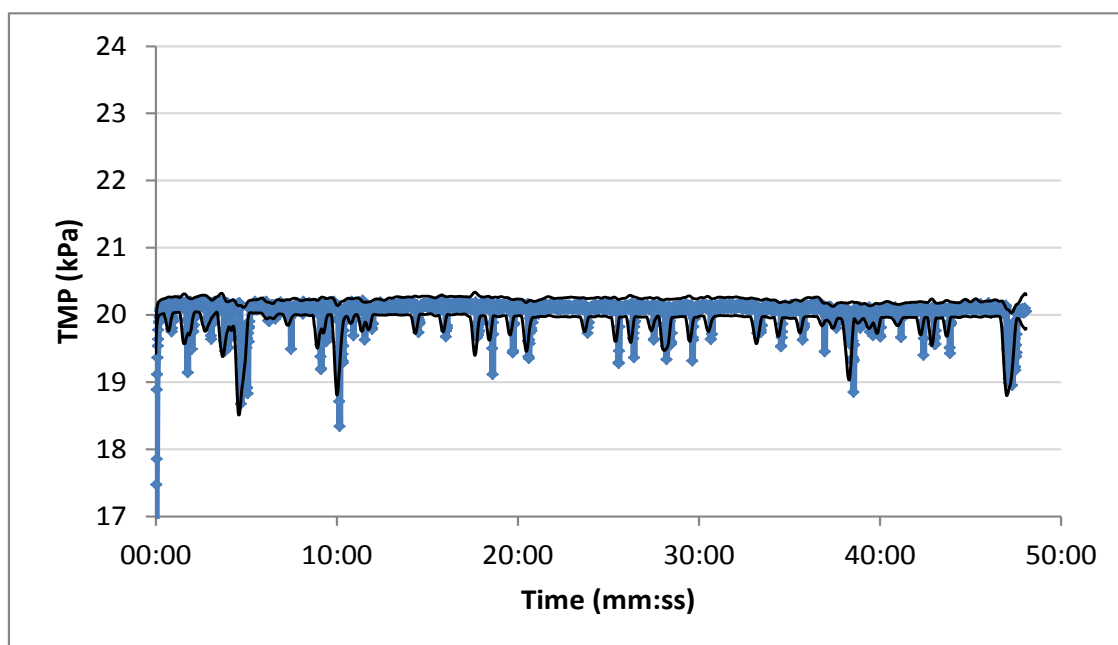


Figure 5-20: TMP for cyclical operation at 37 LMH for flood HA suspension

No cyclical increase in initial TMP was observed over the course of eight filtration cycles due to the effective retention of particles by the PF. Only after 30 minutes of operation did PF filtrate

turbidity start to increase. Filtration of the water from which the most turbidity had been removed did not show a discernible increase in TMP.

5.4 Comparison of pressure drop data

The temperature of the water will affect the rate of fouling by affecting the water's viscosity. At a lower temperature, the viscosity increases and molecular activity decreases, resulting in a slightly lower flux through the membrane. The opposite is true for higher temperatures, where water flows more easily through the membrane.

In order to obtain a representative comparison between experiments that have been carried out at different temperatures, pressure drop data over both the PF and UF membrane had to be corrected to the same temperature.

Normalising pressure drop data with viscosity, as described in 2.2.3 c), was done by correcting the viscosity of the water to a standard temperature using Equation 2.8. This normalisation gave a closer estimation of pressure drop at 20°C, than the method discussed in 2.2.3 c) 1. The comparison between the two methods of calculation is included in Appendix D. Pressure drops over the PF and UF membrane are summarised in Table 5-1

Table 5-1: Normalised pressure drop data for filtration experiments

Water composition	Configuration	Downflow (m/h)	Flux (LMH)	PF pressure drop (20°C)	UF TMP (20°C)
20 mg/L HA 30 mg/L bentonite	Direct UF		37		0.40
	PF UF	8	37	6.45	0.00
	Direct UF		46		0.41
	PF UF	10	46	6.92	0.00
25 mg/L HA 100 mg/L bentonite	Direct UF		46		1.09
	PF UF	10	46	7.10	0.30
400 mg/L bentonite	Direct UF		37		2.56
	PF UF	8	37	4.98	0.90
70 mg/L HA	Direct UF		37		0.63
	PF UF	8	37	8.14	0.00

For the low turbidity suspension (20 mg/L HA and 30 mg/L bentonite), more than 98% of the turbidity was removed by terminating filtration at PF breakthrough (when filtrate turbidity exceeded 1 NTU). The total filtrate volumes at low and high flow rates were very similar, reflecting in the similar pressure drops for both experiments. The addition of pre-filtration caused a 100% decrease in TMP.

For filtration with the high turbidity suspension (25 mg/L HA, 100 mg/L bentonite), operation was carried on past PF breakthrough point, with more particles passing through the PF and depositing onto the UF membrane. At a high flow rate (10 m/h and 46 LMH), the filtration duration was extended from 50 to 60 minutes in order to establish whether operation past the filtration breakthrough point would be possible to increase recovery. Breakthrough already occurred after 15 minutes of operation. TMP increase without pre-filtration was 1 kPa as opposed to 0.3 kPa, with 72% TMP reduction if pre-filtration was added. It was assumed that the particles depositing onto the membrane following pre-filtration caused reversible fouling, as no increase in initial TMP was noted. If the flocs caused reversible fouling, it was because the promotion of destabilised particle collision through the PF bed would potentially aid in the formation of flocs, which would deposit as reversible cake layer.

The successful operation of the filtration units past breakthrough indicated that recovery of the system could be increased by operating the system for a longer duration under certain conditions. However, under too radical conditions the filtration durations cannot be prolonged to increase recovery as PF performance limits this. If operation is extended past required filtration durations for relatively clean water, the duration should not be extended by too much. If water changes radically, the system has to be monitored carefully and filtration durations should be shortened.

Under high suspended solids conditions, PF performance limited filtration duration. When the water was filtered for as long as determined during characterisation, the resistance posed by the PF upon backwashing was too high. Upon expansion, the bed expanded to beyond the visible range. The predetermined backwashing duration was also insufficient to clean the PF. Shortening the duration for low downflow rate filtration from 70 to 50 minutes still enabled 64% reduction of TMP. PF filtrate showed a gradual increase in turbidity with time, with residual turbidity never reaching incoming flocculated water turbidity, indicative of continuous PF floc modification and retention.

Under high organic flood conditions, the PF again removed 100% of TMP, with no increase in TMP when pre-filtration was used. Filtration duration can also possibly be increased under these conditions, although it is not known what the long term effect of deposition of organic foulants would be. Coagulation seemed to be effective in agglomerating HA, as no irreversible fouling occurred for the experimental duration, which would have manifested itself as an increase in overall TMP.

5.5 On-site testing and performance evaluation

The equipment was tested on site after characterisation and laboratory test work. Site test work gave an indication of the robustness of the filter combination, and an indication of the performance of the pilot plant with actual surface water. Laboratory suspensions selected for experimentation did not contain all species typical to surface water, such as pathogens, finer colloids and inorganic molecules, amongst others.

On-site test work was conducted at a drinking water treatment plant located in the Southern Cape. The experimental plan was to operate the set-up for 5 days continuously, firstly with both filters in operation, and secondly only with flocculation onto the UF membrane. Conditions at the plant were closely simulated and replicated where possible.

Firstly the PF had to be characterised for the new water type and different coagulant (aluminium sulphate) used. The downflow rates of 8 and 10 m/h were compared to select an operational rate. The filtration duration was then selected so the pilot plant could be operated at the same recovery as the actual plant, with CEB carried out every 24 hours.

5.5.1 Selection of operation philosophy

Pre-filter performance at different flow rates

The performance of the PF was firstly characterised at a low and high downflow rate to determine the breakthrough curve for each flow rate, and to assist in the selection of an operational philosophy. A platinum-cobalt colour meter was used for testing the colour of treated and untreated water.

The percentage removal of turbidity and colour for the two downflow rates considered are presented in Figure 5-21 and Figure 5-22.

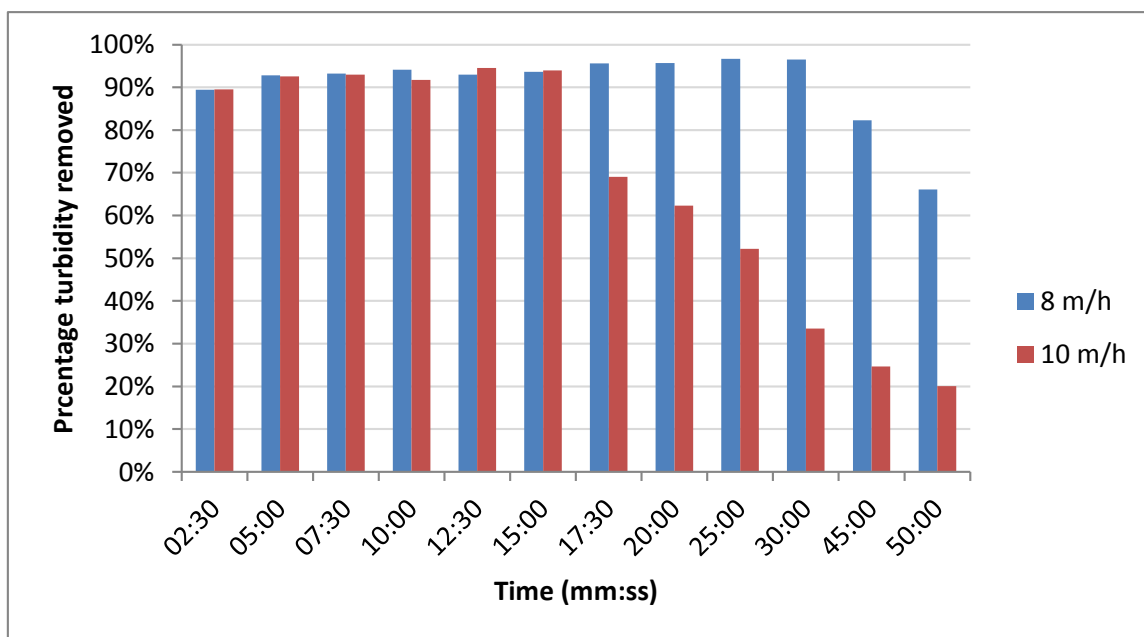


Figure 5-21: Turbidity removal by PF at different downflow rates

Breakthrough occurs at a later time at a lower flow rate, as was anticipated. Destabilised particles have time to agglomerate and form larger flocs, which are captured within the bed. At a downflow rate of 8 m/h, water can be filtered for 45 minutes before breakthrough occurs, while breakthrough would occur after 25 minutes for 10 m/h operation. The PF will not only be operated until breakthrough is reached, but for the duration determined for the downflow rate during characterisation.

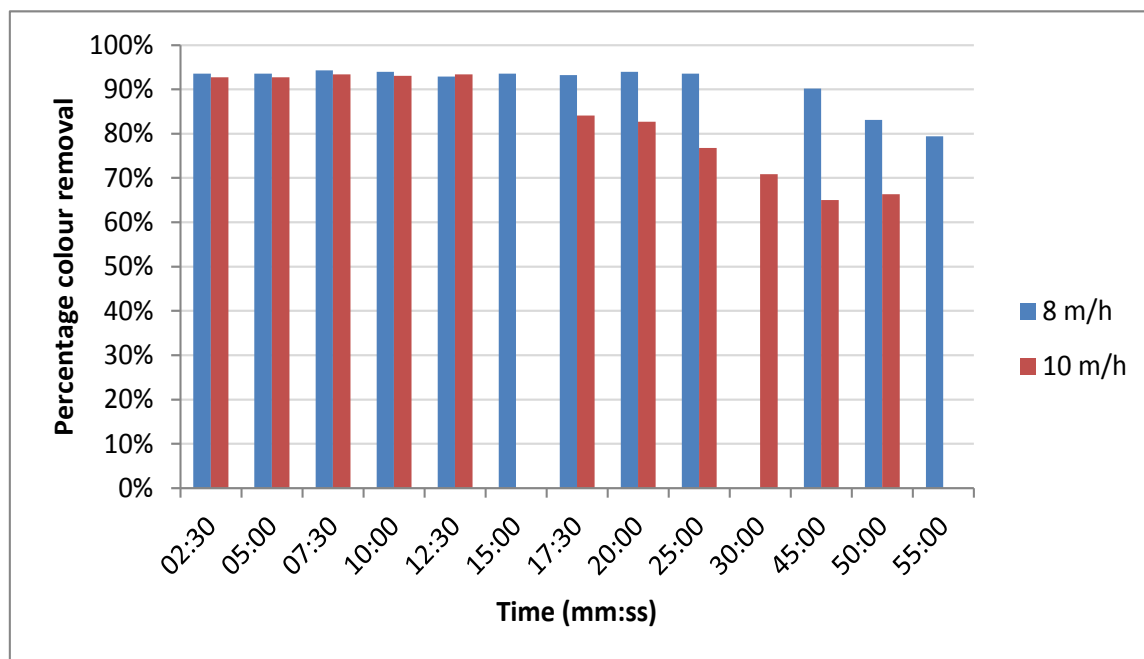


Figure 5-22: Colour removal by PF at different downflow rates

Colour breakthrough occurs much slower than turbidity, with 70% of colour still removed upon PF breakthrough. Again the lower flux filtration showed a more favourable breakthrough curve for water exiting the PF.

As was the case with UV-Visible component removal, the PF was more effective in removing particles that absorb visible light and cause colour than removing turbidity from the water. The agglomeration of dissolved HA could contribute to the turbidity and form pin flocs, which then showed as turbidity rather than colour.

It was decided to operate the PF at 8 m/h downflow rate through the bed, and 37 LMH flux through the membrane. The membrane flux was comparable to the 30 LMH used in the actual plant. The lower flux was also selected as safety measure, as it was unsure how the membrane would perform when filtering actual surface water. River water contains many compounds that were not tested for during lab test work, such as pathogens. Water was filtered for 70 minutes and backwashed for 2 minutes.

Operational duration and recovery

The Southern Cape plant filtered water for 50 minutes, with intermittent backwashing of 50-70 seconds. CEB was carried out every 20 hours. Water was filtered at a rate of 25 m³/h through Inge® membranes at a flux of 30 LMH. At the time of experimentation, they were operating at a recovery of 82% on average.

It was decided to operate the experimental unit at the same recovery as the plant. It was only required to extend filtration duration by 1 minute to reach 82% recovery. Product water used during CEB rinsing was considered in recovery calculations.

5.5.2 Effect of pH on water quality

Initially no adjustment was made to the pH of water during treatment, as this was the manner selected for laboratory experiments and proved to still deliver favourable filtrate. However, aluminium sulphate coagulant is more pH-sensitive.

The reason the actual membrane plant was constructed, was because the existing conventional treatment plant was unable to remove aluminium to the SANS 241 requirement of below 0.2 mg/l. If the membrane plant operated within the recommended pH range of 5.6-6.2, aluminium was removed almost completely. The membrane treated water was then blended with the conventional treatment plant water to ensure a safe aluminium concentration in the final product.

Alum dosage was selected by the operators with jar tests, and reassessed when raw water quality changed. Required dosages ranged between 50-100 mg/L coagulant as alum. These concentrations of alum reduced the pH to between 4.3 and 5 from the raw water pH of 7. As supported by the literature study (Matilainen, et al., 2010), acidic pH leads to the formation of alum-NOM complexes which are small enough to pass through the membrane. Residual aluminium at a pH below 5 gave concentrations exceeding 1 mg/L aluminium as measured on site. The SANS requirement for potable water is an aluminium concentration below 0.2 mg/L. Adjusting the pH to the recommended range resulted in favourable aluminium removal. An additional dosing pump was required on the pilot plant to adjust the pH to this range.

Aluminium measurements were conducted on site with a Hach DR/890 Colorimeter. Table 5-2 contains the residual aluminium readings and the corresponding pH at which the reading was taken.

Table 5-2: pH following UF and resulting residual Al

pH	5.75	5.77	5.88	5.97
Al (mg/L)	0.054	0.046	0.035	0.012

It appears that greater aluminium removal occurs at a pH approaching 6 (Kimura, et al., 2008). For the acidic water (pH below 5), the colorimeter could not measure aluminium as concentrations exceeded 0.8 mg/L.

Samples were brought back to the Process Engineering Department for elemental analysis on the Analytik Jena ControAA 400, but the detected concentrations were too low to be measured accurately. The lower limit for the instrument was 0.1088 mg/L, and samples could not confidently be quantified. For tests conducted at a low pH, aluminium concentrations up to 1 ppm were measured, emphasising the importance of proper pH control.

5.5.3 Surface water filtration through media and membrane filtration

Experiments were firstly conducted including the PF as pre-treatment. The pilot plant was run continuously for 5 days at the low flow rate, with 71 minutes filtration and 2 minutes backwashing. CEB was carried out after each 24-hour experimental cycle, similar to CEB intervals of the actual plant.

Raw water properties over course of experimentation

Raw water colour and turbidity were measured over the course of the experiment, with average readings plotted in Figure 5-23.

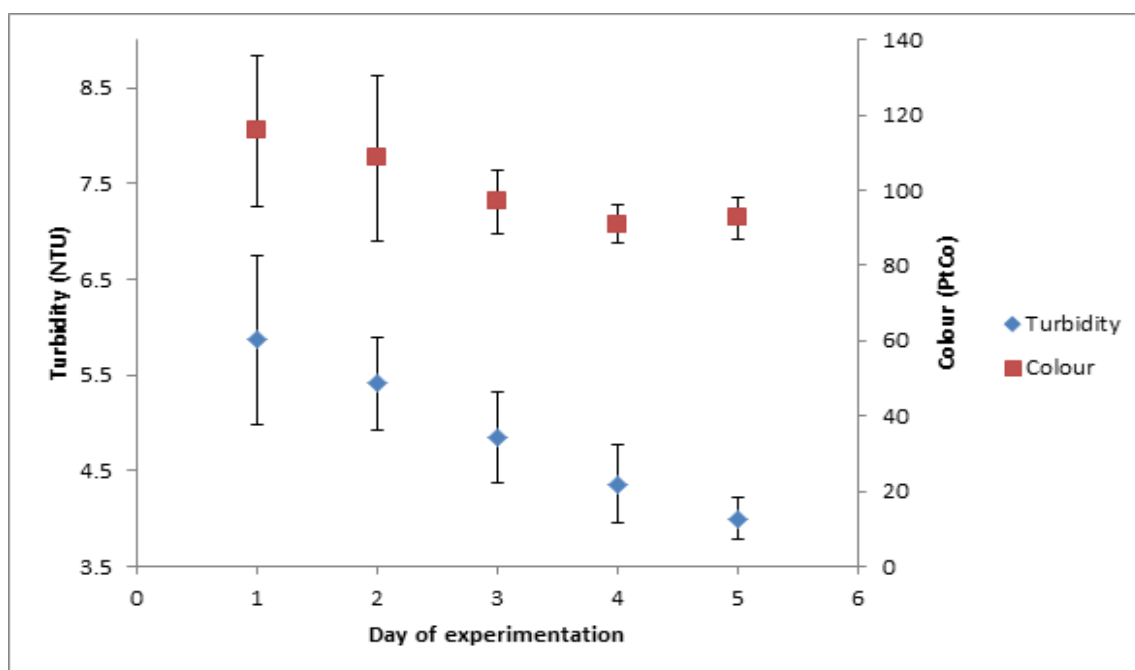


Figure 5-23: Raw water properties over the course of experiment

Raw water quality improved slightly as time passed. The turbidity of the water decreased from 5.9 to 4 NTU, and colour decreased from 116 to 93 mg/L PtCo. An alum dosage of between 50-60 mg/L was required to flocculate the water. Overall the water was less turbid than the 12 NTU water used in lab testing. Based on lab experiments, a PF pressure drop of maximum 6.5 kPa was predicted, with no significant TMP increase per 71-minute filtration cycle. The long term effect of filtration was not yet known and the prevalence of irreversible fouling could not be predicted.

PF pressure drop profile

The pressure sensor measuring pressure above the PF had failed prior to the site visit. Gauge measurements were carefully noted in order to plot pressure drop over the PF. The gauge at the outlet of the membrane housing was also monitored and values logged for use in pressure drop calculations. Pressure drop data for each of the days was measured and compiled into plots illustrated in Figure 5-24.

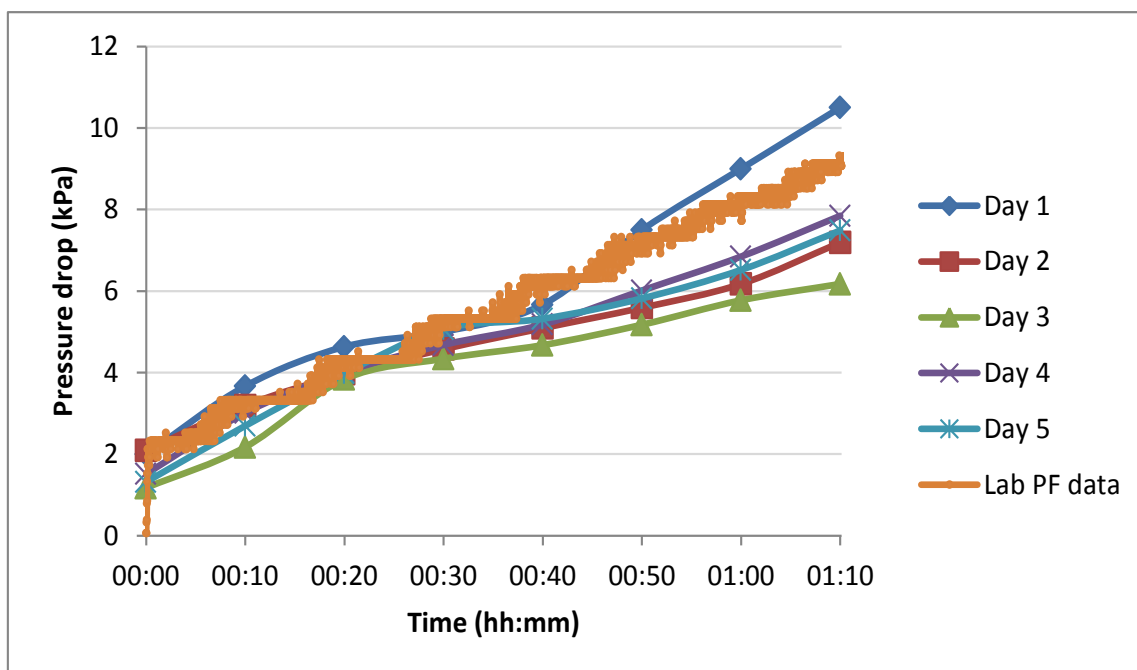


Figure 5-24: Pressure drop over PF for site experiments

Pressure drop on Day 1 was notably higher than the following days, as the water initially had a high turbidity due to rain a few days prior. For the rest of the experiment, pressure drop over the PF was relatively similar at around 6.2 kPa.

The pressure drop was very similar to normalised pressure drop over the PF for lab conditions. The synthetic 12 NTU suspension (20 mg/L HA and 30 mg/L) was filtered at 8 m/h downflow rate for 70 minutes, resulting in a pressure drop of 6.5 kPa, normalised to 25°C. The similar pressure drops between lab and site work could be ascribed to the species present in actual surface water, and potentially the different hydrolysis reactions that took place between the NOM and respective coagulants used. The fact that the lower turbidity actual surface water gave the same pressure drop as lab data could reflect on the fine nature of suspended solids or greater prevalence of dissolved solids, which reacted with the coagulant in such a manner that resistant flocs formed and were retained within the PF bed.

The effectiveness of the coagulant to clarify the river water could further be quantified through the determination of the percentage colour and turbidity removed.

Turbidity and colour removal following pre-filtration

The residual turbidities and colour of PF filtrate were expressed as percentage of raw water turbidity and colour removed for each day and raw water composition (as opposed to flocculated water turbidity as discussed for laboratory test work). Information is summarised in Figure 5-25 and Figure 5-26.

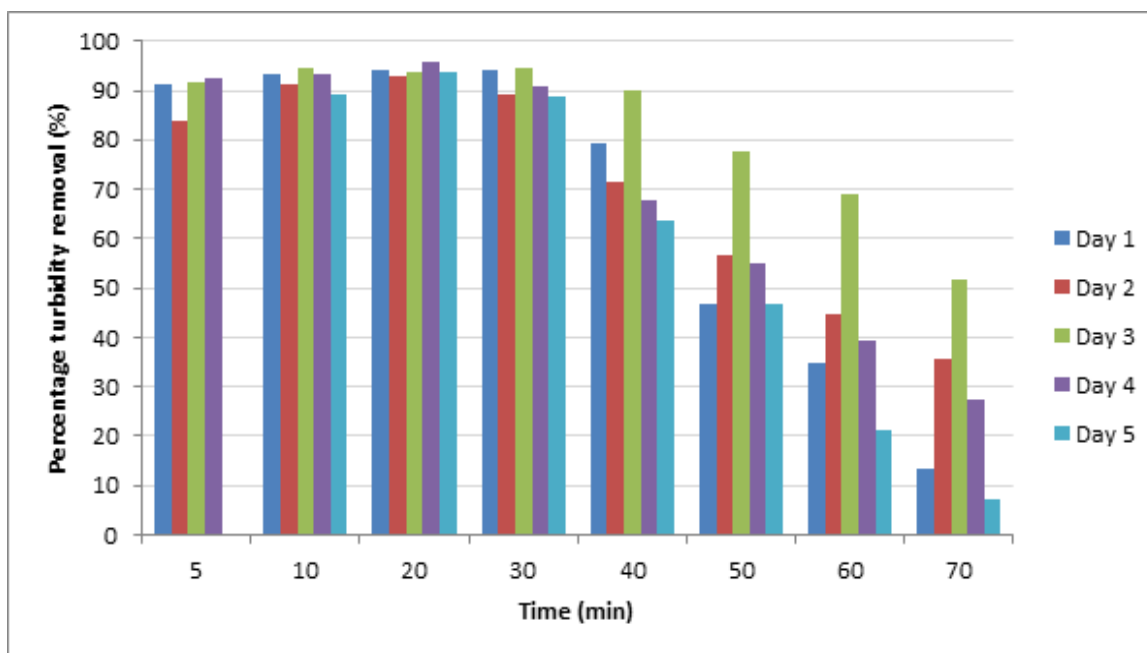


Figure 5-25: Percentage turbidity removal from site water by PF

Turbidity removal exceeded 90% for the first 30 minutes of operation following bed maturation. Breakthrough of the filter occurred after about 45 minutes, which was followed by a rapid decline in turbidity. The PF was operated past breakthrough with poor turbidity removal of around 10-50% occurring in the final 10 minutes of filtration.

Similar trends were found in the colour removal profile, illustrated in Figure 5-26.

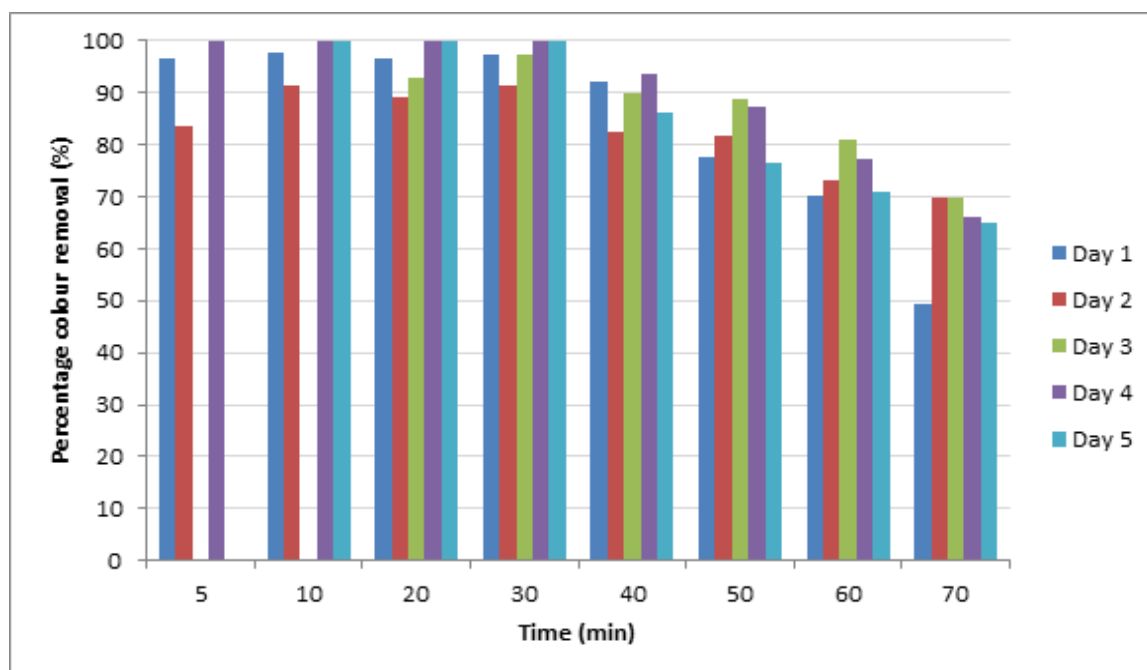


Figure 5-26: Percentage colour removal from site water by PF

As was the case with components causing UV-Vis absorption tested for during lab work, the PF retained a larger fraction of colour causing components than turbidity causing components, with around 50-70% of colour still being removed in the final 10 minutes of filtration. Both UV-Vis and colour measurement are meant to be representative of the HA present in water. The high removal could be ascribed to the greater effectiveness with which the coagulant can remove HA, as opposed to SS agglomeration and removal.

Bed maturation was critical for effective colour removal, as it could be seen that colour removal was slightly lower at 5 minutes than at 10 minutes. Colour breakthrough occurred more gradually than turbidity breakthrough. Even at the turbidity breakthrough point at 45 minutes, relatively high colour removal of around 70-90% still occurred.

Membrane pressure profile

As seen in preceding figures, the PF successfully retained a large percentage of the incoming raw water turbidity, and especially colour causing components (which are said to be responsible for irreversible fouling in membranes (Fan, et al., 2001)). Due to the high turbidity and colour removal achieved throughout the largest part of PF filtration, it was not expected that membrane pressure profiles will show significant increases in TMP over the course of a 71-minute filtration cycle, as found in lab tests under similar conditions.

Following CEB, the filtration sequence started late afternoon for the 5 days the unit operated continuously. Temperatures dropped to around 21°C overnight, and increased to up to 26°C in the last few hours of the cycle. Although data was normalised to account for the difference in temperature, similar trends were still noted in normalised data with temperature variations.

The TMP data was normalised, correcting the actual viscosity of the water (determined from logged temperature readings) to viscosity at a standard temperature. As the site visit occurred in January and temperatures were consistently higher than 20°C, TMP was normalised to 25°C in order to minimise distortions to the readings.

Normalised TMP profiles are plotted in Figure 5-27 to Figure 5-31.

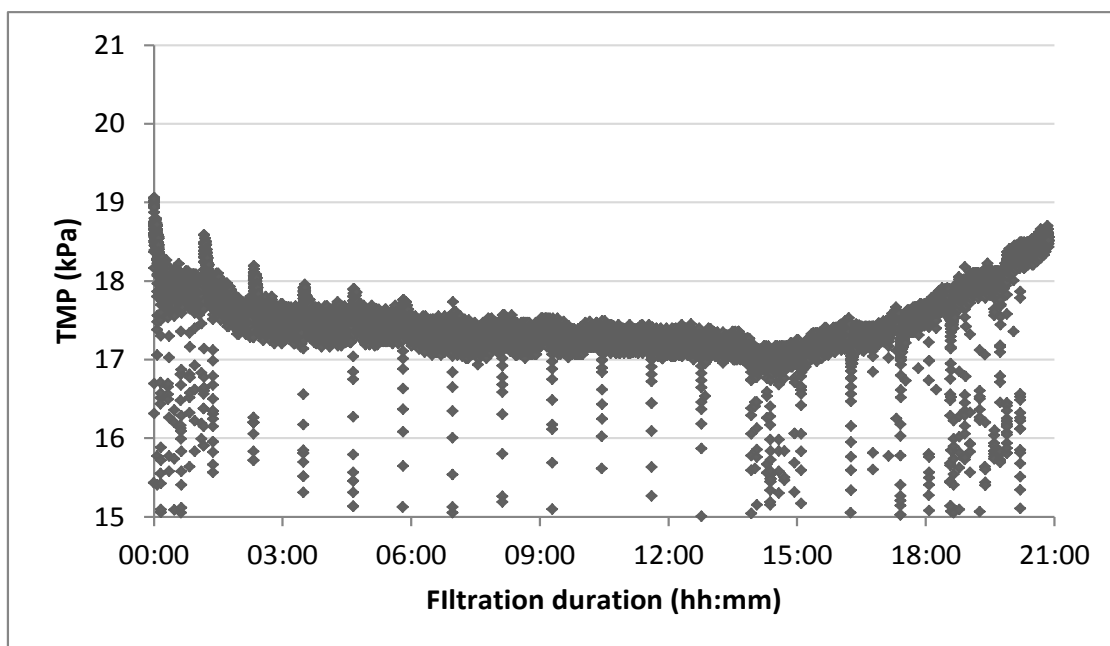


Figure 5-27: Day 1 TMP for filtration of PF permeate

TMP was initially slightly higher at the beginning of a 71-minute filtration cycle than at the end, which could be indicative of membrane relaxation occurring. Following 7 hours of gradual TMP decrease, throughout the course of a 71-minute filtration cycle, the pressure mostly remained constant at 17 kPa. The pilot plant ran through the night between the 5th and 14th hour of operation during which time the temperature remained around 22°C. For filtration after 16 hours, the raw water in the storage tank would heat up and the temperature would exceed 25°C.

At the beginning and end of the 24-hour experimental cycle, temperatures were equal at 26°C and TMP around 18.2 kPa was logged. It was assumed that no irreversible fouling had manifested itself over the course of the experimental cycle, as the initial and terminal TMP was the same.

Following an alkaline and acidic CEB and rinse, filtration was initiated for the second 24-hour experimental cycle.

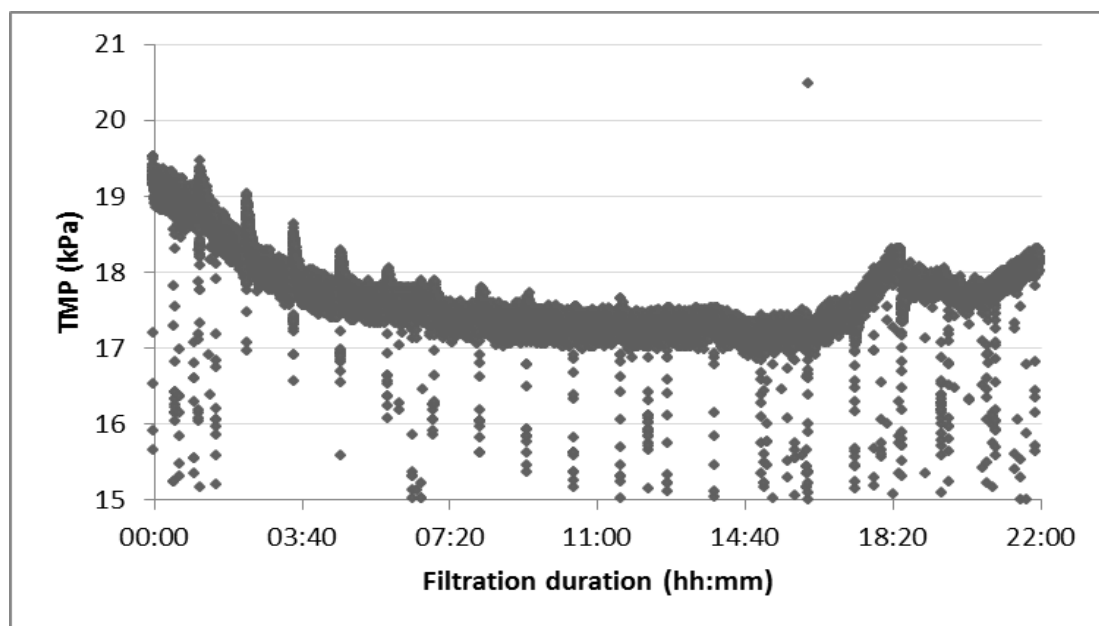


Figure 5-28: Day 2 TMP for filtration of PF permeate

Similar trends and TMP values were noted at the middle and end of the 24-hour cycle as noted for the previous experimental cycle. Water was very warm initially as the raw water storage tank, which was situated outside in the sun, slowly filled for the hour in which CEB was carried out. Upon initiation of the experiment, as raw water was continuously fed to the raw storage tank, the temperature of the water decreased from 27 to 23°C. After 6 hours, temperature did not significantly vary for a further 11 hours and TMP remained relatively constant at 17.4 kPa. TMP did not increase above the 19 kPa measured upon initiation of the 24-hour experimental cycle.

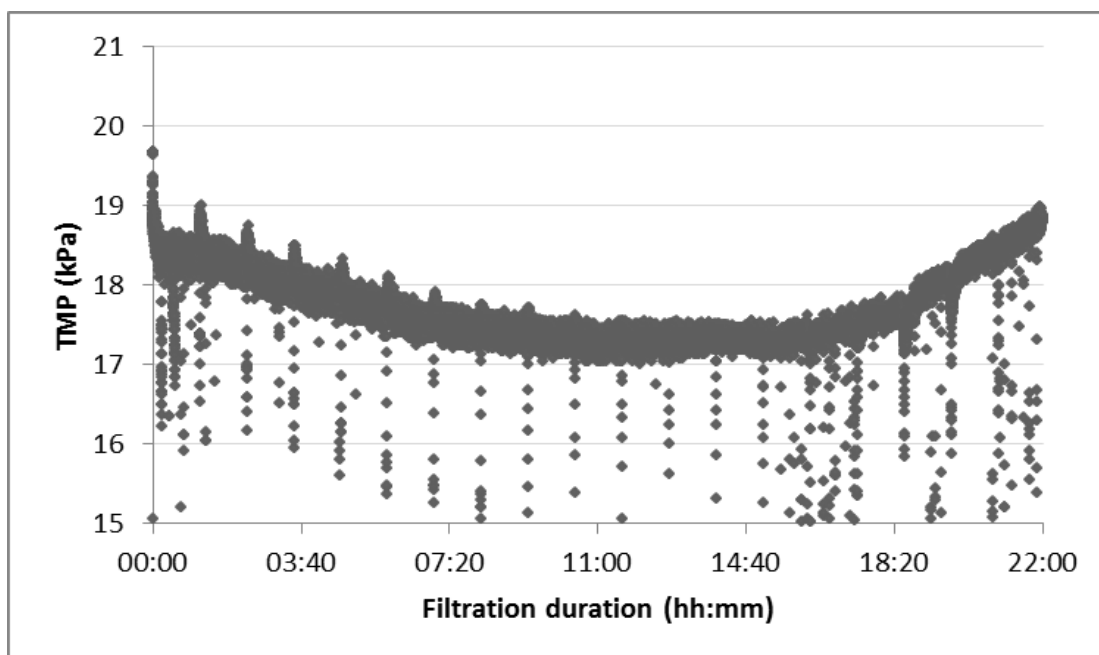


Figure 5-29: Day 3 TMP for filtration of PF permeate

More gradual changes in the TMP profile was noted on the third day of continuous filtration. From this profile, the same TMP magnitudes could be seen as determined previously at specific temperatures. The TMP for the middle section where temperature was recorded as 23°C, remained consistent at 17.2 kPa. This was the same as the TMP measured at 23°C for previous 24-hour experimental cycles. From the consistency of these values, it appears that irreversible fouling had not manifested itself. The regular chemical cleaning of the membrane would assist in the removal of built-up foulants.

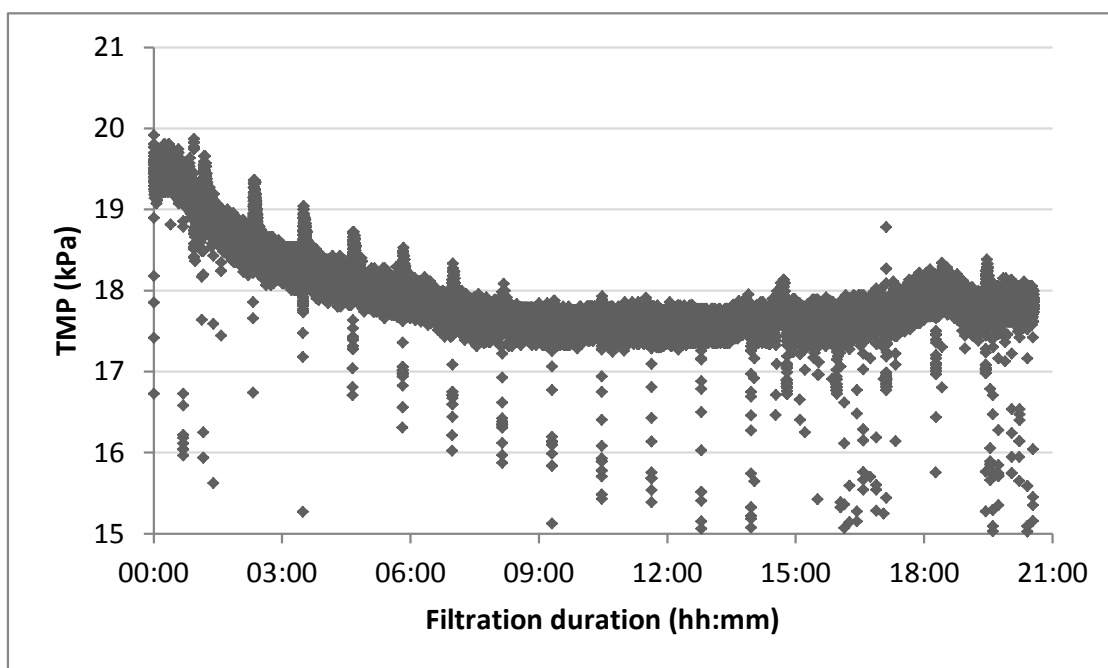


Figure 5-30: Day 4 TMP for filtration of PF permeate

On the fourth day, TMP at 23 °C remained slightly higher than on previous days at 17.4 kPa. At the end of the 24-hour experimental cycle, the TMP reached 18 kPa at a temperature of 25°C, which is similar to measurements made at this temperature on previous days. It was assumed irreversible fouling had not taken place.

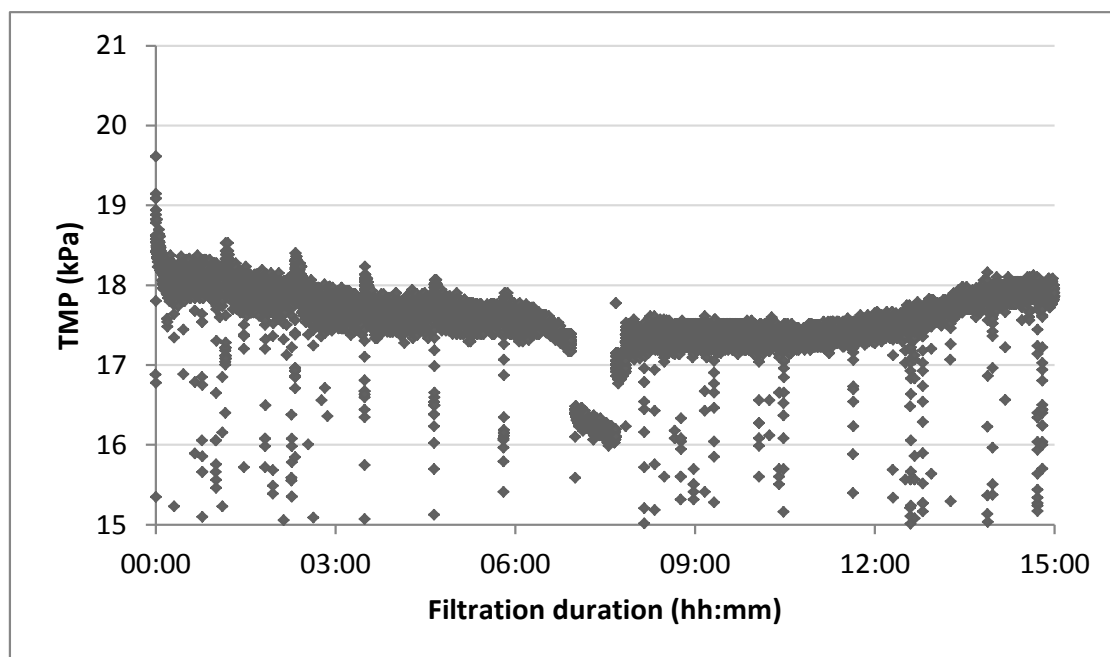


Figure 5-31: Day 5 TMP for filtration of PF permeate

A disruption in operation had taken place on the final day of operation. However, the range within which TMP fell – between 17 and 18.5 kPa – was the same as previous 24 hour experimental cycles within the measured temperature ranges.

Overall, TMP correlated consistently with temperature for the 24-hour experimental cycles conducted over the 5 days. The same variation in TMP values was found, which could be ascribed to the variation of temperature profiles throughout the course of a 24-hour experimental cycle.

For these particular conditions, no rise in TMP was expected, as PF filtration tests conducted in the lab under relatively similar conditions resulted in no TMP rise. The overall experimental duration was perhaps a bit short with CEB carried out at relatively regular intervals, removing adhered foulants which could otherwise have contributed to irreversible fouling. Although this is good and recommended practice, more seldom CEB could have shown more distinct fouling and overall changes in the TMP profile.

Clean water quality

The turbidity of the filtered water was consistently less than 0.18 NTU with a PtCo colour reading of 0, if the pH was maintained within the required operating range. A decrease in pH led to poorer water quality, which reflected in the turbidity and colour readings, and particularly in the residual aluminium readings taken on site.

5.5.4 Surface water filtration through flocculation on membrane

Following the five days of experiments where the UF was pre-treated with the PF, water was continuously flocculated and filtered through the UF membrane alone. The same conditions were maintained as selected for the first set of experiments: filtration at 37 LMH flux through the membrane for 71 minutes, followed by 2 minute backwashing at 200 LMH flux. CEB was conducted every 24 hours. An extra day of filtration was added due to an interruption during experimentation.

Raw water properties over course of experimentation

Over the course of the direct flocculation experiments, the raw water turbidity and colour were relatively similar to water quality measured during the pre-filtered experiment, making for fair comparison. Measured turbidity and colour for the raw water are plotted in Figure 5-32.

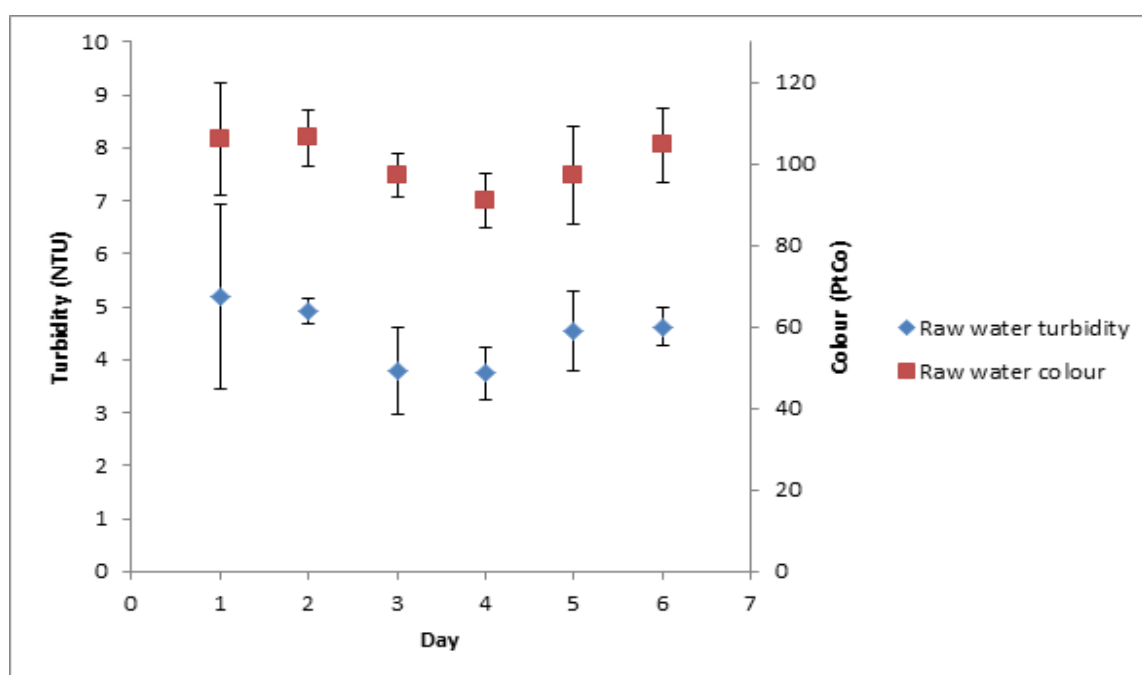


Figure 5-32: Raw water turbidity and colour

Turbidity remained relatively constant between 4.3-5.2 NTU over the 6 days. Colour varied more widely between 91-106 mg/L PtCo. These conditions are considered relatively clean for the river from which surface water is extracted, and low aluminium sulphate dosages of 50-60 mg/L was maintained.

Membrane pressure profile

Whereas there was no notable increase in TMP over the course of one 71-minute filtration cycle if pre-treatment was included, it was predicted than an increase in TMP would occur for direct

flocculation. Lab test work for similar conditions and water treated gave a TMP increase per filtration cycle of 0.4 kPa, and a similar increase was expected for this set of experiments.

Filtration cycles were again initiated late afternoon, with temperature fluctuations similar to the previous experiments. Figure 5-33 to Figure 5-39 contains normalised TMP plots.

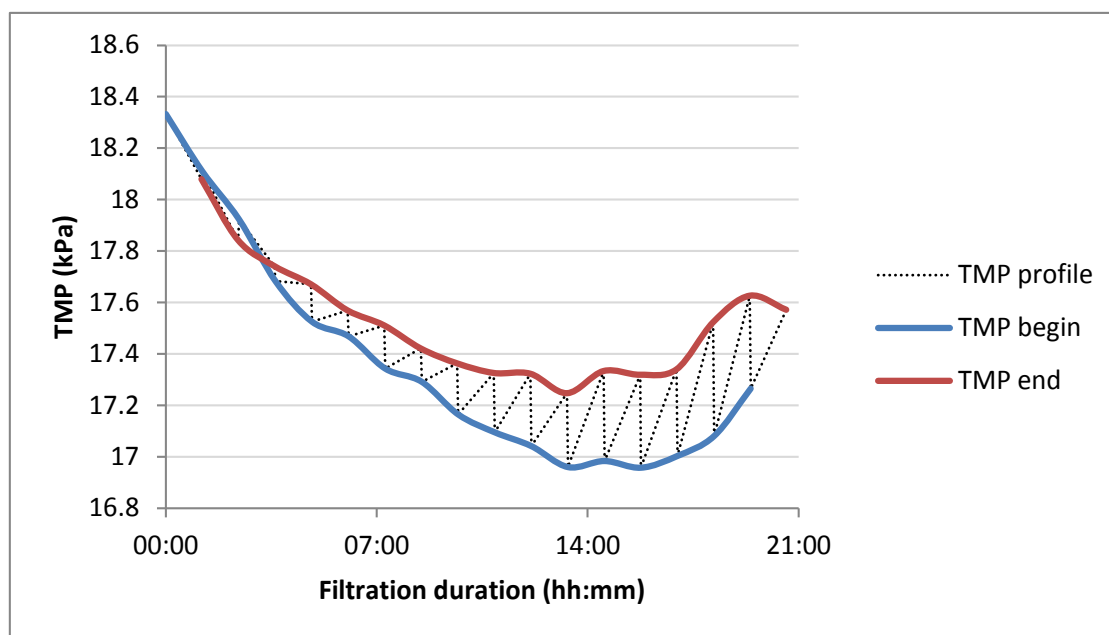


Figure 5-33: Day 1 TMP profile for direct flocculation and filtration through UF

As with filtration including pre-treatment, TMP initially started just above 18 kPa at 25°C and decreased to 17 kPa at a temperature of 22°C in the middle of the 24-hour experimental cycle. Initially, the TMP at the beginning of a filtration cycle was slightly higher, and decreased stepwise upon hydraulic backwashing. This phenomenon is plotted with normalised data in Figure 5-34 and was particularly prevalent in the first few filtration cycles.

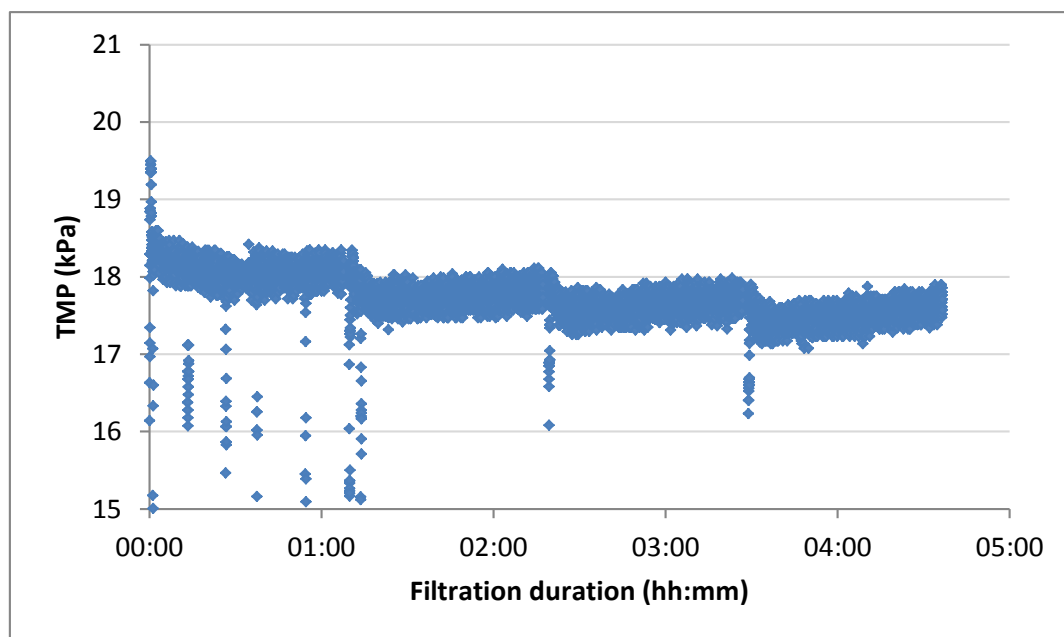


Figure 5-34: Initial TMP profile

Hydraulic washing between 71-minute filtration cycles should not be able to improve permeability of the membrane to this extent. It could be that the acidic wash and soak period during CEB, in which citric acid is used, could leave a residual positive charge on the membrane and affect the type of fouling or floc formed. After a few hydraulic washes, the membrane charge was increasingly neutralised and initial TMP value decreases gradually. The occurrence seems to be temperature dependent, as the temperature during the first 71-minute filtration cycle following CEB is around 25°C, and decreases to 23°C after three 71-minute filtration cycles.

The magnitude of TMP rise during a single 71-minute filtration cycle varied, from no TMP rise initially, to TMP increases of 0.04 kPa after the initial TMP decrease phenomena terminated. The rise in TMP per filtration cycle gradually increased from here onwards. Towards the end of the 24-hour experimental cycle, the TMP increase for a single filtration cycle approached 0.6 kPa. TMP at the beginning and end of the 24-hour experimental cycle was 17.4 kPa at 24°C, indicative that no particles had irreversibly adhered to the membrane over the course of the experiment.

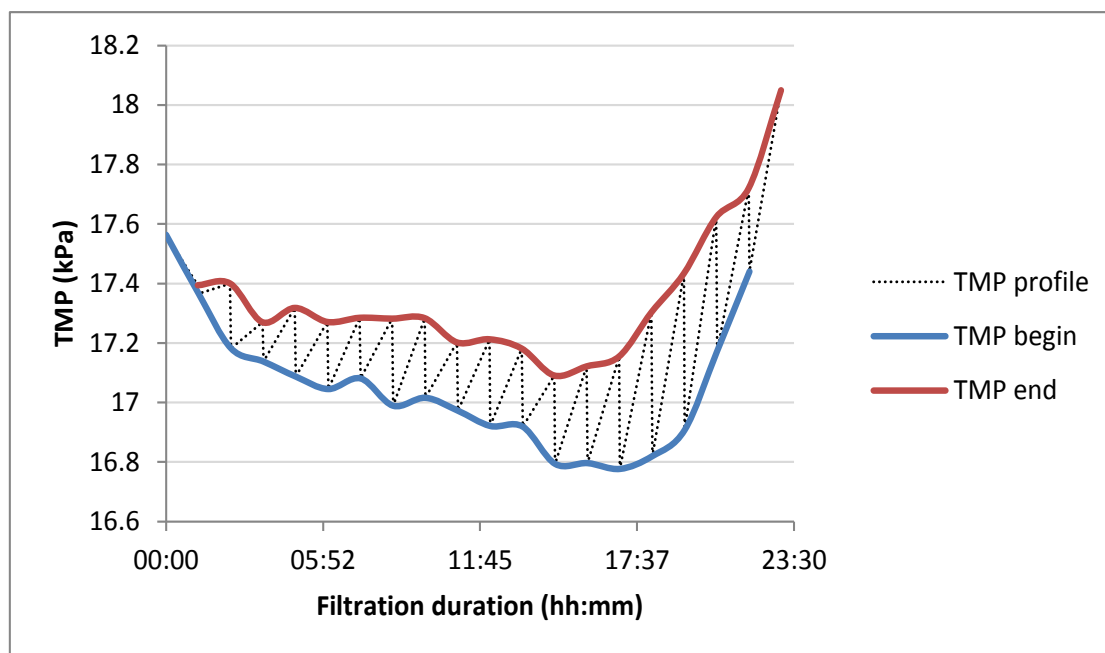


Figure 5-35: Day 2 TMP profile for direct flocculation and filtration through UF

The initial TMP started at a slightly lower TMP than for the previous 24-hour experimental cycle, as the initial temperature was lower than previously at 23°C. Towards the middle of the 24-hour experimental cycle, TMP reached a value of 16.8 kPa at a temperature of 21°C. This was lower than the minimum TMP achieved by the membrane in previous experiments under these conditions, indicative of the temperature dependence of flux and particle deposition rate.

Initially, relatively consistent TMP increases were found per 71-minute filtration cycle at around 0.2 kPa. With time, the magnitude of TMP increases per filtration cycle rose to 0.7 kPa. The higher temperatures at this later point in experimentation could contribute to the increase in TMP rises per filtration cycle.

By the end of a 24-hour experimental cycle, the terminal TMP of 17.4 kPa (at 24°C) was the same as TMP measured at the beginning of the 24-hour cycle (at 23°C), and it did not appear that irreversible fouling had taken place.

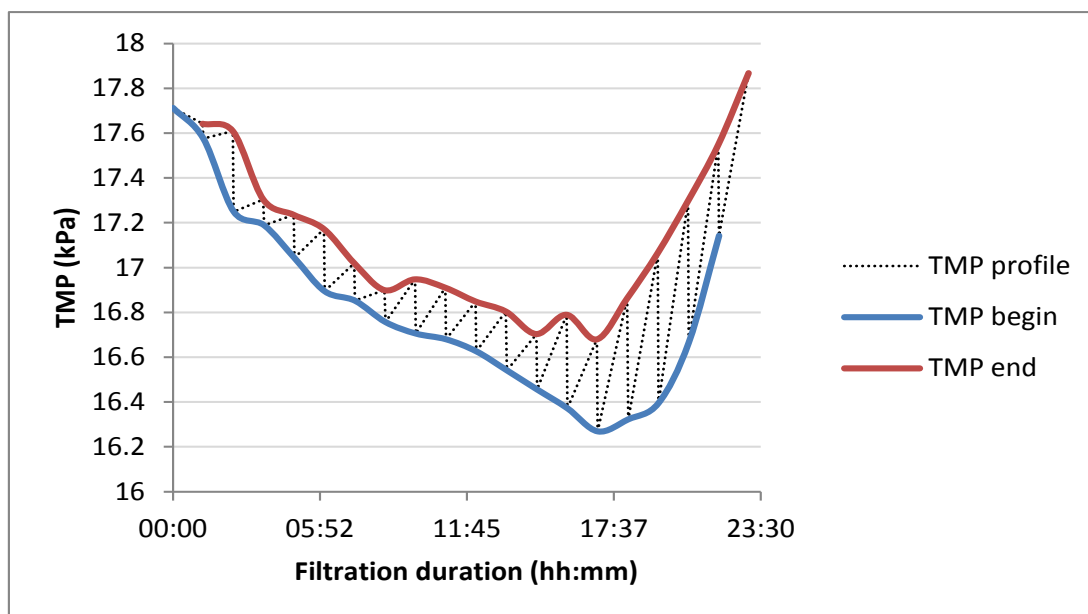


Figure 5-36: Day 3 TMP profile for direct flocculation and filtration through UF

Again TMP increase per filtration cycle was initially less than 0.2 kPa, and the magnitude thereof increased to 0.8 kPa. Potentially due to the lower minimum temperature reached (20°C), a minimum TMP of 16.3 kPa was achieved. TMP at the termination of an experimental 24 hour cycle (at 25°C) did not increase higher than TMP at the beginning of an experimental cycle (at 25°C), and irreversible fouling did not appear to occur.

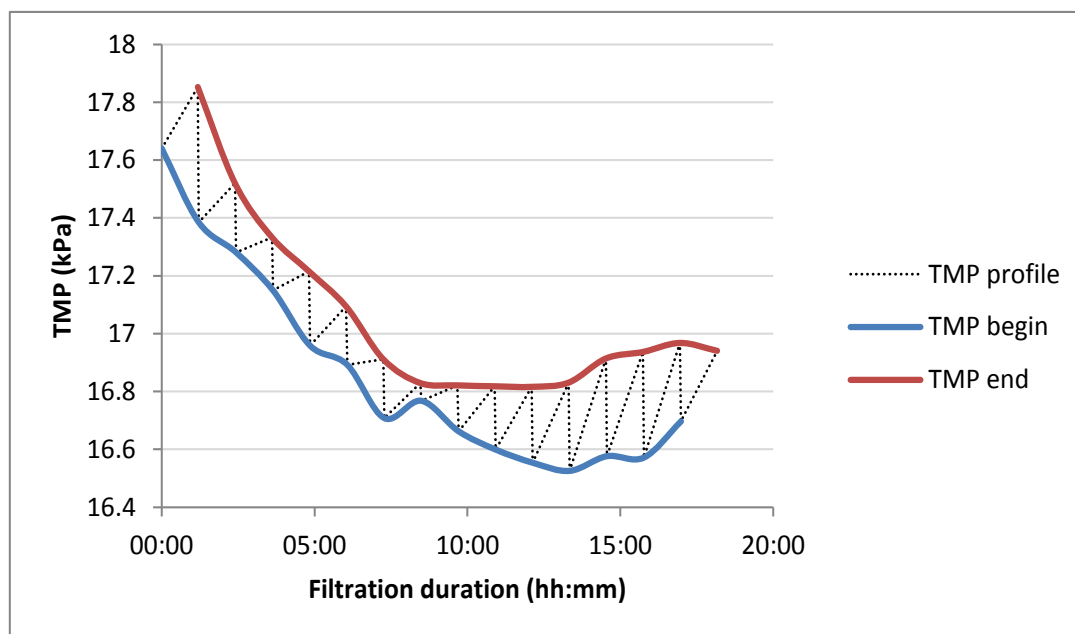


Figure 5-37: Day 4 TMP profile for direct flocculation and filtration through UF

TMP at the beginning and end of the filtration cycles gradually decrease before plateauing and maintaining consistent initial and final values, and consistent TMP rises per filtration cycles at

approximately 0.3 kPa. The cycle had to be terminated early due to a disruption in experimentation, and after CEB was carried out, the following cycle was initiated.

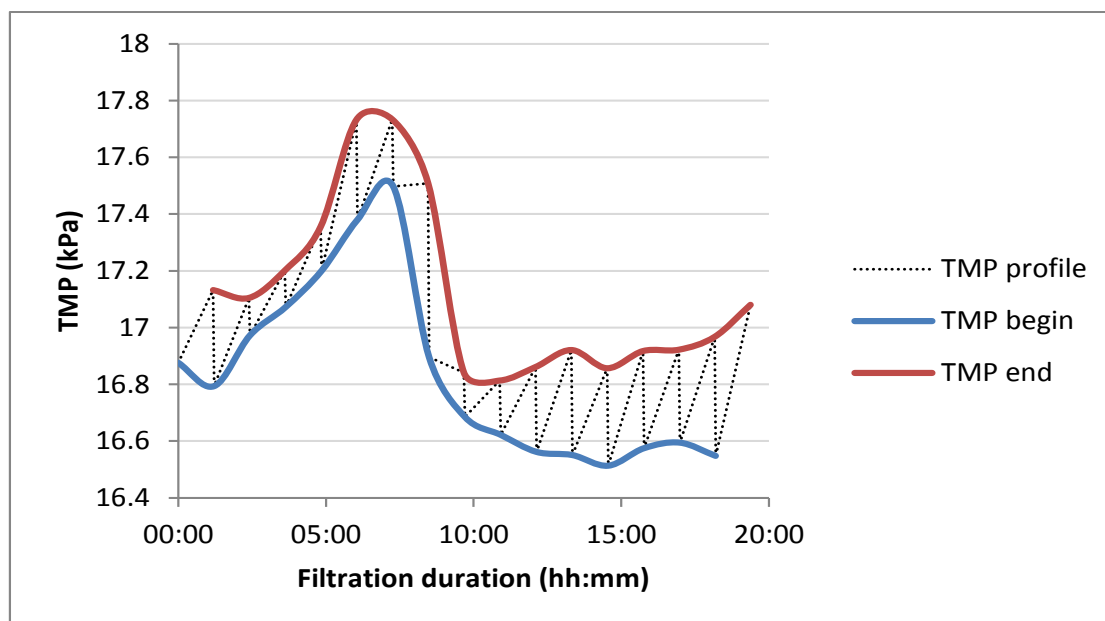


Figure 5-38: Day 5 TMP profile for direct flocculation and filtration through UF

An initial rise in TMP was noted. This increase does not exceed TMP initially measured for previous experimental cycles, and the following decrease in TMP remains within ranges measured on previous days. The 16.6 kPa TMP measured at the lowest point was slightly higher than the TMP of 16.3 kPa measured on a previous day, as the temperature did not decrease below 21°C as it did when 16.3 kPa was reached. Increases in TMP per filtration cycle varied between 0.2 and 0.4 kPa, with the anomalous decreasing section between the 5th and 10th hour potentially due to variations in temperature causing TMP spikes. Initial and final TMP remained within expected ranges.

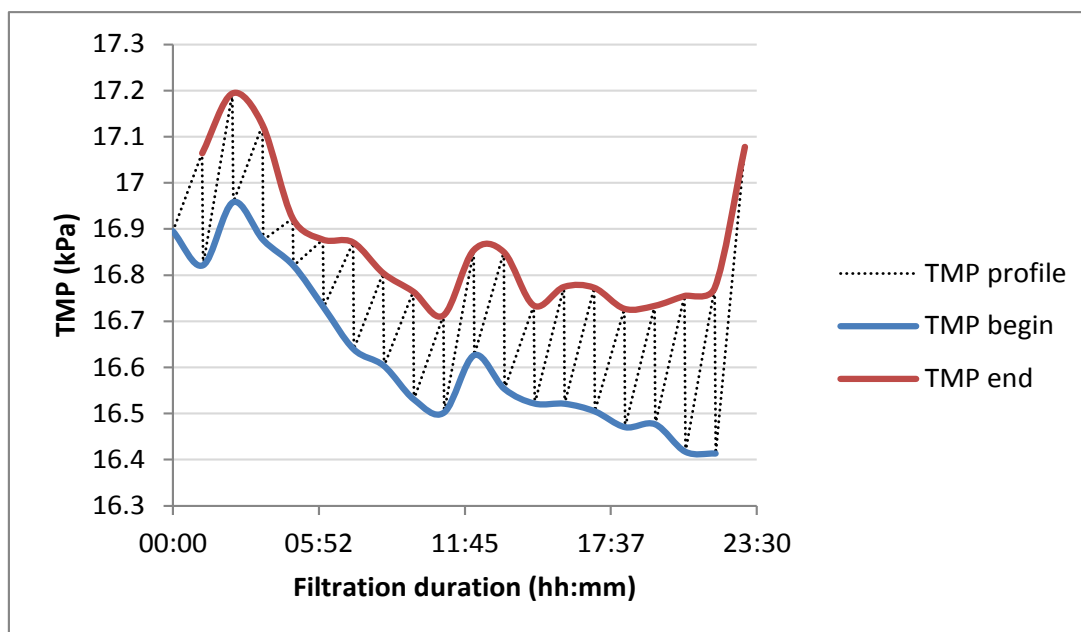


Figure 5-39: Day 6 TMP profile for direct flocculation and filtration through UF

At the end of many days of direct filtration through the membrane, no discernible change in initial or final TMP was noted that could not be ascribed to temperature fluctuations. Even for the normalised data, similar trends were noted indicative that the difference in flux at the different temperatures influenced the mass of foulants deposited per experimental cycle.

Fouling was reversible, as hydraulic backwashing adequately removed the increased TMP built up over the course of an experimental cycle. From similar temperature points over the course of an experimental day, it appears that irreversible fouling did not build up to cause an increase in TMP.

For the UF membrane operated without pre-filtration, TMP increases per filtration cycle varied between less than 0.2 to 0.8 kPa. No increases in TMP could be found when water was pre-filtered through the sand bed. The PF was thus an effective buffer to incoming foulants, as no TMP increase over the membrane occurred when including pre-treatment.

Especially for the treatment of water with such a variable nature, flocculating water directly through the membrane without any measure of pre-treatment is not recommended. If raw water quality should suddenly worsen and carry a large fraction of incoming solids, irreparable damage could be caused to the membrane. For sudden raw water changes, an adjustment in pH dosage is also critical in mitigating fouling. However, the presence of a buffer such as the PF would strain incoming suspended solids which could block capillaries. Using a backwashable pre-treatment, as opposed to a strainer that has to be manually cleaned or discarded, would have a longer usable lifespan. Using a PF showed that even at high SS loading, as tested for

during lab experiments, incoming flocs were modified and half the turbidity causing fraction removed by the PF. Repeating the experiments at a time of year when river water carries a high organics and solids loading, is crucial in determining the viability of using the pilot plant set-up on an actual site.

5.5.5 Temperature influence

Whereas membrane pressure drop data was normalised, trends corresponding with temperature was still noted. An example of a non-normalised curve is shown in Figure 5-40.

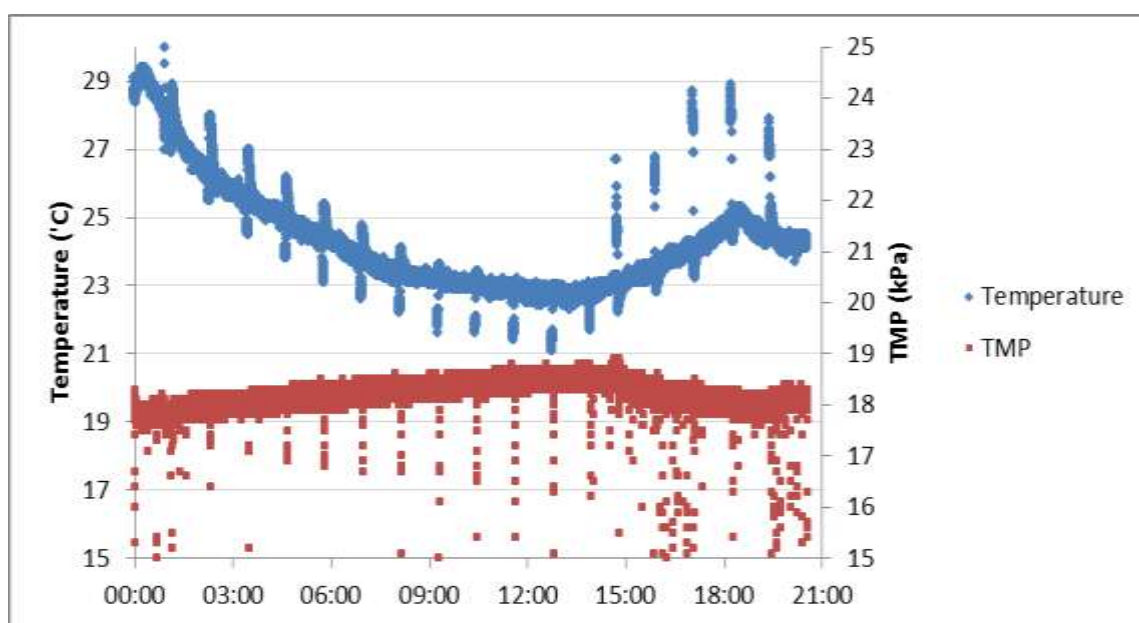


Figure 5-40: Non-normalised TMP plot

The reason for the temperature influence still being present in normalised TMP data could be a result of different flocculation kinetics at different temperatures, with a potential decrease in kinetics overnight when temperature drops. The TMP was calculated using a gauge reading for the permeate pressure, which could have deviated overnight when measurements were not taken. The inaccuracy with measurements made from gauges could also have influenced the TMP profile.

5.5.6 Comparison with plant data

According to Process Operators at the plant, the pressure drop over the membrane plant increases by 1 kPa between CEB cycles, or over the course of 20 hours of filtration. During the time of experimentation, no increase in initial TMP was found in the pilot plant for either set of experiments. It would likely be more comparable to conduct CEB after the same volume of water has been filtered by the unit rather than at similar time intervals.

CHAPTER 6 : CONCLUSIONS AND RECOMMENDATIONS

6.1 Conclusions

In response to the key questions stated:

1. It was possible to establish media bed properties that delivered PF filtrate with a turbidity below 1 NTU for 45-60 minutes for the range of downflow rates considered. Filtration at 12 m/h downflow rate was discredited due to poor overall performance. Screened sand (0.425-0.6 mm) promoted effective particle retention, and a bed depth of 250 mm was suitable to achieve required filtration durations. For downflow through the PF at 8 m/h, residual filtrate turbidity remained below 1 NTU for 70 minutes. At a downflow rate of 10 m/h, this duration shortened to 50 minutes. TMP reduction by inclusion of the PF was 100%. Backwashing duration of 2 minutes, equivalent to 4 displacement volumes, restored PF retention capacity in order to deliver clean filtrate upon backwash termination.
2. For dirtier water than the PF was characterised for, earlier breakthrough occurred.
 - a. For 10 m/h filtration of water with a turbidity of 31 NTU, breakthrough occurred after 15 minutes rather than the 50 minutes the bed was characterised for. The addition of PF was still able to reduce TMP by 72%.
 - b. Under flood conditions, water was filtered at 8 m/h through the PF and 37 LMH through the UF. Filtration duration was shortened from 70 to 50 minutes, explained hereafter. For high (400 mg/L) SS loading, breakthrough was instantaneous. TMP was still reduced by 64% compared to UF without pre-treatment.
 - c. For high (70 mg/L) organics loading, breakthrough occurred after 30 minutes, with 100% of TMP reduction enabled with the inclusion of pre-treatment.

Even upon breakthrough, continued floc retention occurred within the PF. The PF continuously modified the destabilised particles, creating a more gradual filtrate turbidity profile for water to be filtered by UF. The lower filtrate turbidity and the continuous increase of the PF pressure drop are indicative of continuous floc modification and fractional retention by the bed.

3. It was found that for high incoming suspended solids loading, filtration duration had to be shortened considerably from the duration established during characterisation. For high SS filtration at 8 m/h downflow rate, filtration duration had to be decreased from 70 to 50 minutes. Operating at the characterisation duration led to the deposition of very high mass of solids in the bed. Upon backwashing, the media and retained fines expanded past the visible height, meaning the elution of grains could occur. The use of the characterisation duration is a good average guideline which can be adjusted for extreme cases if deemed necessary.

It would be possible to considerably increase filtration duration during times when incoming water is relatively clean, until the membrane showed a predetermined increase in TMP. During times when incoming water is very dirty, the filtration duration would have to be shortened considerably in order to prevent the washing out of grains as found in lab work. The use of a terminal UF pressure drop could signify the end of a filtration cycle for high solids loading.

The backwashing requirement of the PF is fixed and limits the maximum recovery of the pilot scale set-up.

The use of a pre-filter proved an effective safeguard to the UF membrane, as it removed at least 40% of incoming flocculated water turbidity for high SS loading water. For synthetic water concentrations tested in the lab, and for clean site water, the PF aided in creating flocs that built up a reversible foulant on the membrane surface. Further testing and adjustment on site for a wider range of conditions would be necessary to consider the viability of its implementation as surface water UF pre-treatment.

6.2 Recommendations

As lab work could not be done for extended durations as experienced on site, it would be valuable to conduct more site work with the pilot plant, at different times of the year. Operating the pilot plant during a time for which incoming solids suddenly increases would be interesting, and the switch between filtration fluxes and durations could be evaluated.

For the operation of the set-up itself, a few alterations can be made to improve performance:

- On-site testing of equipment following first heavy rains of season to test for worst-case conditions
- Determine the effect of altering the CEB recipe
- Include pressure sensor at membrane outlet for more accurate TMP calculations

- During site work, CEB after the same volume of water has been treated as the plant you're comparing data to, rather than conducting a CEB at the same intervals
- Strainer above PF bed in order to prevent the washing out of media grains, while still allowing for the passage of flocs to the bed

Further alterations to equipment would fall outside the scope of what the unit was initially constructed for, but changes such as the inclusion of air scouring and selection of a higher column could be brought about.

CHAPTER 7 : REFERENCES

- Alam, N, O Ozdimir, M A Hampton, and A V Nguyen. "Dewatering of coal plant tailings: Flocculation followed by filtration." *Fuel*, no. 90 (2011): 26-35.
- American Society of Civil Engineers. *Water treatment plant design*. 5th. New York: McGraw-Hill, 2013.
- Anirudhan, TS, and M Ramachandran. "Surfactant-modified bentonite as adsorbent for the removal of humic acid from wastewaters." *Applied Clay Science*, no. 35 (2007): 276-281.
- Arnal, J M, M Sancho, G Verdu, J Lora, J F Marin, and J Chafer. "Selection of the most suitable ultrafiltration membrane for water disinfection in developing countries." *Desalination*, no. 168 (2004): 265-270.
- Baker, RW. *Membrane Technology and Applications*. 3rd. West Sussex: John Wiley & Sons, 2012.
- Bergamasco, R, L C Konradt-Moraes, M F Vieira, M R Fagundes-Klen, and A M S Vieira. "Performance of a coagulation-ultrafiltration hybrid process for water supply treatment." *Chemical Engineering Journal*, no. 166 (2011): 483-489.
- Bessiere, Y, C Guigui, P J Remize, and C Cabassud. "Coupling air-assisted backwash and rinsing steps: a new way to improve ultrafiltration process operation for inside-out hollow fibre modules." *Desalination*, no. 240 (2009): 71-77.
- Carroll, T, S King, SR Gray, BA Bolto, and NA Booker. "The fouling of microfiltration membranes by NOM after coagulation treatment." *Water Research* 34, no. 11 (2000): 2861-2868.
- Chae, S R, H Yamamura, K Ikeda, and Y Watanabe. "Comparison of fouling characteristics of two different poly-vinylidene fluoride microfiltration membranes in a pilot-scale drinking water treatment system using pre-coagulation/sedimentation, sand filtration, and chlorination." *Water Research*, no. 42 (2008): 2029-2042.
- Chang, H, et al. "Hydraulic irreversibility of ultrafiltration membrane fouling by humic acid: Effects of membrane properties and backwash water composition." *Journal of Membrane Science*, no. 493 (2015): 723-733.

- Chen, JP, SL Kim, and YP Ting. "Optimization of membrane physical and chemical cleaning by a statistically designed approach." *Journal of Membrane Science*, no. 219 (2003): 27-45.
- Chen, Y, BZ Dong, NY Gao, and JC Fan. "Effect of coagulation pretreatment on fouling of an ultrafiltration membrane." *Desalination*, no. 204 (2007): 181-188.
- Cheng, WP, and FH Chi. "A study of coagulation mechanisms of polyferric sulfate A study of coagulation mechanisms of polyferric sulfate method." *Water Research*, no. 36 (2002): 4583-91.
- Cho, M H, C H Lee, and S Lee. "Effect of flocculation conditions on membrane permeability in coagulation-microfiltration." *Desalination*, no. 191 (2006): 386-396.
- City of Tswane, Water and Sanitation Division. "Rietvlei Water Treatment Plant." Tswane: Public Works and Infrastructure Development, 2006.
- Cleasby, J L, and K Fan. "Predicting the fluidisation and expansion of filter media." *Journal of the Environmental Engineering Division*, no. 101 (1981): 455-471.
- Cox, Charles R. *Operation and Control of Water Treatment Processes*. 3rd. Geneva: World Health Organisation, 1969.
- Crittenden, JC, KJ Howe, DW Hand, G Tchobanoglous, and RR Trussell. *Principles of water treatment*. 3rd. New Jersey: John Wiley & Sons, 2012.
- Crozes, G F, J G Jacangelo, G Anselme, and J M Laine. "Impact of ultrafiltration operating conditions on membrane irreversible fouling." *Journal of Membrane Science*, no. 124 (1997): 63-76.
- De Souza, N P, and O D Basu. "Comparative analysis of physical cleaning operations for fouling control of hollow fiber membranes in drinking water treatment." *Journal of Membrane Science*, no. 436 (2013): 28-35.
- Degrémont. *Water Treatment Handbook*. 7th. France: Lavoisier, 2007.
- Dharmarajah, A H, and J L Cleasby. "Predicting the expansion of filter media." *Journal of the American Water Works Association*, no. 78 (1986): 66-76.
- Dialynas, E, and E Diamadopoulos. "Integration of immersed membrane ultrafiltration with coagulation and activated carbon adsorption for advanced treatment of municipal wastewater." *Desalination*, no. 230 (2008): 113-127.

- Dong, BZ, Y Chen, NY Gao, and JC Fan. "Effect of pH on UF membrane fouling." *Desalination*, no. 195 (2006): 201-208.
- DOW. "DOW Water and Process Solutions." 2012. http://msdssearch.dow.com/PublishedLiteratureDOWCOM/dh_095b/0901b8038095b91d.pdf?filepath=/609-00071.pdf&fromPage=GetDoc (accessed July 27, 2016).
- Drioli, E, and L Giorno. *Membrane operations*. Germany: Wiley-VCH, 2009.
- Droste, Ronald L. *Theory and Practice of Water and Wastewater Treatment*. Canada: John Wiley & Sons, 1997.
- Dynamics, Native. "Calculation of flow through nozzles and orifices." 11 February 2015. https://neutrium.net/fluid_flow/calculation-of-flow-through-nozzles-and-orifices/ (accessed June 29, 2016).
- Edzwald, JK, JE Tobiasson, JE Kelley, HJ Dunn, PB Galant, and GS Kaminski. "Impacts of Filter Backwash Recycle on Clarification and Filtration." Denver, Colorado: American Water Works Research, 2001.
- Engineers, American Society of Civil. *Water Treatment Plant Design*. 2nd. New York: McGraw-Hill, 1990.
- Fan, L, JL Harris, FA Roddick, and NA Booker. "Influence of the characteristics of natural organic material on the fouling of microfiltration membranes." *Water Research* 35, no. 18 (2001): 4455-4463.
- Fiksdal, L, and T O Leiknes. "The effect of coagulation with MF/UF membrane filtration for the removal of virus in drinking water." *Journal of Membrane Science*, no. 279 (2006): 364-371.
- Fu, X, T Maruyama, T Sotani, and H Matsuyama. "Effect of surface morphology on membrane fouling by humic acid with the use of cellulose acetate butyrate hollow fiber membranes." *Journal of Membrane Science*, no. 320 (2008): 483-491.
- Gao, W, et al. "Membrane fouling control in ultrafiltration technology for drinking water production: A review." *Desalination*, no. 272 (2011): 1-8.
- GHD. *The GHD Book of Water Treatment*. 1st. Sydney: GHD, 2005.
- Gomez, M, A De La Rua, G Garralon, F Plaza, R Hontoria, and M A Gomez. "Urban wastewater disinfection by filtration technologies." *Desalination*, no. 190 (2006): 16-28.

- Gottfried, A, AD Shepard, K Hardiman, and ME Walsh. "Impact of recycling filter backwash water on organic removal in coagulation-sedimentation processes." *Water research*, no. 42 (2008): 4683-4691.
- Government. "Statistics Souty Africa." 6 October 2010. http://beta2.statssa.gov.za/?page_id=1854&PPN=D0405.8&SCH=4756 (accessed February 25, 2014).
- Graham, NJD. "Filter pore flocculation as a mechanism in rapid filtration." *Water Research*, no. 22 (1988): 1229-1238.
- Gray, N F. *Water Technology: An Introduction for Environmental Scientists and Engineers*. 2nd. Great Britain: Elsevier, 2005.
- Guigui, C, JC Rouch, L Durand-Bourlier, V Bonnelye, and P Aptel. "Impact of coagulation conditions on the in-line coagulation/UF process for drinking water production." *Desalination*, no. 147 (2002): 95-100.
- Guo, X, Z Zhang, L Fang, and L Su. "Study on ultrafiltration for surface water by a polyvinylchloride hollow fiber membrane." *Desalination*, no. 238 (2009): 183-191.
- Henley, Ernest J, J D Seader, and D Keith Roper. *Separation Process Principles*. 3rd. Asia: John Wiley & Sons, 2011.
- Hillis, P, M B Padley, N I Powell, and P M Gallagher. "Effects of backwash conditions on out-to-in membrane microfiltration." *Desalination*, no. 118 (1998): 197-204.
- Ives, KJ. *The Scientific Basis of Filtration*. Cambridge: AW Sijthoff, 1975.
- Jeong, S, and S Vigneswaran. "Assessment of biological activity in contact flocculation filtration used as a pretreatment in seawater desalination." *Chemical Engineering Journal*, no. 228 (2013): 976-983.
- Jin, B, BM Wilen, and P Lant. "A comprehensive insight into floc characteristics and their impact on compressibility and settleability of activated sludge." *Chemical Engineering Journal* (Chemical Engineering Journal), no. 95 (2003): 221-234.
- Johir, A H, C Khorsed, S Vigneswaran, and H K Shon. "In-line flocculation-filtration as pre-treatment to reverse osmosis desalination." *Desalination*, no. 247 (2009): 85-93.
- Johnson, R L, and J L Cleasby. "Effect of backwash on filter effluent quality." *Journal of the Sanitary Engineering Division*, no. 92 (1966): 215-228.

- Judd, SJ, and P Hillis. "Optimisation of combined coagulation and microfiltration for water treatment." *Water Research* 35, no. 12 (2001): 2895-2904.
- Jung, AV, V Chanudet, J Ghanbaja, BS Lartiges, and JL Barsillon. "Coagulation of humic substances and dissolved organic matter with a ferric salt: An electron energy loss spectroscopy investigation." *Water Research*, no. 39 (2005): 3849-3862.
- Kabsch-Korbutowicz, M. "Application of ultrafiltration integrated with coagulation for improved NOM removal." *Desalination*, no. 174 (2005): 13-22.
- Katsoufidou, K, S G Yiantsios, and A J Karabelas. "A study of ultrafiltration membrane fouling by humic acids and flux recovery by backwashing: Experiments and modeling." *Journal of Membrane Science*, no. 266 (2005): 40-50.
- Katsoufidou, K, S G Yiantsios, and A J Karabelas. "An experimental study of UF membrane fouling by humic acid and sodium alginate solutions: the effect of backwashing on flux recovery." *Desalination*, no. 220 (2008): 214-227.
- Kawamura, Susumu. *Integrated Design and Operation of Water Treatment Facilities*. 2nd. Canada: John Wiley & Sons, 2000.
- Kimura, K, T Maeda, H Yamamura, and Y Watanabe. "Irreversible membrane fouling in microfiltration membranes filtering coagulated surface water." *Journal of Membrane Science*, no. 320 (2008): 356-362.
- Kimura, K, Y Hane, Y Watanabe, G Amy, and N Ohkuma. "Irreversible membrane fouling during ultrafiltration of surface water." *Water Research*, no. 38 (2004): 3431-3441.
- Konieczny, K. "Disinfection of surface and ground waters with polymeric ultrafiltration membranes." *Desalination*, no. 119 (1998): 251-258.
- Konieczny, K, D Sakol, J Plonka, M Rajca, and M Bodzek. "Coagulation-ultrafiltration system for river water treatment." *Desalination*, no. 240 (2009): 151-159.
- Konieczny, K, M Bodzek, and M Rajca. "A coagulation-MF system for water treatment using ceramic membranes." *Desalination*, 2006: 92-101.
- Kretzschmar, R, H Holthoff, and H Sticher. "Influence of pH and Humic Acid on Coagulation Kinetics of Kaolinite: A Dynamic Light Scattering Study." *Journal of Colloid and Interface Science*, no. 202 (1998): 95-103.

- Kweon, J H, et al. "Evaluation of coagulation and PAC adsorption pretreatments on membrane filtration for a surface water in Korea: A pilot study." *Desalination*, no. 249\ (2009): 212-216.
- Leiknes, T. "The effect of coupling coagulation and flocculation with membrane filtration in water treatment: A review." *Journal of Environmental Science*, no. 21 (2009): 8-12.
- Li, Q, and M Elimelech. "Synergistic effects in combined fouling of a loose nanofiltration membrane by colloidal materials and natural organic matter." *Journal of membrane science*, no. 278 (2006): 72-82.
- Ma, C, L Wang, S Li, S G J Heijman, L C Rietveld, and X B Su. "Practical experience of backwashing with RO permeate for UF fouling control treating surface water at low temperatures." *Separation and Purification Technology*, no. 119 (2013): 136-142.
- Ma, S, C Liu, K Yang, and D Lin. "Coagulation removal of humic acid-stabilized carbon nanotubes from water by PACl: Influences of hydraulic conditions and water chemistry." *Science of the Total Environment* 439 (2012): 123-128.
- Matamoros, Victor, and Victoria Salvado. "Evaluation of a coagulation/flocculation-lamellar clarifier and filtration-UV-chlorination reactor for removing emerging contaminants at full-scale wastewater treatment plants in Spain." *Journal of environmental management*, no. 117 (2013): 96-102.
- Matilainen, Ann, Mikko Vepsäläinen, and Mika Silanpää. "Natural organic matter removal by coagulation during drinking water treatment: A review." *Advances in Colloid and Interface Science*, no. 159 (2010): 198-197.
- Mierzwa, J C, I Hespanhol, M C C Da Silva, R D B Rodrigues, and C F Giorgi. "Direct drinking water treatment by spiral-wound ultrafiltration membranes." *Desalination*, no. 230 (2008): 41-50.
- Mosqueda-Jimenez, D B, and P M Huck. "Characterization of membrane foulants in drinking water treatment." *Desalination*, no. 198 (2006): 173-182.
- Mosqueda-Jimenez, DB, PM Huck, and OD Basu. "Fouling characteristics of an ultrafiltration membrane used in drinking water treatment." *Desalination* 230 (2008): 79-91.
- Murray, K E, S M Thomas, and A A Bodour. "Prioritizing research for trace pollutants and emerging contaminants in the freshwater environment." *Environmental Pollution*, no. 158 (2010): 3462-3471.

- Nakatsuka, S, I Nakate, and T Miyano. "Drinking water treatment by using ultrafiltration hollow fiber membranes." *Desalination*, no. 106 (1996): 55-61.
- Nazaroff, W W, and L Alvarez-Cohen. *Environmental Engineering Science*. New York: John Wiley & Sons, 2001.
- Nowicki, W, and G Nowicka. "Verification of the Schulze-Hardy Rule: A Colloid Chemistry Experiment." *Journal of Chemical Education* 71 (1994): 624-626.
- Park, S, and T Yoon. "Effects of iron species and inert minerals on coagulation and direct filtration for humic acid removal." *Desalination*, no. 239 (2009): 146-158.
- Peng, X, Z Luan, F Chen, B Tian, and Z Jia. "Adsorption of humic acid onto pillared bentonite." *Desalination*, no. 174 (2005): 135-143.
- Perry, R H, and D W Green. *Perry's Chemical Engineers' Handbook*. 8th. New York: McGraw-Hill, 2008.
- Pourrezaei, P, et al. "Physico-Chemical Processes." *Water Environment Research*, no. 82 (2010): 997-1072.
- Pradhan, M, S Vigneswaran, J Kandasamy, and R B Aim. "Combined effect of air and mechanical scouring of membranes for fouling reduction in submerged membrane reactor." *Desalination (Desalination)*, no. 288 (2012): 58-65.
- Rautenbach, R, and R Albrecht. *Membrane Processes*. 1st. Frankfurt: John Wiley & Sons, 1989.
- Rebhun, M, Z Fuhrer, and A Adin. "Contact flocculation-filtration of humic substances." *Water Research*, no. 18 (1984): 963-970.
- Regula, C, et al. "Chemical cleaning/disinfection and ageing of organic UF membranes: A review." *Water Research*, 2014: doi: 10.1016/j.watres.2014.02.050.
- Rhodes, Martin. *Introduction to Particle Technology*. 2nd. England: John Wiley & Sons, 2008.
- Rodrigues, A, A Brito, P Janknecht, MF Proenca, and R Nogueira. "Quantification of humic acids in surface water: effects of divalent cations, pH and filtration." *Journal of Environmental Monitoring*, 2008: 377-382.
- Salman, M, E Bassam, and F Khalili. "Adsorption of humic acid on bentonite." *Applied Clay Science* 38 (2007): 51-56.

- Scott, K, and R Hughes. *Industrial Membrane Separation Technology*. 1st. London: Blackie Academic & Professional, 1996.
- Serra, C, L Durand-Bourlier, M J Clifton, P Moulin, J C Rouch, and P Aptel. "Use of air sparging to improve backwash efficiency in hollow-fiber modules." *Journal of Membrane Science*, no. 161 (1999): 95-113.
- Shengji, X, Y Juanjuan, and G Naiyun. "An empirical model for membrane flux prediction in ultrafiltration of surface water." *Desalination*, no. 221 (2008): 370-375.
- Sieliechi, JM, et al. "Changes in humic acid conformation during coagulation with ferric chloride: Implications for drinking water treatment." *Water Research*, no. 42 (2008): 2111-2123.
- Slavik, I, A Jehmlich, and W Uhl. "Impact of backwashing procedures on deep bed filtration productivity in drinking water treatment." *Water Research*, no. 47 (2013): 6348-6357.
- Slavik, I, A Jehmlich, and W Uhl. "Impact of backwashing procedures on deep bed filtration productivity in drinking water treatment." *Water Research*, no. 47 (2013): 6348-6357.
- Smith, Paul James, Saravanamuth Vigneswaran, Huu Hao Ngo, Roger Ben-Aim, and Hung Nguyen. "A new approach to backwash initiation in membrane systems." *Journal of Membrane Science*, no. 278 (2006): 381-389.
- Stevenson, David G. *Water Treatment Unit Processes*. 1st. London: Imperial College Press, 1997.
- Tambo, N, and H Hosumi. "Physical aspects of flocculation II: Contact flocculation." *Water Research*, no. 13 (1979): 441.
- Tchobanoglous, G, and ED Schroeder. *Water Quality*. 1st. Canada: Addison-Wesley Publishing Company, 1985.
- Tebbutt, THY. *Principles of Water Quality Control*. 4th. Oxford: Pergamon Press, 1992.
- Uyguner-Demirel, CS, and M Bekbolet. "Significance of analytical parameters for the understanding of natural organic matter in relation to photocatalytic oxidation." *Chemosphere*, no. 84 (2011): 1009-1031.
- Van Duuren, F A. *Water Purification Works Design*. Pretoria: Water Research Commission, 1997.
- Wang, J, and XC Wang. "Ultrafiltration with in-line coagulation for the removal of natural humic acid and membrane fouling mechanism." *Journal of Environmental Sciences* 18, no. 5 (2006): 880-884.

- Wang, J, J Guan, S R Santiwong, and T David Waite. "Characterization of floc size and structure under different monomer and polymer coagulants on microfiltration membrane fouling." *Journal of Membrane Science*, no. 321 (2008): 132-138.
- Wang, L, X Wang, and K Fukushi. "Effects of operational conditions on ultrafiltration membrane fouling." *Desalination*, no. 229 (2008): 181-191.
- Wang, Q, B Gao, Y Wang, Z Yang, W Xu, and Q Yue. "Effect of pH on humic acid removal performance in coagulation-ultrafiltration process and the subsequent effects on chlorine decay." *Separation and Purification Technology*, no. 80 (2011): 549-555.
- Wang, Y, Q Wang, BY Gao, Q Yue, and Y Zhao. "The disinfection by-products precursors removal efficiency and the subsequent effects on chlorine decay for humic acid synthetic water treated by coagulation process and coagulation-ultrafiltration process." *Chemical Engineering Journal*, no. 193 (2012): 59-67.
- Weber, WJ. *Physicochemical Processes for Water Quality Control*. Canada: John Wiley & Sons, 1972.
- Willemse, RJN, and B Voort. "Full-scale recycling of backwash water from sand filters using dead-end membrane filtration." *Water Research*, no. 33 (1999): 3379-3385.
- Zhan, X, B Gao, Q Yue, Y Wang, and B Cao. "Coagulation behavior of polyferric chloride for removing NOM from surface water with low concentration of organic matter and its effect on chlorine decay model." *Separation and Purification Technology*, no. 75 (2010): 61-68.
- Zhang, H, Z Zhong, W Li, W Xing, and W Jin. "River Water Purification via a Coagulation-Porous Ceramic Membrane Hybrid Process." *Chinese Journal of Chemical Engineering* 1, no. 22 (2014): 113-119.
- Zhang, L, P Gu, Z Zhong, D Yang, W He, and H Han. "Characterization of organic matter and disinfection by-products in membrane backwash water from drinking water treatment." *Journal of Hazardous Materials* (Journal of Hazardous Materials), no. 168 (2009): 753-759.
- Zhang, Ling Ling, Dong Yang, Zhi-Ji Zhong, and Ping Gu. "Application of hybrid coagulation-microfiltration process for treatment of membrane backwash water from waterworks." *Separation and Purification Technology*, no. 62 (2008): 415-422.

- Zhu, L J, et al. "Hydrophilic and anti-fouling polyethersulfone ultrafiltration membranes with poly (2-hydroxyethyl methacrylate) grafted silica nanoparticles as additive." *Journal of Membrane Science*, no. 451 (2014): 157-168.
- Zularisam, A W, A F Ismail, and R Salim. "Behaviours of natural organic matter in membrane filtration for surface water treatment — a review." *Desalination*, no. 194 (2006): 211-231.

CHAPTER 8 : APPENDICES

8.1 Appendix A: Characterisation of reagents and materials

Complete information sheets of chemicals attached in the following pages

8.1.1 MSDS sheets

The MSDS sheets for purchased chemicals and chemicals used for CEB present in the Process Engineering Department are attached hereafter.

1. Product name: Bentonite
Product number: 285234

2. Product name: Humic acid sodium salt
Product number: H16752

3. Product name: Iron (III) chloride solution
Product number: 12322

4. Product name: Sodium hydroxide

5. Product name: Sodium hypochlorite

6. Product name: Citric acid

8.1.2 Bentonite particle size distribution

Bentonite was analysed to determine the particle sizes and gauge the type of fouling that could occur.

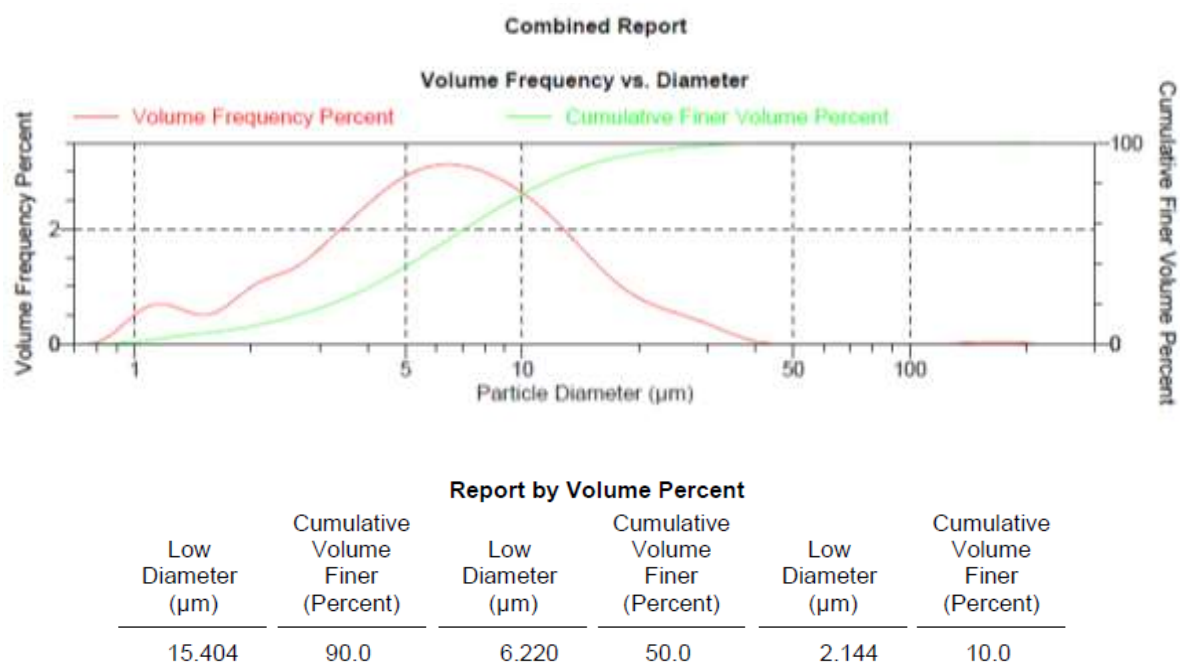


Figure 8-1: Bentonite particle size distribution

Bentonite particle sizes are consistently larger than the nominal UF pore size, even at the lowest detected limit at 2 micron. The bentonite particle sizes are of such a nature that it would predominantly build up as a cake layer on the membrane surface.

8.1.3 Sand particle size distribution

Figure 8-2 illustrates the different sand types considered and their particle size distributions as given by Consol datasheets.

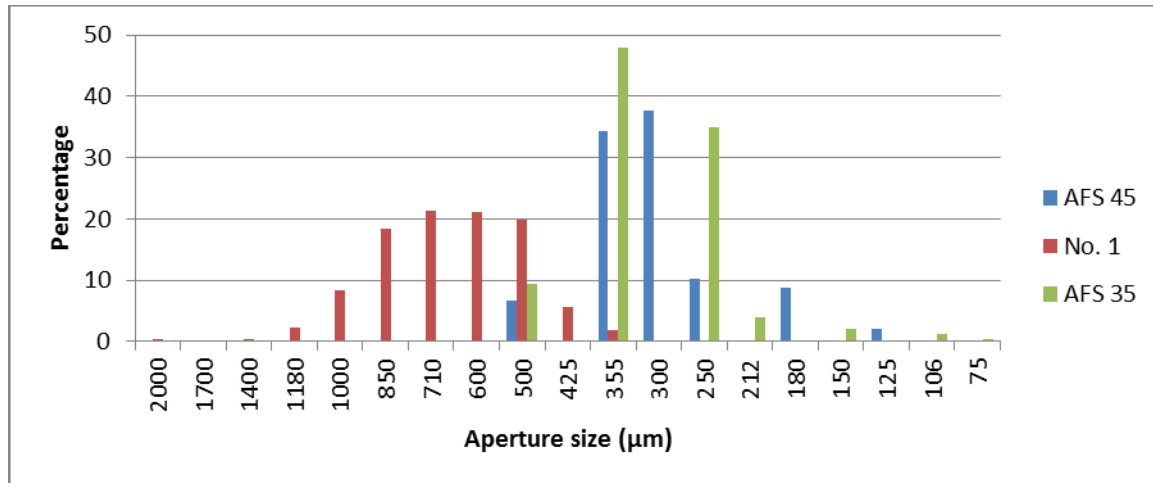


Figure 8-2: Silica sand grading and particle size distribution

The shape of the media is illustrated in the following figure:



Figure 8-3: Silica filtration media

8.1.4 Turbidity of humic acids and bentonite suspensions

Suspension	Humic acid conc. (mg/L)	Bentonite conc. (mg/L)	Measured turbidity (NTU)	Calculated turb. (NTU)
Base	0	0	0.14	
HA1	5	0	1.47	
HA2	10	0	2.71	
HA3	15	0	3.95	
HA4	20	0	5.02	
HA5	25	0	6.02	
Base	0	0	0.14	
B1	0	5	1.14	
B2	0	10	2.05	
B3	0	20	3.52	
B4	0	30	5.49	
B5	0	40	6.64	
B6	0	50	8.08	
B7	0	60	9.75	
B8	0	80	12.8	
B9	0	100	16.5	
M1	10	10	4.41	4.76
M2	20	20	8.16	8.54
M3	20	40	11.1	11.66
M4	25	50	14.1	14.1
M5	25	100	22.3	22.52

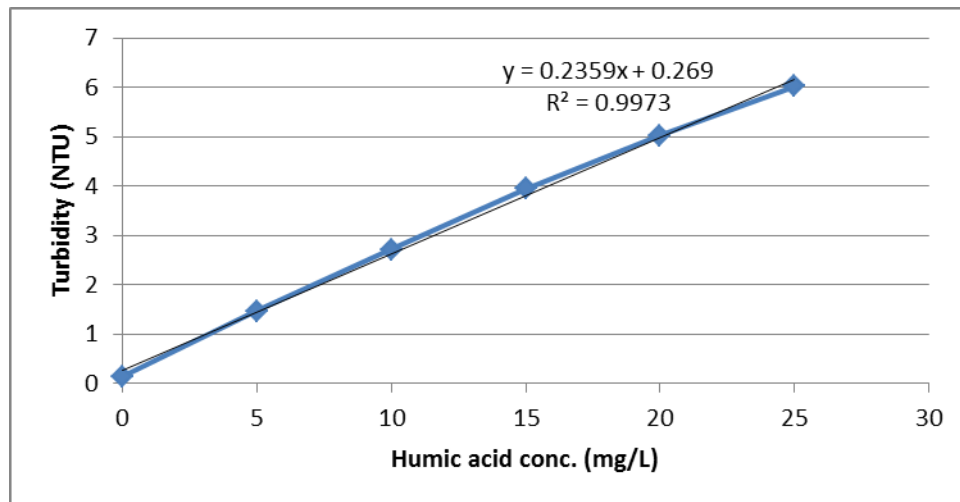


Figure 8-4: Humic acid contribution to water turbidity

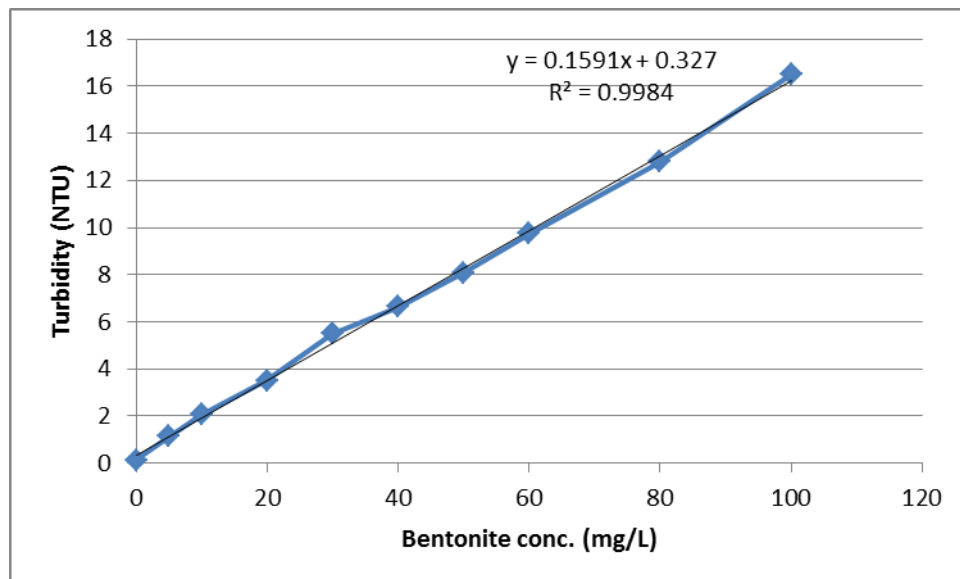
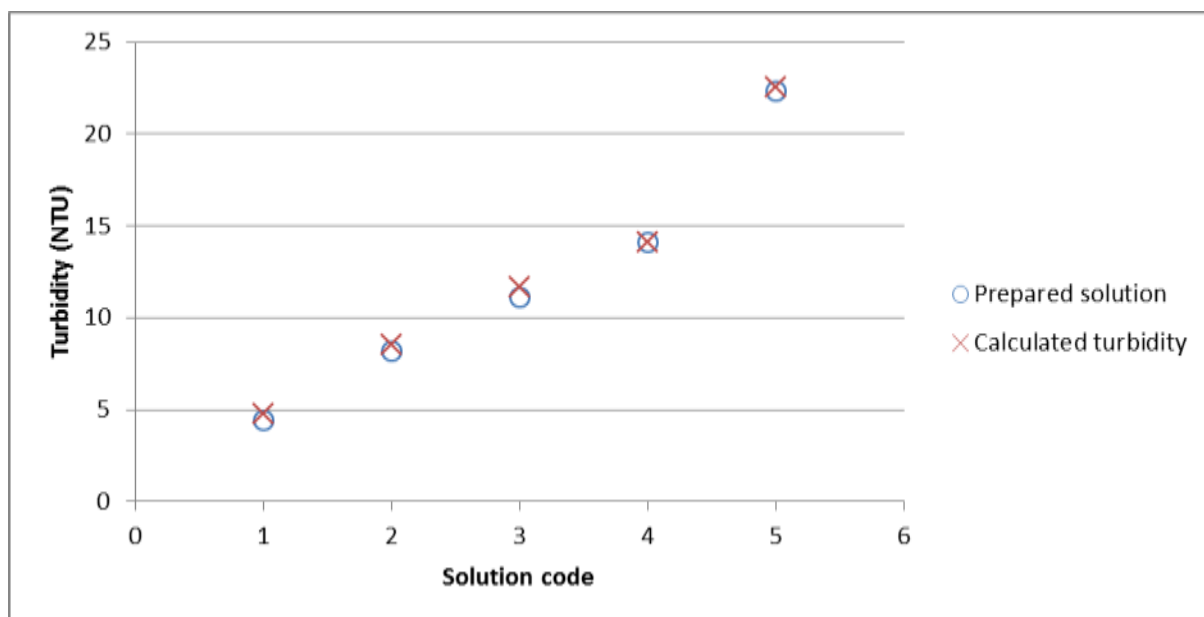


Figure 8-5: Bentonite contribution to water turbidity



This confirmation was necessary to determine whether water with a required turbidity could be made up through selection of humic acid and bentonite concentrations.

8.1.5 Operation of conventional surface water treatment plant

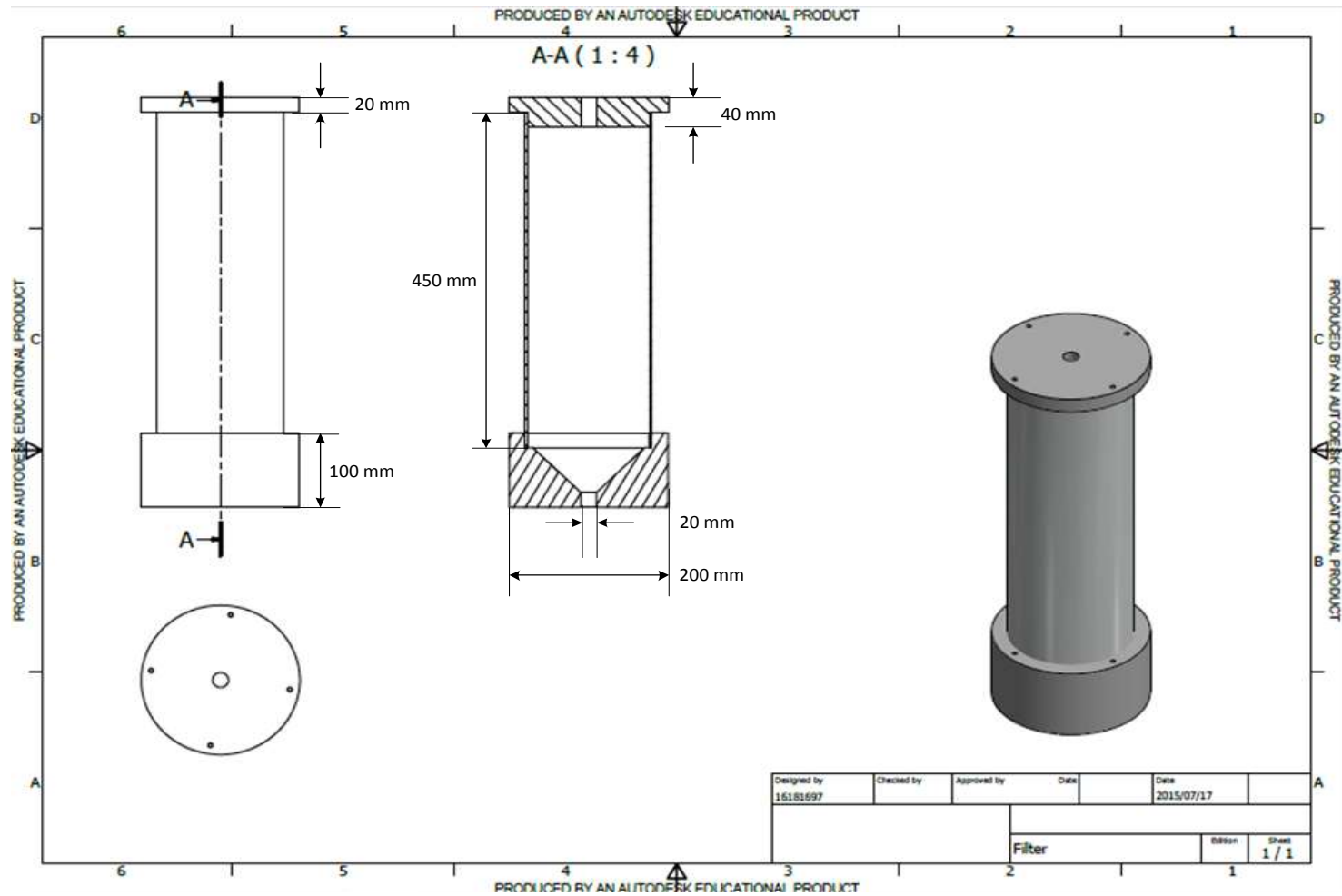
The production of potable water is most commonly done through conventional water treatment in South Africa. Conventional water treatment is done as follows:

- Plant feed intake from raw water source (river, catchment dam)
- Chemical dosing to alter pH of raw water
- Coagulant dosing
- Rapid mixing (at point of coagulant dosage)
- Slow mixing (water flow through channels to promote destabilised particle contact)
- Sedimentation: settling of flocs
- Filtration of supernatant through media beds
- Disinfection (chlorination/UV treatment/ozonation)

The sludge separated from the supernatant following sedimentation is pumped to settling dams.

8.2 Appendix B: Equipment construction and operation

8.2.1 Media filter Inventor drawing



8.2.2 Equipment list

Unit	Code	Description
Water tank	T-101	1000 L raw water storage
Mixer	M-101	Motor with three blade impeller to agitate contents of raw water storage tank
Feed pump	P-101	Grundfos CMBE centrifugal booster pump
Dosing pump	P-102	Watson-Marlow 520S dosing pump
Static mixer	M-102	Fitting for variable orifice plate
Media filter	F-101	PVC filter of varying depth
Ultrafiltration module	F-102	inge® dizzer® P4040-4.0 ultrafiltration module
Backwashing pump	P-103	DAB 0.47 kW centrifugal pump
Water tank	T-102	200 L water storage of filtered water for use in backwashing
Flow meter	FE	Flow sensor for measuring water flow rate of forward washing water
Flow meter	FE	Flow sensor for measuring water flow rate of backwashing water
Pressure transmitter	PT	Pressure transmitter for measuring pressure in line
Pressure transmitter	PT	Pressure transmitter for measuring pressure in line
Temperature probe	TE	PT-100 probe for measuring water temperature
Non-return valves	NRV-101	Nylon check valve
	NRV-102	Nylon check valve
Actuated valves	AV-101	Netafim solenoid valve
	AV-102	Netafim solenoid valve
	AV-103	Netafim solenoid valve
Manual valves	MV-101 to MV-112	PVC ball valves controlling flow path

8.2.3 Layout, construction and assembly of experimental unit

The layout of the experimental unit was done by considering the sizes of all the units and their proximity to one another. They were assembled in the sequence determined in the process flow diagram with consideration of practical requirements and limitations, and units were arranged in the most compact and functional way considered practically feasible.

Based on the most compact manner of assembly of the units, dimensions were calculated for a frame which could contain all units. Support structures, such as beams or planks on which units can rest, and brackets for the membrane module, were added. Upon adding wheels and painting the frame, units were added to the frame starting with the largest components, namely the filters and pumps. Rigid PVC pipe sections were cut to the desired length and glued to the necessary fittings. Hose barbs for flexible tubing were inserted where necessary, and the tubing secured with hose clamps. Fittings for the flow meters and pressure gauges were custom made in the workshop. Different orifice plates were made which would ensure flow of between 9 and 11 m/s for the different flow rates used during experimentation.

The water storage tanks were not considered in the assembly of the mobile unit, and just had to be placed in close proximity to the set-up. The large raw water storage tank includes a motor with a mixing impeller which prevents suspended components in the water from settling. The experimental unit was placed close to drainage so that the overflow of clean water and backwashing and dilution water can be washed away.

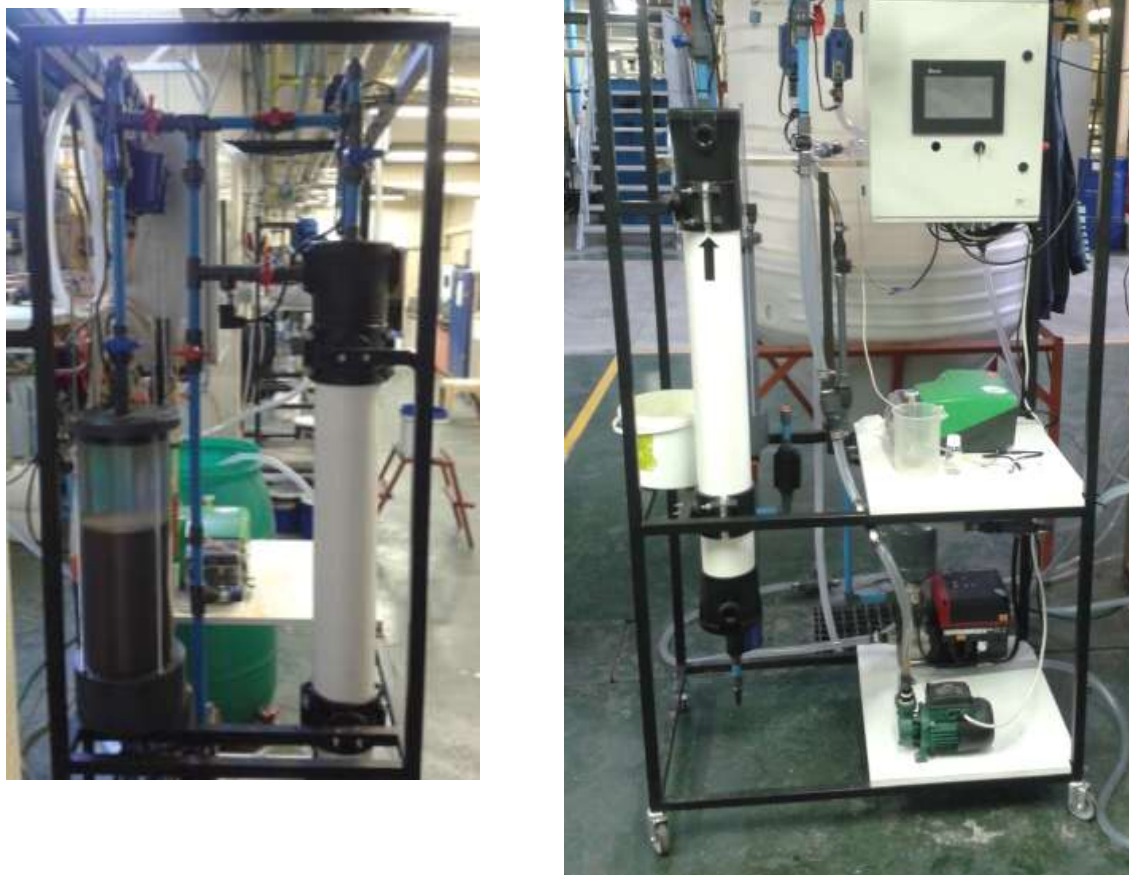


Figure 8-6: Experimental set-up (left) side and (right) front view

8.2.4 Commissioning of completed water treatment unit

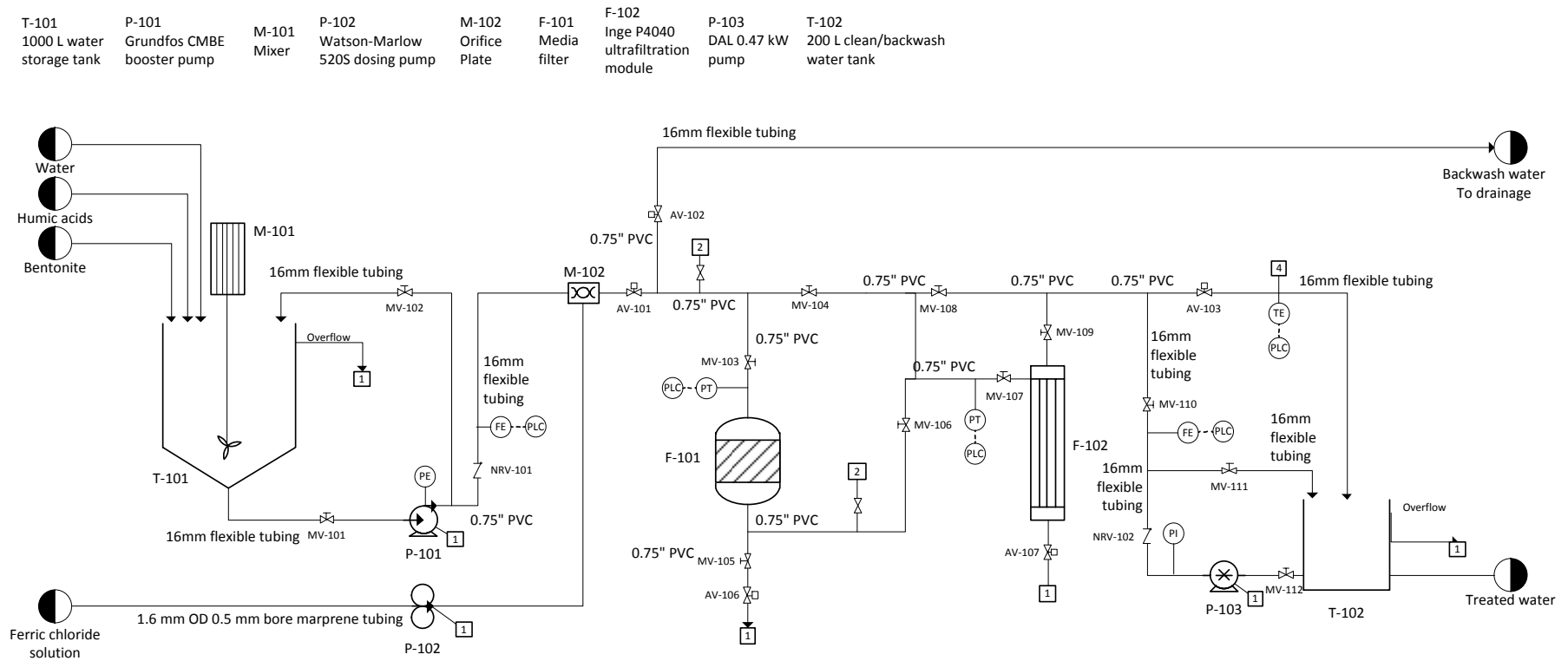
Following the assembly of the treatment unit and the required electronic commands to render it functional, the unit is treated through clean water runs to determine whether it can successfully be operated at the conditions and within the ranges it was designed for. Water is used in experimental work to test whether the unit can achieve the desired flow rates, and the commissioning period is used to address electronic and hydraulic problems that arose during testing. Faulty solenoid valves were fixed or replaced, and leaking areas were addressed. Minor changes were made to the set-up following the completion of construction to improve the functionality thereof. Maintenance of the set-up occurs throughout experimentation, and the potential effect of minor changes to the set-up should be carefully considered before they are made in order to reduce interference.

8.2.5 Electronic requirements and instrumentation required

A PLC controls the automated operation of the experimental set-up. It can change the pump speed through a variable speed drive to maintain an entered flow rate set point. It is necessary for the user to ensure the correct manual valves are open for the required operation, the correct orifice plate is inserted and the correct PID parameters for the specific experiment are entered. Upon entry of a flow rate set point, operational and backwashing durations, the operation of the unit is automated. After the required forward washing time has reached completion, backwashing is initiated by the PLC. Upon the completion of each cycle, the required actuated valves used in each mode are either opened or closed based on the requirement, and required pumps are switched either on or off.

8.2.6 Final process flow diagram




Attached hereafter.



Utility connections

1. Drainage
2. Sample port
3. Compressed air
4. Vent to atmosphere

Key to valve symbols

- | | |
|---|------------------|
|  | Manual valve |
|  | Actuated valve |
|  | Non-return valve |

8.2.7 Complete operating procedure for experimental set-up

Loading new sand into the system

Prior to operation, it has to be checked that sand of the required size is loaded in the bed at the required depth. If the bed is too shallow, a slurry of sand can be carefully fed through the top of the media bed. If the entire contents of the bed has to be replaced, the following sequence of steps has to be followed.

Removing sand from filter

- Close all ball and solenoid valves feeding water to or from the plant.
- Close ball valves in-line before and after media filter.
- Drain water from media filter through bottom manual valve. Loosen union above to speed up draining.
- Unfasten winged bolts fixing lid of media bed to the body, and remove the lid.
- Scoop all sand out of the tube from top, being careful not to leave sand that could fall through to bottom of filter after lifting tube.
- After removing tubing, carefully scrape sand off mesh support after removing mesh. No sand should fall through, as it could possibly be subsequently transported to pressure sensor or ultrafiltration membrane.
- Remove, clean and dry components (sieves, distributor, o-rings), making sure all sand is flushed out by rinsing with clean water.

Load new sand to system

- Put in distributor, rough mesh, fine mesh sieve and rubber seal in base of media filter. Put o-rings in and around base and lid, adding generous amounts of Vaseline to seals.
- Secure PVC tube in base and add the required amount of selected sand. When close to the required depth, close and fasten lid – upon adding water to the media bed, more sand can always be added through a slurry. It is more difficult to remove sand from the bed than it is to add it to achieve required depth.
- Seal and secure lid of media filter with winged nuts.
- Ensure manual valves required are opened. Repeat forward and backwashes until system is waterlogged. Air will be trapped in bed – when backwashing, pass more water over bed than through bed to avoid entrainment of sand and blocking of solenoid valve ports.

- Tap sides of media filter once system is waterlogged. Add more sand if bed is too shallow.

Once the system contains appropriate sand to required depth, preparation for experimental work can be done.

PID parameter determination

For each sand type and depth, unique PID parameters have to be determined for each flow rate tested. The appropriate orifice plate for each flow rate in question has to be inserted in the system, and the system has to be filled with water upon changing orifice fitting.

PID parameter determination was prescribed by the providers of the PID Wizard used in the PLC, and for reference the procedure is included. However, appropriate parameters could not be found by following the steps set out, and rather an iterative approach was taken to determine values.

- Set sampling time as 50 (0.5 s).
- Set I, D = 0.
- Verify that lower and upper pump speed limits are adequate.
- Set a value for P before starting the pump. For each subsequent run, incrementally increase the value (5, 10, 20 +).
- With pump start up, see how flow rate reaches set point: not too steep incline and no drastic overshoot, steady at rate close to set point.
- For set P, gradually increase I (1, 2, 4 +) and see response. I should not exceed P and set point should be reached (slight overshoot okay).
- Vary D with set P and I (0.01, 0.05, 0.1, 0.2) - D should not exceed 10% of I. Can leave as 0.

Ciancone correlations have also not provided the author with reliable PID parameters, and an iterative experimental approach is most successful in finding suitable parameters. Both the P and I constants were between 200-300 with integral upper limit set as 1500.

Prepare water and flocculant for run

Water preparation

- Weigh bentonite and humic acids as required for needed water composition selected.
- Carefully dissolve and suspend components in RO water - sufficient mixing is required to avoid lump formation. Alternatively, regular mixing assists with bentonite

suspension. Suspensions are usually mixed together the day prior to experimentation to avoid lumps of bentonite.

- Add to big water tank and mix to dissolve suspension. Add remainder of water to make up required volume of suspension.

Flocculant solution

- Make up flocculant to required percentage – 20% FeCl_3 solution was used in experimentation. 15% solution can be dosed more accurately, but no discernible difference in efficiency was noted when tested.
- Ensure flocculant line is filled by first speeding up RPM in running water before setting to required rate for selected flux.

Start-up

- Ensure all air is evacuated from system by doing forward and backwashing runs.
- Ensure backwashing recycle line is always submerged, otherwise it lets air into system
- Enter required flow rate set point, and corresponding PID parameter values and pump speed limits. Make sure the right orifice plate is used.
- Enter required operational and backwashing durations.
- Insert flash drive into USB port before starting experiments, to log

During a run

- Measure and log turbidity of raw water, and monitor throughout experimentation to see if it changes.
- Sample at selected time intervals and measure for turbidity.
- Extract samples for UV-Vis analysis if it is required.
- Run operation for pre-determined amount of time/cycles/until water suspension depleted.

End

- Stop all pumps, and close solenoid and manual valves.
- Before switching off PLC, go to Data Logging tab and click on “Remove Storage” – VERY important, otherwise all data is lost!
- Clean up around set-up.
- Drain water and rinse with clean water if possible.
- Rinse set-up thoroughly with water if it will be left for a while. For long shut-down period, drain set-up.

- Carry out chemically enhanced backwash on ultrafilter if filtered water was dirty.

CEB

Carry out CEB on a system that has been backwashed and washed completely with clean water.

- Open ball valves to allow for the flow of water only through membrane.
- Prepare 50 l each of a caustic soda solution (pH of 11.5) with 15 ppm NaOCl, and a 2% citric acid solution.
- Place the backwashing line in a container, and capture both the base and acid solution to check the pH before sending the solution to drainage.
- First, and starting with a low flow rate, fill the system with the basic solution. Let it soak for 10-30 minutes before rinsing with the remaining chemicals at a higher flow rate. Rinse blue bucket with RO water and wash water through entire system with water until all chemicals have been displaced.
- Repeat the same procedure with citric acid solution. Verify that pH doesn't drop below 2.
- Neutralise backwashing solution prior to discarding to drainage if necessary.
- Rinse system thoroughly with water before starting a new experiment

8.2.8 Control philosophy

Attached hereafter, with explanation of sub-processes following the main ssequence.

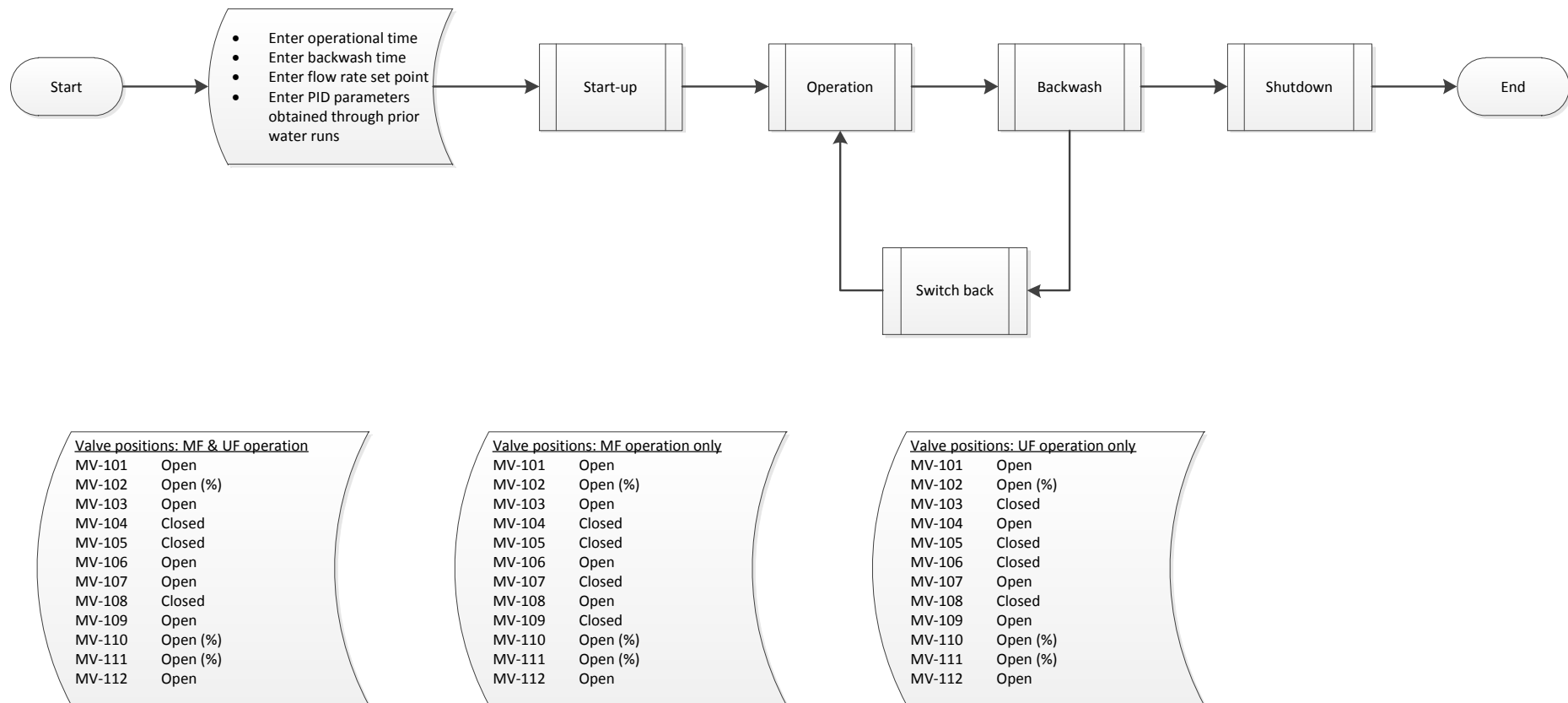


Figure 8-7: Experimental sequence

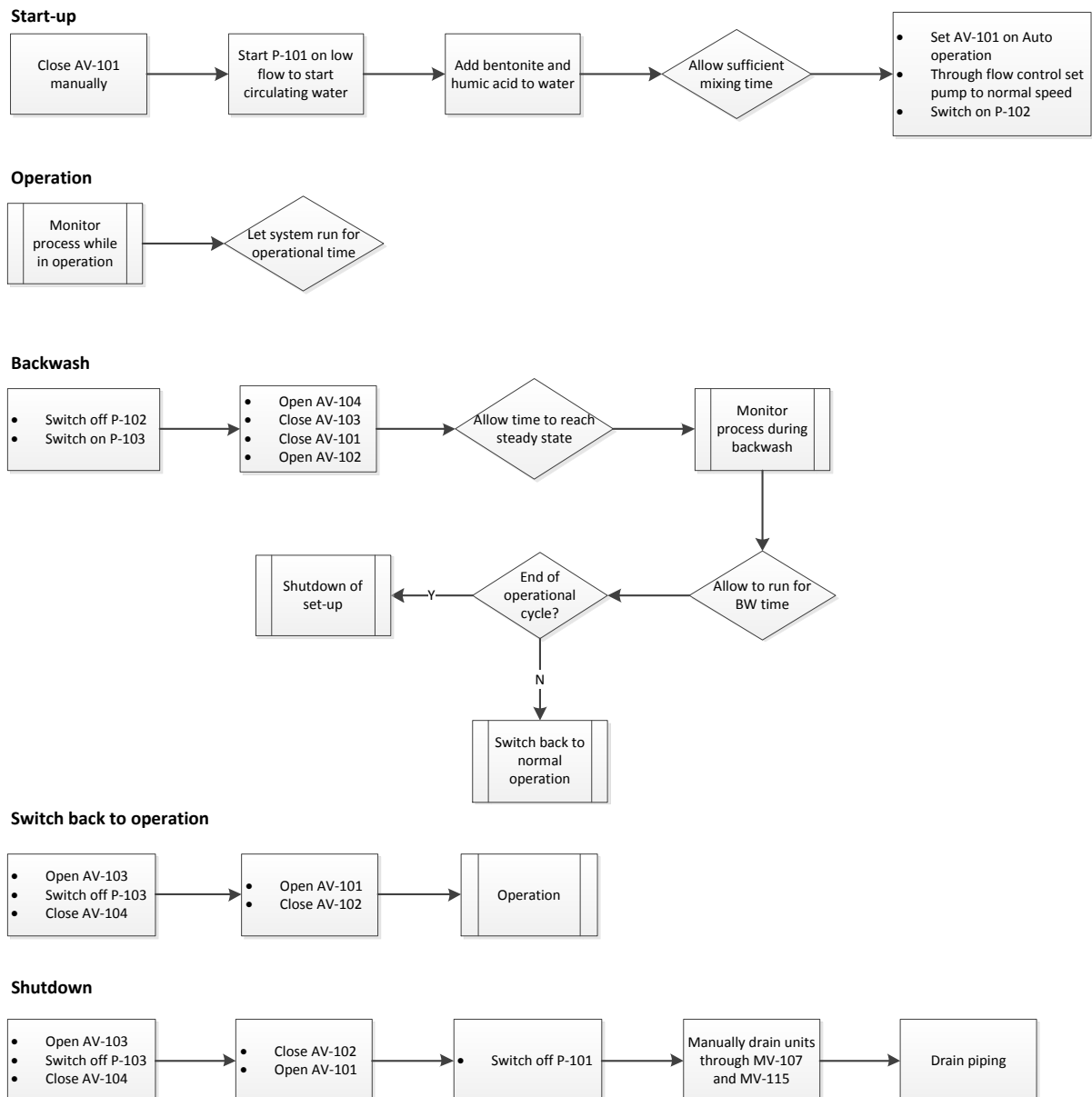


Figure 8-8: Subprocesses for experimentation

8.2.9 Southern Cape plant operation

Raw river water is extracted from the source river, with overflow recycled back. It is screened before being pumped to the membrane treatment plant. Water is firstly dosed with aluminium sulphate. Dosage rates are determined through jar tests, which are repeated regularly depending on the turbidity and colour of raw water, and of the water quality following pre-treatment. The aluminium sulphate used by the plant was also used by the author, made up in a 10% aluminium sulphate solution.

Caustic is added to increase the pH following the dosage of the aluminium sulphate. This is an important step in ensuring the effective removal of aluminium from the water, as the author found. Aluminium sulphate is highly acidic, and the rate of caustic dosage is set to be sufficient to raise the pH of the water to between 5.6 and 6.2, as determined by plant engineers. Following the dosage of aluminium sulphate and caustic, the water is passed through three flocculation mixing tanks, in which the speed decreases step wise in the last two tanks following rapid mixing in the first tank. Water passes through a pipe flocculator to a lamellar clarifier, where the water is given approximately 15 minutes retention time for floc growth. Following the pre-treatment, water is first passed through a 60 micron screen before being filtered through the membranes. Product water is blended with the conventionally treated water to meet SANS standards for safe water.

8.3 Appendix C: Omitted graphs and data

8.3.1 Flocculated water turbidity

The following graph indicates residual turbidity following jar testing flood suspension of HA water. The turbidity after settling is plotted for different dosages of ferric chloride added. The optimal dosage is selected where residual turbidity is lowest.

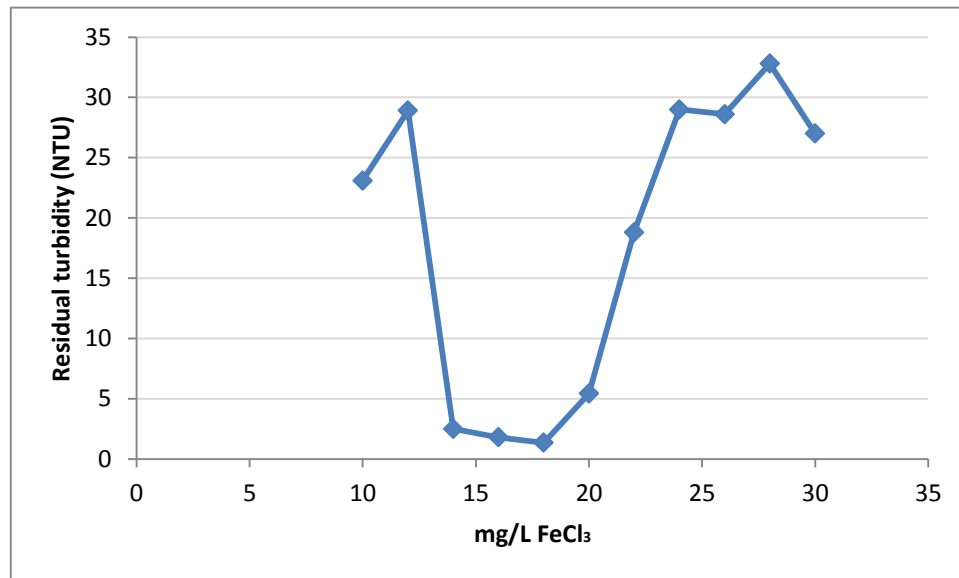


Figure 8-9: Residual turbidity for flood HA coagulant dosage

8.3.2 Pre-filter characterisation

Coarse sand (0.5-1 mm)

Filtrate quality is shown in the following Figures at different downflow rates for a shallow (150 mm) bed depth.

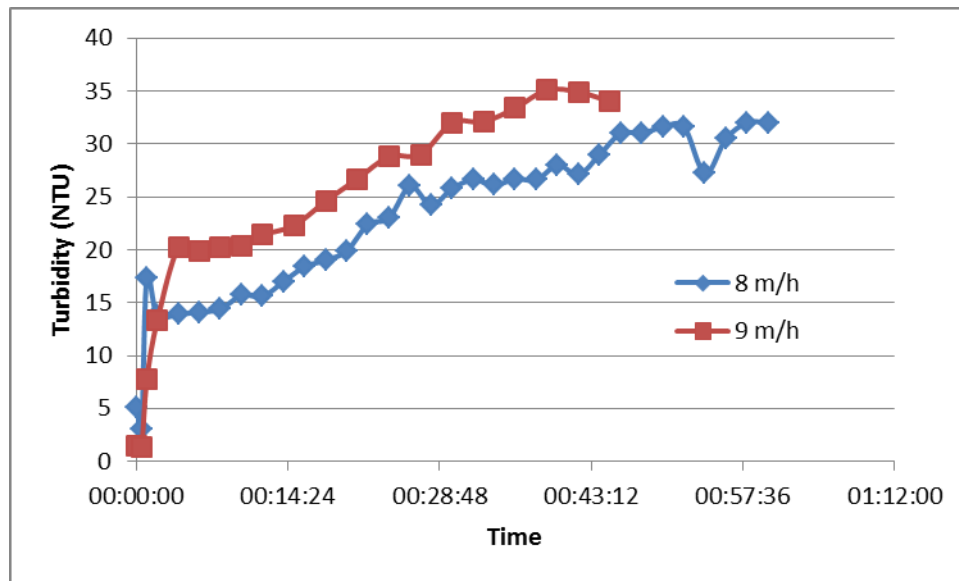


Figure 8-10: Residual turbidity for 8 and 9 m/h downflow through coarse 150 mm bed

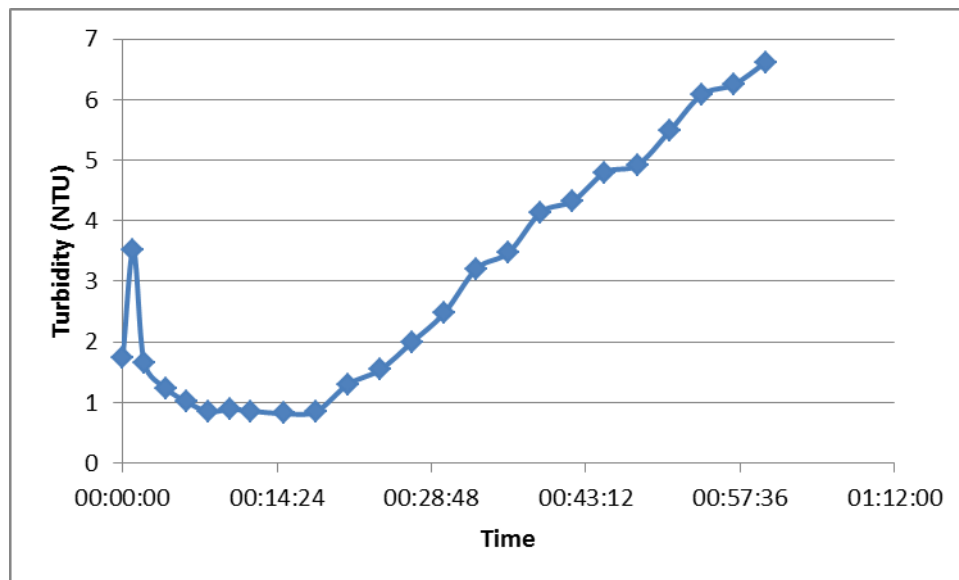


Figure 8-11: 11 m/h downflow rate through shallow bed of screened sand

Ineffective filtration occurred with short delivery time of clean water for a 150 mm bed made of sand 0.425-0.6 mm diameter. The PF bed had to be made deeper in order to more effectively retain particles.

Vary bed depths

For filtration of clean synthetic river water (12 NTU), pressure drop profiles are constructed for the different bed depths.

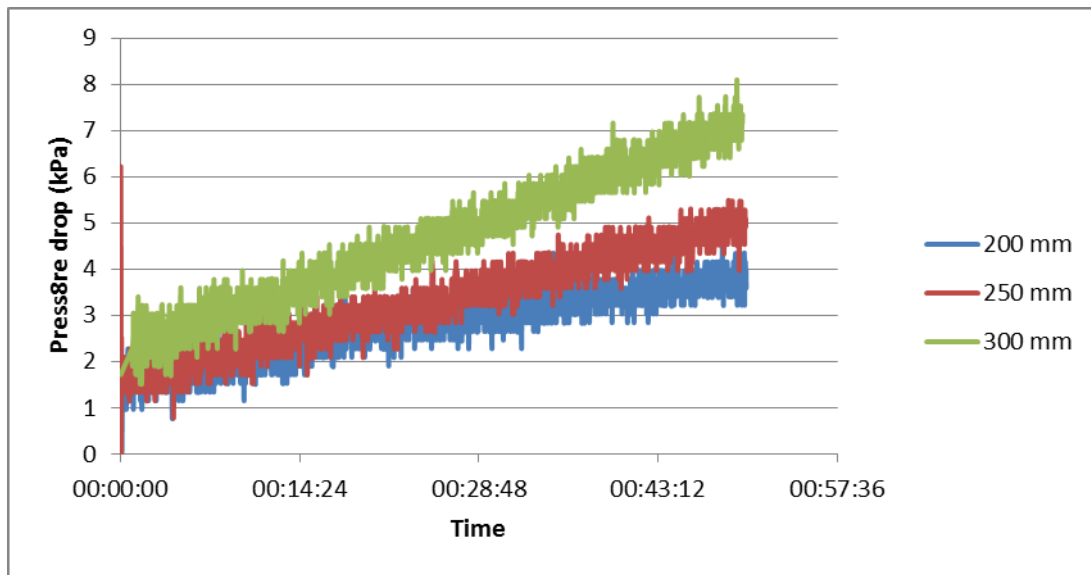


Figure 8-12: Pressure drop over PF at 8 m/h downflow rate

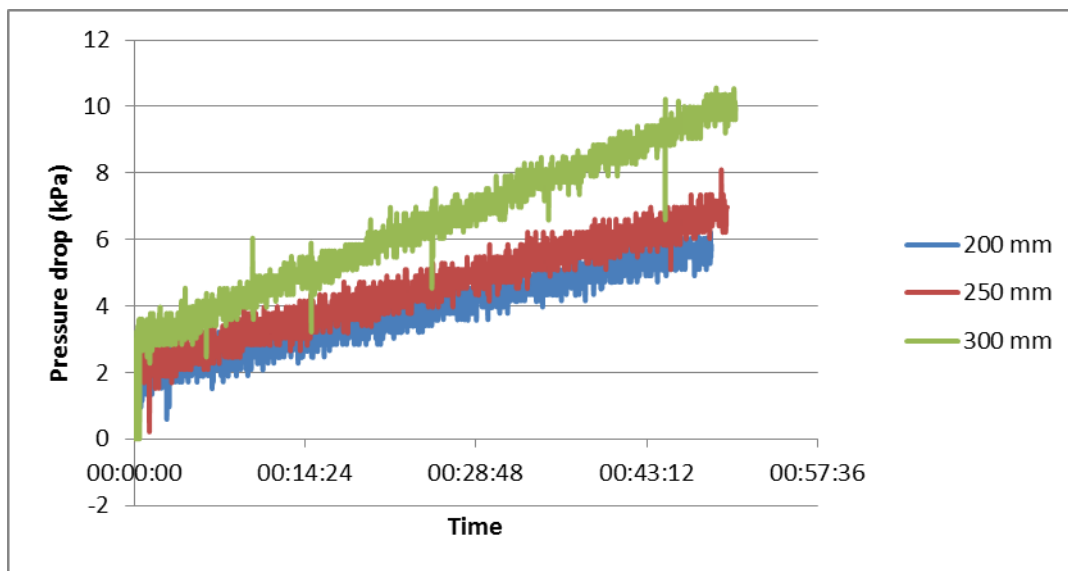


Figure 8-13: Pressure drop over PF at 10 m/h downflow rate

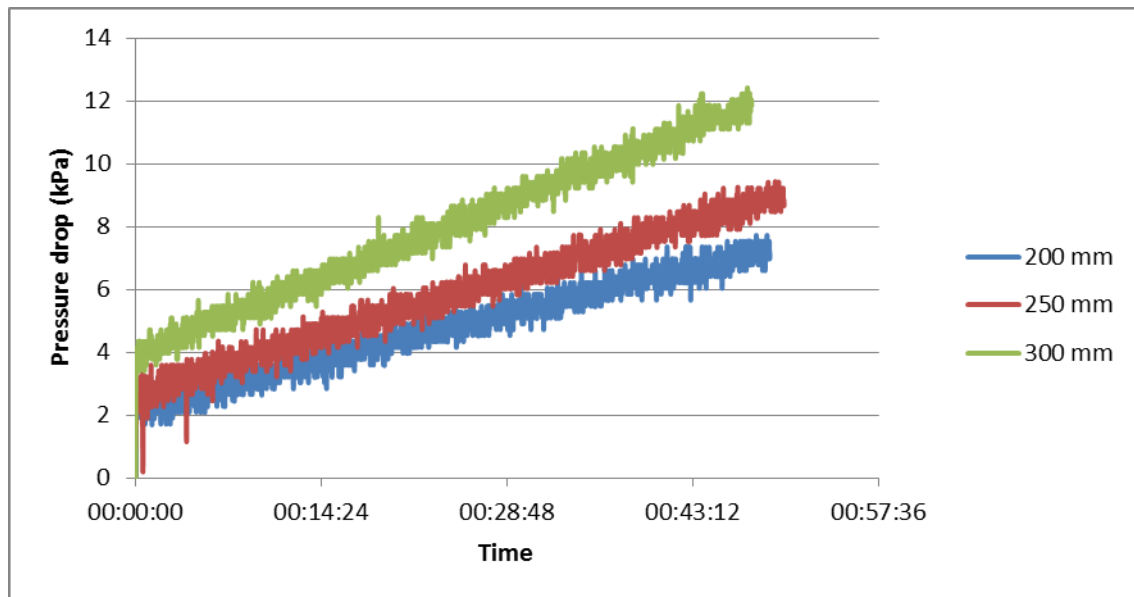


Figure 8-14: Pressure drop over PF at 12 m/h downflow rate

Vary flow rates

For a fixed bed depth, pressure drop over the PF is plotted for different downflow rates.

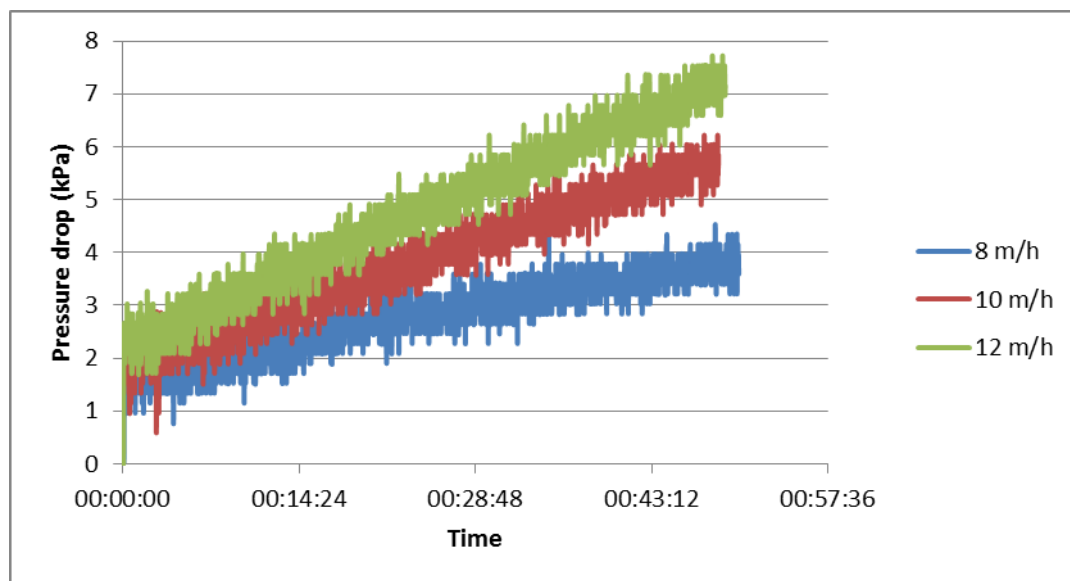


Figure 8-15: Pressure drop over 200 mm PF

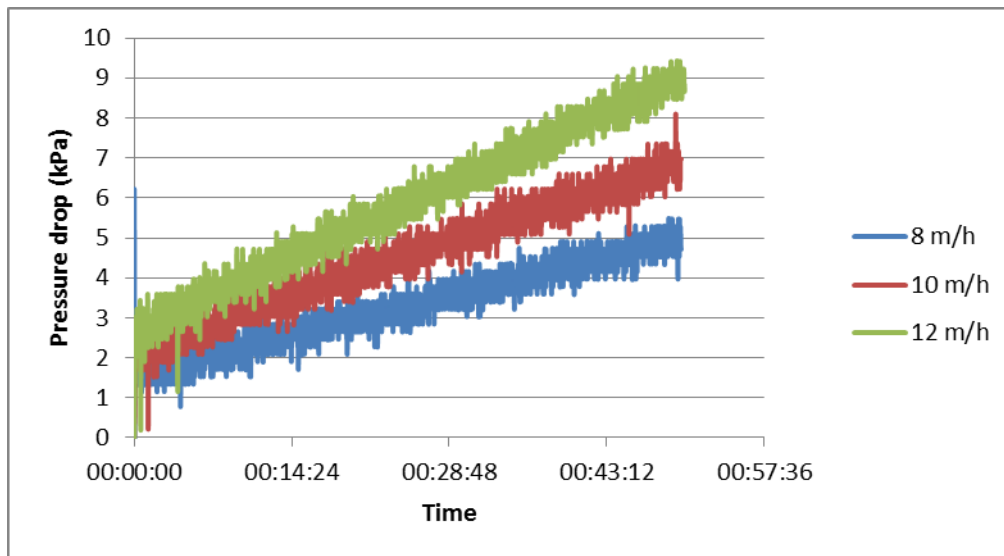


Figure 8-16: Pressure drop over 250 mm PF

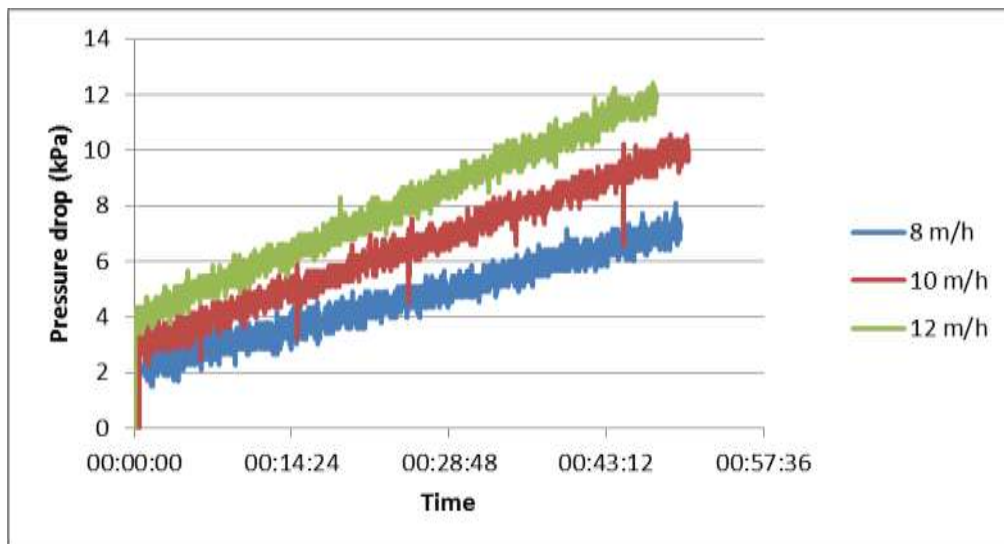


Figure 8-17: Pressure drop over 300 mm PF

Vary backwashing duration

Residual turbidity profiles were plotted for PF filtrate for cyclical operation with 10 m/h downflow rate for 50 minutes, with different backwashing durations between cycles. Backwashing durations were selected based on number of displacement volumes (DV).

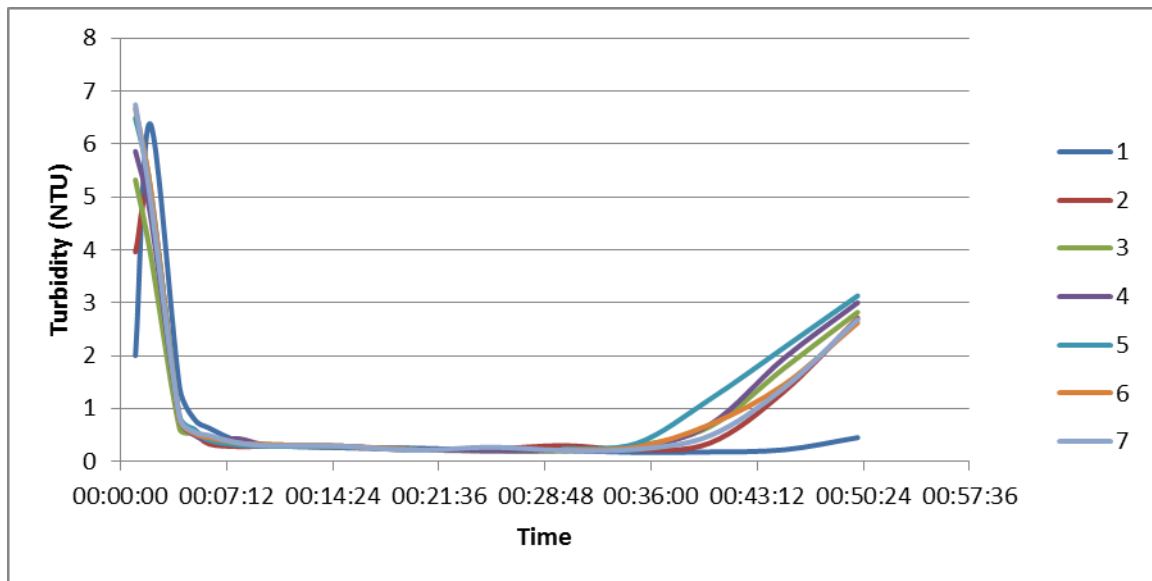


Figure 8-18: Residual turbidity for repeated 50 minute cycles of 10 m/h with 2 DV backwashing

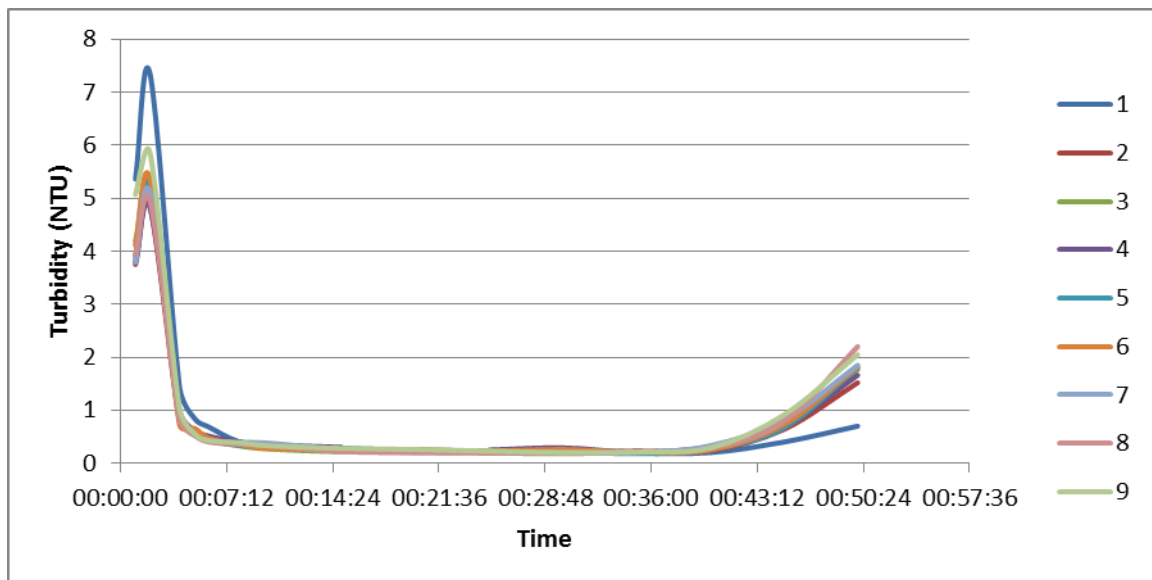


Figure 8-19: Residual turbidity for repeated 50 minute cycles of 10 m/h with 3 DV backwashing

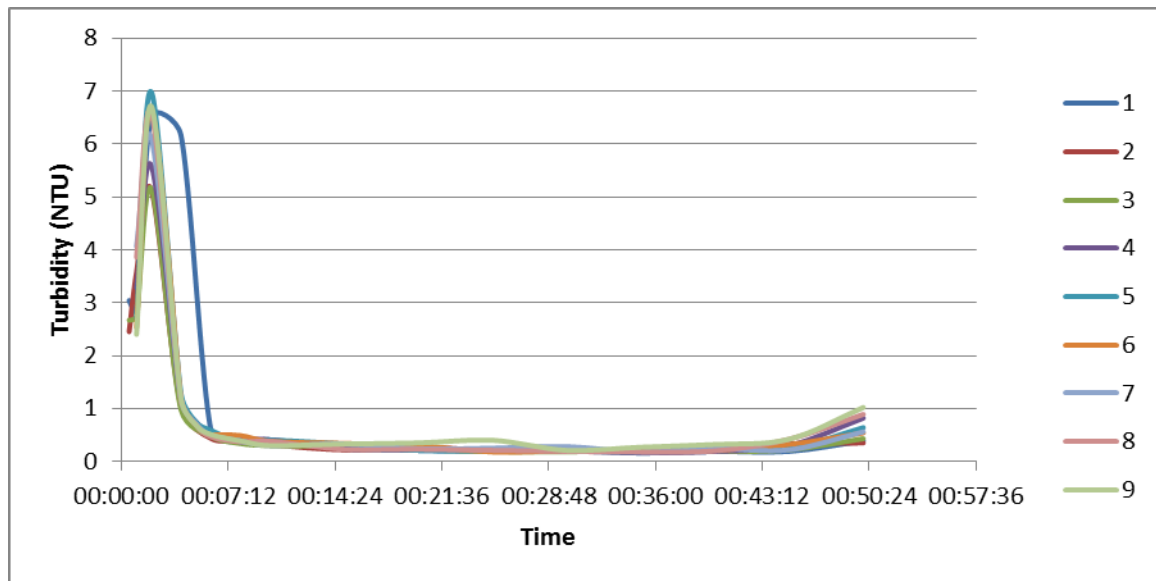


Figure 8-20: Residual turbidity for repeated 50 minute cycles of 10 m/h with 4 DV backwashing

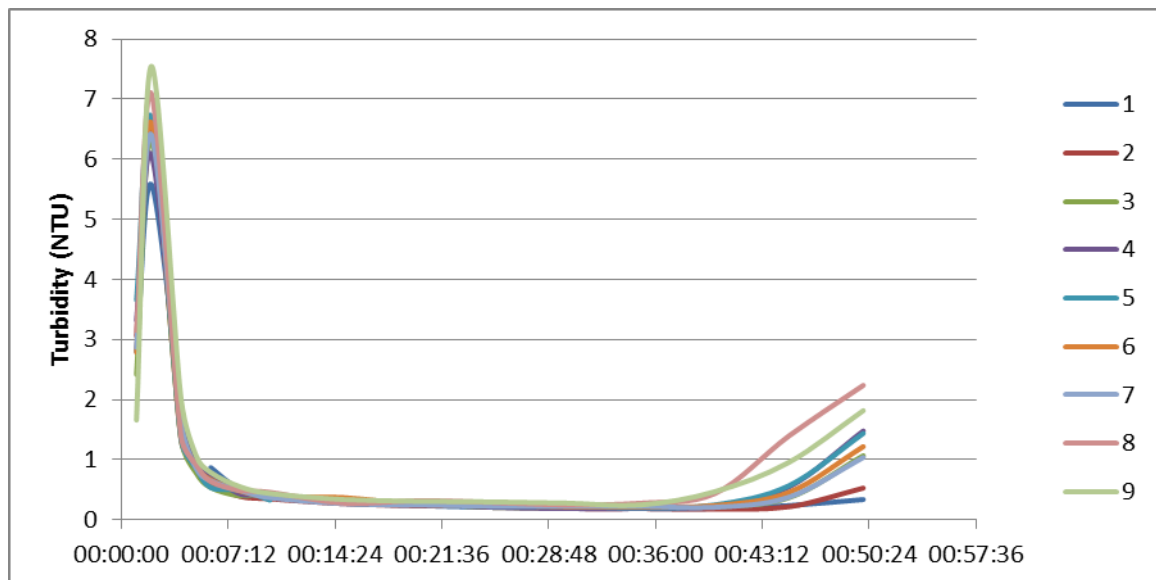


Figure 8-21: Residual turbidity for repeated 50 minute cycles of 10 m/h with 6 DV backwashing

The initial residual turbidity spike is characteristic of the maturation period of a media filter. It is the turbidity at the end of the cycle indicating the breakthrough point that is important in the selection of backwashing duration.

8.3.3 Combined filter effectiveness

Clean water pre-filter and UF, dump first 5 minutes suspension

Operation at 37 LMH flux

Normal suspension prepared; dump first 5 minutes (relatively high turbidity spike at 4 minutes around 7 NTU)

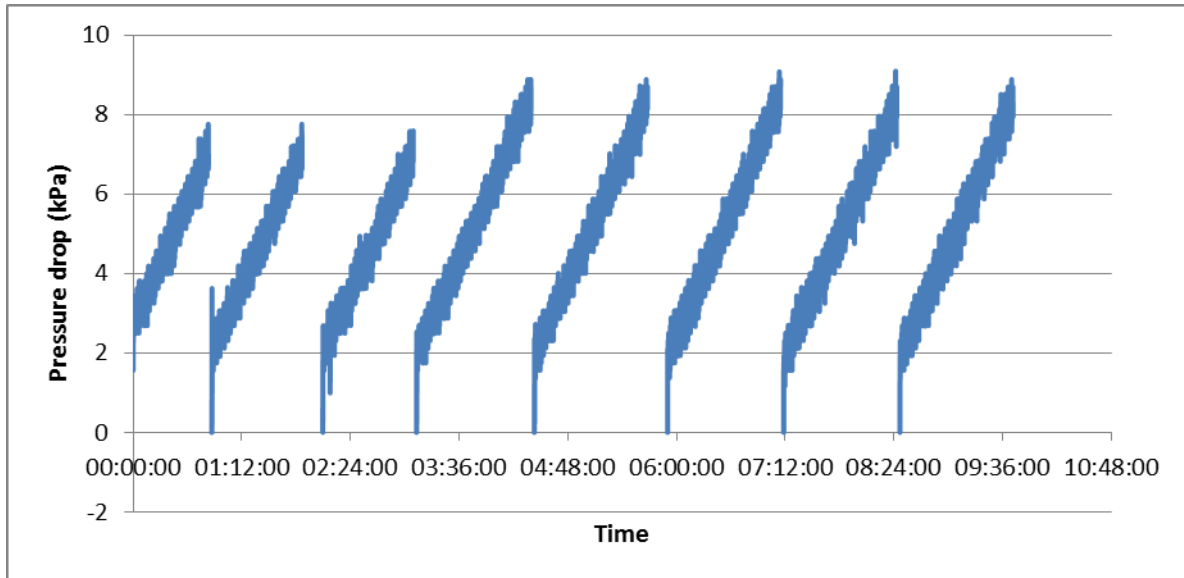


Figure 8-22: Pressure drop profile over media bed for 3x60 5x75 min 36 LMH cycles with 2 min backwashing

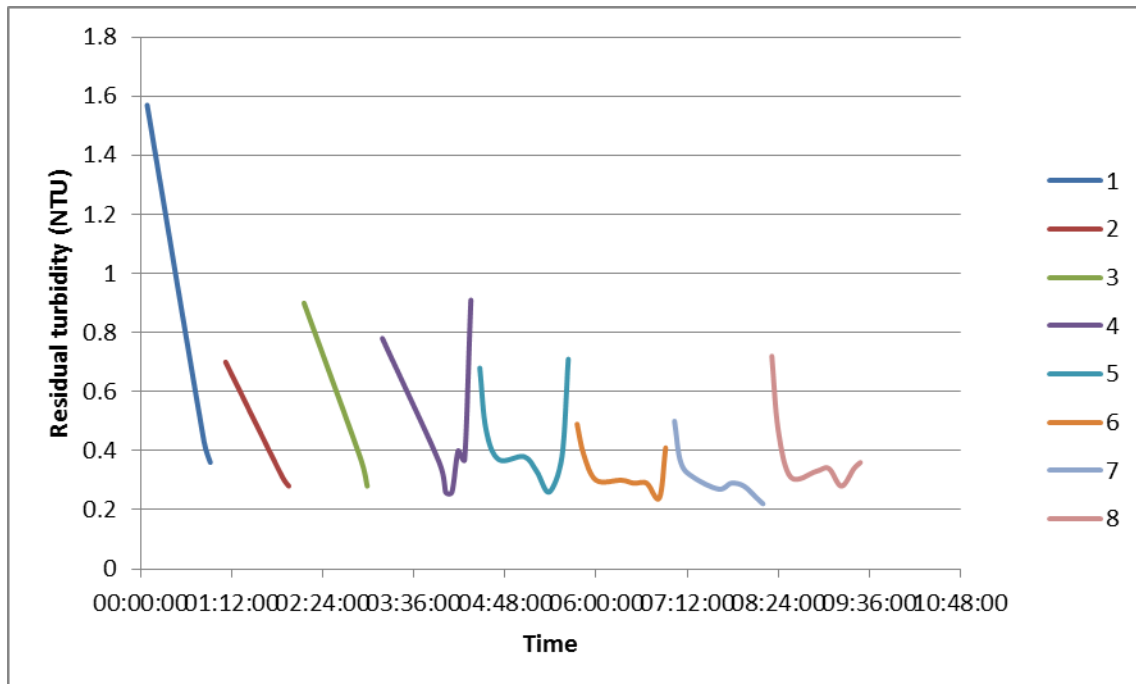


Figure 8-23: Residual turbidity profile following media filtration for 36 LMH operation with 2 min BW

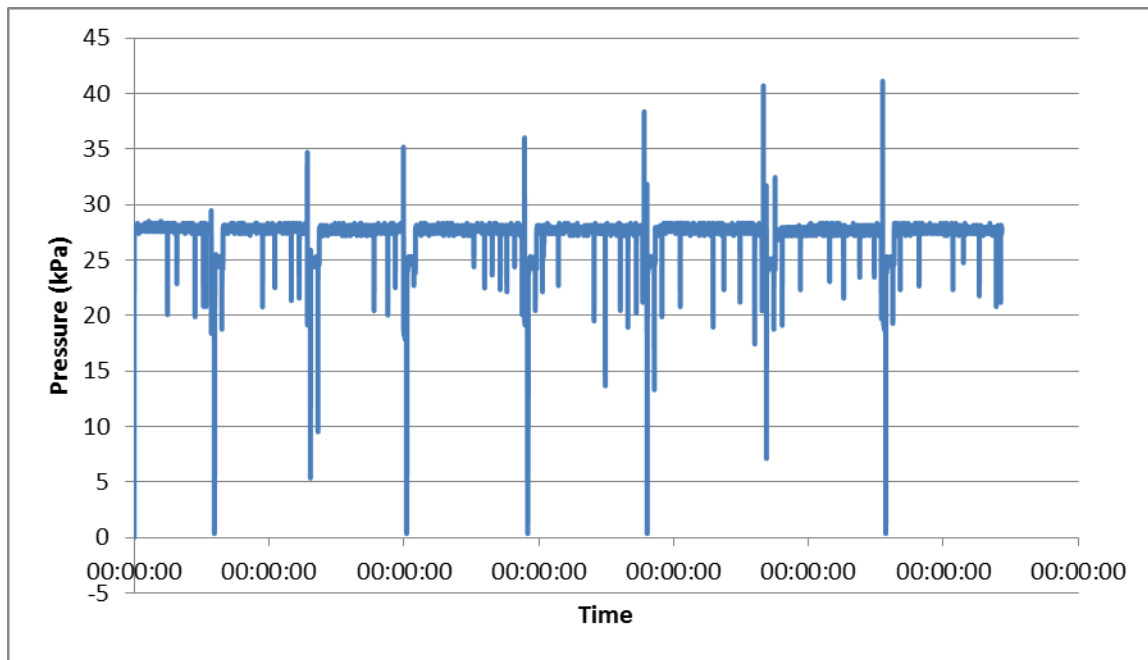


Figure 8-24: Membrane pressure for 3x60 5x75 min 36 LMH cycles with 2 min backwashing

Operation at 46 LMH flux

Greater operational flux is induced while still bypassing the membrane for the first 5 minutes of operation, allowing for the maturation of the media bed without depositing the particles responsible for the initial turbidity peak onto the membrane surface.

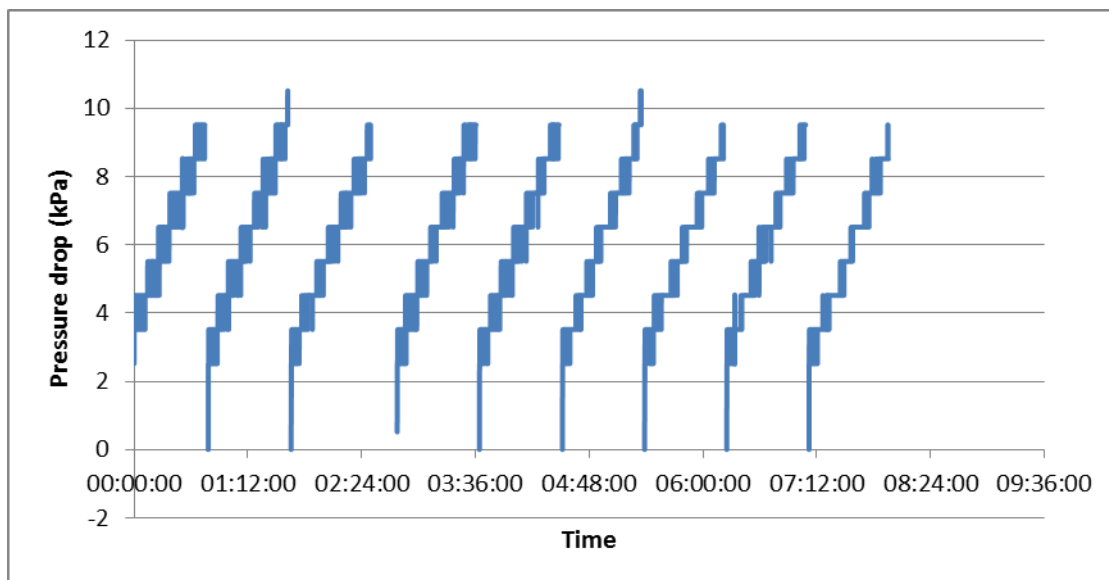


Figure 8-25: Pressure drop over media bed for 50 min 46 LMH

Linear increase in pressure.

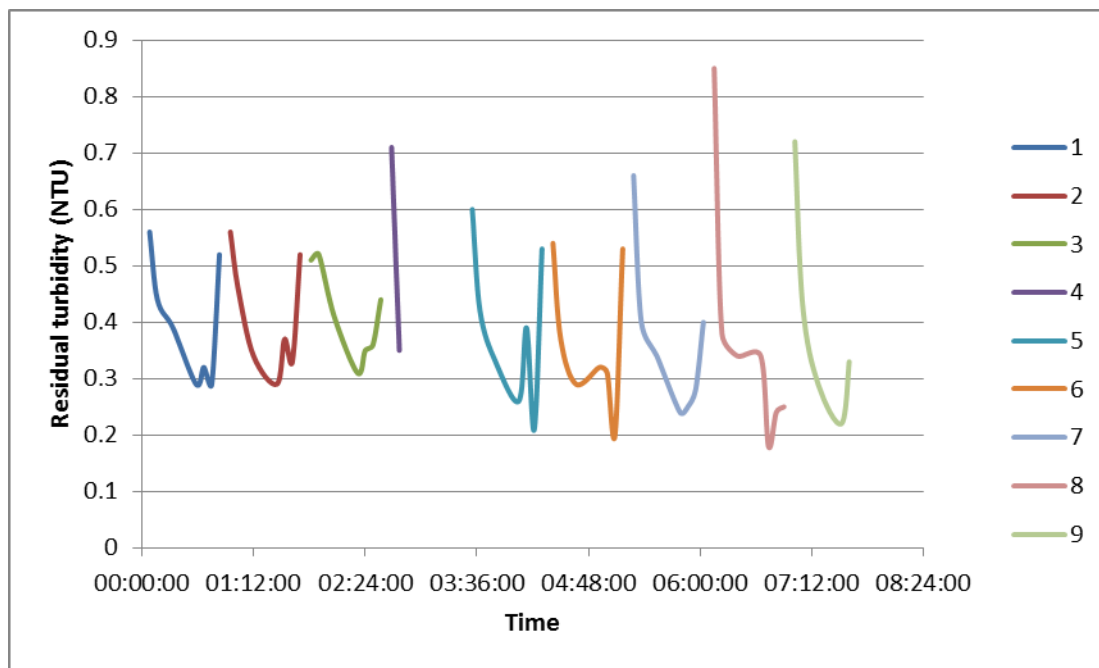


Figure 8-26: Residual turbidity profile following media filtration

Turbidities are consistently very low – almost no solids remaining to deposit onto membrane.

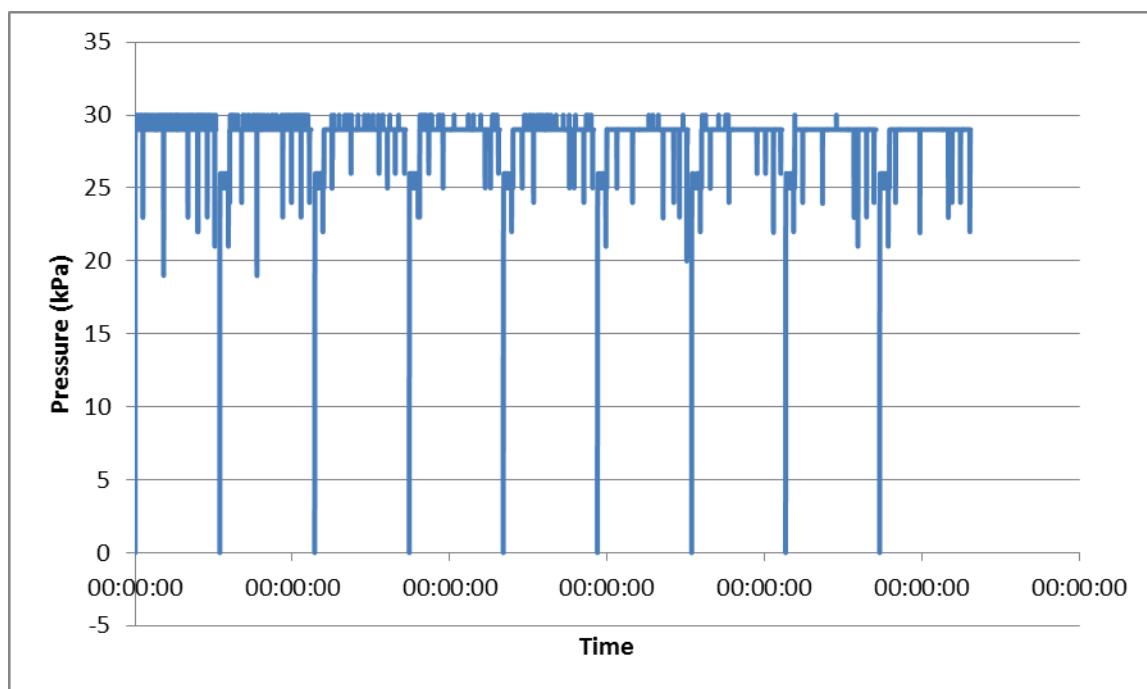


Figure 8-27: Membrane pressure for 50 min 47 LMH cycles with 2 min backwashing

Maintain clean membrane pressure – exit pressure data unavailable.

Site work operation at unadjusted pH (too low, insufficient Al removal)

Pre-filter pressure profile

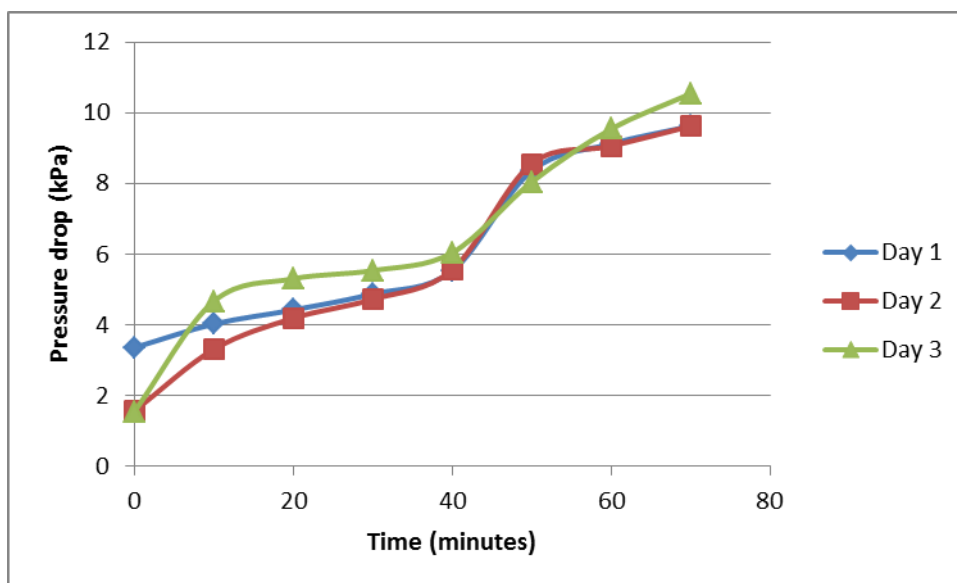


Figure 8-28: Pressure drop over pre-filter

Residual turbidity and colour following pre-filter

Water properties before membrane filtration

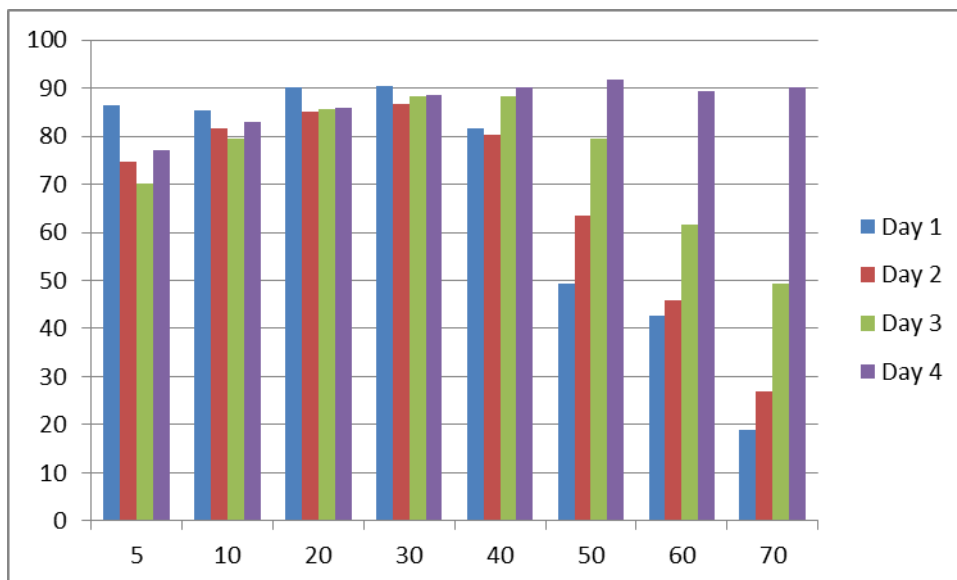


Figure 8-29: Percentage turbidity removed by pre-filter

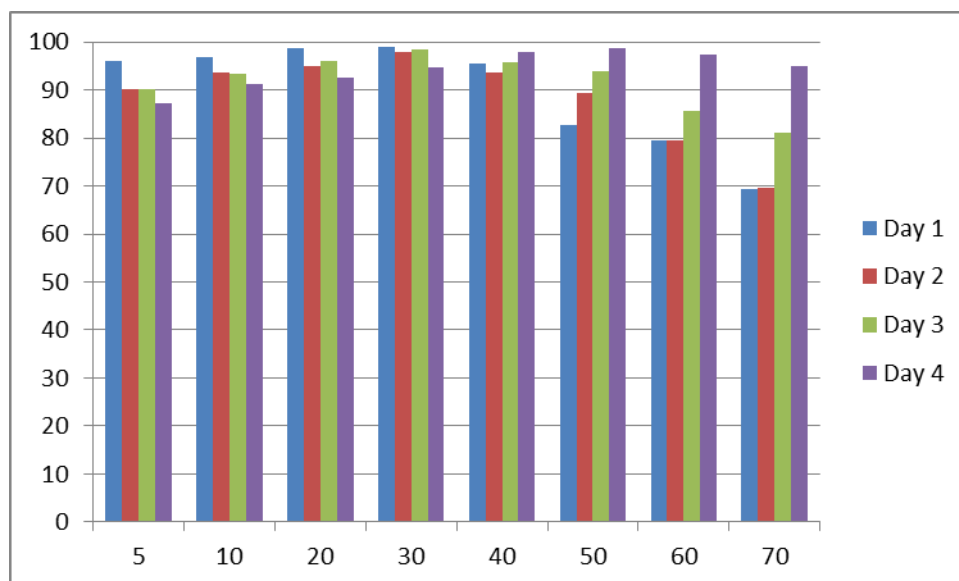


Figure 8-30: Percentage colour removed by pre-filter

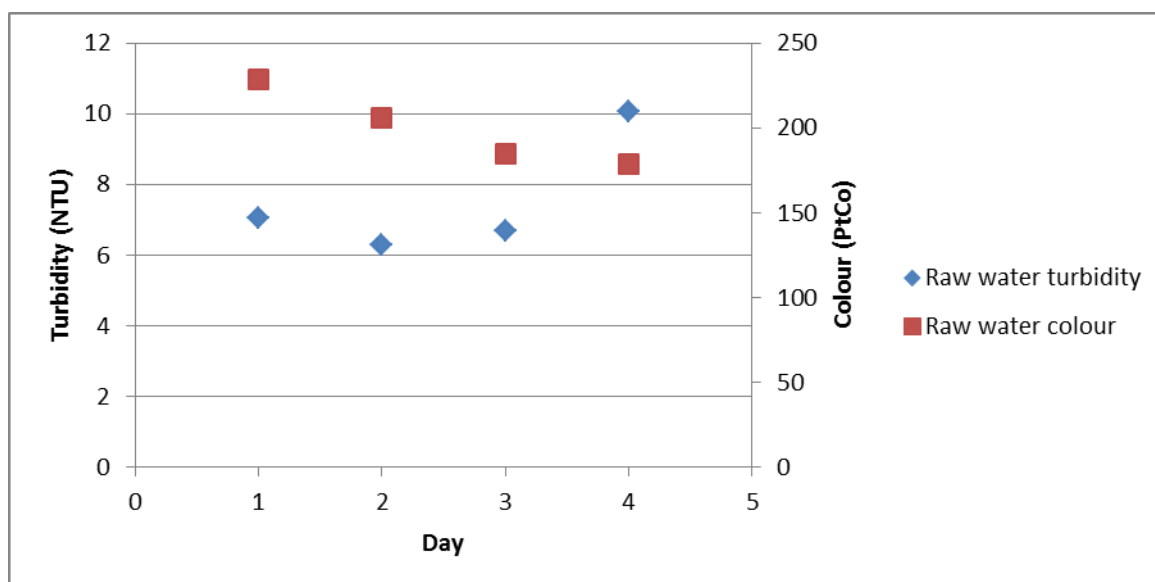


Figure 8-31: Raw water properties over course of experiment

Membrane pressure profile

As the filtered water was used for hydraulic backwashing, the acidic backwash also contributed to fouling.

Clean water quality

Turbidity 0.14 NTU; colour 0 PtCo

8.4 Appendix D: Sample calculations

PF area determination

Select operational fluxes for both filters. Search through manufacturer specifications for pilot scale surface areas for UF membranes. From inge®'s dizzy® range, modules with surface areas of 4 and 6 m² were found to be most suitable. The 4 m² membrane would give a larger flux for fixed flow rates (constrained by system design), and was selected for experimentation.

The average flux for membrane filtration was selected as 50 LMH, and the average downflow rate for media filtration was selected as 10 m/h. Set values in Equation 3.1 and determine PF size capable of handling mid-range fluxes through both filters.

$$J_{UF}A_{UF} = J_{media}A_{media}$$

$$\frac{50 \text{ LMH} \cdot 4 \text{ m}^2}{10 \text{ m/h}} = A_{media} = \pi \frac{d^2}{4}$$

Iteratively select most appropriate PF surface area and correlate with commercially available PVC pipe sizes to select suitable diameter. Piping with a diameter of 0.154 m was found to be most suitable.

From selected range of downflow rates: 8-12 m/h, the flow rate through the system could be determined and correlated with membrane flux.

PF downflow rate

Convert downflow rate to volumetric flow rate through following conversion:

$$Downflow \left(\frac{m}{h} \right) \cdot \frac{1h}{60min} \cdot (m^2)_{PF} \cdot \frac{1000L}{1m^3} = Flow \text{ rate} \left(\frac{L}{min} \right)$$

$$8 \frac{m}{h} \cdot \frac{1h \cdot 1000L}{60min \cdot 1m^3} \cdot 0.019m^2 = 2.47 \frac{L}{min}$$

UF flux

Convert water flow rate to correct units through following conversion:

$$Flow \text{ rate} \left(\frac{L}{min} \right) \cdot \frac{60 \text{ min}}{1 \text{ h}} \cdot (m^2)_{UF} = Flux \text{ (LMH)}$$

$$2.47 \times \frac{60}{1} = 148.2 \text{ LMH}$$

Substitute flux, measured TMP and viscosity in Equation 2.2 to find membrane resistance.

$$J = \frac{\Delta P - \Delta \Pi}{\mu(R_T)}$$

$$37LMH = \frac{9.2kPa - 0kPa}{0.001Pa \cdot s \cdot (R_m)}$$

$$R_m = \frac{9200Pa}{37 \frac{L}{m^2h} \cdot \frac{1h \cdot 1m^3}{3600s \cdot 1000L} \cdot 0.001Pa \cdot s}$$

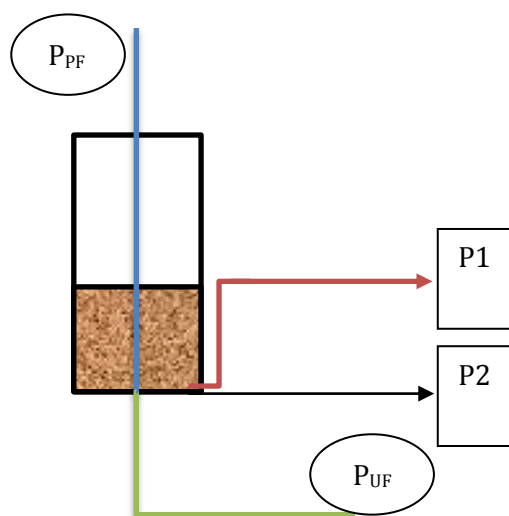
$$R_m = 8.95 \cdot 10^{11} m^{-1}$$

The resistance of the membrane is calculated using clean membrane flux. More foulants will adhere to the membrane as dirty water is filtered, and the fouling resistance will contribute to the total resistance. The contribution of fouling to the total resistance can be determined by evaluating clean membrane resistance. It can be used to determine when hydraulic or chemical cleaning should be initiated.

Measured pressure drop over PF

Sensor readings are used to determine the pressure drop over the bed. Hydrostatic pressures are used to correct the two pressure readings to a common point at the bottom of the filter media. The difference in the two readings gives the pressure drop caused by friction through the bed and by the resistance posed by fouling.

Hydrostatic pressure drop is added to the sensor above the bed, and subtracted from the sensor at the bottom of the bed. Three bends between the PF outlet and UF pressure sensor are included as minor losses. Calculations are based on filtering water at 20°C at a downflow rate of



8 m/h.

Figure 8-32: PF pressure drop calculation

$$\Delta P = P_1 - P_2$$

$$\Delta P = [P_{PF} + ((\text{height } P_{PF} \text{ above } P_1) \cdot \rho_{\text{water}} \cdot g)] - [P_{UF} - ((\text{height } P_{UF} \text{ below } P_2) \cdot \rho_{\text{water}} \cdot g)] - \text{minor losses bends}$$

$$\Delta P = \left[P_{PF} + \frac{(0.08 + 0.45) \cdot 999 \cdot 9.81}{1000} \right] - \left[P_{UF} - \frac{(0.32 + \frac{V^2}{2g} (\sum K) \cdot 999 \cdot 9.81)}{1000} \right]$$

$$\Delta P = 1.02 \text{ kPa}$$

Theoretical pressure drop over PF

In order to calculate the theoretical pressure drop, other PF characteristics firstly have to be determined.

- Bed voidage [Equation 2.11]

The weight of sand is gravimetrically determined and substituted along with other bed properties in order to determine voidage. Expanded PF bed height of 275 mm was used.

$$\varepsilon = 1 - \frac{6.75 \text{ kg}}{998 \frac{\text{kg}}{\text{m}^3} \cdot \left(\pi \frac{0.1536^2}{4} \cdot 0.275 \right) \text{ m}^3}$$

$$\varepsilon = 0.5$$

- Reynolds flow through a packed bed [Equation 2.16]

The flow regime through the bed is determined by calculating the Reynolds number for flow through a packed bed. Flow at 8 m/h flux at 20°C is considered.

$$Re^* = \frac{0.005 \text{ m} \cdot 0.002 \frac{\text{m}}{\text{s}} \cdot 998 \frac{\text{kg}}{\text{m}^3}}{0.001 \cdot (1 - 0.5)}$$

$$Re^* = 2.27$$

For Re^* below 10, flow is laminar (Rhodes, 2008).

- Determine equivalent mean surface-volume diameter to account for degree of non-sphericity of particles [Equation 18]

Several actual pressure drop data values, along with the corresponding downflow rate, are used to determine x_{sv} . The value used in theoretical calculations is the average of a minimum of three calculated values.

$$x_{sv} = \sqrt{\frac{150 \cdot (0.001 \text{ Pa} \cdot \text{s}) \cdot \left(0.002177 \frac{\text{m}}{\text{s}}\right) \cdot 0.275 \text{ m}}{1020 \text{ Pa} \cdot 0.5^3}}$$

$$x_{sv} = 0.00042 \text{ m}$$

- Determine theoretical laminar pressure drop using Ergun equation [Equation 2.19]

Using the above parameters and required water properties, theoretical pressure drop can be calculated:

$$\frac{\Delta P}{0.275 \text{ m}} = 150 \frac{0.001 \text{ Pa} \cdot \text{s} \cdot 0.002177 (1 - 0.5)^2}{(0.00042)^2 \cdot 0.5^3} + 1.75 \frac{998 \frac{\text{kg}}{\text{m}^3} \left(0.002177 \frac{\text{m}}{\text{s}}\right)^2 (1 - 0.5)}{0.00042 \cdot 0.5^3}$$

$$\Delta P = 1141 \text{ Pa}$$

A slight deviation exists between the actual and theoretical pressure drop, which could be due to the degree of non-sphericity being slightly different to the calculated average.

Transmembrane pressure

As there is no permeate pressure drawn from the unit, TMP calculation is simplified from Equation 2.1 to:

$$TMP = P_{inlet} - P_{permeate}$$

Pressure drop over membrane for 37 LMH flux:

$$TMP = 28.4 \text{ kPa} - 10 \text{ kPa} = 18.4 \text{ kPa}$$

This value is used in pressure calculations for the membrane and is symbolised by the pressure drop ΔP for the membrane.

Velocity gradient for orifice plate mixing

The determination of several parameters is required to determine the velocity gradient incurred by the orifice plate. Flow at 2.42 L/min (8 m/h downflow and 37 LMH flux) at 20°C is considered. A 2 mm orifice plate had been found to be suitable for mixing at a low flow rate.

- Head loss over orifice plate [Equation 2.31]

The value of β is expressed as the ratio of the orifice diameter over the pipe diameter:

$$\beta = \frac{d_{\text{orifice}}}{d_{\text{pipe}}} = \frac{2 \text{ mm}}{12 \text{ mm}} = 0.1667$$

Using this parameter and other water and structural properties, the head loss caused by the orifice plate can be calculated. The discharge coefficient for the orifice plate, C_d , is 0.61.

$$h_L = \frac{1}{2 \cdot 9.81 \frac{m}{s^2}} (1 - (0.1667)^4) \left(\frac{4.12 \cdot 10^{-5} \frac{m^3}{s}}{0.61 \cdot 3.14 \cdot 10^{-6} m^2} \right)^2$$

$$h_L = 23.5 \text{ m}$$

- Power number [Equation 2.30]

Following the calculation of h_L , its value can be substituted into Equation 2.30 to calculate the power number:

$$P = 4.12 \cdot 10^{-5} \cdot 998 \cdot 23.5 = 9.49 \frac{kg \cdot m}{s}$$

- Velocity gradient [Equation 2.32]

In order to determine this value, an assumption had to be made about the mixing volume upon expansion following the orifice plate. It is assumed that the volume of turbulent flow following the orifice plate is equal to ten times the pipe diameter.

$$G = \sqrt{\frac{9.49}{\left(\frac{0.012^2}{4}\right) \cdot 0.12 \cdot 10 \cdot 0.001}} = 35\,398$$

The high value could be due to an incorrect assumption made for the calculation. The format of the velocity gradient calculation is usually used to determine the velocity gradient for mixing vessels.

Sensor accuracy

The accuracy of the sensor is expressed as a percentage of its measurable range.

$$\text{Range } (0 - 400 \text{ kPa}) \times 1\% = 4 \text{ kPa}$$

Although this value is high compared to the low pressure drops measured over the PF, it was found that the sensors were accurate. Theoretically determined pressure drop consistently

correlated well with the actual pressure drop when comparing clean bed pressure drop at the beginning of a PF pressure drop cycle.

For site test work, more accurate sensors were procured, with the following accuracy:

$$\text{Range } (0 - 160 \text{ kPa}) \times 0.25\% = 0.4 \text{ kPa}$$

Measurements could now much more confidently be believed.

Percentage turbidity removed

Percentage turbidity removed is calculated using turbidity readings of raw water and filtrate:

$$\frac{\text{Incoming NTU} - \text{outgoing NTU}}{\text{Incoming NTU}} \times 100\%$$

The same calculations can be done with colour and UV absorbance to determine the effectiveness of filtration.

Recovery

The overall system recovery is calculated using Equation 2.10. In the backwashing water term, W_B , the water used during CEB was also included. Depending on filtration and backwashing duration, the amount of cycles carried out between CEB (in a 24 hour period, as selected in this project) was calculated and used to determine recovery.

$$\text{Recovery} = \frac{W_F - W_B}{W_F} \cdot 100$$

For 8 m/h downflow and 37 LMH flux, with 70 minute filtration and 2 minute backwashing:

$$\frac{24 \text{ hours} \cdot \frac{60 \text{ min}}{1 \text{ h}}}{70 + 2 \text{ min}} = 20 \text{ cycles between CEBs}$$

$$\frac{\left[20 \cdot 2.42 \frac{\text{L}}{\text{min}} \cdot 70 \text{ min} \right] - \left[20 \cdot 13.3 \frac{\text{L}}{\text{min}} \cdot 2 \text{ min} + 2 \cdot 13.3 \frac{\text{L}}{\text{min}} \cdot 3 \text{ min} \right]}{\left[20 \cdot 2.42 \frac{\text{L}}{\text{min}} \cdot 70 \text{ min} \right]} \cdot 100\%$$

$$\text{Recovery} = 81.9\%$$

Recovery is thus 82% for the selected conditions. It can be improved by increasing the filtration duration slightly. Required backwashing duration is fixed and cannot be altered to improve recovery.

Displacement volume correlation with backwashing duration

Determine one displacement volume by calculating the sum of volumes in system:

$$\sum Area \times Length = \pi r^2 \times l$$

Account for PF bed voidage. Sum of all volumes = one DV, which amounted to 6.3 L.

Backwashing flow rate is fixed at 13.3 L/min. One DV thus takes $13.3/6.3 = 0.5$ min to wash out of the system. Different DV and backwashing durations were investigated.

Temperature normalisation for flux

Two sets calculations were considered for flux normalisation to the same temperature, as temperature varied during experimentation. As experiments were mostly conducted at or below 20°C, all data were corrected to 20°C.

As an example, temperature normalisation of

- Method 1: DOW normalisation
 - Determine normalised volumetric flow rate [Equation 2.4]

$$Q_{20} = Q_T e^{-0.0239(T-20)}$$

- Determine temperature correction factor for experimental temperature:

$$TCF = e^{\left[3020\left(\frac{1}{293} - \frac{1}{273+T}\right)\right]}, T \leq 20^\circ\text{C} \quad [2.6]$$

$$TCF = e^{\left[2640\left(\frac{1}{293} - \frac{1}{273+T}\right)\right]}, T \geq 20^\circ\text{C} \quad [2.7]$$

The temperature correction factor for the standard temperature of 20°C is 1.

- Substitute volumetric flow rate at experimental flow rate and pressure drop at experimental temperature into Equation 2.5:

$$Q_{20} = Q_T \cdot \frac{TCF_{20}}{TCF_T} \cdot \frac{\left(P_{feed} - \frac{\Delta P}{2} - P_{permeate}\right)_{20}}{\left(P_{feed} - \frac{\Delta P}{2} - P_{permeate}\right)_T}$$

This manner of normalisation is used for RO and NF.

- Method 2: Correct viscosity to standard temperature [Equation 2.8]

In order to use this correction, assumptions had to be made about the flux remaining constant, depositing equivalent amounts of foulants in order to assume the R_T term remains constant for the system at standard and experimental temperatures.

$$J = \frac{\Delta P_S}{\mu_S(R_T)_S} = \frac{\Delta P_T}{\mu_T(R_T)_T}$$

$$\Delta P_{20} = \frac{\Delta P_T \mu_{20}}{\mu_T}$$

For experiments conducted close to standard temperatures, the second method introduced the least distortion to the actual pressure drop data. Comparison between the pressure drop readings calculated using both methods are summarised in Table 8-1.

Table 8-1: Comparison of temperature normalisation effectiveness for Methods 1 and 2

Flux (LMH)	Temperature (°C)	Measured dP (kPa)	Corrected ΔP (kPa)		Deviation measured (%)	
			Method 1	Method 2	Method 1	Method 2
37 combined	21.5	0	0.00	0.00		
37 direct UF	20.5	0.2	0.17	0.20	15.41%	-1.22%
46 combined	19.5	0	0.00	0.00		
46 direct UF	20.8	0.2	0.17	0.20	15.13%	-1.95%
46 combined	20.6	0.15	0.13	0.15	15.31%	-1.46%
46 direct UF	16.3	0.6	0.48	0.55	19.45%	8.81%
37 combined	16	0.5	0.40	0.45	19.75%	9.51%
37 direct UF	16.4	1.4	1.13	1.28	19.36%	8.58%
37 combined	16	0	0.00	0.00		
37 direct UF	15.6	0.35	0.28	0.31	20.14%	10.43%

For normalisation of data close to 20°C, there should be no distortion to the data as it is a small correction that has to be done. Equation 2.8 was thus used in normalisation calculations. The same correction was made for PF pressure drop data to account for the variance in temperature.

As temperatures during site visit was generally much higher than lab tests, pressure drop data was corrected to 25°C.

Error bar determination

Experiments were conducted as a set of repeated cycles. The standard deviation of recorded data was calculated, and the positive and negative values of the standard deviation was shown on the graph. For graphs with data points (where e.g. turbidity was measured at discrete

intervals), the standard deviations was shown as an error bar above and below each point. For continuously measured data, the positive and negative standard deviations were shown as lines.

For the PF site data: turbidities measured after 20 minutes:

Table 8-2: Determination of average turbidity and corresponding standard deviation

Day	Recorded turbidity readings (NTU)				Average	Standard deviation
1	0.34	0.31	0.41	0.38	0.36	0.043969687
2	0.2	0.97	0.74	0.5	0.636667	0.329886344
3	0.23	0.34	0.2		0.256667	0.073711148
4	0.53	0.34			0.435	0.134350288
5	0.47				0.47	0

SAFETY DATA SHEET

according to Regulation (EC) No. 1907/2006

Version 5.1 Revision Date 29.04.2014

Print Date 26.09.2014

GENERIC EU MSDS - NO COUNTRY SPECIFIC DATA - NO OEL DATA

SECTION 1: Identification of the substance/mixture and of the company/undertaking

1.1 Product identifiers

Product name : Bentonite

Product Number : 285234

Brand : Sigma-Aldrich

REACH No. : A registration number is not available for this substance as the substance or its uses are exempted from registration, the annual tonnage does not require a registration or the registration is envisaged for a later registration deadline.

CAS-No. : 1302-78-9

1.2 Relevant identified uses of the substance or mixture and uses advised against

Identified uses : Laboratory chemicals, Manufacture of substances

1.3 Details of the supplier of the safety data sheet

Company : Sigma-Aldrich (Pty.) Ltd.
17 Pomona Street
Aviation Park, Unit 4
KEMPTON PARK
1619 SOUTH AFRICA

Telephone : +27 11 979 1188

Fax : +27 11 979 1119

1.4 Emergency telephone number

Emergency Phone # :

SECTION 2: Hazards identification

2.1 Classification of the substance or mixture

Not a hazardous substance or mixture according to Regulation (EC) No. 1272/2008.
This substance is not classified as dangerous according to Directive 67/548/EEC.

2.2 Label elements

The product does not need to be labelled in accordance with EC directives or respective national laws.

2.3 Other hazards - none

SECTION 3: Composition/information on ingredients

3.1 Substances

Synonyms : Montmorillonite

CAS-No. : 1302-78-9

EC-No. : 215-108-5

No components need to be disclosed according to the applicable regulations.

SECTION 4: First aid measures

4.1 Description of first aid measures

If inhaled

If breathed in, move person into fresh air. If not breathing, give artificial respiration.

In case of skin contact

Wash off with soap and plenty of water.

In case of eye contact

Flush eyes with water as a precaution.

If swallowed

Never give anything by mouth to an unconscious person. Rinse mouth with water.

4.2 Most important symptoms and effects, both acute and delayed

The most important known symptoms and effects are described in the labelling (see section 2.2) and/or in section 11

4.3 Indication of any immediate medical attention and special treatment needed

no data available

SECTION 5: Firefighting measures

5.1 Extinguishing media

Suitable extinguishing media

Use water spray, alcohol-resistant foam, dry chemical or carbon dioxide.

5.2 Special hazards arising from the substance or mixture

Aluminum oxide, silicon oxides

5.3 Advice for firefighters

Wear self contained breathing apparatus for fire fighting if necessary.

5.4 Further information

no data available

SECTION 6: Accidental release measures

6.1 Personal precautions, protective equipment and emergency procedures

Avoid dust formation. Avoid breathing vapours, mist or gas.
For personal protection see section 8.

6.2 Environmental precautions

Do not let product enter drains.

6.3 Methods and materials for containment and cleaning up

Sweep up and shovel. Keep in suitable, closed containers for disposal.

6.4 Reference to other sections

For disposal see section 13.

SECTION 7: Handling and storage

7.1 Precautions for safe handling

Provide appropriate exhaust ventilation at places where dust is formed. Normal measures for preventive fire protection.
For precautions see section 2.2.

7.2 Conditions for safe storage, including any incompatibilities

Store in cool place. Keep container tightly closed in a dry and well-ventilated place.

7.3 Specific end use(s)

Apart from the uses mentioned in section 1.2 no other specific uses are stipulated

SECTION 8: Exposure controls/personal protection

8.1 Control parameters

Components with workplace control parameters

8.2 Exposure controls

Appropriate engineering controls

General industrial hygiene practice.

Personal protective equipment

Eye/face protection

Use equipment for eye protection tested and approved under appropriate government standards such as NIOSH (US) or EN 166(EU).

Skin protection

Handle with gloves. Gloves must be inspected prior to use. Use proper glove removal technique (without touching glove's outer surface) to avoid skin contact with this product. Dispose of contaminated gloves after use in accordance with applicable laws and good laboratory practices. Wash and dry hands.

The selected protective gloves have to satisfy the specifications of EU Directive 89/686/EEC and the standard EN 374 derived from it.

Full contact

Material: Nitrile rubber

Minimum layer thickness: 0,11 mm

Break through time: 480 min

Material tested: Dermatrill® (KCL 740 / Aldrich Z677272, Size M)

Splash contact

Material: Nitrile rubber

Minimum layer thickness: 0,11 mm

Break through time: 480 min

Material tested: Dermatrill® (KCL 740 / Aldrich Z677272, Size M)

data source: KCL GmbH, D-36124 Eichenzell, phone +49 (0)6659 87300, e-mail sales@kcl.de, test method: EN374

If used in solution, or mixed with other substances, and under conditions which differ from EN 374, contact the supplier of the CE approved gloves. This recommendation is advisory only and must be evaluated by an industrial hygienist and safety officer familiar with the specific situation of anticipated use by our customers. It should not be construed as offering an approval for any specific use scenario.

Body Protection

Choose body protection in relation to its type, to the concentration and amount of dangerous substances, and to the specific work-place. The type of protective equipment must be selected according to the concentration and amount of the dangerous substance at the specific workplace.

Respiratory protection

Respiratory protection is not required. Where protection from nuisance levels of dusts are desired, use type N95 (US) or type P1 (EN 143) dust masks. Use respirators and components tested and approved under appropriate government standards such as NIOSH (US) or CEN (EU).

Control of environmental exposure

Do not let product enter drains.

SECTION 9: Physical and chemical properties

9.1 Information on basic physical and chemical properties

- | | |
|---------------|---------------------------------------|
| a) Appearance | Form: granules
Colour: grey, beige |
| b) Odour | no data available |

c) Odour Threshold	no data available
d) pH	6,0 - 9,0
e) Melting point/freezing point	no data available
f) Initial boiling point and boiling range	no data available
g) Flash point	not applicable
h) Evaporation rate	no data available
i) Flammability (solid, gas)	no data available
j) Upper/lower flammability or explosive limits	no data available
k) Vapour pressure	no data available
l) Vapour density	no data available
m) Relative density	2,400 g/cm ³
n) Water solubility	no data available
o) Partition coefficient: n-octanol/water	no data available
p) Auto-ignition temperature	no data available
q) Decomposition temperature	no data available
r) Viscosity	no data available
s) Explosive properties	no data available
t) Oxidizing properties	no data available

9.2 Other safety information

no data available

SECTION 10: Stability and reactivity

10.1 Reactivity

no data available

10.2 Chemical stability

Stable under recommended storage conditions.

10.3 Possibility of hazardous reactions

no data available

10.4 Conditions to avoid

no data available

10.5 Incompatible materials

Strong acids

10.6 Hazardous decomposition products

Other decomposition products - no data available

In the event of fire: see section 5

SECTION 11: Toxicological information

11.1 Information on toxicological effects

Acute toxicity

LD50 Intravenous - rat - 35 mg/kg

Remarks: Lungs, Thorax, or Respiration:Acute pulmonary edema.

Skin corrosion/irritation

no data available

Serious eye damage/eye irritation

no data available

Respiratory or skin sensitisation

no data available

Germ cell mutagenicity

no data available

Carcinogenicity

Carcinogenicity - mouse - Oral

Tumorigenic:Equivocal tumorigenic agent by RTECS criteria. Liver:Tumors.

IARC: No component of this product present at levels greater than or equal to 0.1% is identified as probable, possible or confirmed human carcinogen by IARC.

Reproductive toxicity

no data available

Specific target organ toxicity - single exposure

no data available

Specific target organ toxicity - repeated exposure

no data available

Aspiration hazard

no data available

Additional Information

RTECS: CT9450000

Lung irritation, Asthma

SECTION 12: Ecological information

12.1 Toxicity

Toxicity to fish LC50 - Oncorhynchus mykiss (rainbow trout) - 19.000 mg/l - 96 h

12.2 Persistence and degradability

no data available

12.3 Bioaccumulative potential

no data available

12.4 Mobility in soil

no data available

12.5 Results of PBT and vPvB assessment

PBT/vPvB assessment not available as chemical safety assessment not required/not conducted

12.6 Other adverse effects

no data available

SECTION 13: Disposal considerations**13.1 Waste treatment methods****Product**

Offer surplus and non-recyclable solutions to a licensed disposal company.

Contaminated packaging

Dispose of as unused product.

SECTION 14: Transport information**14.1 UN number**

ADR/RID: -

IMDG: -

IATA: -

14.2 UN proper shipping name

ADR/RID: Not dangerous goods

IMDG: Not dangerous goods

IATA: Not dangerous goods

14.3 Transport hazard class(es)

ADR/RID: -

IMDG: -

IATA: -

14.4 Packaging group

ADR/RID: -

IMDG: -

IATA: -

14.5 Environmental hazards

ADR/RID: no

IMDG Marine pollutant: no

IATA: no

14.6 Special precautions for user

no data available

SECTION 15: Regulatory information

This safety datasheet complies with the requirements of Regulation (EC) No. 1907/2006.

15.1 Safety, health and environmental regulations/legislation specific for the substance or mixture

no data available

15.2 Chemical Safety Assessment

For this product a chemical safety assessment was not carried out

SECTION 16: Other information**Further information**

Copyright 2014 Sigma-Aldrich Co. LLC. License granted to make unlimited paper copies for internal use only.

The above information is believed to be correct but does not purport to be all inclusive and shall be used only as a guide. The information in this document is based on the present state of our knowledge and is applicable to the product with regard to appropriate safety precautions. It does not represent any guarantee of the properties of the product. Sigma-Aldrich Corporation and its Affiliates shall not be held liable for any damage resulting from handling or from contact with the above product. See www.sigma-aldrich.com and/or the reverse side of invoice or packing slip for additional terms and conditions of sale.

SAFETY DATA SHEET

according to Regulation (EC) No. 1907/2006

Version 6.7 Revision Date 29.04.2015

Print Date 14.11.2016

GENERIC EU MSDS - NO COUNTRY SPECIFIC DATA - NO OEL DATA

SECTION 1: Identification of the substance/mixture and of the company/undertaking

1.1 Product identifiers

Product name : Sodium hydroxide

Product Number : S8045
Brand : Sigma-Aldrich
Index-No. : 011-002-00-6
REACH No. : 01-2119457892-27-XXXX
CAS-No. : 1310-73-2

1.2 Relevant identified uses of the substance or mixture and uses advised against

Identified uses : Laboratory chemicals, Manufacture of substances

1.3 Details of the supplier of the safety data sheet

Company : Sigma-Aldrich (Pty.) Ltd.
17 Pomona Street
Aviation Park, Unit 4
KEMPTON PARK
1619 SOUTH AFRICA

Telephone : +27 11 979 1188
Fax : +27 11 979 1119

1.4 Emergency telephone number

Emergency Phone # :

SECTION 2: Hazards identification

2.1 Classification of the substance or mixture

Classification according to Regulation (EC) No 1272/2008

Corrosive to metals (Category 1), H290
Skin corrosion (Category 1A), H314

For the full text of the H-Statements mentioned in this Section, see Section 16.

Classification according to EU Directives 67/548/EEC or 1999/45/EC

C Corrosive R35

For the full text of the R-phrases mentioned in this Section, see Section 16.

2.2 Label elements

Labelling according Regulation (EC) No 1272/2008

Pictogram



Signal word : Danger

Hazard statement(s)

H290 : May be corrosive to metals.
H314 : Causes severe skin burns and eye damage.

Precautionary statement(s)

P280 : Wear protective gloves/ protective clothing/ eye protection/ face

P303 + P361 + P353	protection. IF ON SKIN (or hair): Take off immediately all contaminated clothing. Rinse skin with water/shower.
P304 + P340 + P310	IF INHALED: Remove person to fresh air and keep comfortable for breathing. Immediately call a POISON CENTER or doctor/ physician.
P305 + P351 + P338	IF IN EYES: Rinse cautiously with water for several minutes. Remove contact lenses, if present and easy to do. Continue rinsing.
Supplemental Hazard Statements	none

2.3 Other hazards

This substance/mixture contains no components considered to be either persistent, bioaccumulative and toxic (PBT), or very persistent and very bioaccumulative (vPvB) at levels of 0.1% or higher.

SECTION 3: Composition/information on ingredients

3.1 Substances

Synonyms	: Caustic soda
Formula	: NaOH
Molecular weight	: 40,00 g/mol
CAS-No.	: 1310-73-2
EC-No.	: 215-185-5
Index-No.	: 011-002-00-6
Registration number	: 01-2119457892-27-XXXX

Hazardous ingredients according to Regulation (EC) No 1272/2008

Component	Classification	Concentration
Sodium hydroxide		
CAS-No. 1310-73-2 EC-No. 215-185-5 Index-No. 011-002-00-6 Registration number 01-2119457892-27-XXXX	Met. Corr. 1; Skin Corr. 1A; H290, H314	<= 100 %

Hazardous ingredients according to Directive 1999/45/EC

Component	Classification	Concentration
Sodium hydroxide		
CAS-No. 1310-73-2 EC-No. 215-185-5 Index-No. 011-002-00-6 Registration number 01-2119457892-27-XXXX	C, R35	<= 100 %

For the full text of the H-Statements and R-Phrases mentioned in this Section, see Section 16

SECTION 4: First aid measures

4.1 Description of first aid measures

General advice

Consult a physician. Show this safety data sheet to the doctor in attendance.

If inhaled

If breathed in, move person into fresh air. If not breathing, give artificial respiration. Consult a physician.

In case of skin contact

Take off contaminated clothing and shoes immediately. Wash off with soap and plenty of water. Consult a physician.

In case of eye contact

Rinse thoroughly with plenty of water for at least 15 minutes and consult a physician.

If swallowed

Do NOT induce vomiting. Never give anything by mouth to an unconscious person. Rinse mouth with water. Consult a physician.

4.2 Most important symptoms and effects, both acute and delayed

The most important known symptoms and effects are described in the labelling (see section 2.2) and/or in section 11

4.3 Indication of any immediate medical attention and special treatment needed

No data available

SECTION 5: Firefighting measures**5.1 Extinguishing media****Suitable extinguishing media**

Use water spray, alcohol-resistant foam, dry chemical or carbon dioxide.

5.2 Special hazards arising from the substance or mixture

Sodium oxides

5.3 Advice for firefighters

Wear self-contained breathing apparatus for firefighting if necessary.

5.4 Further information

No data available

SECTION 6: Accidental release measures**6.1 Personal precautions, protective equipment and emergency procedures**

Wear respiratory protection. Avoid dust formation. Avoid breathing vapours, mist or gas. Ensure adequate ventilation. Evacuate personnel to safe areas. Avoid breathing dust.
For personal protection see section 8.

6.2 Environmental precautions

Prevent further leakage or spillage if safe to do so. Do not let product enter drains. Discharge into the environment must be avoided.

6.3 Methods and materials for containment and cleaning up

Pick up and arrange disposal without creating dust. Sweep up and shovel. Keep in suitable, closed containers for disposal.

6.4 Reference to other sections

For disposal see section 13.

SECTION 7: Handling and storage**7.1 Precautions for safe handling**

Avoid formation of dust and aerosols.
Provide appropriate exhaust ventilation at places where dust is formed.
For precautions see section 2.2.

7.2 Conditions for safe storage, including any incompatibilities

Store in cool place. Keep container tightly closed in a dry and well-ventilated place.

7.3 Specific end use(s)

Apart from the uses mentioned in section 1.2 no other specific uses are stipulated

SECTION 8: Exposure controls/personal protection

8.1 Control parameters

Components with workplace control parameters

Derived No Effect Level (DNEL)

Application Area	Exposure routes	Health effect	Value
Workers	Inhalation	Long-term local effects	1 mg/m ³
Consumers	Inhalation	Long-term local effects	1 mg/m ³

8.2 Exposure controls

Appropriate engineering controls

Handle in accordance with good industrial hygiene and safety practice. Wash hands before breaks and at the end of workday.

Personal protective equipment

Eye/face protection

Face shield and safety glasses Use equipment for eye protection tested and approved under appropriate government standards such as NIOSH (US) or EN 166(EU).

Skin protection

Handle with gloves. Gloves must be inspected prior to use. Use proper glove removal technique (without touching glove's outer surface) to avoid skin contact with this product. Dispose of contaminated gloves after use in accordance with applicable laws and good laboratory practices. Wash and dry hands.

The selected protective gloves have to satisfy the specifications of EU Directive 89/686/EEC and the standard EN 374 derived from it.

Full contact

Material: Nitrile rubber

Minimum layer thickness: 0,11 mm

Break through time: 480 min

Material tested:Dermatril® (KCL 740 / Aldrich Z677272, Size M)

Splash contact

Material: Nitrile rubber

Minimum layer thickness: 0,11 mm

Break through time: 480 min

Material tested:Dermatril® (KCL 740 / Aldrich Z677272, Size M)

data source: KCL GmbH, D-36124 Eichenzell, phone +49 (0)6659 87300, e-mail sales@kcl.de, test method: EN374

If used in solution, or mixed with other substances, and under conditions which differ from EN 374, contact the supplier of the CE approved gloves. This recommendation is advisory only and must be evaluated by an industrial hygienist and safety officer familiar with the specific situation of anticipated use by our customers. It should not be construed as offering an approval for any specific use scenario.

Body Protection

Complete suit protecting against chemicals, The type of protective equipment must be selected according to the concentration and amount of the dangerous substance at the specific workplace.

Respiratory protection

Where risk assessment shows air-purifying respirators are appropriate use a full-face particle respirator type N100 (US) or type P3 (EN 143) respirator cartridges as a backup to engineering controls. If the respirator is the sole means of protection, use a full-face supplied air respirator. Use respirators and components tested and approved under appropriate government standards such as NIOSH (US) or CEN (EU).

Control of environmental exposure

Prevent further leakage or spillage if safe to do so. Do not let product enter drains. Discharge into the environment must be avoided.

SECTION 9: Physical and chemical properties**9.1 Information on basic physical and chemical properties**

a) Appearance	Form: pellets Colour: white
b) Odour	odourless
c) Odour Threshold	No data available
d) pH	14 at 50 g/l at 20 °C
e) Melting point/freezing point	Melting point/range: 318 °C
f) Initial boiling point and boiling range	1.390 °C
g) Flash point	Not applicable
h) Evaporation rate	No data available
i) Flammability (solid, gas)	No data available
j) Upper/lower flammability or explosive limits	No data available
k) Vapour pressure	< 24,00 hPa at 20 °C 4,00 hPa at 37 °C
l) Vapour density	1,38 - (Air = 1.0)
m) Relative density	2,1300 g/cm ³
n) Water solubility	ca.1.260 g/l at 20 °C
o) Partition coefficient: n-octanol/water	No data available
p) Auto-ignition temperature	No data available
q) Decomposition temperature	No data available
r) Viscosity	No data available
s) Explosive properties	No data available
t) Oxidizing properties	No data available

9.2 Other safety information

Bulk density	ca.1.150 kg/m ³
Relative vapour density	1,38 - (Air = 1.0)

SECTION 10: Stability and reactivity**10.1 Reactivity**

No data available

10.2 Chemical stability

Stable under recommended storage conditions.

10.3 Possibility of hazardous reactions

No data available

- 10.4 Conditions to avoid**
No data available
- 10.5 Incompatible materials**
Strong oxidizing agents, Strong acids, Organic materials
- 10.6 Hazardous decomposition products**
Other decomposition products - No data available
In the event of fire: see section 5

SECTION 11: Toxicological information

11.1 Information on toxicological effects

Acute toxicity

No data available

Skin corrosion/irritation

Skin - Rabbit

Result: Causes severe burns. - 24 h

Serious eye damage/eye irritation

Eyes - Rabbit

Result: Corrosive - 24 h

Respiratory or skin sensitisation

Will not occur

Germ cell mutagenicity

No data available

Carcinogenicity

IARC: No component of this product present at levels greater than or equal to 0.1% is identified as probable, possible or confirmed human carcinogen by IARC.

Reproductive toxicity

No data available

Specific target organ toxicity - single exposure

No data available

Specific target organ toxicity - repeated exposure

No data available

Aspiration hazard

No data available

Additional Information

RTECS: WB4900000

Material is extremely destructive to tissue of the mucous membranes and upper respiratory tract, eyes, and skin.

To the best of our knowledge, the chemical, physical, and toxicological properties have not been thoroughly investigated.

SECTION 12: Ecological information

12.1 Toxicity

Toxicity to fish	LC50 - Gambusia affinis (Mosquito fish) - 125 mg/l - 96 h
	LC50 - Oncorhynchus mykiss (rainbow trout) - 45,4 mg/l - 96 h
Toxicity to daphnia and other aquatic invertebrates	Immobilization EC50 - Daphnia (water flea) - 40,38 mg/l - 48 h

12.2 Persistence and degradability

The methods for determining the biological degradability are not applicable to inorganic substances.

12.3 Bioaccumulative potential

No data available

12.4 Mobility in soil

No data available

12.5 Results of PBT and vPvB assessment

This substance/mixture contains no components considered to be either persistent, bioaccumulative and toxic (PBT), or very persistent and very bioaccumulative (vPvB) at levels of 0.1% or higher.

12.6 Other adverse effects

Harmful to aquatic life.

SECTION 13: Disposal considerations

13.1 Waste treatment methods

Product

Offer surplus and non-recyclable solutions to a licensed disposal company. Dissolve or mix the material with a combustible solvent and burn in a chemical incinerator equipped with an afterburner and scrubber.

Contaminated packaging

Dispose of as unused product.

SECTION 14: Transport information

14.1 UN number

ADR/RID: 1823

IMDG: 1823

IATA: 1823

14.2 UN proper shipping name

ADR/RID: SODIUM HYDROXIDE, SOLID

IMDG: SODIUM HYDROXIDE, SOLID

IATA: Sodium hydroxide, solid

14.3 Transport hazard class(es)

ADR/RID: 8

IMDG: 8

IATA: 8

14.4 Packaging group

ADR/RID: II

IMDG: II

IATA: II

14.5 Environmental hazards

ADR/RID: no

IMDG Marine pollutant: no

IATA: no

14.6 Special precautions for user

No data available

SECTION 15: Regulatory information

This safety datasheet complies with the requirements of Regulation (EC) No. 1907/2006.

15.1 Safety, health and environmental regulations/legislation specific for the substance or mixture

15.2 Chemical Safety Assessment

A Chemical Safety Assessment has been carried out for this substance.

SECTION 16: Other information

Full text of H-Statements referred to under sections 2 and 3.

H290

May be corrosive to metals.

H314

Causes severe skin burns and eye damage.

Met. Corr.

Corrosive to metals

Skin Corr. Skin corrosion

Full text of R-phrases referred to under sections 2 and 3

C Corrosive
R35 Causes severe burns.

Further information

Copyright 2015 Sigma-Aldrich Co. LLC. License granted to make unlimited paper copies for internal use only.

The above information is believed to be correct but does not purport to be all inclusive and shall be used only as a guide. The information in this document is based on the present state of our knowledge and is applicable to the product with regard to appropriate safety precautions. It does not represent any guarantee of the properties of the product. Sigma-Aldrich Corporation and its Affiliates shall not be held liable for any damage resulting from handling or from contact with the above product. See www.sigma-aldrich.com and/or the reverse side of invoice or packing slip for additional terms and conditions of sale.

SAFETY DATA SHEET

according to Regulation (EC) No. 1907/2006

Version 5.0 Revision Date 27.04.2012

Print Date 14.11.2016

GENERIC EU MSDS - NO COUNTRY SPECIFIC DATA - NO OEL DATA

1. IDENTIFICATION OF THE SUBSTANCE/MIXTURE AND OF THE COMPANY/UNDERTAKING

1.1 Product identifiers

Product name : Citric acid

Product Number : C83155

Brand : Sigma-Aldrich

CAS-No. : 77-92-9

1.2 Relevant identified uses of the substance or mixture and uses advised against

Identified uses : Laboratory chemicals, Manufacture of substances

1.3 Details of the supplier of the safety data sheet

Company : Sigma-Aldrich (Pty.) Ltd.
17 Pomona Street
Aviation Park, Unit 4
KEMPTON PARK
1619 SOUTH AFRICA

Telephone : +27 11 979 1188

Fax : +27 11 979 1119

1.4 Emergency telephone number

Emergency Phone # :

2. HAZARDS IDENTIFICATION

2.1 Classification of the substance or mixture

Classification according to Regulation (EC) No 1272/2008 [EU-GHS/CLP]

Eye irritation (Category 2)

Classification according to EU Directives 67/548/EEC or 1999/45/EC

Irritating to eyes.

2.2 Label elements

Labelling according Regulation (EC) No 1272/2008 [CLP]

Pictogram



Signal word : Warning

Hazard statement(s)
H319 : Causes serious eye irritation.

Precautionary statement(s)
P305 + P351 + P338 : IF IN EYES: Rinse cautiously with water for several minutes. Remove contact lenses, if present and easy to do. Continue rinsing.

Supplemental Hazard
Statements : none

According to European Directive 67/548/EEC as amended.

Hazard symbol(s)



R-phrases)

R36

Irritating to eyes.

S-phrases)

S26

In case of contact with eyes, rinse immediately with plenty of water and seek medical advice.

2.3 Other hazards - none

3. COMPOSITION/INFORMATION ON INGREDIENTS

3.1 Substances

Formula : $C_6H_8O_7$

Molecular Weight : 192,12 g/mol

Component		Concentration
Citric acid		
CAS-No.	77-92-9	-
EC-No.	201-069-1	

4. FIRST AID MEASURES

4.1 Description of first aid measures

General advice

Consult a physician. Show this safety data sheet to the doctor in attendance.

If inhaled

If breathed in, move person into fresh air. If not breathing, give artificial respiration. Consult a physician.

In case of skin contact

Wash off with soap and plenty of water. Consult a physician.

In case of eye contact

Rinse thoroughly with plenty of water for at least 15 minutes and consult a physician.

If swallowed

Never give anything by mouth to an unconscious person. Rinse mouth with water. Consult a physician.

4.2 Most important symptoms and effects, both acute and delayed

Vomiting, Diarrhoea, Damage to tooth enamel., Dermatitis, To the best of our knowledge, the chemical, physical, and toxicological properties have not been thoroughly investigated.

4.3 Indication of any immediate medical attention and special treatment needed

no data available

5. FIREFIGHTING MEASURES

5.1 Extinguishing media

Suitable extinguishing media

Use water spray, alcohol-resistant foam, dry chemical or carbon dioxide.

5.2 Special hazards arising from the substance or mixture

Carbon oxides

5.3 Advice for firefighters

Wear self contained breathing apparatus for fire fighting if necessary.

5.4 Further information

no data available

6. ACCIDENTAL RELEASE MEASURES

6.1 Personal precautions, protective equipment and emergency procedures

Use personal protective equipment. Avoid dust formation. Avoid breathing vapors, mist or gas. Ensure adequate ventilation. Avoid breathing dust.

6.2 Environmental precautions

Do not let product enter drains.

6.3 Methods and materials for containment and cleaning up

Pick up and arrange disposal without creating dust. Sweep up and shovel. Keep in suitable, closed containers for disposal.

6.4 Reference to other sections

For disposal see section 13.

7. HANDLING AND STORAGE

7.1 Precautions for safe handling

Avoid contact with skin and eyes. Avoid formation of dust and aerosols. Provide appropriate exhaust ventilation at places where dust is formed.

7.2 Conditions for safe storage, including any incompatibilities

Store in cool place. Keep container tightly closed in a dry and well-ventilated place.

7.3 Specific end uses

no data available

8. EXPOSURE CONTROLS/PERSONAL PROTECTION

8.1 Control parameters

Components with workplace control parameters

8.2 Exposure controls

Appropriate engineering controls

Handle in accordance with good industrial hygiene and safety practice. Wash hands before breaks and at the end of workday.

Personal protective equipment

Eye/face protection

Safety glasses with side-shields conforming to EN166 Use equipment for eye protection tested and approved under appropriate government standards such as NIOSH (US) or EN 166(EU).

Skin protection

Handle with gloves. Gloves must be inspected prior to use. Use proper glove removal technique (without touching glove's outer surface) to avoid skin contact with this product. Dispose of contaminated gloves after use in accordance with applicable laws and good laboratory practices. Wash and dry hands.

The selected protective gloves have to satisfy the specifications of EU Directive 89/686/EEC and the standard EN 374 derived from it.

Immersion protection

Material: Nitrile rubber

Minimum layer thickness: 0,11 mm

Break through time: > 480 min

Material tested: Dermatrill® (Aldrich Z677272, Size M)

Splash protection

Material: Nitrile rubber

Minimum layer thickness: 0,11 mm

Break through time: > 30 min

Material tested: Dermatrill® (Aldrich Z677272, Size M)

data source: KCL GmbH, D-36124 Eichenzell, phone +49 (0)6659 873000, e-mail sales@kcl.de, test method: EN374

If used in solution, or mixed with other substances, and under conditions which differ from EN 374, contact the supplier of the CE approved gloves. This recommendation is advisory only and must be evaluated by an Industrial Hygienist familiar with the specific situation of anticipated use by our customers. It should not be construed as offering an approval for any specific use scenario.

Body Protection

impervious clothing, The type of protective equipment must be selected according to the concentration and amount of the dangerous substance at the specific workplace.

Respiratory protection

For nuisance exposures use type P95 (US) or type P1 (EU EN 143) particle respirator. For higher level protection use type OV/AG/P99 (US) or type ABEK-P2 (EU EN 143) respirator cartridges. Use respirators and components tested and approved under appropriate government standards such as NIOSH (US) or CEN (EU).

9. PHYSICAL AND CHEMICAL PROPERTIES**9.1 Information on basic physical and chemical properties**

a) Appearance	Form: crystalline Colour: white
b) Odour	no data available
c) Odour Threshold	no data available
d) pH	1,8 at ca.50 g/l at 25 °C
e) Melting point/freezing point	Melting point/range: 153 - 159 °C - lit.
f) Initial boiling point and boiling range	no data available
g) Flash point	no data available
h) Evaporation rate	no data available
i) Flammability (solid, gas)	no data available
j) Upper/lower flammability or explosive limits	Lower explosion limit: 8 %(V)
k) Vapour pressure	no data available
l) Vapour density	no data available
m) Relative density	no data available
n) Water solubility	383 g/l at 25 °C
o) Partition coefficient: n-octanol/water	log Pow: -1,64 at 20 °C
p) Autoignition temperature	no data available
q) Decomposition temperature	no data available
r) Viscosity	no data available
s) Explosive properties	no data available
t) Oxidizing properties	no data available

9.2 Other safety information

no data available

10. STABILITY AND REACTIVITY**10.1 Reactivity**

no data available

10.2 Chemical stability

no data available

- 10.3 Possibility of hazardous reactions**
no data available
- 10.4 Conditions to avoid**
no data available
- 10.5 Incompatible materials**
Oxidizing agents, Bases, Reducing agents, Nitrates
- 10.6 Hazardous decomposition products**
Other decomposition products - no data available

11. TOXICOLOGICAL INFORMATION

11.1 Information on toxicological effects

Acute toxicity

LD50 Oral - rat - 5.400 mg/kg

LD50 Dermal - rat - > 2.000 mg/kg

Skin corrosion/irritation

Skin - rabbit - Mild skin irritation - OECD Test Guideline 404

Serious eye damage/eye irritation

Eyes - rabbit - Irritating to eyes. - OECD Test Guideline 405

Respiratory or skin sensitization

Prolonged or repeated exposure may cause allergic reactions in certain sensitive individuals.

Germ cell mutagenicity

no data available

Carcinogenicity

IARC: No component of this product present at levels greater than or equal to 0.1% is identified as probable, possible or confirmed human carcinogen by IARC.

Reproductive toxicity

no data available

Specific target organ toxicity - single exposure

no data available

Specific target organ toxicity - repeated exposure

no data available

Aspiration hazard

no data available

Potential health effects

Inhalation	May be harmful if inhaled. May cause respiratory tract irritation.
Ingestion	May be harmful if swallowed.
Skin	May be harmful if absorbed through skin. May cause skin irritation.
Eyes	Causes serious eye irritation.

Signs and Symptoms of Exposure

Vomiting, Diarrhoea, Damage to tooth enamel., Dermatitis, To the best of our knowledge, the chemical, physical, and toxicological properties have not been thoroughly investigated.

Additional Information

RTECS: GE7350000

12. ECOLOGICAL INFORMATION

12.1 Toxicity

Toxicity to fish mortality LC50 - Leuciscus idus melanotus - 440 mg/l - 48 h
Method: OECD Test Guideline 203

Toxicity to daphnia and static test - Daphnia magna (Water flea) - 1.535 mg/l - 24 h
other aquatic
invertebrates

12.2 Persistence and degradability

no data available

12.3 Bioaccumulative potential

no data available

12.4 Mobility in soil

no data available

12.5 Results of PBT and vPvB assessment

no data available

12.6 Other adverse effects

no data available

13. DISPOSAL CONSIDERATIONS

13.1 Waste treatment methods

Product

Offer surplus and non-recyclable solutions to a licensed disposal company. Dissolve or mix the material with a combustible solvent and burn in a chemical incinerator equipped with an afterburner and scrubber.

Contaminated packaging

Dispose of as unused product.

14. TRANSPORT INFORMATION

14.1 UN number

ADR/RID: -

IMDG: -

IATA: -

14.2 UN proper shipping name

ADR/RID: Not dangerous goods

IMDG: Not dangerous goods

IATA: Not dangerous goods

14.3 Transport hazard class(es)

ADR/RID: -

IMDG: -

IATA: -

14.4 Packaging group

ADR/RID: -

IMDG: -

IATA: -

14.5 Environmental hazards

ADR/RID: no

IMDG Marine pollutant: no

IATA: no

14.6 Special precautions for user

no data available

15. REGULATORY INFORMATION

This safety datasheet complies with the requirements of Regulation (EC) No. 1907/2006.

15.1 Safety, health and environmental regulations/legislation specific for the substance or mixture

no data available

15.2 Chemical Safety Assessment

no data available

16. OTHER INFORMATION

Further information

Copyright 2012 Sigma-Aldrich Co. LLC. License granted to make unlimited paper copies for internal use only.

The above information is believed to be correct but does not purport to be all inclusive and shall be used only as a guide. The information in this document is based on the present state of our knowledge

and is applicable to the product with regard to appropriate safety precautions. It does not represent any guarantee of the properties of the product. Sigma-Aldrich Corporation and its Affiliates shall not be held liable for any damage resulting from handling or from contact with the above product. See www.sigma-aldrich.com and/or the reverse side of invoice or packing slip for additional terms and conditions of sale.

SAFETY DATA SHEET

according to Regulation (EC) No. 1907/2006

Version 5.0 Revision Date 23.11.2012

Print Date 26.09.2014

GENERIC EU MSDS - NO COUNTRY SPECIFIC DATA - NO OEL DATA

1. IDENTIFICATION OF THE SUBSTANCE/MIXTURE AND OF THE COMPANY/UNDERTAKING

1.1 Product identifiers

Product name : Iron(III) chloride solution

Product Number : 12322

Brand : Sigma-Aldrich

1.2 Relevant identified uses of the substance or mixture and uses advised against

Identified uses : Laboratory chemicals, Manufacture of substances

1.3 Details of the supplier of the safety data sheet

Company : Sigma-Aldrich (Pty.) Ltd.
17 Pomona Street
Aviation Park, Unit 4
KEMPTON PARK
1619 SOUTH AFRICA

Telephone : +27 11 979 1188

Fax : +27 11 979 1119

1.4 Emergency telephone number

Emergency Phone # :

2. HAZARDS IDENTIFICATION

2.1 Classification of the substance or mixture

Classification according to Regulation (EC) No 1272/2008 [EU-GHS/CLP]

Corrosive to metals (Category 1)

Skin irritation (Category 2)

Serious eye damage (Category 1)

Chronic aquatic toxicity (Category 2)

Classification according to EU Directives 67/548/EEC or 1999/45/EC

Harmful if swallowed. Irritating to skin. Risk of serious damage to eyes.

2.2 Label elements

Labelling according Regulation (EC) No 1272/2008 [CLP]

Pictogram



Signal word : Danger

Hazard statement(s)

H290

May be corrosive to metals.

H315

Causes skin irritation.

H318

Causes serious eye damage.

H411

Toxic to aquatic life with long lasting effects.

Precautionary statement(s)

P273

Avoid release to the environment.

P280

Wear protective gloves/ eye protection/ face protection.

P305 + P351 + P338

IF IN EYES: Rinse cautiously with water for several minutes. Remove contact lenses, if present and easy to do. Continue rinsing.

Supplemental Hazard Statements none

According to European Directive 67/548/EEC as amended.

Hazard symbol(s)



R-phrases)

R22

Harmful if swallowed.

R38

Irritating to skin.

R41

Risk of serious damage to eyes.

S-phrases(s)

S26

In case of contact with eyes, rinse immediately with plenty of water and seek medical advice.

S39

Wear eye/face protection.

2.3 Other hazards - none

3. COMPOSITION/INFORMATION ON INGREDIENTS

3.2 Mixtures

Synonyms : Ferric chloride

Formula : Cl_3Fe

Molecular Weight : 162,20 g/mol

Component		Classification	Concentration
Iron trichloride			
CAS-No.	7705-08-0	Met. Corr. 1; Acute Tox. 4; Skin Irrit. 2; Eye Dam. 1; Aquatic Chronic 2; H290, H302, H315, H318, H411 Xn, R22 - R38 - R41	50 - 100 %
EC-No.	231-729-4		

For the full text of the H-Statements and R-Phrases mentioned in this Section, see Section 16

4. FIRST AID MEASURES

4.1 Description of first aid measures

General advice

Consult a physician. Show this safety data sheet to the doctor in attendance.

If inhaled

If breathed in, move person into fresh air. If not breathing, give artificial respiration. Consult a physician.

In case of skin contact

Wash off with soap and plenty of water. Consult a physician.

In case of eye contact

Rinse thoroughly with plenty of water for at least 15 minutes and consult a physician.

If swallowed

Never give anything by mouth to an unconscious person. Rinse mouth with water. Consult a physician.

4.2 Most important symptoms and effects, both acute and delayed

spasm, inflammation and edema of the larynx, spasm, inflammation and edema of the bronchi, pneumonitis, pulmonary edema, Overdose of iron compounds may have a corrosive effect on the gastrointestinal mucosa and be followed by necrosis, perforation, and stricture formation. Several hours may elapse before symptoms that can include epigastric pain, diarrhea, vomiting, nausea, and hematemesis occur. After apparent recovery a person may experience metabolic acidosis, convulsions, and coma hours or days later. Further complications may develop leading to acute liver necrosis that can result in death due to hepatic coma., To the best of our knowledge, the chemical, physical, and toxicological properties have not been thoroughly investigated.

- 4.3 Indication of any immediate medical attention and special treatment needed**
no data available

5. FIREFIGHTING MEASURES

5.1 Extinguishing media

Suitable extinguishing media

Use water spray, alcohol-resistant foam, dry chemical or carbon dioxide.

5.2 Special hazards arising from the substance or mixture

Hydrogen chloride gas, Iron oxides

5.3 Advice for firefighters

Wear self contained breathing apparatus for fire fighting if necessary.

5.4 Further information

no data available

6. ACCIDENTAL RELEASE MEASURES

6.1 Personal precautions, protective equipment and emergency procedures

Use personal protective equipment. Avoid breathing vapors, mist or gas. Ensure adequate ventilation. Evacuate personnel to safe areas.

6.2 Environmental precautions

Prevent further leakage or spillage if safe to do so. Do not let product enter drains. Discharge into the environment must be avoided.

6.3 Methods and materials for containment and cleaning up

Soak up with inert absorbent material and dispose of as hazardous waste. Keep in suitable, closed containers for disposal.

6.4 Reference to other sections

For disposal see section 13.

7. HANDLING AND STORAGE

7.1 Precautions for safe handling

Avoid contact with skin and eyes. Avoid inhalation of vapour or mist.

7.2 Conditions for safe storage, including any incompatibilities

Store in cool place. Keep container tightly closed in a dry and well-ventilated place. Containers which are opened must be carefully resealed and kept upright to prevent leakage.

7.3 Specific end uses

no data available

8. EXPOSURE CONTROLS/PERSONAL PROTECTION

8.1 Control parameters

Components with workplace control parameters

8.2 Exposure controls

Appropriate engineering controls

Handle in accordance with good industrial hygiene and safety practice. Wash hands before breaks and at the end of workday.

Personal protective equipment

Eye/face protection

Tightly fitting safety goggles. Faceshield (8-inch minimum). Use equipment for eye protection tested and approved under appropriate government standards such as NIOSH (US) or EN 166(EU).

Skin protection

Handle with gloves. Gloves must be inspected prior to use. Use proper glove removal technique (without touching glove's outer surface) to avoid skin contact with this product. Dispose of

contaminated gloves after use in accordance with applicable laws and good laboratory practices. Wash and dry hands.

The selected protective gloves have to satisfy the specifications of EU Directive 89/686/EEC and the standard EN 374 derived from it.

Body Protection

Complete suit protecting against chemicals, The type of protective equipment must be selected according to the concentration and amount of the dangerous substance at the specific workplace.

Respiratory protection

Where risk assessment shows air-purifying respirators are appropriate use a full-face respirator with multi-purpose combination (US) or type ABEK (EN 14387) respirator cartridges as a backup to engineering controls. If the respirator is the sole means of protection, use a full-face supplied air respirator. Use respirators and components tested and approved under appropriate government standards such as NIOSH (US) or CEN (EU).

9. PHYSICAL AND CHEMICAL PROPERTIES

9.1 Information on basic physical and chemical properties

- | | |
|---|-------------------|
| a) Appearance | Form: liquid |
| b) Odour | no data available |
| c) Odour Threshold | no data available |
| d) pH | no data available |
| e) Melting point/freezing point | no data available |
| f) Initial boiling point and boiling range | no data available |
| g) Flash point | no data available |
| h) Evaporation rate | no data available |
| i) Flammability (solid, gas) | no data available |
| j) Upper/lower flammability or explosive limits | no data available |
| k) Vapour pressure | no data available |
| l) Vapour density | no data available |
| m) Relative density | no data available |
| n) Water solubility | no data available |
| o) Partition coefficient: n-octanol/water | no data available |
| p) Autoignition temperature | no data available |
| q) Decomposition temperature | no data available |
| r) Viscosity | no data available |
| s) Explosive properties | no data available |
| t) Oxidizing properties | no data available |

9.2 Other safety information

no data available

10. STABILITY AND REACTIVITY

10.1 Reactivity

no data available

10.2 Chemical stability

no data available

10.3 Possibility of hazardous reactions

no data available

10.4 Conditions to avoid

no data available

10.5 Incompatible materials

Bases, Alkali metals, Strong oxidizing agents, Potassium, Exothermic in contact with water, Forms shock-sensitive mixtures with certain other materials.

10.6 Hazardous decomposition products

Other decomposition products - no data available

11. TOXICOLOGICAL INFORMATION

11.1 Information on toxicological effects

Acute toxicity

no data available

Skin corrosion/irritation

no data available

Serious eye damage/eye irritation

no data available

Respiratory or skin sensitization

no data available

Germ cell mutagenicity

no data available

Carcinogenicity

IARC: No component of this product present at levels greater than or equal to 0.1% is identified as probable, possible or confirmed human carcinogen by IARC.

Reproductive toxicity

no data available

Specific target organ toxicity - single exposure

no data available

Specific target organ toxicity - repeated exposure

no data available

Aspiration hazard

no data available

Potential health effects

Inhalation

May be harmful if inhaled. Causes respiratory tract irritation.

Ingestion

Harmful if swallowed.

Skin

May be harmful if absorbed through skin. Causes skin irritation.

Eyes

Causes eye burns.

Signs and Symptoms of Exposure

spasm, inflammation and edema of the larynx, spasm, inflammation and edema of the bronchi, pneumonitis, pulmonary edema, Overdose of iron compounds may have a corrosive effect on the gastrointestinal mucosa and be followed by necrosis, perforation, and stricture formation. Several hours may elapse before symptoms that can include epigastric pain, diarrhea, vomiting, nausea, and hematemesis occur. After apparent recovery a person may experience metabolic acidosis, convulsions,

and coma hours or days later. Further complications may develop leading to acute liver necrosis that can result in death due to hepatic coma., To the best of our knowledge, the chemical, physical, and toxicological properties have not been thoroughly investigated.

Additional Information

RTECS: Not available

12. ECOLOGICAL INFORMATION

12.1 Toxicity

no data available

12.2 Persistence and degradability

no data available

12.3 Bioaccumulative potential

no data available

12.4 Mobility in soil

no data available

12.5 Results of PBT and vPvB assessment

no data available

12.6 Other adverse effects

Toxic to aquatic life with long lasting effects.

13. DISPOSAL CONSIDERATIONS

13.1 Waste treatment methods

Product

Offer surplus and non-recyclable solutions to a licensed disposal company.

Contaminated packaging

Dispose of as unused product.

14. TRANSPORT INFORMATION

14.1 UN number

ADR/RID: 2582

IMDG: 2582

IATA: 2582

14.2 UN proper shipping name

ADR/RID: FERRIC CHLORIDE SOLUTION

IMDG: FERRIC CHLORIDE SOLUTION

IATA: Ferric chloride solution

14.3 Transport hazard class(es)

ADR/RID: 8

IMDG: 8

IATA: 8

14.4 Packaging group

ADR/RID: III

IMDG: III

IATA: III

14.5 Environmental hazards

ADR/RID: yes

IMDG Marine pollutant: yes

IATA: no

14.6 Special precautions for user

no data available

15. REGULATORY INFORMATION

This safety datasheet complies with the requirements of Regulation (EC) No. 1907/2006.

15.1 Safety, health and environmental regulations/legislation specific for the substance or mixture

no data available

15.2 Chemical Safety Assessment

no data available

16. OTHER INFORMATION**Text of H-code(s) and R-phrases mentioned in Section 3**

Acute Tox.	Acute toxicity
Aquatic Chronic	Chronic aquatic toxicity
Eye Dam.	Serious eye damage
H290	May be corrosive to metals.
H302	Harmful if swallowed.
H315	Causes skin irritation.
H318	Causes serious eye damage.
H411	Toxic to aquatic life with long lasting effects.
Met. Corr.	Corrosive to metals
Skin Irrit.	Skin irritation
Xn	Harmful
R22	Harmful if swallowed.
R38	Irritating to skin.
R41	Risk of serious damage to eyes.

Further information

Copyright 2012 Sigma-Aldrich Co. LLC. License granted to make unlimited paper copies for internal use only.

The above information is believed to be correct but does not purport to be all inclusive and shall be used only as a guide. The information in this document is based on the present state of our knowledge and is applicable to the product with regard to appropriate safety precautions. It does not represent any guarantee of the properties of the product. Sigma-Aldrich Corporation and its Affiliates shall not be held liable for any damage resulting from handling or from contact with the above product. See www.sigma-aldrich.com and/or the reverse side of invoice or packing slip for additional terms and conditions of sale.

SAFETY DATA SHEET

according to Regulation (EC) No. 1907/2006

Version 5.2 Revision Date 06.02.2014

Print Date 26.09.2014

GENERIC EU MSDS - NO COUNTRY SPECIFIC DATA - NO OEL DATA

SECTION 1: Identification of the substance/mixture and of the company/undertaking

1.1 Product identifiers

Product name : Humic acid sodium salt

Product Number : H16752

Brand : Aldrich

REACH No. : A registration number is not available for this substance as the substance or its uses are exempted from registration, the annual tonnage does not require a registration or the registration is envisaged for a later registration deadline.

CAS-No. : 68131-04-4

1.2 Relevant identified uses of the substance or mixture and uses advised against

Identified uses : Laboratory chemicals, Manufacture of substances

1.3 Details of the supplier of the safety data sheet

Company : Sigma-Aldrich (Pty.) Ltd.
17 Pomona Street
Aviation Park, Unit 4
KEMPTON PARK
1619 SOUTH AFRICA

Telephone : +27 11 979 1188

Fax : +27 11 979 1119

1.4 Emergency telephone number

Emergency Phone # :

SECTION 2: Hazards identification

2.1 Classification of the substance or mixture

Not a hazardous substance or mixture according to Regulation (EC) No. 1272/2008.
This substance is not classified as dangerous according to Directive 67/548/EEC.

2.2 Label elements

The product does not need to be labelled in accordance with EC directives or respective national laws.

2.3 Other hazards - none

SECTION 3: Composition/information on ingredients

3.1 Substances

Chemical characterization : Natural product

CAS-No. : 68131-04-4

EC-No. : 268-608-0

No components need to be disclosed according to the applicable regulations.

SECTION 4: First aid measures

4.1 Description of first aid measures

If inhaled

If breathed in, move person into fresh air. If not breathing, give artificial respiration.

In case of skin contact

Wash off with soap and plenty of water.

In case of eye contact

Flush eyes with water as a precaution.

If swallowed

Never give anything by mouth to an unconscious person. Rinse mouth with water.

4.2 Most important symptoms and effects, both acute and delayed

The most important known symptoms and effects are described in the labelling (see section 2.2) and/or in section 11

4.3 Indication of any immediate medical attention and special treatment needed

no data available

SECTION 5: Firefighting measures

5.1 Extinguishing media

Suitable extinguishing media

Use water spray, alcohol-resistant foam, dry chemical or carbon dioxide.

5.2 Special hazards arising from the substance or mixture

Nature of decomposition products not known.

5.3 Advice for firefighters

Wear self contained breathing apparatus for fire fighting if necessary.

5.4 Further information

no data available

SECTION 6: Accidental release measures

6.1 Personal precautions, protective equipment and emergency procedures

Avoid dust formation. Avoid breathing vapours, mist or gas.
For personal protection see section 8.

6.2 Environmental precautions

Do not let product enter drains.

6.3 Methods and materials for containment and cleaning up

Sweep up and shovel. Keep in suitable, closed containers for disposal.

6.4 Reference to other sections

For disposal see section 13.

SECTION 7: Handling and storage

7.1 Precautions for safe handling

Provide appropriate exhaust ventilation at places where dust is formed.
For precautions see section 2.2.

7.2 Conditions for safe storage, including any incompatibilities

Store in cool place. Keep container tightly closed in a dry and well-ventilated place.

7.3 Specific end use(s)

Apart from the uses mentioned in section 1.2 no other specific uses are stipulated

SECTION 8: Exposure controls/personal protection

8.1 Control parameters

Components with workplace control parameters

8.2 Exposure controls

Appropriate engineering controls

General industrial hygiene practice.

Personal protective equipment

Eye/face protection

Use equipment for eye protection tested and approved under appropriate government standards such as NIOSH (US) or EN 166(EU).

Skin protection

Handle with gloves. Gloves must be inspected prior to use. Use proper glove removal technique (without touching glove's outer surface) to avoid skin contact with this product. Dispose of contaminated gloves after use in accordance with applicable laws and good laboratory practices. Wash and dry hands.

The selected protective gloves have to satisfy the specifications of EU Directive 89/686/EEC and the standard EN 374 derived from it.

Full contact

Material: Nitrile rubber

Minimum layer thickness: 0,11 mm

Break through time: 480 min

Material tested: Dermatrill® (KCL 740 / Aldrich Z677272, Size M)

Splash contact

Material: Nitrile rubber

Minimum layer thickness: 0,11 mm

Break through time: 480 min

Material tested: Dermatrill® (KCL 740 / Aldrich Z677272, Size M)

data source: KCL GmbH, D-36124 Eichenzell, phone +49 (0)6659 87300, e-mail sales@kcl.de, test method: EN374

If used in solution, or mixed with other substances, and under conditions which differ from EN 374, contact the supplier of the CE approved gloves. This recommendation is advisory only and must be evaluated by an industrial hygienist and safety officer familiar with the specific situation of anticipated use by our customers. It should not be construed as offering an approval for any specific use scenario.

Body Protection

Choose body protection in relation to its type, to the concentration and amount of dangerous substances, and to the specific work-place. The type of protective equipment must be selected according to the concentration and amount of the dangerous substance at the specific workplace.

Respiratory protection

Respiratory protection is not required. Where protection from nuisance levels of dusts are desired, use type N95 (US) or type P1 (EN 143) dust masks. Use respirators and components tested and approved under appropriate government standards such as NIOSH (US) or CEN (EU).

Control of environmental exposure

Do not let product enter drains.

SECTION 9: Physical and chemical properties

9.1 Information on basic physical and chemical properties

- | | |
|---------------|-------------------|
| a) Appearance | Form: solid |
| b) Odour | no data available |

c) Odour Threshold	no data available
d) pH	no data available
e) Melting point/freezing point	Melting point/range: > 300 °C - lit.
f) Initial boiling point and boiling range	no data available
g) Flash point	no data available
h) Evaporation rate	no data available
i) Flammability (solid, gas)	The product is not flammable. - Flammability (solids)
j) Upper/lower flammability or explosive limits	no data available
k) Vapour pressure	no data available
l) Vapour density	no data available
m) Relative density	1,52 g/cm ³ at 20 °C
n) Water solubility	369 g/l at 20 °C - soluble
o) Partition coefficient: n-octanol/water	log Pow: -2,08 at 23 °C
p) Auto-ignition temperature	> 400 °C at 1.013 hPa
q) Decomposition temperature	no data available
r) Viscosity	no data available
s) Explosive properties	Not explosive
t) Oxidizing properties	no data available

9.2 Other safety information

Surface tension	66,6 mN/m at 20 °C
-----------------	--------------------

SECTION 10: Stability and reactivity

10.1 Reactivity

no data available

10.2 Chemical stability

Stable under recommended storage conditions.

10.3 Possibility of hazardous reactions

no data available

10.4 Conditions to avoid

no data available

10.5 Incompatible materials

Strong oxidizing agents

10.6 Hazardous decomposition products

Other decomposition products - no data available

In the event of fire: see section 5

SECTION 11: Toxicological information

11.1 Information on toxicological effects

Acute toxicity

LD50 Oral - rat - female - > 2.000 mg/kg
(Directive 67/548/EEC, Annex V, B.1.)

LD50 Dermal - rat - male and female - > 2.000 mg/kg
(Directive 67/548/EEC, Annex V, B.3.)

LD50 Intraperitoneal - rat - 502 mg/kg

LD50 Intraperitoneal - mouse - 1.176 mg/kg

Skin corrosion/irritation

Skin - rabbit

Result: No skin irritation - 4 h

(Directive 67/548/EEC, Annex V, B.4.)

Serious eye damage/eye irritation

Eyes - rabbit

Result: No eye irritation - 24 h

(Directive 67/548/EEC, Annex V, B.5.)

Respiratory or skin sensitisation

no data available

Germ cell mutagenicity

no data available

Ames test

S. typhimurium

Result: negative

Directive 67/548/EEC, Annex V, B.12.

rat - male and female

Result: negative

Carcinogenicity

IARC: No component of this product present at levels greater than or equal to 0.1% is identified as probable, possible or confirmed human carcinogen by IARC.

Reproductive toxicity

Reproductive toxicity - rat - Intraperitoneal

Effects on Fertility: Post-implantation mortality (e.g., dead and/or resorbed implants per total number of implants).

no data available

Specific target organ toxicity - single exposure

no data available

Specific target organ toxicity - repeated exposure

no data available

Aspiration hazard

no data available

Additional Information

Repeated dose toxicity - rat - male and female - Oral - No observed adverse effect level - 500 mg/kg
RTECS: MT6550000

To the best of our knowledge, the chemical, physical, and toxicological properties have not been thoroughly investigated.

SECTION 12: Ecological information

12.1 Toxicity

Toxicity to fish	static test LC50 - <i>Poecilia reticulata</i> (guppy) - > 128 mg/l - 96 h (Directive 67/548/EEC, Annex V, C.1.)
Toxicity to daphnia and other aquatic invertebrates	static test EC50 - <i>Daphnia magna</i> (Water flea) - > 113 mg/l - 48 h (Directive 67/548/EEC, Annex V, C.2.)
Toxicity to algae	static test EC50 - <i>Desmodesmus subspicatus</i> (green algae) - > 89,2 mg/l - 72 h (Directive 67/548/EEC, Annex V, C.3.)

12.2 Persistence and degradability

Biodegradability	aerobic - Exposure time 28 d Result: 4,9 % - Not readily biodegradable. (C.4-E of the COUNCIL REGULATION (EC) No 440/2008)
------------------	--

12.3 Bioaccumulative potential

no data available

12.4 Mobility in soil

no data available

12.5 Results of PBT and vPvB assessment

PBT/vPvB assessment not available as chemical safety assessment not required/not conducted

12.6 Other adverse effects

no data available

SECTION 13: Disposal considerations

13.1 Waste treatment methods

Product

Offer surplus and non-recyclable solutions to a licensed disposal company.

Contaminated packaging

Dispose of as unused product.

SECTION 14: Transport information

14.1 UN number

ADR/RID: -	IMDG: -	IATA: -
------------	---------	---------

14.2 UN proper shipping name

ADR/RID: Not dangerous goods
IMDG: Not dangerous goods
IATA: Not dangerous goods

14.3 Transport hazard class(es)

ADR/RID: -	IMDG: -	IATA: -
------------	---------	---------

14.4 Packaging group

ADR/RID: -	IMDG: -	IATA: -
------------	---------	---------

14.5 Environmental hazards

ADR/RID: no	IMDG Marine pollutant: no	IATA: no
-------------	---------------------------	----------

14.6 Special precautions for user

no data available

SECTION 15: Regulatory information

This safety datasheet complies with the requirements of Regulation (EC) No. 1907/2006.

15.1 Safety, health and environmental regulations/legislation specific for the substance or mixture

no data available

15.2 Chemical Safety Assessment

For this product a chemical safety assessment was not carried out

SECTION 16: Other information

Further information

Copyright 2014 Sigma-Aldrich Co. LLC. License granted to make unlimited paper copies for internal use only.

The above information is believed to be correct but does not purport to be all inclusive and shall be used only as a guide. The information in this document is based on the present state of our knowledge and is applicable to the product with regard to appropriate safety precautions. It does not represent any guarantee of the properties of the product. Sigma-Aldrich Corporation and its Affiliates shall not be held liable for any damage resulting from handling or from contact with the above product. See www.sigma-aldrich.com and/or the reverse side of invoice or packing slip for additional terms and conditions of sale.

SAFETY DATA SHEET

according to Regulation (EC) No. 1907/2006

Version 5.7 Revision Date 25.07.2016

Print Date 14.11.2016

GENERIC EU MSDS - NO COUNTRY SPECIFIC DATA - NO OEL DATA

SECTION 1: Identification of the substance/mixture and of the company/undertaking

1.1 Product identifiers

Product name : Sodium hypochlorite solution

Product Number : 425044

Brand : Sigma-Aldrich

REACH No. : A registration number is not available for this substance as the substance or its uses are exempted from registration, the annual tonnage does not require a registration or the registration is envisaged for a later registration deadline.

1.2 Relevant identified uses of the substance or mixture and uses advised against

Identified uses : Laboratory chemicals, Manufacture of substances

1.3 Details of the supplier of the safety data sheet

Company : Sigma-Aldrich (Pty.) Ltd.
17 Pomona Street
Aviation Park, Unit 4
KEMPTON PARK
1619 SOUTH AFRICA

Telephone : +27 11 979 1188

Fax : +27 11 979 1119

1.4 Emergency telephone number

Emergency Phone #

SECTION 2: Hazards identification

2.1 Classification of the substance or mixture

Classification according to Regulation (EC) No 1272/2008

Skin corrosion (Category 1B), H314

Acute aquatic toxicity (Category 1), H400

For the full text of the H-Statements mentioned in this Section, see Section 16.

2.2 Label elements

Labelling according Regulation (EC) No 1272/2008

Pictogram



Signal word : Danger

Hazard statement(s)

H314

Causes severe skin burns and eye damage.

H400

Very toxic to aquatic life.

Precautionary statement(s)

P273

Avoid release to the environment.

P280 Wear protective gloves/ protective clothing/ eye protection/ face protection.
P305 + P351 + P338 IF IN EYES: Rinse cautiously with water for several minutes. Remove contact lenses, if present and easy to do. Continue rinsing.
P310 Immediately call a POISON CENTER/doctor.
Supplemental Hazard information (EU)
EUH031 Contact with acids liberates toxic gas.

2.3 Other hazards

This substance/mixture contains no components considered to be either persistent, bioaccumulative and toxic (PBT), or very persistent and very bioaccumulative (vPvB) at levels of 0.1% or higher.

SECTION 3: Composition/information on ingredients

3.2 Mixtures

Formula : ClNaO
Molecular weight : 74,44 g/mol

Hazardous ingredients according to Regulation (EC) No 1272/2008

Component		Classification	Concentration
Sodium hypochlorite			
CAS-No.	7681-52-9	Skin Corr. 1B; Aquatic Acute 1; H314, H400 Concentration limits: ≥ 5 %: , EUH031; M-Factor - Aquatic Acute: 10	≥ 10 - < 20 %
EC-No.	231-668-3		
Index-No.	017-011-00-1		

For the full text of the H-Statements mentioned in this Section, see Section 16.

SECTION 4: First aid measures

4.1 Description of first aid measures

General advice

Consult a physician. Show this safety data sheet to the doctor in attendance.

If inhaled

If breathed in, move person into fresh air. If not breathing, give artificial respiration. Consult a physician.

In case of skin contact

Take off contaminated clothing and shoes immediately. Wash off with soap and plenty of water. Consult a physician.

In case of eye contact

Rinse thoroughly with plenty of water for at least 15 minutes and consult a physician.

If swallowed

Do NOT induce vomiting. Never give anything by mouth to an unconscious person. Rinse mouth with water. Consult a physician.

4.2 Most important symptoms and effects, both acute and delayed

The most important known symptoms and effects are described in the labelling (see section 2.2) and/or in section 11

4.3 Indication of any immediate medical attention and special treatment needed

No data available

SECTION 5: Firefighting measures

5.1 Extinguishing media

Suitable extinguishing media

Dry powder

5.2 Special hazards arising from the substance or mixture

No data available

5.3 Advice for firefighters

Wear self-contained breathing apparatus for firefighting if necessary.

5.4 Further information

No data available

SECTION 6: Accidental release measures

6.1 Personal precautions, protective equipment and emergency procedures

Wear respiratory protection. Avoid breathing vapours, mist or gas. Ensure adequate ventilation.

Evacuate personnel to safe areas.

For personal protection see section 8.

6.2 Environmental precautions

Prevent further leakage or spillage if safe to do so. Do not let product enter drains. Discharge into the environment must be avoided.

6.3 Methods and materials for containment and cleaning up

Soak up with inert absorbent material and dispose of as hazardous waste. Do not flush with water. Keep in suitable, closed containers for disposal.

6.4 Reference to other sections

For disposal see section 13.

SECTION 7: Handling and storage

7.1 Precautions for safe handling

Avoid inhalation of vapour or mist.

For precautions see section 2.2.

7.2 Conditions for safe storage, including any incompatibilities

Store in cool place. Keep container tightly closed in a dry and well-ventilated place. Containers which are opened must be carefully resealed and kept upright to prevent leakage.

Never allow product to get in contact with water during storage. Do not store near acids.

Recommended storage temperature 2 - 8 °C

7.3 Specific end use(s)

Apart from the uses mentioned in section 1.2 no other specific uses are stipulated

SECTION 8: Exposure controls/personal protection

8.1 Control parameters

Components with workplace control parameters

8.2 Exposure controls

Appropriate engineering controls

Handle in accordance with good industrial hygiene and safety practice. Wash hands before breaks and at the end of workday.

Personal protective equipment

Eye/face protection

Tightly fitting safety goggles. Faceshield (8-inch minimum). Use equipment for eye protection tested and approved under appropriate government standards such as NIOSH (US) or EN 166(EU).

Skin protection

Handle with gloves. Gloves must be inspected prior to use. Use proper glove removal technique (without touching glove's outer surface) to avoid skin contact with this product. Dispose of contaminated gloves after use in accordance with applicable laws and good laboratory practices. Wash and dry hands.

The selected protective gloves have to satisfy the specifications of EU Directive 89/686/EEC and the standard EN 374 derived from it.

Full contact

Material: Nitrile rubber

Minimum layer thickness: 0,11 mm

Break through time: 480 min

Material tested: Dermatrill® (KCL 740 / Aldrich Z677272, Size M)

Splash contact

Material: Nitrile rubber

Minimum layer thickness: 0,11 mm

Break through time: 480 min

Material tested: Dermatrill® (KCL 740 / Aldrich Z677272, Size M)

data source: KCL GmbH, D-36124 Eichenzell, phone +49 (0)6659 87300, e-mail sales@kcl.de, test method: EN374

If used in solution, or mixed with other substances, and under conditions which differ from EN 374, contact the supplier of the CE approved gloves. This recommendation is advisory only and must be evaluated by an industrial hygienist and safety officer familiar with the specific situation of anticipated use by our customers. It should not be construed as offering an approval for any specific use scenario.

Body Protection

Complete suit protecting against chemicals, The type of protective equipment must be selected according to the concentration and amount of the dangerous substance at the specific workplace.

Respiratory protection

Where risk assessment shows air-purifying respirators are appropriate use a full-face respirator with multi-purpose combination (US) or type ABEK (EN 14387) respirator cartridges as a backup to engineering controls. If the respirator is the sole means of protection, use a full-face supplied air respirator. Use respirators and components tested and approved under appropriate government standards such as NIOSH (US) or CEN (EU).

Control of environmental exposure

Prevent further leakage or spillage if safe to do so. Do not let product enter drains. Discharge into the environment must be avoided.

SECTION 9: Physical and chemical properties

9.1 Information on basic physical and chemical properties

- | | |
|--|-------------------|
| a) Appearance | Form: liquid |
| b) Odour | No data available |
| c) Odour Threshold | No data available |
| d) pH | No data available |
| e) Melting point/freezing point | -30 - -20 °C |
| f) Initial boiling point and boiling range | 111 °C |

g) Flash point	Not applicable
h) Evaporation rate	No data available
i) Flammability (solid, gas)	No data available
j) Upper/lower flammability or explosive limits	No data available
k) Vapour pressure	23,3 hPa at 20 °C
l) Vapour density	No data available
m) Relative density	1,206 g/mL at 25 °C
n) Water solubility	completely miscible
o) Partition coefficient: n-octanol/water	No data available
p) Auto-ignition temperature	No data available
q) Decomposition temperature	No data available
r) Viscosity	No data available
s) Explosive properties	No data available
t) Oxidizing properties	No data available

9.2 Other safety information

No data available

SECTION 10: Stability and reactivity

10.1 Reactivity

No data available

10.2 Chemical stability

Stable under recommended storage conditions.

10.3 Possibility of hazardous reactions

No data available

10.4 Conditions to avoid

No data available

10.5 Incompatible materials

Strong acids, Organic materials, Powdered metals, Forms shock-sensitive mixtures with certain other materials., Amines, Reacts violently with ammonium salts, aziridine, methanol, and phenylacetonitrile, sometimes resulting in explosions. Reacts with primary aliphatic or aromatic amines to form explosively unstable n-chloroamines. Reaction with formic acid becomes explosive at 55°C.

10.6 Hazardous decomposition products

Hazardous decomposition products formed under fire conditions. - Hydrogen chloride gas, Sodium oxides
Other decomposition products - No data available
In the event of fire: see section 5

SECTION 11: Toxicological information

11.1 Information on toxicological effects

Acute toxicity

No data available

Skin corrosion/irritation

No data available

Serious eye damage/eye irritation

No data available

Respiratory or skin sensitisation

No data available

Germ cell mutagenicity

No data available

Carcinogenicity

IARC: A4 - Not classifiable as a human carcinogen (Sodium hypochlorite)

3 - Group 3: Not classifiable as to its carcinogenicity to humans (Sodium hypochlorite)

IARC: No component of this product present at levels greater than or equal to 0.1% is identified as probable, possible or confirmed human carcinogen by IARC.

Reproductive toxicity

No data available

Specific target organ toxicity - single exposure

No data available

Specific target organ toxicity - repeated exposure

No data available

Aspiration hazard

No data available

Additional Information

RTECS: Not available

burning sensation, Cough, wheezing, laryngitis, Shortness of breath, spasm, inflammation and edema of the larynx, spasm, inflammation and edema of the bronchi, pneumonitis, pulmonary edema, Material is extremely destructive to tissue of the mucous membranes and upper respiratory tract, eyes, and skin., To the best of our knowledge, the chemical, physical, and toxicological properties have not been thoroughly investigated.

SECTION 12: Ecological information**12.1 Toxicity**

No data available

12.2 Persistence and degradability

No data available

12.3 Bioaccumulative potential

No data available

12.4 Mobility in soil

No data available

12.5 Results of PBT and vPvB assessment

This substance/mixture contains no components considered to be either persistent, bioaccumulative and toxic (PBT), or very persistent and very bioaccumulative (vPvB) at levels of 0.1% or higher.

12.6 Other adverse effects

Very toxic to aquatic life with long lasting effects.

SECTION 13: Disposal considerations**13.1 Waste treatment methods****Product**

Offer surplus and non-recyclable solutions to a licensed disposal company.

Dispose of as unused product.

14.1 UN number

IMDG: 1791

IATA: 1791

ADR/RID: HYPOCHLORITE SOLUTION

IMDG: HYPOCHLORITE SOLUTION

IATA: Hypochlorite solution

ADR/RID: 8

IMDG: 8

IATA: 8

ADR/RID: III

IMDG: III

IATA: III

ADR/RID: yes

IMDG Marine pollutant: yes

IATA: no

No data available

15.1 Safety, health and environmental regulations/legislation specific for the substance or mixture

This safety datasheet complies with the requirements of Regulation (EC) No. 1907/2006.

For this product a chemical safety assessment was not carried out

Full text of H-Statements referred to under sections 2 and 3.

EUH031 Contact with acids liberates toxic gas.

H314 Causes severe skin burns and eye damage.

H400 Very toxic to aquatic life.

Further information

Copyright 2016 Sigma-Aldrich Co. LLC. License granted to make unlimited paper copies for internal use only.

The above information is believed to be correct but does not purport to be all inclusive and shall be used only as a guide. The information in this document is based on the present state of our knowledge and is applicable to the product with regard to appropriate safety precautions. It does not represent any guarantee of the properties of the product. Sigma-Aldrich Corporation and its Affiliates shall not be held liable for any damage resulting from handling or from contact with the above product. See www.sigma-aldrich.com and/or the reverse side of invoice or packing slip for additional terms and conditions of sale.